Regulation of layer-specific axon targeting in the developing visual system of *Drosophila*

Katarina Timofeev

June 2012

Division of Molecular Neurobiology

MRC National Institute for Medical Research

The Ridgeway

Mill Hill, London

NW7 1AA, UK

Department of Cell and Developmental Biology

University College London

A thesis submitted to University College London

for the degree of Doctor of Philosophy

Declaration

I, Katarina Timofeev, confirm that the work presented in this thesis is my own. Where information has been derived from other sources, I confirm that this has been indicated in the thesis.

Chapter 3, 4 and 5 include data generated and kindly provided by W. Joly, D. Hadjieconomou and I. Salecker. This has been specifically indicated in the main text and the figure legends.

Abstract

The ability of a nervous system to correctly process sensory information depends on the precise wiring of axonal and dendritic projections. The visual system of vertebrates and invertebrates consists of many neuron subtypes, whose neurites are organized into columns and layers. Layered pathways are pivotal to enable parallel processing of several visual features within a network, such as motion and color detection. Despite their functional relevance, the molecular mechanisms controlling their formation are still poorly understood.

In the visual system of *Drosophila*, photoreceptor neurons (R-cells, R1-R8) extend axons into the optic lobe. R1-R6 axons target to the lamina, while R8 and R7 axons terminate in two distinct neuropil layers in the medulla, called M3 and M6. This thesis investigated the roles of Netrin ligands and the attractive receptor Frazzled and repellent receptor Unc-5 in mediating layer-specific targeting of R8 axons during development. Immunohistological and genetic analyses showed that Frazzled is expressed and cell-autonomously required in R8 photoreceptors for targeting their axons to layer M3. Netrin-B is specifically localized in this layer due to axonal release primarily by lamina neurons L3 and ligand capture by Frazzled expressed in target neurons. Loss of Netrins in the target area causes similar defects as loss of Netrins in R-cells. Netrin-B expression in L3 is sufficient to substantially rescue these R8-axon targeting defects. R8 axons target normally despite replacement of diffusible Netrin-B by membrane-tethered ligands, indicating that they act at short-range. Netrin localization is instructive, as expression of a tethered ligand-variant in ectopic layers can retarget R8 axons. Finally, R8 axons also express and require Unc-5 for layer-specific targeting suggesting a modulatory role of repellent input in this process. Together, this provides evidence for a distinct mechanism that uses the release of localized chemotropic guidance cues to precisely direct axons to a positionally defined layer.

Contents

Title		1
Declaration		2
Abstract		3
Table of contents		4
List of figures and tables		7
Abbreviations		9
Chapter 1 Introduction		10
1.1	Wiring the nervous system	11
1.1.1	Axon pathfinding during development	12
1.1.2	Guidance systems at the CNS midline	13
1.1.2.1	Netrins and their DCC and Unc-5 receptors guide neurons at the midline	14
1.1.2.2	Repulsive function of Slit guidance cues and Robo receptors at the midline	16
1.1.2.3	Semaphorin and Ephrin guidance cues and their receptors mediate repulsion at the midline	17
1.1.3	Guidance molecules steer growth cones by regulating cytoskeleton dynamics	19
1.1.4	Cell adhesion molecules	20
1.1.5	Organization of neural maps	22
1.2	The visual system as a model to study layer-specific axon targeting	26
1.2.1	The visual system of vertebrates	27
1.2.2	The *Drosophila* visual system	29
1.2.3	Retinotopic map formation during development	31
1.2.4	R1-R6 targeting in the lamina	32
1.2.5	Layer-specific targeting in the medulla	33
1.2.6	Molecules involved in axon targeting to columns and layers in the medulla	35
1.3	Strategies for layer-specific targeting in the visual system	39
1.4	The Netrin, Frazzled and Unc-5 guidance system	42
1.4.1	Roles of Netrins and their receptors beyond the midline	42
1.4.2	Structural organization of Netrin, DCC and Unc-5	44
1.4.3	Downstream signaling of Netrins and their receptors DCC and Unc-5	45
1.4.4	Roles of Netrins and their receptors in the visual system	47
1.5	Aims of the work presented in this thesis	48
Chapter 2 Material and Methods		49
2.1	Genetics	50
2.1.1	Stocks and crosses used in this study	50
2.1.2	Generation of the *unc-5*$^{8\text{-}2a}$ allele	53
2.1.3	RNAi knock-down approach in several genetic backgrounds	53
2.2	Immunohistochemistry	54
2.3	Production of the Unc-5 antibody	56
2.4	Molecular biology	56
2.4.1	Genomic DNA extraction	56
2.4.2	Standard polymerase chain reaction	57

2.4.3 Cloning of the *NetB*^{V5} and *NetB*^{cd8} constructs into *pMT-V5* vectors to use in cell based assays 58
2.4.4 Cloning of the *UAS-NetB* and *UAS-NetB*^{cd8} constructs into *pKC* vectors for the generation of transgenic flies 60
2.4.5 Cloning of the *Fra*^{Fl} and *Fra*$^{ECD-HA}$ constructs to use in cell based aggregation assays into *pMT-V5* vectors 60
2.4.6 Cloning of the *Fra-mCherry* construct into *pMT-V5* vector to use in cell based assays 62
2.5 Cell assays 63
2.5.1 S2 and S2R+ Schneider cell culture 63
2.5.2 Transient transfection of S2 / S2R+ cells 63
2.5.3 Concentration of secreted NetB and Fra^{ECD-HA} proteins from conditioned medium 64
2.5.4 Binding assays 64
2.5.5 Fixation and immunohistochemistry 65
2.5.6 Western blot analysis 66

Chapter 3 The role of Frazzled in R8 axons 68
3.1 Introduction 69
3.2 Results 71
3.2.1 Fra is expressed in the optic lobe during pupal development 71
3.2.2 Fra is expressed in R8 cells along the cell body membrane and in the developing rhabdomeres 72
3.2.3 Fra is localized to the growth cones of R8 axons 73
3.2.4 *fra* is required for R8 axon targeting 74
3.2.5 *fra* is required in R8 axons for the targeting to the final layer M3 76
3.2.6 Knock-down of *fra* using the RNAi approach leads to R8 axon targeting defects 79
3.2.7 Fra is not sufficient for layer-specific axon targeting 80
3.3 Discussion 82
3.3.1 Fra is required for R8 axon targeting to the M3 layer 82
3.3.2 Fra is not sufficient to mediate layer-specificity 83

Chapter 4 The role of Netrins in regulating layer-specific R8 axon targeting 85
4.1 Introduction 86
4.2 Results 87
4.2.1 Netrin expressing neurons in the optic lobe 88
4.2.2 NetB is dynamically expressed in the developing visual system with a strong localization to the emerging M3 layer 88
4.2.3 NetA and NetB are expressed redundantly in a similar set of neurons 91
4.2.4 Netrins are required for R8 axon targeting to the M3 layer 93
4.2.5 *NetA and NetB* are required in the target-associated neurons for layer-specific targeting 95
4.3 Discussion 97
4.3.1 Netrins are expressed in the M3 layer and mediate layer-specific R8 axon targeting 97

Chapter 5 Mechanisms of layer-specific Netrin localization 99
5.1 Introduction 100
5.2 Results 102

5.2.1 Netrins act at short-range 102
5.2.2 Fra in target neurons localizes NetB in the M3 layer 105
5.2.3 Cell-based binding assay to analyze Fra and Netrin in a ternary complex 113
5.2.4 Layer-specific targeting is mediated by local axonal release of NetB 123
5.2.5 Cell-type specific RNAi knock-down of *NetA* and *NetB* 124
5.2.6 Rescue of aberrant R8 axon targeting in $NetAB^{\Delta}$ mutants 128
5.3 Discussion 132
5.3.1 NetB mediates short-range attraction of R8 axons to the M3 layer 132
5.3.2 Role of Fra in target neurons in the localization of NetB to the M3 layer 132
5.3.3 Role for L3 lamina neurons in local release of NetB into the M3 layer 136

Chapter 6 The role of ectopic NetB for R8 axon targeting 138
6.1 Introduction 139
6.2 Results 140
6.2.1 Co-expression of NetB and Fra in ectopic layers 140
6.2.2 Ectopic expression of NetB with truncated Fra in the M1/M2 layers 142
6.2.3 Misexpression of NetB in R-cells 145
6.2.4 Ectopic expression of membrane-tethered $NetB^{cd8}$ 147
6.3 Discussion 156
6.3.1 Layer-specific localization of NetB is sufficient to target R8 axons 156

Chapter 7 The role of the Unc-5 guidance receptor in R8 axons 159
7.1 Introduction 160
7.2 Results 161
7.2.1 Unc-5 is expressed in the optic lobe during pupal development 161
7.2.2 *unc-5* is required for layer-specific targeting of R8 axons 162
7.2.3 *unc-5* is required to maintain R8 axons at the medulla neuropil border during the first half of pupal development 164
7.2.4 Ectopic expression of *unc-5* in R-cells prevents targeting to the lamina and medulla neuropils 166
7.3 Discussion 168
7.3.1 *unc-5* is required for R8 axon targeting during early pupal development 168
7.3.2 Unc-5 likely interacts with Fra in the Netrin mediated R8 axon targeting to the M3 layer 169

Chapter 8 Concluding remarks and future work 173
8.1 Strategies to form synaptic layers in the visual system 173
8.2 NetB regulates R8 axon targeting through both Fra and Unc-5 receptors 173
8.3 L3 lamina neurons function as intermediate targets for R8 axons 176
8.4 Hierarchy in the neuropils: Top-down control to connect synaptic neuropils 177

References 179
Acknowledgments 196

List of figures and tables

Chapter 1 - Introduction
Figure 1. The growth cone guides axons towards their targets. 13
Figure 2. Axon guidance at the CNS midline. 19
Figure 3. The adult visual system of higher vertebrates. 28
Figure 4. Layer- and column-specific connections in the adult fly visual system. 31
Figure 5. Two-step layer-specific R8 and R7 axon targeting during development. 35
Figure 6. Molecules involved in column- and layer-specific R7 and R8 axon targeting in the medulla. 38
Figure 7. Interaction of Netrin with DCC and Unc-5. 44
Figure 8. Signaling pathways downstream of DCC and Unc-5 receptors. 46

Chapter 2 – Material and methods
Table 1: Activity of the *act>>Gal4* FLPout approaches in different areas in the optic lobe. 54
Table 2: Solutions. 54
Table 3: Primary antibodies. 54
Table 4: Secondary antibodies. 55
Table 5: Primers used for sequence analysis of *unc-5*. 57
Table 6: Primers used for sequence analysis and cloning of *NetB* constructs. 59
Table 7: Primers used for sequence analysis and cloning of Fra constructs. 61

Chapter 3 - The role of Frazzled in R8 axons
Figure 9. Fra expression in R-cells and the optic lobe during pupal development and in the adult. 72
Figure 10. Fra is expressed on R8 cell bodies and in developing rhabdomeres. 73
Figure 11. Fra is localized to the growth cones of R8 axons. 74
Figure 12. *fra* is required for R8 axon targeting to the M3 layer. 76
Figure 13. *fra* is required for R8 axon targeting to the M3 layer during pupal development. 78
Figure 14. Knock-down of *fra* using RNAi. 80
Figure 15. Prolonged ectopic expression of *fra* in all R-cells leads to aberrant targeting of R8 axons. 81

Chapter 4 - The role of Netrins for layer-specific R8 axon targeting
Figure 16. Analysis of the expression pattern of Netrin releasing neurons. 88
Figure 17. The secreted ligand NetB is localized in the M3 layer. 90
Figure 18. Analysis of YFP-protein traps show that NetA and NetB are expressed in a similar set of neurons. 92
Figure 19. *NetA/B* are required for R8 axon targeting to the M3 layer. 94
Figure 20. Knock-down of *NetA* and *NetB* in the eye and target neurons. 96

Chapter 5- Mechanisms of layer-specific Netrin localization
Figure 21. *NetB* acts at short-range. 103
Figure 22. R8 axons bridge the distance to localized NetB in the M3 layer by extending filopodia. 105
Figure 23. NetB localization in *fra* knock-down experiments. 107
Figure 24. Fmi localization in *fra* knock-down experiments. 109

Figure 25. Membrane-tethered NetB^{TMmyc} localization in *fra* knock-down experiments. 111
Figure 26. Expression of Fra in target neurons. 112
Figure 27. *NetB*^{V5}, *NetB*^{cd8} and *Fra*$^{ECD-HA}$ and *Fra*^{Fl} constructs used in cell-based assays. 115
Figure 28. Cell assays to demonstrate binding of Fra and NetB 117
Figure 29. Cell assays to demonstrate a binding of *Fra-GFP* to *NetB*^{V5} and *Fra*$^{ECD-HA}$. 119
Figure 30. Cell assays to demonstrate binding of *Fra*$^{ECD-HA}$ and *NetB*^{cd8}. 120
Figure 31. Clustering Fra-GFP R+ cells and Fra-Cherry R+ cells. 122
Figure 32. Analysis of *NP4151-*, and *NP0831-Gal4* insertions adjacent to *NetB* and *NetA* loci 124
Figure 33. Knock-down of *NetA* and *NetB* using *NP4151-Gal4* and *NP0831-Gal4*. 125
Figure 34. Knock-down using *UAS-NetA*^{RNAi}, *UAS-NetB*^{RNAi} in target neuron subtypes. 127
Figure 35. Analysis of the enhancer trap *MH56-Gal4* expression pattern. 129
Figure 36. *MH56-Gal4* ectopically releases NetB into the M3 layer. 130
Figure 37. M3 layer-specific expression of *UAS-NetB* rescues R8 axon targeting defects. 131

Chapter 6 - The role of ectopic NetB for R8 axon targeting
Figure 38. *MH919-Gal4* and *MH728-Gal4* drivers were used to co-express *UAS-fra* and *UAS-NetB*. 141
Figure 39. *MH939-Gal4* is used to co-express of *UAS-fra* and *UAS-NetB*. 142
Figure 40. Ectopic layer of NetB is created by co-expression of *UAS-fra*$^{\Delta Cmyc}$ and *UAS-NetB*. 143
Figure 41. Analysis of the *MH502-Gal4* expression pattern during development. 144
Figure 42. Truncated *UAS-fra*$^{\Delta Cmyc}$ was co-expressed with *UAS-NetB* using *MH502-Gal4*. 145
Figure 43. Ectopic expression of NetB in R-cells leads to stalling at the medulla neuropil border. 146
Figure 44. Ectopic expression of *UAS-NetB*^{cd8} in the M1/2 layers. 148
Figure 45. GFP-reporter expression under the control of *MH502-Gal4* with suppressed expression in R-cells. 150
Figure 46. Ectopic expression of *UAS-NetB*^{cd8} using *MH502-Gal4*. 152
Figure 47. *ap-Gal4* expression during pupal development and in the adult. 153
Figure 48. *UAS-NetB*^{cd8} over-expression broadly in the target neurons in the medulla using *ap-Gal4*. 155

Chapter 7 - The role of the Unc-5 guidance receptor in R8 axons
Figure 49. The guidance receptor Unc-5 is dynamically expressed in the visual system. 162
Figure 50. *unc-5* is required for R8 axon targeting. 163
Figure 51. *unc-5* is required during early pupal development. 165
Figure 52. Unc-5 acts as a repellent receptor when expressed ectopically in R-cells. 167

Abbreviations

APF	After puparium formation	**LN**	Lamina neuron
Babo	Baboon	**Lo**	Lobula
CadN	N-Cadherin	**Lp**	Lobula plate
CAM	Cell adhesion molecule	**MAPK**	mitogen activated protein kinase
Caps	Capricious	**MARCM**	Mosaic analysis with a repressible cell marker
CNS	Central nervous system	**Me**	Medulla
Comm	Commissureless	**MF**	Morphogenetic furrow
DCC	Deleted in Colorectal Cancer	**MN**	Medulla neuron
Dpp	Decapentaplegic	**NCAM**	Neuronal cell adhesion molecule
Dscam	Down syndrome cell adhesion molecule	**Nel**	Neural epidermal growth factor-like
EGF	Epidermal growth factor	**NetA**	Netrin-A
EMS	Ethyl methanesulfonate	**NetB**	Netrin-B
Ey	Eyeless	**OR**	Odorant receptor
FAK	Focal adhesion kinase	**ORN**	Olfactory receptor neuron
FasII	Fasciclin II	**PTP69D**	Protein tyrosine phosphatase protein 69D
Fmi	Flamingo	**RGC**	Retinal ganglion cell
Fn	Fibronectin	**RNAi**	RNA interference
Fra	Frazzled	**Robo**	Roundabout
GFP	Green fluorescent protein	**Sens**	Senseless
GMR	Glass multimer reporter	**Seq**	Sequoia
Gogo	Golden Goal	**TM**	Transmembrane domain
Hh	Hedgehog	**TSP**	Thrombospondin domain
Ig	Immunoglobulin	**Tutl**	Turtle
IPL	Inner plexiform layer	**Unc-5**	Uncoordinated-5
La	Lamina	**VDRC**	Vienna Drosophila RNAi Center
LAR	Leukocyte-antigen-related-like	**YFP**	Yellow fluorescent protein

Chapter 1

Introduction

1.1 Wiring of the nervous system

The mature nervous system of vertebrates and invertebrates fulfills a variety of diverse functions that are essential for everyday tasks such as feeding, mating, fighting or fleeing, and ultimately also for the survival of an animal. The ability of a nervous system to correctly process information depends on functioning neural circuits that consist of series of interconnected neurons. The organization of neural circuits in the nervous system varies greatly according to the intended function. Neural circuits are organized into structures such as glomeruli that are components of a discrete / convergent map in the olfactory system, or columns in the continuous / retinotopic map in the visual system, which allows a correct topographic representation of the external world. Synaptic layers are a frequently used form of organization and allow parallel information processing in the brain. How neural circuits are established during development and how specificity of connections between afferent neurons and their postsynaptic partners in synaptic units, such as layers, are achieved remains an intriguing and pivotal question in neurobiology.

During development, neural circuits are established in a stepwise fashion. Axons of neurons navigate during pathfinding, find specific target areas, identify target neurons and establish functioning synapses with appropriate synaptic partners. The mechanisms underlying axon guidance are highly conserved between vertebrates and invertebrates. Studies at the CNS midline allowed the identification of guidance molecules and their receptors, and provided significant insights into the mechanisms of pathfinding. However, much less is understood about how axons target to precise positions, such as layers, during circuit formation.

1.1.1 Axon pathfinding during development

In the developing nervous system, neurons extend axons towards appropriate target areas following specific paths. The highly reproducible pattern of axons navigating along distinct trajectories suggests that axons are guided by cues in their surroundings (Tessier-Lavigne and Goodman, 1996). They are guided over long distances towards their synaptic targets by a motile structure at the leading edge, called the growth cone (Figure 1) (y Cajal, S.R. 1890). The growth cone plays a key role in axon guidance, perceiving frequently changing signals in its environment, as it navigates to its targets (Tessier-Lavigne and Goodman, 1996; Dent et al., 2011). Equipped with distinct receptors, it is actively guided along pathways. Growth cones contain veil-like protrusions, the lamellipodia, and finger-like filopodia, which are characterized by high levels of bundled F-actin (Lowery and Van Vactor, 2009). At the proximal part of the growth cone, this actin network is associated with microtubules. Growth cone motility is induced through the activation of cell surface receptors that signal through complex pathways via Rho, Rac and Cdc42 family members of small GTPases, to ultimately control the assembly or disassembly of actin filaments (Huber et al., 2003).

Pioneer neurons lay down the very first axonal trajectories, which are then followed by later emerging axons (Bate, 1976). They extend their axons along stereotypic pathways into the central nervous system (CNS), following guidance cues. While in the early embryo growing distances are small and guidance cues are reachable, pioneer neurons lay out a basic scaffold (Hidalgo and Brand, 1997). Follower axons can then navigate efficiently along the fascicles established by the pioneer axons and the cues they provide.

To overcome the complex task for axons to navigate towards a target area over long distances, the trajectory is divided into multiple consecutive guidance steps. Axon

pathfinding frequently relies on intermediate targets (Bentley and Caudy, 1983; Chao et al., 2009). Initially, growth cones navigate towards these intermediate targets but then continue to grow to eventually reach their target area. How growth cones adjust their direction and make choices at these intermediate targets is a key question in axon guidance.

Guidance forces determine the route by a combination of attractive and repulsive cues that can be either localized and act at short-range, or act over long distances (Tessier-Lavigne and Goodman, 1996; Dickson, 2002). Intermediate targets often provide these guidance cues in the environment. Change of the repertoire of guidance receptors allows the growth cone to navigate towards and then away to reach the next intermediate or final target (Tessier-Lavigne and Goodman, 1996).

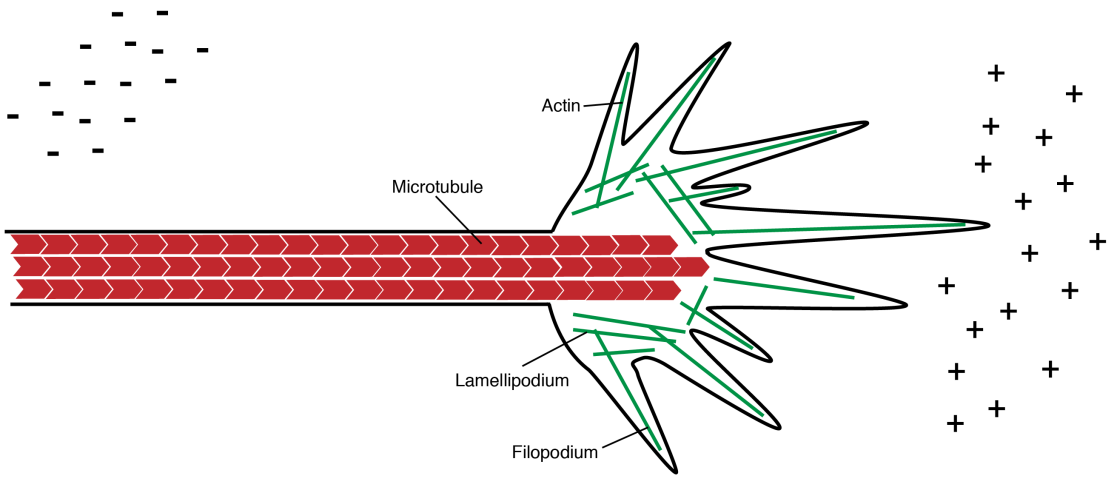

Figure 1. The growth cone guides axons towards their targets. The growth cone cytoskeleton is organized from microtubules and actin. At its tip it contains veil-like protrusions, the lamellipodia, and finger-like filopodia. Attractive (+ in schematic) and repulsive (-) guidance forces provide a path that the growth cone follows mediated through the activation of attractant or repellent cell surface receptors.

1.1.2 Guidance systems at the CNS midline

The most extensively studied and well-understood example of axon pathfinding is the CNS midline (Figure 2). Four major families of guidance cues have been intensively

studied in axon pathfinding at the ventral midline in *C. elegans*, vertebrates and *Drosophila*. These include the Netrins, Slits, Semaphorins, and Ephrins (Dickson, 2002).

1.1.2.1 Netrins and their DCC and Unc-5 receptors guide neurons at the midline

In an EMS (Ethyl methanesulfonate) mutagenesis screen to identify viable behavioral mutants in *C. elegans*, S. Brenner isolated the *unc-6, unc-40* and *unc-5* mutants and mapped their linkage group (Brenner, 1974). These belong to a large group of about 400 *uncoordinated (unc)* mutants characterized by a lack of control of motion. Subsequent studies found that these mutants had profound neuroanatomical defects and that the affected genes are required to control circumferential axon guidance of pioneer axons at the midline in *C. elegans* (Hedgecock et al., 1990; Ishii et al., 1992).

Intriguingly in vertebrates, commissural neurons of spinal cord explants from chick embryos showed a significant outgrowth in the presence of floor plate cells (Serafini et al., 1994). A screen to determine the molecular nature of these diffusible factors responsible for this behavior, led to the identification of a novel attractive guidance molecule. This protein was named Netrin, after the Sanskrit word "netr", which means “one who guides” (Kennedy et al., 1994; Serafini et al., 1994). Sequence analysis revealed that it shared significant homology with Unc-6 in *C. elegans* (Serafini et al., 1994). Subsequent analysis demonstrated that also in the *Drosophila* ventral nerve cord, similar to floor plate cells in vertebrates, Netrins are secreted by midline cells (Harris et al., 1996; Mitchell et al., 1996; Serafini et al., 1996; Shirasaki et al., 1996).

Netrins act as bifunctional guidance molecules that work as attractants or repellents, depending on the receptor they activate. The attractive receptor is called Unc-40 in *C. elegans* (Chan et al., 1996). The homolog in vertebrates is Deleted in Colorectal Cancer (DCC) and Frazzled (Fra) in *Drosophila* (Fazeli et al., 1997; Keino-Masu et al.,

1996; Kolodziej et al., 1996). Unc-5 in *C. elegans* and its homologs in vertebrates and *Drosophila* are the repulsive receptors (Keleman and Dickson, 2001; Leonardo et al., 1997; Leung-Hagesteijn et al., 1992; Wadsworth et al., 1996).

In circumferential axon guidance in *C. elegans*, growth cones migrate along the body wall between the epidermis and basement membrane in response to a gradient of Netrin/Unc-6 that is secreted at the ventral midline. Neurons expressing the attractive receptor Unc-40 migrate ventrally, while those expressing the repellent Unc-5 receptor alone, or both Unc-5 and Unc-40, migrate dorsally (Hedgecock et al., 1990; Hong et al., 1999; Merz and Culotti, 2000; Merz et al., 2001).

In the vertebrate spinal cord, DCC mediates the attraction of commissural axons to Netrins in the ventral midline (Fazeli et al., 1997; Keino-Masu et al., 1996). Similarly in *Drosophila,* Fra is required for Netrin-mediated attraction (Kolodziej et al., 1996). In contrast, Unc-5 was shown to mediate repulsive responses to Netrins. In *Drosophila,* misexpression of Unc-5 in commissural axons prevents these to cross the midline (Keleman and Dickson, 2001).

In *Drosophila*, the Down syndrome cell adhesion molecule (Dscam) is suggested to function as an attractive receptor for Netrin, promoting CNS midline crossing likely in parallel to Fra (Andrews et al., 2008). In vertebrates, Dscam is also suggested to be a putative Netrin receptor and may act in parallel to DCC, however the involvement of Dscam in Netrin mediated axon guidance remains uncertain (Liu et al., 2009; Ly et al., 2008).

1.1.2.2 Repulsive function of Slit guidance cues and Robo receptors at the midline

Once commissural axons have crossed the midline, they do not re-cross but proceed away from the midline. For that, they need to become insensitive to the attractive Netrins, as well as being prevented from re-crossing the midline mediated through repulsion (Stein and Tessier-Lavigne, 2001; Zou et al., 2000). The midline secretes diffusible repellent proteins. One such important chemorepulsive molecule is Slit. Slit prevents neurons from crossing and re-crossing the midline via the Roundabout (Robo) receptor, which is expressed by growth cones of ipsilateral and commissural neurons (Brose et al., 1999; Kidd et al., 1999; Kidd et al., 1998; Mastick et al., 2010; Simpson et al., 2000). In *Drosophila*, to enable commissural neurons to cross the midline and to overcome Slit mediated repulsion, Robo is absent from commissural growth cones, as they approach the midline. This is mediated by a small transmembrane protein called Commissureless (Comm) (Keleman et al., 2002a; Seeger et al., 1993; Tear et al., 1996). Comm controls the intracellular sorting of Robo, thereby preventing the receptor from reaching the growth cone membrane surface. Once across the midline, growth cones express Robo at the cell surface and therefore cannot re-cross. This results in the establishment of longitudinal tracts on the contralateral side of the midline. Ipsilateral neurons do not express Comm. Consequently, the growth cone continuously expresses Robo, which prevents midline crossing (Georgiou and Tear, 2002; Keleman et al., 2002b).

Surprisingly in *Drosophila,* Fra has a second Netrin-independent function at the midline, in addition to its canonical function mediated through Netrins. Fra is suggested to activate *comm* transcription, thereby coupling Netrin-mediated attraction to the down-regulation of Slit mediated repulsion in pre-crossing commissural axons (Yang et al., 2009).

In vertebrates, the Slit/Robo guidance system works together with Netrin/DCC to mediate commissural axon guidance across the midline (Mambetisaeva et al., 2005; Stein and Tessier-Lavigne, 2001). Before crossing the midline, commissural axons express Robo1, which mediates repulsion through midline-derived Slit. Robo1 in turn prevents DCC from binding to Netrin. Upon reaching the midline commissural neurons start expressing Rig-1/Robo3, which blocks Robo1 expression (Camurri et al., 2004; Sabatier et al., 2004). Thus, Robo1 no longer binds to Slit nor blocks DCC. Therefore, Slit mediated repulsion is silenced and Netrin at the midline mediates attraction through the DCC receptor allowing the axons to cross. Once they crossed the midline, Rig-1/Robo3 is downregulated and Robo1 upregulated, thus preventing commissural axons re-cross the midline (Sabatier et al., 2004).

1.1.2.3 Semaphorin and Ephrin guidance cues and their receptors mediate repulsion at the midline

In addition to the Slit/Robo guidance system, Semaphorins and their Plexin receptors mediate repulsion in the vertebrate spinal cord (Long et al., 2004; Zou et al., 2000). For instance, Sema3B is expressed at the vertebrate midline in floor plate cells and has no effect on commissural axons before crossing, but act as strong repellents after crossing (Nawabi et al., 2010). An intricate coordination of signaling between the floor plate cells and commissural axons allows initial crossing but prevents re-entry through the Plexin-A1/Neuropilin-2 receptor in the growth cone (Nawabi et al., 2010). At the pre-crossing stage, commissural neurons are not responsive to Sema3B due to low levels of Plexin-A1 at the growth cone. This is mediated by the cysteine protease calpain1 that cleaves the extracellular domain of Plexin-A1 (Nawabi et al., 2010). However, upon reaching the midline, calpain1 is inhibited through a signal from floor plate cells, and

Plexin-A1 accumulates in the growth cone to form a receptor complex together with Neuropilin-2. Commissural axons expressing Plexin-A1/Neuropilin-2 become responsive to Sema3B that is secreted from the floor plate cells and are thus repelled from the midline.

Finally, also members of the Eph receptor tyrosine kinase family and their ephrin ligands have been shown to act as prominent organizers of axon guidance at the midline (Palmer and Klein, 2003). EphrinB ligands function as selective repellents for subsets of axons and thereby prevent them from crossing the midline (Brittis et al., 2002; Imondi et al., 2000). However, pre-crossing axons of commissural neurons are Eph-negative and therefore do not respond to ephrins. Upon crossing the midline, EphB1 and EphA2 accumulate in the growth cones of commissural axons. These are unable to re-cross but follow longitudinal tracts, as they are not permitted to enter the midline by ephrinB ligands.

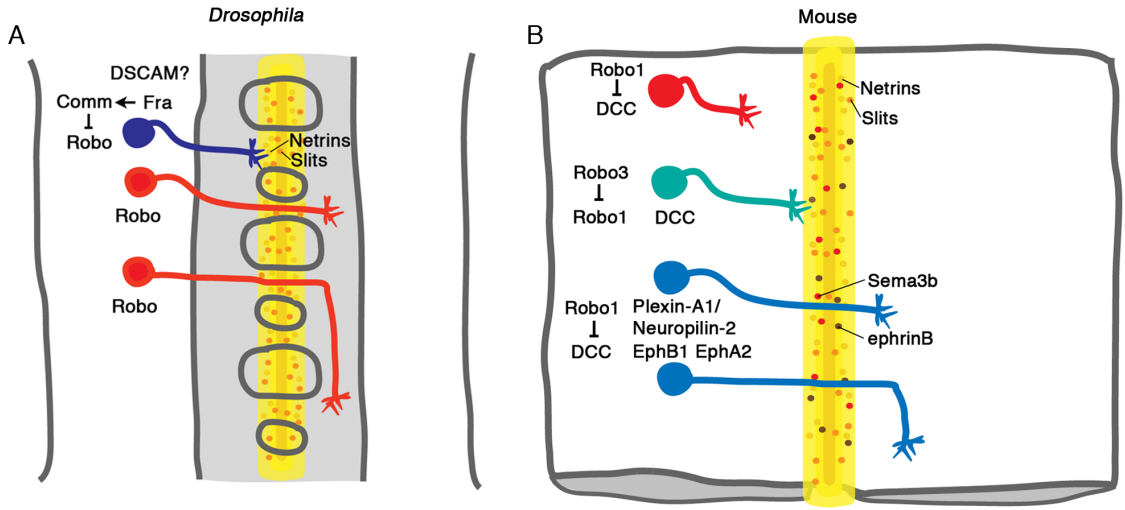

Figure 2. Axon guidance at the CNS midline. (A) *Drosophila* embryonic ventral nerve cord. The midline is depicted in yellow. Commissural axons approaching the midline are sensitive to Netrins and are attracted through the Fra receptor. Slit/Robo signaling is prevented through Fra transcriptionally upregulating Comm, which in turn prevents Robo from reaching the growth cone. Upon crossing the midline, Comm is downregulated and Slit mediated repulsion via Robo prevents axons from re-crossing, thus establishing longitudinal tracts on the contralateral side. (B) Mouse spinal cord shown as an open-book preparation. The floor plate (yellow) secrets guidance cues such as Netrins, Slit, Sema3b and ephrinB. On pre-crossing axons Robo1 binds to Slit and at the same time prevents DCC mediated Netrin attraction. Upregulation of Robo3 allows axon to approach the floor plate as it blocks Robo1 expression. Robo1 no longer binds to Slit nor blocks DCC. Netrin at the midline mediates attraction through the DCC receptor allowing the axons to cross. Once across Robo3 is downregulated and Robo1 upregulated thus commissural axons do not re-cross. Sema3b mediates repulsion through the Plexin-A1/Neuropilin-2 complex and ephrinB through the EphB1 and EphA2 receptors thus pushing the axons away from the midline. Anterior is up, posterior is down. Schematic adapted from Evans and Bashaw, 2010.

1.1.3 Guidance molecules steer growth cones by regulating cytoskeleton dynamics

The correct spatial and temporal expression of attractants and repellents in the environment and of receptors on the growth cone are crucial for regulating the dynamic behavior of axons. Depending on the signals a growth cone encounters, it reacts by reducing or stimulating growth in a given direction. Therefore, precise mechanisms downstream of the guidance receptors are required to ultimately regulate the growth cone cytoskeleton (Geraldo and Gordon-Weeks, 2009; Kalil and Dent, 2005).

However, the growth cone is a great distance from away from the cell body nucleus, where gene expression takes place. Local translation in the growth cone may enhance the efficiency and speed of action of guidance cues at the tip of an axon. Chemotropic guidance cues have been shown to stimulate axonal growth through activation of local protein synthesis (Campbell and Holt, 2001; Ming et al., 2002). Experiments with rat retinal ganglion cells demonstrated that isolated retinal growth cones immediately lose their ability to expand towards a chemotropic gradient of Netrin1 or Sema3A when translation was inhibited (Piper et al., 2006). Recent studies revealed a direct link between Netrin signaling and the intracellular translation machinery through the transmembrane DCC receptor (Tcherkezian et al., 2010). Upon Netrin signaling, DCC interacts with the protein synthesis machinery at the membrane in the growth cone, therefore influencing protein translation required for axon outgrowth. As a possible further component in this cascade, the polarity protein and cytoskeleton regulator - PAR complex protein Par3 – is suggested to be involved in axonal elongation via local translation of its mRNA in the growth cone. This stimulated outgrowth is mediated through signaling of netrin-1 and nerve growth factor (NGF), thus coupling guidance cues with regulation of actin and microtubule dynamics to control growth cone motility and promoting directional steering in axons (Hengst et al., 2009).

1.1.4 Cell adhesion molecules

Cell adhesion is fundamentally important in axon pathfinding, axon targeting and synapse formation. Information is transmitted to the growth cone through cell adhesion molecules (CAMs) that facilitate interactions with the environment. The Immunoglobulin (Ig)- superfamily members, neuronal cell adhesion molecule (NCAM) and the *Drosophila* homologue Fasciclin 2 (Fas2), were the first to be implicated in regulating cell

adhesion (Holmes and Heilig, 1999; Kamiguchi, 2007; Rutishauser et al., 1988). For instance, homophilic interactions of Fas2 are thought to be critical for the fasciculation of axons that share the same trajectory in the embryonic CNS (Lin et al., 1994). Moreover, NCAM and Fas2 regulate synapse function. NCAM for instance localizes at the developing synapse and is playing a role in synaptic plasticity (Bukalo et al., 2004; Uryu et al., 1999). Similiarly, studies at the neuromuscular junction in *Drosophila* showed that Fas2 is enriched in motor axon growth cones and their target muscles, and is involved in synapse stabilization (Schuster et al., 1996). Furthermore, Fas2 was implicated in axon guidance in the mushroom body neurons, where it is suggested to function in olfactory learning and short-term memory formation (Cheng et al., 2001).

Other CAMs have additional intracellular catalytic domains that are kinases or phosphatases. Examples are the receptor protein tyrosine phosphatase proteins such as PTP69D and *Drosophila* Leukocyte-antigen-related-like (Lar). Both have been implicated in targeting of motor axons in the *Drosophila* embryo (Desai et al., 1997; Krueger et al., 1996). Additionally, DLAR, PTP69D, PTP10Dand PTP99A contribute to midline axon guidance in the CNS through positively regulating Slit/Robo repulsive signaling (Sun et al., 2000). Mutant analyses have shown that in the absence of all protein tyrosine phosphatase proteins, non-crossing longitudinal axons do form commissures that cross the midline. These findings place tyrosine phosphorylation in the downstream cascade that regulates how a growth cone responds to midline signals (Sun et al., 2000).

The cadherin family of cell adhesion molecules are calcium-dependent adherent proteins and are structurally distinct from the other cell-adhesion receptors. The classical cadherins, such as the neural N-Cadherin (CadN), contain five cadherin repeats and play crucial roles in axon guidance, as well as stabilization of connections of axons with

their synaptic targets (Lee et al., 2001; Matsunaga et al., 1988; Poskanzer et al., 2003; Riehl et al., 1996; Shapiro et al., 1995; Yonekura et al., 2007).

1.1.5 Organization of neural maps

Once the axon has reached its designated target area, they then have to select precise locations within the target area and the appropriate postsynaptic partners among multiple potential target neurons. The formation of specific and stable contacts is essential for a fully functioning nervous system and is achieved in several succeeding steps (Holt and Harris, 1998; Huberman et al., 2010). Differential cell adhesion provides a mechanism for axons to defasciculate from the axon bundle they have traveled with and to enter the appropriate target area (Aberle, 2009). Furthermore, guidance cues acting in a gradient or at short-range allow the axon to recognize and enter a specific position in the target area (Dickson, 2002; Tessier-Lavigne and Goodman, 1996). Within the target area, to create a faithful representation of the external world, sensory neuron projections are organized into neural maps (Luo and Flanagan, 2007). Neural maps can be classified into two broad categories, continuous/topographic and discrete/convergent maps, based on differences in the anatomical organization and functional requirements (Inan and Crair, 2007; Luo and Flanagan, 2007). The organization of continuous and discrete maps is strikingly similar in vertebrate and invertebrate nervous systems (Clandinin and Feldheim, 2009; Feldheim and O'Leary, 2010; Imai et al., 2010; Sakano, 2010).

The key characteristics of continuous maps is that axonal projections in the target area maintain their spatial order relative to their neighboring neurons from the sensory area. An important example is the retinotopic map in the visual system. In a retinotopic map, to spatially preserve the visual representation, retinal neurons have to locate in the

target area in the brain in precise positions next to their neighbors from the retina (Luo and Flanagan, 2007; McLaughlin and O'Leary, 2005).

The idea of chemically guided formation of continuous retinotopic maps in the visual system goes back to Roger Sperry, who proposed that specificity of circuit formation during development is determined by molecular cues, which are expressed in gradients in the retina and the target area (Sperry, 1963). Thus, based on their position in the retina, axons of retinal neurons project to defined positions in the target field. Members of the Eph receptor tyrosine kinases and their respective ephrin ligands are expressed in a graded fashion in the developing retina and visual target areas, and have been found to provide a molecular substrate for the formation of a retinotopic map (Cheng and Flanagan, 1994; Drescher, 1997; Drescher et al., 1995). For instance, nasal and temporal retinal axons express different levels of the EphA receptor and are guided to their target areas within the tectum through differential expression of the ephrinA ligands, which establish a gradient with low expression in the anterior tectum and high expression in the posterior tectum. Temporal RGC axons, with a high expression of EphA3 receptor, are repelled by high levels of ephrinA2 and are therefore prevented from growing into the posterior tectum, but remain anteriorly. Nasal axons do not express EphA3 or at vey low levels, and are therefore allowed to enter the posterior tectum (Drescher, 1997; Feldheim et al., 2000). In the retina, a countergradient is established by the expression of ephrinA2 ligands (Hornberger et al., 1999). Retinal expression of the ephrinA2 ligand in the nasal region allows the modulation of the EphA receptor expression in these cells, thus it keeps EphA expression at low levels. This establishes an EphA gradient that allows sorting of nasal and temporal axon projections in the tectum (Drescher, 1997; Feldheim et al., 2000). Importantly, in the tectum opposing gradients of ephrinA ligands and EphA receptors are pivotal for correct branching of

retinal axons (Rashid et al., 2005). In vertebrates, the refinement of synaptic maps and elimination of inappropriate synapses is dependent on synaptic activity. This transforms developing, immature circuits into proper synaptic connections (Katz and Shatz, 1996; Huberman et al., 2008).

In contrast, in a discrete map, axons from spatially dispersed sensory neurons with the same identity project onto one location in the target field (Luo and Flanagan, 2007; Mombaerts, 2006). In the vertebrate olfactory system, olfactory receptor neurons (ORNs) are located in the olfactory epithelium and express a single odorant receptor (OR) (Mombaerts, 2006). ORNs that express the same OR, and thus convey the same odorant information, target to the same region in the target area, called olfactory bulb, which is subdivided into functional subunits called glomeruli (Sakano, 2010).

In the mouse olfactory system, it is now well established that ORs play an instructive role in ORN axon targeting to defined glomeruli (Feinstein and Mombaerts, 2004; Mombaerts, 1996). Furthermore, recent studies have provided a molecular link between OR identity and axon guidance decisions (Imai et al., 2006; Serizawa et al., 2006). Different ORs mediate different levels of cAMP, which in turn mediate differential expression of Nrp1 and Sema3A (Imai et al., 2006; Imai et al., 2009; Schwarting et al., 2004). Some ORN axons express the Nrp1 receptor and others the Sema3A ligand, thus mediating a sorting of ORN axons by repulsive axon-axon interactions. Moreover, Sema3A is also expressed in a graded fashion in the target area in the olfactory bulb, therefore establishing targeting along the anterior-posterior axis (Imai et al., 2009). Similarly, different levels of cell adhesion molecules can provide a mechanism that allows axon sorting through fasciculation of axons. For instance, adhesion molecules Kirrel2 and Kirrel3 mediate axon targeting through their differential expression in subtypes of ORNs and in distinct glomeruli in the olfactory bulb (Serizawa et al., 2006).

In contrast in *Drosophila,* ORs do not specify targeting decisions of ORN axons (Dobritsa et al., 2003). Nevertheless, targeting of subtypes of ORNs is also mediated by axon guidance molecules such as Sema-1a and its receptor plexinA that enable sorting by axon-axon interactions (Komiyama et al., 2007; Lattemann et al., 2007). This mechanism allows the formation of a coarse map that is refined by matching of axons and dendrites.

Moreover, dendrites of target neurons have been suggested to play active roles in synaptic specificity to ensure proper connectivity of ORNs and their postsynaptic partners in the developing olfactory system in *Drosophila* (Jefferis et al., 2004). In a process called dendritic targeting, dendrites help to form specific connections with presynaptic partners as they extend dendritic filopodia choosing between potential synaptic partners. Dendrites of projection neurons (PNs), originating from the CNS, form a coarse glomerular map in the target area, the antennal lobe, before ORN axons innervate this region (Jefferis et al., 2004). Thus, PN dendrites and ORN axons initially target independently to appropriate regions in the antennal lobe. However, additional molecular mechanisms ensure the matching of pre- and postsynaptic partners.

The conserved family of transmembrane proteins called Teneurins have been reported to play a role in circuit assembly in the nervous systems of vertebrates and invertebrates (Tucker and Chiquet-Ehrismann, 2006; Tucker et al., 2007; Young and Leamey, 2009). Moreover, in *Drosophila,* differential expression of two Teneurins, *ten-a* and *ten-m,* mediates homophilic interactions between distinct PN and ORN subtypes, thus regulating the matching of pre- and postsynaptic partners in the antennal lobe (Hong et al., 2012).

The organization of neuronal projections into sensory maps allows the correct representation of the external world. However, to enable parallel information processing,

target areas are organized into synaptic subunits, such as layers. This general principle of layer-specific organization is used in many brain areas such as the cerebellum, cerebral cortex, the hippocampus or the visual system (Holt and Harris, 1998; Huberman et al., 2010).

Thus far, studies concerning the development of neural maps allowed the identification of the underlying mechanisms of axon targeting. However, our understanding of the logic and molecular and cellular mechanisms that control layer-specific axon targeting is much less advanced. To study the underlying mechanisms of axon targeting into layered synaptic subunits, the visual system provides a powerful model.

1.2 The visual system as a model to study layer-specific axon targeting

The organization of visual representation in a retinotopic map is pivotal for maintaining topographic information about the external world during processing in deeper brain regions. To enable parallel information processing, such as motion detection and color vision, the visual target areas are further organized into layers. Moreover, during the development of a precise map in the visual system, organization of neuronal processes into distinct layers ensures the correct wiring of different types of neurons, as it allows to bring partner neurons into spatial proximity thus minimizing the number of possible synaptic partners (Huberman et al., 2010).

The vertebrate and fly visual systems consist of many layered structures (Huberman et al., 2010). Furthermore, over the past decades, studies revealed that they share common molecular mechanisms and strategies for correct circuit assembly (Sanes and Zipursky, 2010).

1.2.1 The visual system of vertebrates

The adult vertebrate retina consists of nuclear layers containing the cell bodies of neurons, and neuropil-like plexiform layers that only contain neuronal processes; the latter can be divided into sub-layers based on the innervation pattern of distinct cell types (Masland, 2001b; Mumm et al., 2005; Sanes and Zipursky, 2010) (Figure 3). Situated in the outer nuclear layer are the light-sensitive photoreceptor cells, the rods and the cones. Rods detect contrast in low light conditions, while cones are required for the perception of color (Masland, 2001a). They send processes into the first neuropil layer, the outer plexiform layer (OPL). The inner nuclear layer contains the cell bodies of interneurons called horizontal, amacrine and bipolar cells (Masland, 2001a). The latter connect the OPL with the inner plexiform layer (IPL) and convey visual information to the retinal ganglion cells (RGCs). Cell bodies of RGCs are located in the ganglion cell layer. With their dendritic arborizations in the IPL, RGCs collect the visual information and through their axons relay this information to higher visual processing centers in the brain. Specifically, they connect with targets in the midbrain (generally referred to as optic tectum in birds or superior colliculus in mammals) and the lateral geniculate nucleus (LGN) in the dorsal thalamus, which then transmits information to visual cortex areas (Masland, 2001b). These areas are also highly layered, thus providing the structural basis for parallel information processing.

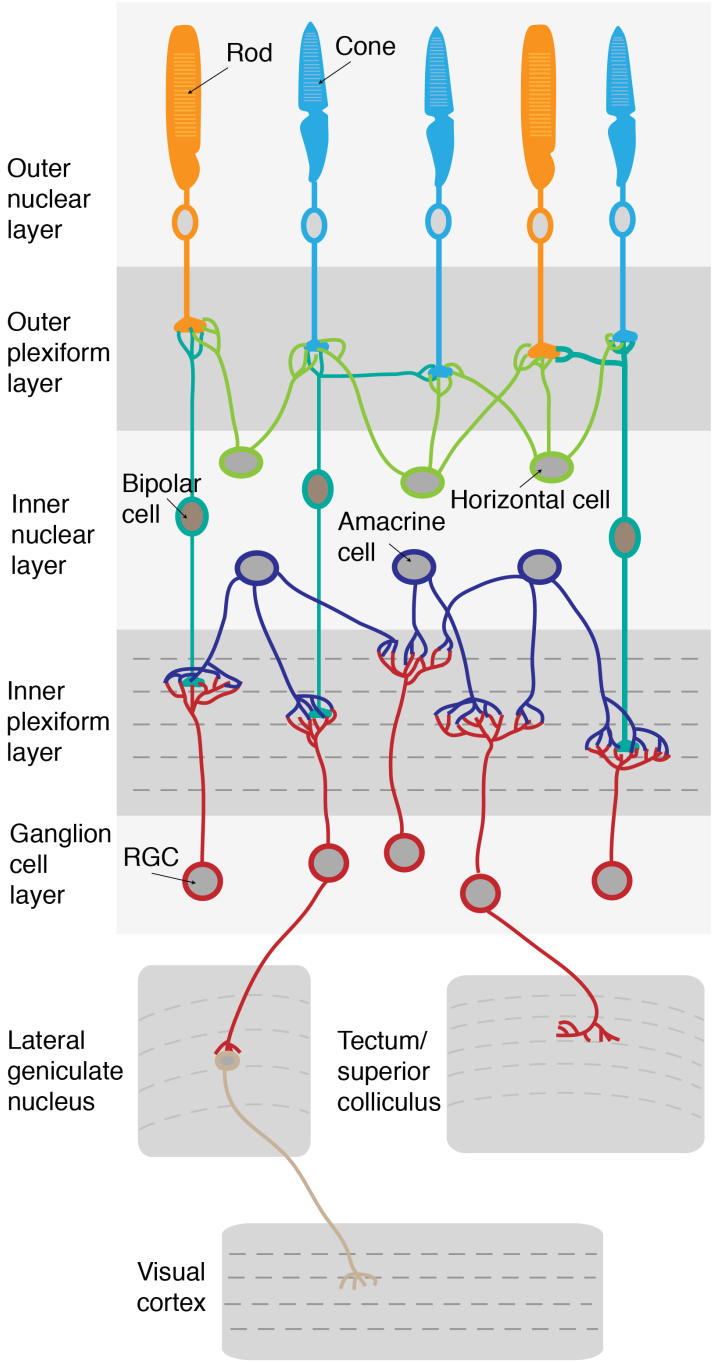

Figure 3. The adult visual system of higher vertebrates. It consists of the retina, the lateral geniculate nucleus, the tectum/superior colliculus and the visual cortex. The retina is subdivided into nuclear layers that contain the cell bodies, and plexiform layers that consist of projections and synapses. The outer nuclear layer contains the light-sensitive photoreceptor cells, the rods and the cones. They target into the first neuropil layer, the outer plexiform layer (OPL). The inner nuclear layer contains the cell bodies of horizontal, amacrine and bipolar cells. Bipolar cells connect the OPL with the inner plexiform layer (IPL). The cell bodies of retinal ganglion cells (RGCs) are located in the ganglion cell layer. They arborize in the IPL and send axons into the tectum /superior colliculus and the lateral geniculate nucleus (LGN). Cells from the LGN send processes to the visual cortex. Modified from Sanes and Zipursky, 2010.

1.2.2 The *Drosophila* visual system

In the *Drosophila* visual system, neurons form stereotypic projections during development that result in a highly precise and invariant connectivity pattern in the adult fly (Clandinin and Feldheim, 2009; Hadjieconomou et al., 2011b; Sanes and Zipursky, 2010). Visual circuit development in *Drosophila* is thought to be genetically hardwired (Hiesinger et al., 2006). Thus, it provides a suitable model system for the identification of the underlying molecular mechanisms that mediate the establishment of neuronal circuits. In addition, the availability of genetic tools with single-cell resolution and for functional manipulations makes it a strong model to study as to how layers are established.

The adult visual system of *Drosophila* consists of the compound eye and four optic ganglia namely, lamina, medulla, lobula and lobula plate (Figure 4). The compound eye is composed of an array of approximately 800 ommatidia, each containing eight photoreceptor cells (R-cells, R1-R8) arranged in a stereotypic pattern. R-cells are divided into three classes based on their rhodopsin expression, as well as their projection patterns (Clandinin and Zipursky, 2002). R1-R6 cells mediate motion detection and express the rhodopsin Rh1, which is sensitive to a broad spectrum of visible light (Ostroy et al., 1974; Rister et al., 2007). R7 cells express Rh3 and Rh4 rhodopsins that detect light in the ultraviolet range, and R8 cells express green and blue light sensitive Rh5 and Rh6 rhodopsins (Montell et al., 1987; Papatsenko et al., 1997; Salcedo et al., 1999). Both R7 and R8 neurons are involved in color detection (Morante and Desplan, 2008) and recently have been also implicated in orientation behavior (Rister et al., 2007). R-cell axons project into the optic lobe with remarkable precision. In the adult visual system, R1-R6 axons terminate in the lamina, and form synaptic connections with lamina

neurons L1-L3, amacrine cells and centrifugal interneurons in so-called lamina cartridges (Fischbach and Dittrich, 1989).

The medulla is subdivided into columnar units and 10 distinct layers. The distal M1 – M6 medulla layers are innervated by R8 and R7 axons and the lamina neurons L1-L5 in a layer-specific manner (Figure 4) (Fischbach and Dittrich, 1989). The layers in the proximal medulla are implemented in motion processing (Borst and Euler, 2011). There are at least 57 medulla neuron subtypes (Meinertzhagen and Sorra, 2001). Medulla neurons and numerous ascending higher order neurons branch within one or more of these 10 layers in defined patterns (Fischbach and Dittrich, 1989). For instance, medulla neurons that connect the distal medulla and the lobula are transmedullary (Tm) neurons, while TmY neurons connect the medulla with the lobula and lobula plate. Ascending T1 neurons connect the medulla and the lamina and for ascending neurons such as T2 neurons connect the proximal medulla and the lobula. Finally, C2 neurons branch in the medulla and the lamina.

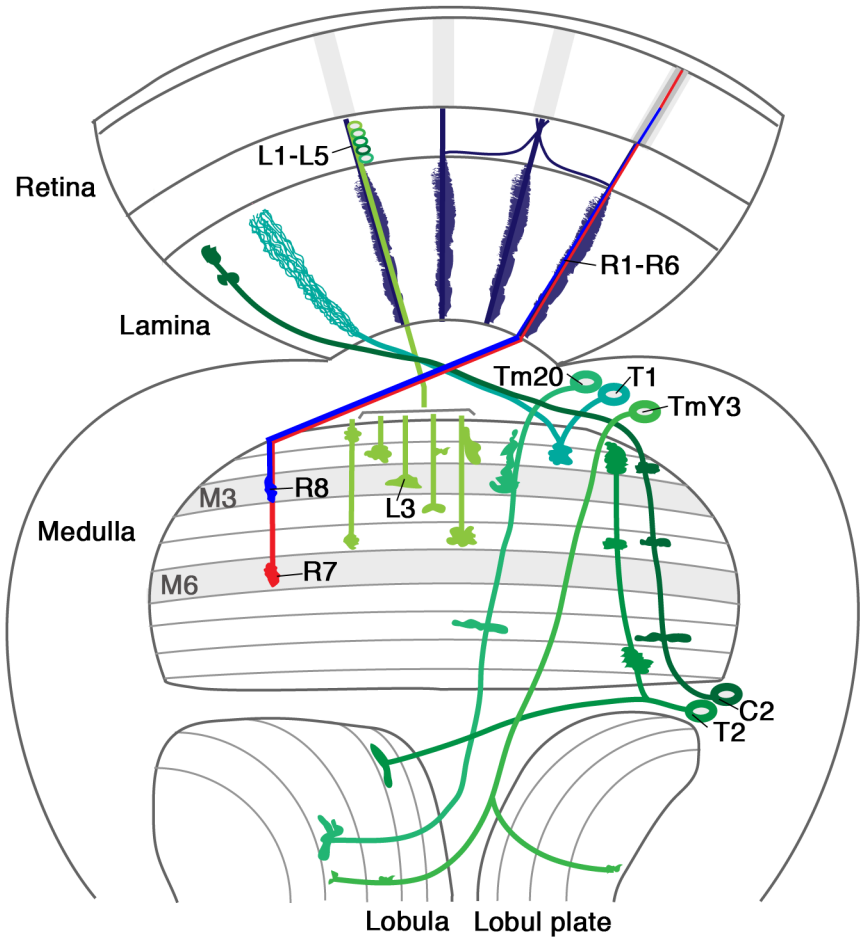

Figure 4. Layer- and column-specific connections in the adult fly visual system. The optic lobe consists of four ganglia, the lamina, medulla, lobula and lobula plate. In the lamina, R1-R6 axons and lamina neurons (L1-L5) form columnar synaptic units, called cartridges. The medulla is organized into columns and layers. R8 and R7 axons, as well as lamina and medulla neurons innervate distinct layers in the medulla neuropil. R8 and R7 axons terminate in the M3 and M6 layers, respectively.

1.2.3 Retinotopic map formation during development

During development, R-cell axons project from the retina to the target area in the optic lobe in a series of interdependent steps. Several mechanisms ensure the formation of a precise projection pattern. Eye development is initiated at the 3rd instar larval stage. An indentation within the eye imaginal disc, called morphogenetic furrow, sweeps from posterior to anterior. Morphogens such as Decapentaplegic (Dpp) and Hedgehog (Hh)

initiate specification and differentiation of R-cells (Borod and Heberlein, 1998; Dominguez and Hafen, 1997; Heberlein et al., 1993; Pignoni and Zipursky, 1997).

R-cell axons subsequently extend into the optic lobe and induce the development of the lamina. They release Hh and Spitz, a fly homolog of the vertebrate Epidermal growth factor (EGF), to sequentially induce lamina neuron proliferation and differentiation (Clandinin and Zipursky, 2002; Huang and Kunes, 1996; Huang et al., 1998; Umetsu et al., 2006). Moreover, Hh signaling promotes the expression of Single-minded (Sim), a basic helix-loop-helix Per-Arnt-Sim (bHLH-PAS) protein, in lamina neurons to mediate their incorporation into columns (Umetsu et al., 2006). These signals ensure the matching of incoming axons and sets of developing neurons in the target field and allow the formation of a retinotopic map along the anterior-posterior axis. In addition, DWnt4, a secreted ligand of the Wnt family, plays a role in establishing R-cell projections along the dorso-ventral axis (Sato et al., 2006).

During larval development, R8 axons are thought to extend first to pass through the lamina and terminate in the medulla neuropil. R1-R6 neurons from the same ommatidium take the same path as R8 axons and terminate between rows of glial cells in the lamina, which provide a stop signal to the incoming R1-R6 axons (Poeck et al., 2001). R7 axons project last and terminate beneath R8 axons in the medulla neuropil.

1.2.4 R1-R6 axon targeting in the lamina

To enable correct retinotopic map formation, visual input is organized in columns with each column representing a point in the visual space. However, as a consequence of the curvature and structure of the fly eye, each subtype of R1-R6 cells that see the same point in space are positioned in six neighboring ommatidia. Therefore, to convey the same information, R1-R6 cells from one ommatidium have to innervate different

lamina cartridges according to their orientation (Clandinin and Zipursky, 2000; Hadjieconomou et al., 2011b). Initially, R1-R6 axons from the same ommatidium leave the optic stalk and project towards the lamina as a fascicle. During early pupal development, they defasciculate and R1-R6 cells from one ommatidium innervate different lamina cartridges. This sorting of axons during the process called neural superposition allows R-cells, which perceive the same optical information, to connect with the correct target neurons in the lamina.

The receptor protein tyrosine phosphatase protein Lar and the scaffolding protein Liprin-α are suggested to act in R-cells mediating the exit from the original fascicle in interaction with the cadherin cell adhesion molecule CadN (Choe et al., 2006; Prakash et al., 2005). In addition, the receptor tyrosine phosphatase PTP69D is required for ganglion specific targeting to the lamina neuropil (Garrity et al., 1999). In PTP69D mutants, R1-R6 project through the lamina and terminate in the medulla neuropil. Furthermore, CadN mediates homophilic interactions between growth cones of R1-R6 cells and lamina neurons L1-L5 (Prakash et al., 2005). In addition, cartridge-specific targeting of R1-R6 axons requires the non-classical cadherin cell adhesion molecule Flamingo (Fmi), which provides a sorting mechanism through level-dependent homophilic interactions between axons (Chen and Clandinin, 2008; Lee et al., 2003).

1.2.5 Layer-specific targeting in the medulla

The medulla represents the largest and most complex ganglion in the optic lobe (Fischbach and Dittrich, 1989; Takemura et al., 2008). The medulla is organized into vertically arranged columns that represent visual information of a precise point in space. To enable parallel information processing, such as encoding color or motion, the me-

dulla is further subdivided into 10 layers (Meinertzhagen and Hansen, 1993; Fischbach and Dittrich, 1989).

Layer-specific connectivity is achieved with enormous precision in a two-step layer selection process during pupal development (Ting et al., 2005) (Figure 5). R8 and R7 axons start to extend sequentially into the medulla neuropil from the late 3rd instar larval stage onwards and terminate closely adjacent to each other in their correct columns. During the early layer selection phase between 17 hours – 40 hours after puparium formation (APF), R-cell growth cones segregate into distinct temporary layers in the medulla neuropil. R8 axons are located at the border of the medulla neuropil, while R7 axons terminate deeper in the medulla neuropil (Ting et al., 2005). This process of initial targeting enables the synchronization of ingrowing photoreceptor axons and the coordination with the development of target neurons.

During the late phase of layer selection starting at mid-pupal stages (~50 hours APF) growth cones regain motility and progress to their final target layers. R8 axons project past the L1/L2 lamina neuron arbors and terminate in their final layer M3. This layer also contains arborizations of the lamina neurons L3 (Fischbach and Dittrich, 1989; Takemura et al., 2008). R7 growth cones extend to the final R7 recipient layer M6. Finally at adult stages, R8 growth cones consolidate into axonal terminals in the M3 layer, whereas the R7 terminals are located in the M6 layer (Clandinin and Zipursky, 2002; Fischbach and Hiesinger, 2008; Morante and Desplan, 2004). Consequently, all visual information converges in the medulla, indirectly from R1-R6 axons via the lamina neurons and directly from the R8 and R7 axons.

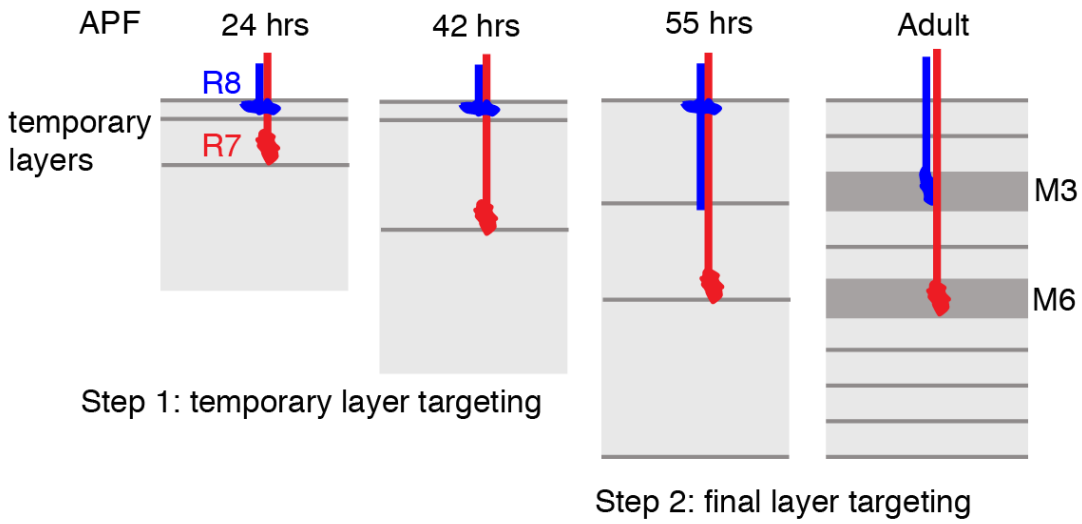

Figure 5. Two-step layer-specific R8 and R7 axon targeting during pupal development. R8 and R7 axons target to their final layers in a two-step targeting process. Initially, during the first half of pupal development, R8 axons stay in their temporary layer at the medulla neuropil border, while R7 terminate deeper in the medulla neuropil. During the initiation of the second targeting step, R8 axons regain motility and proceed to their final target layer M3, whereas R7 innervate the M6 layer. Adapted from Hadjieconomou et al., 2011b.

1.2.6 Molecules involved in axon targeting to columns and layers in the medulla

Several guidance determinants have been identified to regulate targeting of R-cell axons to layers and columns in the medulla. These have distinct, as well as overlapping functions in R8 and R7 axon targeting (Figure 6). The cell adhesion molecules Flamingo (Fmi), Golden goal (Gogo) and Capricious (Caps) are crucially required for correct columnar and layer-specific targeting of R8 axons.

The leucine-rich repeat cell adhesion molecule Caps is the only molecule identified so far to be differentially expressed in R-cells and the target neurons in the corresponding medulla layers (Shinza-Kameda et al., 2006). It is specifically expressed in R8 axons and the target layers M1-M4. *Caps* is required in R8 axons for proper layer selection and topographic projection, as removal of *caps* leads to severe targeting defects.

Ectopic expression of Caps in R7 neurons, which normally do not express Caps, redirects their axons in the R8 recipient layer M3.

The transmembrane receptor Gogo and the non-classical cadherin cell adhesion molecule Fmi are required in R8 axon targeting through regulating axon-target interactions (Hakeda-Suzuki et al., 2011; Tomasi et al., 2008). Removal of either *gogo* or *fmi* leads to similar defects with R8 axons stalling at the distal medulla neuropil border. Fmi and Gogo are dynamically expressed during development in all R-cell subtypes including R8 and R7 axons. Fmi is further expressed broadly in the medulla, suggesting a role in targeting of afferent and target neuron axons through homophilic interactions. Gogo and Fmi have been proposed to mediate R8 inter-axonal repulsion to maintain correct spacing, but also R8 axon-target interactions, therefore enabling R8 axons to find their correct target columns and layer in the medulla (Hakeda-Suzuki et al., 2011).

In addition to the above mentioned retrograde signaling during targeting, where incoming afferent axons are influenced by target neurons to terminate in the target region, an anterograde mechanism mediates the formation of neuronal connections and is likewise essential (Bazigou et al., 2007). The ligand Jelly belly (Jeb) is primarily generated by R-cells to activate Anaplastic Lymphoma Kinase (Alk) signaling in target neurons. This in turn directly or indirectly controls the expression of the cell-adhesion molecules Kin-of-Irre (Kirre), Irregular Chiasm (IrreC) and Fmi. This mechanism coordinates R-cell ingrowth with the local expression of guidance determinants in the target field, thereby in turn regulating layer-specific R8 axon targeting.

R7 axon targeting depends on the cell adhesion molecule CadN, receptor protein tyrosine phosphatases PTP69D and Lar, and the adapter protein Liprin-α (Hofmeyer et al., 2006; Lee et al., 2001; Maurel-Zaffran et al., 2001). CadN is required for R7 axon targeting to the M6 layer, as mutant analyses have shown that R7 axons that lack CadN

incorrectly innervate the R8 recipient layer M3 (Lee et al., 2001). However, ectopic expression of CadN in R8 axons does not alter layer-specificity. Furthermore, CadN is present in isoforms, however their isoform-specific function remains unclear (Nern et al., 2005; Ting et al., 2005).

The receptor tyrosine phosphatase Lar is required in R7 axons to select their appropriate target layer in the medulla (Maurel-Zaffran et al., 2001). In *Lar* mutants, R7 axons initially correctly extend to the M6 layer, but subsequently retract to the R8 recipient layer M3. This suggest a role in stabilizing synaptic connections between afferent and target processes. This function of Lar is independent of its phosphatase activity, but requires the wedge domain that allows recruitment of for instance Liprin-α or CadN (Hofmeyer et al., 2006).

In addition, columnar restriction of R7 axon projections is crucial for information processing. This mechanism is referred to as tiling, by which processes of adjacent same-type neurons fill a neuropil in a complete, yet non-overlapping manner (Ting et al., 2007). Loss of the components of the signaling pathway via Activin/TGF-ß receptor Baboon (Babo), its ligand Activin, the downstream effectors dSmad2 or Importin-α3 (Imp-α3) cause R7 axons to invade neighboring columns (Ting et al., 2007). In addition, a member of the Ig superfamily of CAMs, Turtle (Tutl), regulates the tiling of R7 axons and acts in parallel to the Activin pathway (Ferguson et al., 2009). Tutl mediates homophilic repellent cell-cell interactions in R7 axons, therefore restricting them to single medulla columns.

CadN is repeatedly used for layer-specific targeting in the medulla. Its ubiquitous expression in the medulla neuropil suggests that processes of target neurons employ this guidance determinant for targeting. Lamina neurons innervate specific layers in the medulla neuropil independently of R-cell axon targeting events (Nern et al., 2008). How-

ever, similarly to R-cell axons, axonal projections of lamina neurons are also guided to distinct medulla columns and layers by using CadN (Nern et al., 2008). In mutants for *CadN*, lamina neurons L1, L3 and L4 project aberrantly to deeper medulla layers. Lamina neurons L5 require *CadN* for the branch formation in the M1/M2 layers, whereas in the M5 layer it is required for tiling to a single column. In addition, Dscam2 was recently identified in regulating tiling of lamina neurons L1 (Millard et al., 2007).

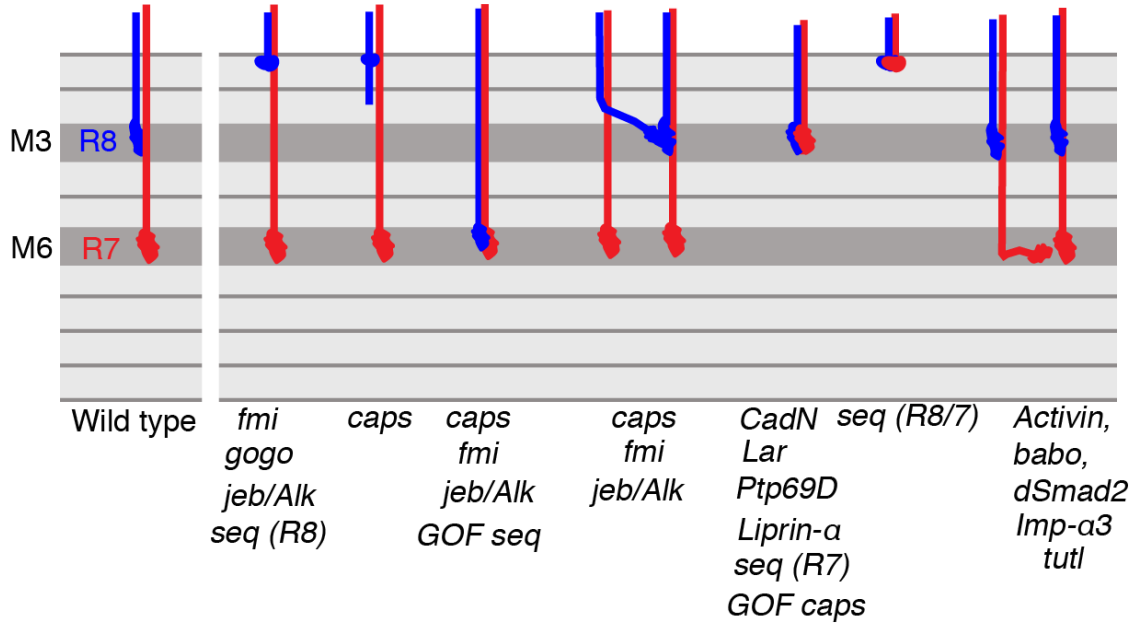

Figure 6. Molecules involved in column- and layer-specific R7 and R8 axon targeting in the medulla. Layer- and column-specific targeting of R8 and R7 axonsis regulated by distinct and partially overlapping molecular programs. For instance loss of *fmi, gogo, caps, jeb/Alk*, and *seq* or overexpression of *seq* lead R8 axons stalling at the medulla neuropil border, extend axon deeper into the medulla or extending into adjacent coumns. For R7 axon targeting loss of *CadN, Lar, Ptp69D, and Liprin-a* or ectopic expression of *caps* leads to incorrect innervation of the R8 recipient layer M3. Loss of *seq* in R7 leads to a similar phenotype, while loss in R8 and R7 causes axons to terminate at the medulla neuropil border. Tiling of R7 axons depends on autocrine signaling mediated by *Activin, babo, dSmad2*, and *imp-a3*, and on repellent homotypic interactions mediated by tutl. Adapted from Hadjieconomou et al., 2011b.

1.3 Strategies for layer-specific targeting in the visual system

Given the complexity of the nervous system and the precision, with which pre- and postsynaptic cells match during neuronal wiring, it is striking as to how a limited number of guidance molecules can orchestrate this process. Several general strategies have been identified that regulate layer-specific axon targeting in the visual system.

Firstly, pre- and postsynaptic neuron subsets can express a combinatorial set of homophilic cell surface molecules that promote the recognition and stabilization of contacts between matching processes. Several molecules have been identified that provide instructive information for layer selection. For instance, the IPL in the vertebrate retina is divided into five sub-layers containing synapses of amacrine and bipolar cells as well as RGCs (Masland, 2001b; Mumm et al., 2005). The cell type specific expression of four immunoglobulin superfamily adhesion molecules - Dscam, DscamL1, Sidekick-1 and Sidekick-2 determine the segregation of processes from subsets of bipolar, amacrine and RGCs into distinct layers in the IPL in the developing vertebrate retina (Yamagata and Sanes, 2008). In *Drosophila*, the leucine-rich repeat protein Capricious (Caps) may play an analogous role in promoting homophilic interactions to stabilize connections within correct columns and layers in R8 axons (Shinza-Kameda et al., 2006). This mechanism provides crucial information to correctly match pre- and postsynaptic partners.

In addition, both cell adhesion molecules and specific ligand-receptor interactions contribute to layer-specific axon targeting. Yet most guidance determinants are expressed ubiquitously in the target field. This leads to the question as to how they can provide layer-specific positional information. As a second mechanism, recent studies have shown that transcriptional control of temporal responsiveness of axons provides layer-specific information using a ubiquitously expressed cell adhesion molecule. In

Drosophila, the zinc finger transcription factor *Sequoia* (*Seq)* controls R8 and R7 axon targeting (Petrovic and Hummel, 2008). During axon targeting Seq expression in R8 and R7 cells is highly dynamic and correlates with the targeting events to their recipient layers M3 and M6, respectively. Thus, Seq regulates their "targeting competence", which is the temporally restricted ability of the growth cone to actively interact with the target field via temporal regulation of CadN expression levels. Loss of *seq* expression leads to mistargeting of R7 axons to the R8 recipient layer M3. In contrast, prolonged *seq* expression results in co-innervation of R8 and R7 axons in the layer M6. Therefore, Seq provides a temporally restricted targeting competence for the extending growth cones that controls synaptic layer selection of R8 and R7 axons.

In addition, coupling of the regulation of cell fate and the expression of axon guidance molecules by the same transcriptional control provides an efficient mechanism to regulate neural circuit assembly. The NF-YC subunit of the heterotrimeric transcription factor NF-Y (nuclear factor Y) regulates R7 layer-specific axon targeting by actively suppressing the R8 cell fate and axon targeting program (Morey et al., 2008). The R8 cell fate program is executed by the transcription factor Senseless (Sens). Sens in turn regulates Caps expression directly through binding to its promotor, therefore mediating R8 axon targeting to the M3 layer. However, both the absence of Sens and the presence of R7 cell fate determinant Prospero (Pros) are required and sufficient for correct layer-specific targeting of R7 axons.

Thirdly, the action of repellent guidance cues is an equally strong force in layer-specific targeting through signals that drive axons away from improper synaptic layers. A repulsive mechanism was reported to mediate layer-specificity in the vertebrate retina. RGCs, amacrine cells and bipolar cells establish layer-specific neurite arborizations to form functional neuronal circuits within distinct sub-layers in the IPL. Recent find-

ings demonstrated that the membrane-bound Semaphorin family member Sema6A controls layer-specific targeting via repulsive signaling through its receptor PlexinA4 (PlexA4) in the IPL of the mouse retina (Matsuoka et al., 2011). Sema6A and PlexA4 are expressed in complementary layers therefore segregating neurites into layers through repulsion.

In the tectum, the repulsive Slit/Robo guidance system has been implicated in guidance of RGC axons to defined layers. In zebrafish the Slit/Robo signaling has been proposed to mediate layer-specificity. RGC axons that express Robo2 respond to tectum-derived Slit1, which is accumulated by Collagen IV in the basement membrane at the surface of the optic tectum, thus positionally restricting their arborizations (Xiao et al., 2011). However, Slit1 is not localized in a layer-specific pattern but is suggested to provide layer-specificity through a spatial gradient. In a similar way, the secreted glycoprotein Neural epidermal growth factor-like (Nel) is suggested to act as an extracellular layer-specific positional cue (Jiang et al., 2009). Nel is expressed by target neurons and is layer-specifically localized in the developing chick optic tectum. These layers are normally not innervated by retinal axons, therefore Nel is suggested to act as an inhibitory guidance cue for retinal axons. Thus, it provides layer-specific positional information by excluding retinal axons from specific layers.

Taken together, the following mechanisms have been uncovered to mediate layer-specificity: (i) matching of pre-and postsynaptic partners through a combinatorial code of cell-adhesion molecules, (ii) transcriptional control of responsiveness to ubiquitous adhesion molecules and (iii) exclusion from distinct layers via repulsion. However, these so far identified mechanisms are unlikely to provide a complete picture, as they leave important issues open. One such central question is for instance, as to how axons

can precisely target to a given layer at a specific position. Theoretically, layer-specific axon targeting could also be mediated by an attractive mechanism, for instance by the layer-specific expression of attractive guidance determinants providing positional information to axons that express the respective receptor.

1.4 The Netrin, Frazzled and Unc-5 guidance system

1.4.1 Roles of Netrins and their receptors beyond the midline

The Netrin family of secreted ligands plays fundamental and diverse roles as chemotopic guidance cues during development of the nervous system of vertebrates and invertebrates (Harris et al., 1996; Hedgecock et al., 1990; Ishii et al., 1992; Kennedy et al., 1994; Serafini et al., 1994). Apart from their prominent role in axon pathfinding at the midline, they are pivotal for motor axon targeting in the *Drosophila* embryo (Kolodziej et al., 1996). The attractive Fra receptor mediates motor axon targeting to the Netrin expressing dorsal muscles 1 and 2 in the periphery (Kolodziej et al., 1996; Mitchell et al., 1996). By contrast, the repulsive Unc-5 receptor functions to prevent motor neuron axons from innervating inappropriate muscles (Labrador et al., 2005).

Furthermore, Netrins have been implicated in organizing dendritic targeting of leg motor neurons within the CNS (Brierley et al., 2009; Furrer et al., 2003; Mauss et al., 2009). Midline-derived Netrin and Slit guidance cues are used by subtypes of Fra and Robo expressing motor neurons for the precise positioning of their dendrites into discrete territories with respect to the CNS midline (Brierley et al., 2009; Mauss et al., 2009).

Outside the nervous system, they engage in diverse functions such as cell migration during the formation of the vasculature and the development of the heart and lung (Adams and Eichmann, 2010). For instance, Unc-5 is required for Netrin-mediated formation of the *Drosophila* heart, as *unc-5* mutant embryos fail to form a properly established heart lumen (Albrecht et al., 2011).

1.4.2 Structural organization of Netrin, DCC and Unc-5

Netrins are secreted chemotopic guidance molecules structurally related to Laminins (Harris et al., 1996; Ishii et al., 1992; Kennedy et al., 1994; Serafini et al., 1994). Netrins/Unc-6 contain a laminin N-terminal domain (Lam^{NT}) and three Laminin-type epidermal growth factor (EGF)-like repeats (Yurchenco and Wadsworth, 2004). These also constitute the binding sites for the DCC and Unc-5 receptors (Geisbrecht et al., 2003; Kruger et al., 2004; Lim and Wadsworth, 2002). Furthermore, the C-terminal Netrin-like domain (NTR) is not homologous to Laminins, but contains several repeats of basic residues that are for instance found in the immune system complement C345 protein family and also in tissue inhibitors of metalloproteases (Bányai and Patthy, 1999; Ishii et al., 1992).

DCC and Unc-5 are single-pass transmembrane proteins. The DCC extracellular region contains four immunoglobulin (Ig) repeats and six type III fibronectin (Fn) domains (Keino-Masu et al., 1996). The extracellular region of Unc-5 is composed of two Ig domains and two thrombospondin (TSP) type I domains (Leonardo et al., 1997; Leung-Hagesteijn et al., 1992). DCC can bind Netrin with the 4^{th} and 5^{th} Fn III domains, whereas Unc-5 requires each Ig domain for binding (Geisbrecht et al., 2003).

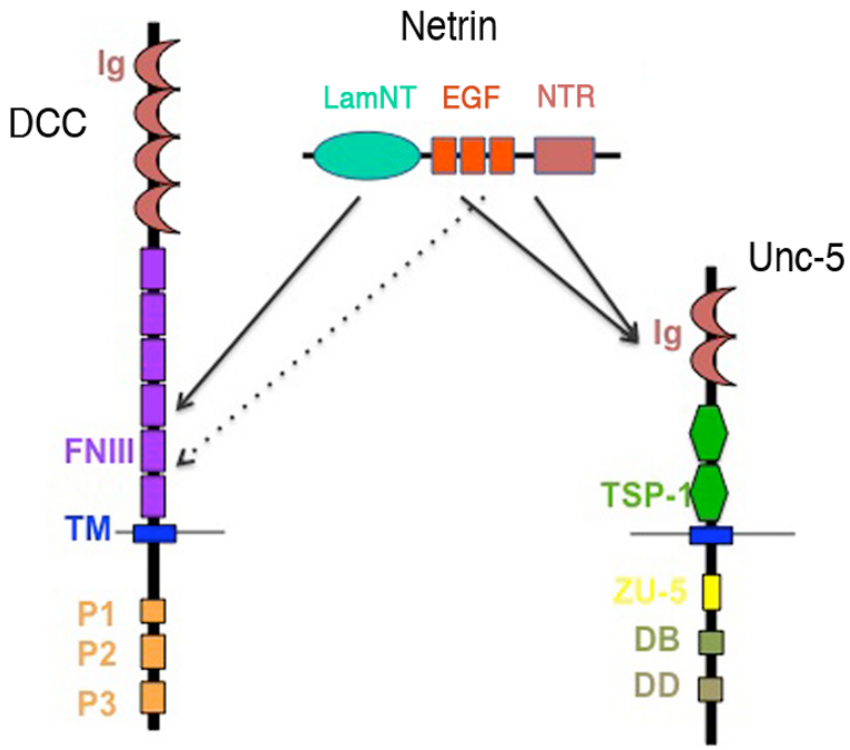

Figure 7. Interaction of Netrin with DCC and Unc-5. Netrin interacts with DCC through binding of its N-terminal Laminin domain (Lam^{NT}) to the 4th Fn III domain of DCC. The Laminin-type EGF repeats are suggested to bind to the 5th Fn III domain of DCC. With Unc-5, Netrin interacts by binding to each Ig with its EGF-like repeats and the C-terminal Netrin-like domain (NTR). Schematic adapted from Kruger et al., 2004.

1.4.3 Downstream signaling of Netrins and their receptors DCC and Unc-5

The cytoplasmic domains of DCC and Unc-5 are pivotal in both recruiting and interacting with signaling as well as adapter proteins. Kinases are implicated in Netrin mediated signaling. For instance, upon DCC activation through Netrin, ERK2, a member of the mitogen activated protein kinase (MAPK) family, binds to the conserved intracellular P1 domain, and subsequently activates MAPK signaling components (Forcet et al., 2002; Ma et al., 2010). This provides a mechanism for the regulation of the cytoskeleton by small GTPases of Rac, Cdc42 and RhoA families (Antoine-Bertrand et

al., 2011; Li et al., 2006; Li et al., 2002; Picard et al., 2009). In addition, DCC recruits components of the translational machinery to the cell membrane (Tcherkezian et al., 2010). This regulation of protein synthesis is also mediated through the P1 domain of DCC likely by ERK2 activation of translational components (Herbert et al., 2002; Tcherkezian et al., 2010).

The focal adhesion kinase (FAK) is constitutively bound to the intracellular domains of DCC and Unc-5. For Netrin-mediated attraction, DCC and FAK are phosphorylated, which in turn leads to the recruitment Src and Fyn tyrosine-protein kinases and subsequent downregulation of RhoA activity, but upregulation of Rac1 and Cdc42 (Antoine-Bertrand et al., 2011). This in turn affects the cytoskeleton dynamics by positively regulating filopodia and lamellipodia extensions (Wen and Zheng, 2006).

Through the adapter protein Nck and Trio, DCC can also activate Rac1 thus affecting lamellipodia extensions (Barallobre et al., 2005). Furthermore, an increase of levels of the second messenger cAMP mediates Ca^{2+} influx which also activates Rac1 and Cdc42 (Round and Stein, 2007). Interaction of DCC and Unc-5 effect repulsion through decreased cAMP levels and thus prevented Ca^{2+} influx that in turn activates RhoA (Nishiyama et al., 2003). RhoA affects stress fiber formation and induces actin disassembly. Moreover, Netrin mediates repulsion through phosphorylation of the Unc-5 receptor and the FAK and Src kinases. Recent studies identified that Unc-5a can activate RhoA in the leading edge of outgrowing neurites, thus affecting outgrowth (Picard et al., 2009).

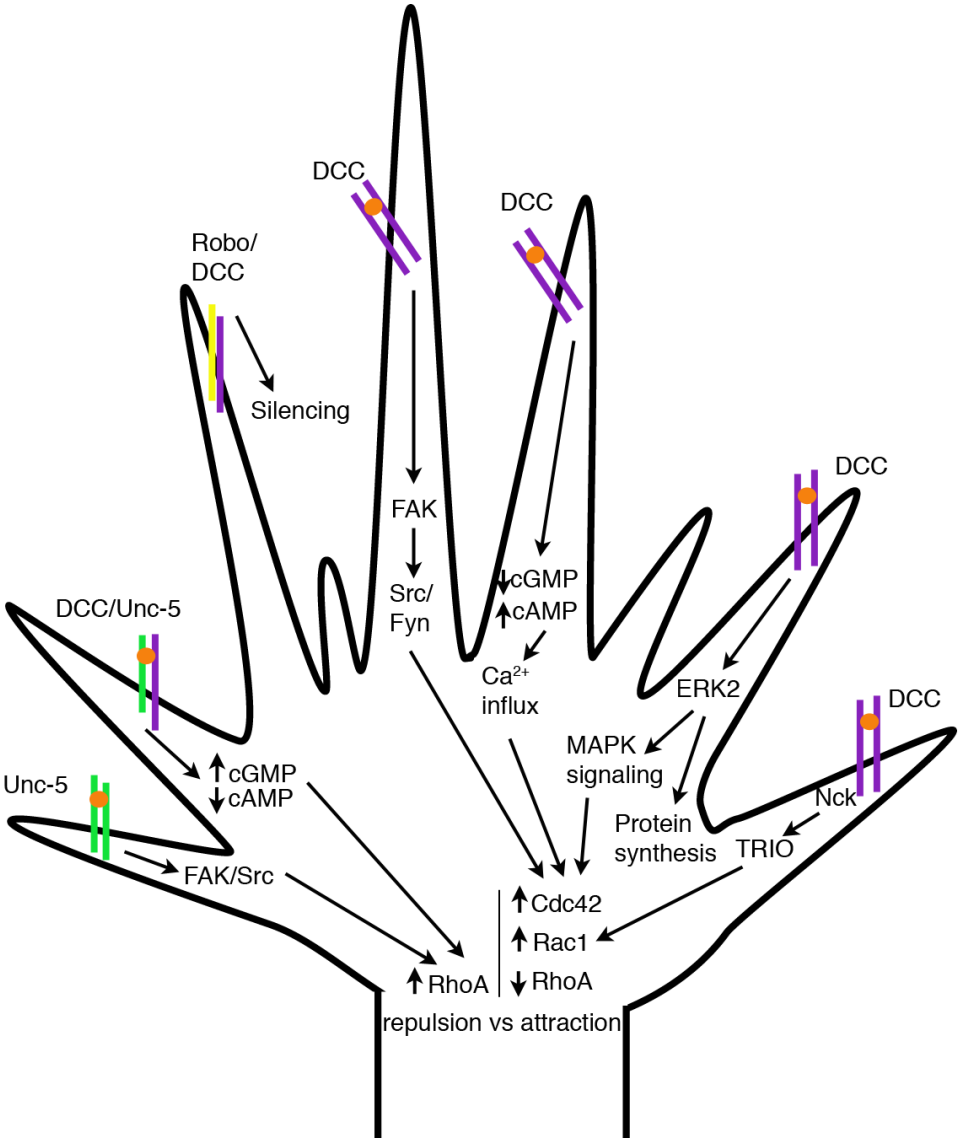

Figure 8. Signaling pathways downstream of DCC and Unc-5 receptors. The focal adhesion kinase (FAK) is constitutively bound to the intracellular domains of DCC. Upon Netrin signaling, FAK is phosphorylated and recruits Src and Fyn tyrosine-protein kinases. This results in an upregulation of Cdc42 and Rac1 GTPases and downregulation of RhoA activity. This affects the cytoskeleton by positively regulating filopodia and lamellipodia extensions thus mediating attraction. Unc-5 and FAK phosphorylation results in an upregulation of RhoA mediating repulsion. DCC activation through Netrin leads to ERK2 phosphorylation and subsequent activation of MAPK signaling components resulting in the phosphorylation of downstream regulators of the cytoskeleton. In addition, regulation of protein synthesis is also mediated through DCC binding to ERK2. Upon Netrin-mediated DCC activation, Nck and Trio activate Rac1. Furthermore, increased levels of the second messenger cAMP and decreased levels of cGMP mediate Ca^{2+} influx, which also activates Rac1 and Cdc42 and promotes axon outgrowth. Interaction of DCC and Unc-5 effect repulsion through decreased cAMP levels and thus prevented Ca^{2+} influx that in turn activates RhoA. Interaction of Robo1 and DCC results in the silencing of attraction. Schematic was adapted from Bradford et al., 2009.

1.4.4 Roles of Netrins and their receptors in the visual system

In the visual system of vertebrates, Netrins were identified to elicit growth cone turning of *Xenopus* retinal ganglion cells (RGCs) towards a Netrin source *in vitro* (de la Torre et al., 1997). Furthermore, Netrin-1 is secreted by cells in the optic disc in the retina and required for proper entry of RGC axons into the optic nerve (Deiner et al., 1997). In mice mutant for *Netrin-1*, many axons fail to leave the eye and grow randomly around the optic disc thus resulting in a disrupted optic nerve.

In *Drosophila,* in the 3rd instar larval optic lobe Netrins are expressed in lamina precursor cells (Gong et al., 1999). Removal of Netrins using a deficiency does neither affect R-cell axon targeting to the lamina, nor neuronal or glial differentiation of lamina precursor cells in the 3rd instar larval optic lobe. However, misexpression of Netrins in R-cells leads to severe defects such as stalling of R-cell axons in the optic stalk, while misexpression in the lamina causes incorrect axon bundle spacing (Gong et al., 1999). The attractive guidance receptor Fra is expressed in R-cell axons, as well as in the lamina. Loss of *fra* in R-cells does not lead to projection defects in the 3rd instar larva, while loss in the lamina interferes with R-cell axon innervation of lamina columns (Gong et al., 1999). As these studies only focused on R-cell axon targeting in the *Drosophila* 3rd instar larval optic lobe, it is not known as to whether Netrins and Fra could have a function at later developmental stages.

Taken together, while Netrins and their receptors have been shown to play diverse roles within the developing nervous system and beyond (Adams and Eichmann, 2010; Cirulli and Yebra, 2007; Lai Wing Sun et al., 2011), it has not been tested as to whether they could mediate layer-specific axon targeting.

1.5 Aims of the work presented in this thesis

One key question during the wiring of the nervous system is as to how matching axons and dendrites of synaptic partners find each other in the large number of different alternatives. To limit possibilities, axons and dendrites of partner neurons have to be organized in spatial proximity (Huberman et al., 2010). One strategy is to form synaptic units, such as columns or layers. In this study, the *Drosophila* visual system was used to address the question as to how layers are established during development.

The work presented here focuses on elucidating the molecular mechanism that directs axons of one sensory photoreceptor cell, the R8, into a distinct layer in the medulla, thus bringing them in the vicinity of processes of respective target partner neurons. Specifically, I have investigated the role of the Netrin, Fra and Unc-5 guidance system in this process.

Experiments described in Chapter 3 address as to which role the Fra guidance receptor plays in R8 axons for layer-specific targeting. Chapter 4 focuses on the activating Netrin ligands and their role in mediating layer-specific R8 axon targeting during development. Chapter 5 focuses on determining the mechanisms, which allow the secreted chemo-attractant molecule Netrin to be localized in a distinct layer. Furthermore, I have investigated as to whether localized Netrins are instructive for layer-specific R8 axon targeting. The results are described in Chapter 6. Chapter 7 describes preliminary data exploring the function of the repulsive Unc-5 receptor in mediating layer-specific targeting of R8 axons.

Chapter 2

Material and Methods

2.1 Genetics

Stocks were cultivated in *Drosophila* standard media at temperature of 25°C, except for RNA interference (RNAi) experiments, for which progeny were shifted to 29ºC at 24 hours after egg laying (AEL).

2.1.1 Stocks and crosses used in this study

Fra expression analysis:

- *caps-Gal4* x *UAS-cd8GFP* (*caps-Gal4:* Shinza-Kameda et al., 2006)

***fra ey$^{3.5}$-FLP* analysis:**

- *ey$^{3.5}$-FLP; FRT42D Ubi-GFP PCNA^{775}/CyO; ato-τ-myc/TM6B* x *FRT42D fra^{3}/Gla Bc*; *ato-τ-myc/TM6B* (*ey$^{3.5}$-FLP:* Bazigou et al., 2007, *fra^{3}*: Kolodziej et al., 1996)

***fra* MARCM (Lee and Luo, 1999):**

- elav-Gal4^{c155}, UAS-cd8GFP, hs-FLP^{1}; FRT42D tub-Gal80/CyO x FRT42D fra^{3}/Gla Bc; Rh6-lacZ/TM6B

***fra* gain-of-function analysis:**

- *Rh6-eGFP/CyO*; *lGMR-Gal4/TM6B* x *UAS-fra* (*UAS-fra:* Kolodziej et al., 1996)

Netrin expression analysis:

- *NetA$^{\Delta}$ B^{myc}/FM6* (*NetA$^{\Delta}$ B^{myc}*: Brankatschk and Dickson, 2006)

- *NetA$^{\Delta}$ B^{TMmyc}/FM6* (*NetA$^{\Delta}$ B^{TMmyc}*: Brankatschk and Dickson, 2006)

- NetA$^{\Delta}$ B^{TMmyc}/FM6 x cn bw/CyO;Rh6-lacZ/TM2

- *NP4151-Gal4* x *UAS-cd8GFP* (*NP4151-Gal4:* Kyoto DGRC)

- *NP0831-Gal4* x *UAS-cd8GFP* (*NP0831-Gal4:* Kyoto DGRC)

- *NP4151-Gal4* x *UAS-syt^{HA}/Y; UAS-cd8GFP/+* (*UAS-syt^{HA}*: Chou et al., 2010)

- *NP0831-Gal4* x *UAS-syt^{HA}/Y*

- *NetB$^{CPTI-000168}$* and *NetA$^{CPTI-002152}$* (Kyoto DGRC)

Flybow:

For Flybow experiments, 24 hour embryo collections were subjected to two 30 min heat shocks at 48 and 72 hours AEL in a 37 ºC water bath.

- *pGMR-Gal4; hs-mFLP5/TM6B* x *FB1.1^{260b}* (*FB1.1^{260b}* : Hadjieconomou et al., 2011a)

***fra* RNAi and Netrin expression analysis:**

- *ey$^{3.5}$-FLP; act>y^{+}>Gal4 UAS-cd8GFP/CyO* x *UAS-Dcr2, UAS-fra^{RNAi}*

(*UAS-fra^{RNAi}*: W. Joly)

- *ey-FLP; act>y^{+}>Gal4 UAS-cd8GFP/CyO* x *UAS-Dcr2, UAS-fra^{RNAi}*;

- *ey$^{3.5}$-Gal80; ey-FLP/CyO; UAS-Dcr2, UAS-fra^{RNAi}/TM6B* x *act>y^{+}>Gal4 UAS-GFP/CyO; lGMR-Gal80/TM6B (ey$^{3.5}$-Gal80*: Chotard et al., 2005; *lGMR-Gal80*: kindly provided by C. Desplan)

Netrin rescue experiments:

Mill Hill (MH)-Gal4 lines were generated in an enhancer trap Gal4 screen in our laboratory to identify drivers active in restricted cell types in the visual system (unpublished, H. Apitz, C. Chotard, L. Fereira, W. Joly, I. Salecker). Inverse PCR was used to determine P element insertion sites (H. Apitz, D. Hadjieconomou). *MH56-Gal4* represents an enhancer trap insertion into the *dpr3* locus (encoding the Ca_{2+} release activated Ca_{2+} channel modulator 2).

- *MH56-Gal4* x *UAS-cd8GFP*

- *MH56-Gal4* x *UAS-NetB*

- *MH56-Gal4* x *UAS-syt^{HA}/Y*

- *NetAB$^{\Delta}$/FM6; Rh6-lacZ/TM3* x *MH56-Gal4/Gla Bc; UAS-NetB/TM6B*;

(*UAS-NetB:* Mitchell et al., 1996, *NetAB*^{A}: Brankatschk and Dickson, 2006)

Netrin RNAi analysis:

- *ey*$^{3.5}$*-FLP; act>>Gal4 UAS-cd8GFP/CyO; Rh6-lacZ/TM6B* x *UAS-NetA*^{RNAi}*/Gla Bc; UAS-Dcr2, UAS-NetB*^{RNAi}*/TM6B* (*UAS-NetA*^{RNAi}, VDRC; *UAS-NetB*^{RNAi}, W. Joly)

- *ey-FLP; act>>Gal4 UAS-cd8GFP/CyO; lGMR-Gal80/TM6B* x *ey*$^{3.5}$*-Gal80; UAS-NetA*^{RNAi}*/Gla Bc;UAS-Dcr2, UAS-NetB*^{RNAi}*/TM6B*

- *NP4151-Gal4* x *UAS-NetA*^{RNAi}*/Gla Bc; UAS-Dcr2, UAS-NetB*^{RNAi}*/TM6B*

- *NP0831-Gal4* x *UAS-NetA*^{RNAi}*/Gla Bc; UAS-Dcr2, UAS-NetB*^{RNAi}*/TM6B*

- *MH56-Gal4* x *UAS-NetA*^{RNAi}*/Gla Bc; UAS-Dcr2, UAS-NetB*^{RNAi}*/TM6B*

- *MH919-Gal4* x *UAS-NetA*^{RNAi}*/Gla Bc; UAS-Dcr2, UAS-NetB*^{RNAi}*/TM6B*

- *MH939-Gal4* x *UAS-NetA*^{RNAi}*/Gla Bc; UAS-Dcr2, UAS-NetB*^{RNAi}*/TM6B*

- *9.9-Gal4* x *UAS-NetA*^{RNAi}*/Gla Bc; UAS-Dcr2, UAS-NetB*^{RNAi}*/TM6B*

Ectopic expression of membrane-tethered NetB:

- *MH919-Gal4* x (a) *UAS-cd8GFP*; (b) *UAS-NetB*^{cd8}*/Gla Bc* (*UAS-NetB*^{cd8}: this study, K.Timofeev)

- *MH939-Gal4* x (a) *UAS-cd8GFP*; (b) *UAS-NetB*^{cd8}*/Gla Bc*

- *MH728-Gal4* x (a) *UAS-cd8GFP*; (b) *UAS-NetB*^{cd8}*/Gla Bc*

- *ap-Gal4* x (a) *UAS-cd8GFP*; (b) *UAS-NetB*^{cd8}*/Gla Bc; Rh6-lacZ/TM6B*

- *NP1086-Gal4* x *UAS-cd8GFP* (*NP1086-Gal4*: Kyoto DGRC)

- *NP1086-Gal4* x *UAS-NetB*^{cd8}

- *MH502-Gal4/CyO; UAS-cd8GFP/TM6B (MH502-Gal4* is inserted into *Oatp30B*, encoding the Organic anion transporting polypeptide 30B)

- *ey*$^{3.5}$*-Gal80; MH502-Gal4/CyO;UAS-cd8GFP/TM6B* x *CyO/Gla Bc; lGMR-Gal80*

- *ey*$^{3.5}$*-Gal80; MH502-Gal4/CyO;UAS-cd8GFP/TM6B* x *UAS-Net*^{cd8}*/TM6B*

- *ey$^{3.5}$-Gal80; MH502-Gal4/Gla Bc; Rh6-lacZ/TM2* x *UAS-Net^{cd8}/Gla Bc; lGMR-Gal80/TM6B*

- *ey$^{3.5}$-Gal80; MH502-Gal4/CyO; UAS-cd8GFP/TM6B* x *UAS-syt^{HA}*

***unc-5 ey$^{3.5}$-FLP* analysis:**

- *ey$^{3.5}$-FLP; FRT42D Ubi-GFP PCNA^{775}/CyO; ato-τ-myc/TM6B* x *FRT42D unc-5^{8-2a}/Gla Bc*; *ato-τ-myc/TM6B* (*unc-5^{8-2a}* : this study, K. Timofeev; original stock *unc-5^{8}:* Labrador et al., 2005)

- *ey$^{3.5}$-FLP; FRT42D Ubi-GFP PCNA^{775}/CyO* x *FRT42D unc-5^{8-2a}/Gla Bc*; *Rh6-lacZ/TM6B*

***unc-5* gain-of-function analysis:**

- *Rh6-eGFP/CyO*; *lGMR-Gal4/TM6B* x *UAS-unc-5 (UAS-unc-5:* Keleman and Dickson, 2001)

2.1.2 Generation of the *unc-5^{8-2a}* allele

The *unc-5^{8}* null mutant allele was generated using ethyl methanesulfonate (EMS) mutagenesis (Labrador et al., 2005). This allele contains a P{GS} element as it was originally generated for a gain-of-function suppressor screen. To avoid unspecific effects of the P{GS} element, the P-element excision strategy was used to remove this. The resulting new allele, *unc-5^{8-2a}*, was subsequently recombined onto a *FRT42D* containing chromosome.

2.1.3 RNAi knock-down approach in several genetic backgrounds

RNAi knock-down experiments were performed using variations of the *act>>Gal4* FLPout approach in combination with RNAi to knock-down gene functions in the eye, the eye and the target neurons, or the target neurons only (Table 1).

More precisely, in all experiments the *act>>Gal4* FLPout approach was combined with the *FLP* recombinase under the control of either the *eyeless*$^{3.5}$ promotor *(ey*$^{3.5}$*-FLP)* (Bazigou et al., 2007) or the *eyeless* promotor *(ey-FLP)*. The *ey*$^{3.5}$*-FLP* activity is restricted to R-cells. In contrast, the *ey* enhancer is described to be active in the R-cells, as well as approximately 50% of the population of target neurons in the medulla (Morante and Desplan, 2008). Further, to restrict the *ey* activity to target neurons only and prevent expression in the R-cells, the *ey-FLP, act>>Gal4* FLPout approach was combined with the early active *ey*$^{3.5}$*-Gal80* and the late acting *lGMR-Gal80* transgenes that are expressed in R-cells thereby preventing *Gal4* activity in these cells.

Table 1: Activity of the *act>>Gal4* FLPout approaches in different areas in the optic lobe.

ey$^{3.5}$*-FLP; act>>Gal4*	*ey-FLP; act>>Gal4*	*ey-FLP; act>>Gal4 +* *ey*$^{3.5}$*-Gal80 and lGMR-Gal80*
R-cells	R-cells & target neurons	Target neurons only

2.2 Immunohistochemistry

Eye-brain complexes of both pupal and adult brains were dissected in phosphate buffered saline (PBS) and fixed in 2% paraformaldehyde (PFA), lysine, sodium phosphatate containing buffer (PLP) for 1 hour at room temperature. Three subsequent washing steps in 0.5% Triton®X-100/PBS (PBT) removed the fixative. The samples were preincubated in 10% normal goat serum (NGS) in PBS for 15 minutes at room temperature and then incubated with the primary antibody diluted in 10% NGS in PBT at 4°C overnight. Next, the samples were washed in 0.5% PBT for 15 minutes, incubated with the secondary antibody for 2.5 hours at RT. Samples were washed twice in PBT and twice

in PBS for at least one hour before mounting and embedding in Vectashield. Images were acquired using a laser scanning Zeiss/Bio-Rad Radiance 2100 or Leica SP5 confocal microscope. Images were processed with Adobe Photoshop.

Table 2: Solutions

PFA 8%	**PBL**	**PBS**	**PBT**
0.8 g paraformal-aldehyde	3.6 g lysine-HCL in 100ml	130 mM NaCl 7 mM Na_2HPO_4	0.1% Triton X-100 in PBS
10 ml ddH_2O	100 mM Na_2HPO_4	3 mM KH_2HPO_4	
70 µl 1M NaOH	pH 7.4	2.7 mM KCl	
		pH 7.4	

Table 3: Primary antibodies

Name	**Origin**	**Dilution**	**Source**
mAB24b10 (anti-Chaoptin)	Mouse	1:50	L. Zipursky
anti-Frazzled	Rabbit	1:250	Kolodziej et al., 1996
anti-Unc-5	Rabbit	1:500	generated in our laboratory
anti-NetB	Rabbit	1:500	B. Altenhein (Albrecht et al., 2011)
anti-GFP	Rabbit	1:1000	Molecular Probes
anti-myc	Rabbit	1:300	Santa Cruz
anti-ß-Galactosidase	Mouse	1:300	Molecular Probes

Table 4: Secondary antibodies

Specificity	Conjugation	Dilution	Source
Goat anti-Rabbit	Cy3, Cy5	1:500, 1:200	Jackson ImmunoResearch Laboratories
Goat anti-Rat	Cy3, Cy5	1:500, 1:200	Jackson ImmunoResearch Laboratories
Goat anti-Mouse	Cy3, Cy5	1:500, 1:200	Jackson ImmunoResearch Laboratories

2.3 Production of the Unc-5 antibody

The peptide antigen KNNAELLGNSSEDENVRPQQGSSSamid is directed against aminoacids (aa) 71 – 94 in a non-conserved sequence stretch downstream of the signal peptide and 44 aa upstream of the fifth Ig-like domain of Unc-5. Two rabbits were immunized following a rapid 77 day schedule at Cambridge Research Biochemicals. Peptides were purified by 16 mg peptide affinity columns. Antibodies were tested for expression in the visual system in wild type, loss-of-function and gain-of-function genetic backgrounds using our standard protocol for immunohistochemistry.

2.4 Molecular biology

2.4.1 Genomic DNA extraction

Eppendorf tubes containing 30-40 flies were frozen at -80°C for 30 minutes. Flies were grinded in 200 μl Buffer A (100 mM Tris-HCl, pH 7.5, 100 mM NaCl, 100 mM EDTA and 0.5% SDS) and incubated at 65°C for 30 minutes. 800 μl of LiCl / KAc (5M KAc : 6M LiCl , 1:2.5) were added and incubated on ice for 15 minutes. The cell debris was

precipitated by centrifugation for 15 minutes at 13000 rpm and the supernatant was transferred into a new eppendorf tube. The DNA was precipitated by adding 600 μl of isopropanol and centrifuged for 17 minutes at 13,000 rpm. The supernatant was discarded and the pellet washed with 1 ml 70% ethanol and centrifuged for 10 minutes at 13,000 rpm. Supernatant was discarded and the pellet dried by aspiration. The pellet was finally resuspended in 100 μl H_2O.

2.4.2 Standard polymerase chain reaction

A standard polymerase chain reaction (PCR) protocol was used to confirm the removal of the P{GS} insertion in the 5' upstream sequence of *unc-5* by a P element mobilization strategy. Additionally, PCR and sequence analysis was conducted to confirm the presence of the described EMS induced point mutation in the encoding sequence of *unc-5* at amino acid position 19 leading to a base pair change from CAG to TAG and thus a premature stop (Labrador et al., 2005).

Table 5: Primers used for sequence analysis of *unc-5*

Primer	Purpose	Sequence 5' – 3'
unc-5 mut for	To sequence *unc-5*	ACGTGAACAAAGCGAGTGTG
unc5 mut rev	To sequence *unc-5*	TTGAAACGTGGAAACAAGCC
unc5 pgs for	To sequence *unc-5*	CTTACCTCGCGCACAACAAA
unc5 pgs rev	To sequence *unc-5*	GCGCTCGAAAGTACGAAACT

The PCR mix contained 1 µl of 50 ng/µl template DNA, 1 µl of 5' hybridizing primer (100 µM), 1 µl of 3' hybridizing primer (100 µM), 5 µl of 10x PCR buffer, 1 µl of dNTPs (10 mM) and 0.8 µl Taq Polymerase (High Fidelity PCR system by Roche). The

reaction was performed as follows: An initial denaturation was performed at 94°C for 5 minutes, and followed by 30 cycles of subsequent steps of denaturation at 94°C for 1 minute, 30 seconds for primer annealing at 58°C and 1 minute of elongation at 72°C. A final elongation step of 10 minutes was performed to terminate the reaction. 5 µl of the PCR products were analyzed by electrophoresis on a 1% agarose gel stained with ethidium bromide.

2.4.3 Cloning of the *NetB^{V5}* and *NetB^{cd8}* constructs into *pMT-V5* vectors to use in cell based assays

Netrin-B (*NetB*) cDNA was amplified using a standard PCR protocol with designed primers NetB 8 containing a NotI restriction site and NetB 11 containing a KpnI site. A fragment of 2.4 kb was gel-purified (Qiagen) and subcloned into the *pCR-Topo2.1* vector using the Topo TA cloning kit (Invitrogen). Sequence analysis using primers NetB 1-6 confirmed the correct sequence of *NetB* inserted into the *pCR-Topo2.1* vector. Subsequently, the KpnI and NotI restriction sites were used to excise and clone the entire *NetB* insert into the *pMTV5* vector (Ligation ratio of insert to vector 1:3, in a total volume of 10μl using T4 DNA ligase (Roche) at 18°C for 2 hours) resulting in a *pMT-V5-NetB^{V5}* construct.

For the generation of the *NetB^{cd8}* construct, the *Cerulean-cd8-V5* sequence (D. Hadjieconomou) was amplified using PCR with the primers cer-cd8-V5 1 and 2 and subcloned into *pCR-Topo2.1* vector. Subsequently, the *Cerulean-cd8-V5* fragment was cloned into the *pMT-V5-NetB^{V5}* plasmid using XhoI and NotI restriction enzymes resulting in the *pMT-V5-NetB^{cd8}* construct.

Table 6: Primers used for the Sequence analysis and cloning of *NetB* constructs

Primer	Purpose	Sequence 5' – 3'
NetB 8	To amplify NetB, NotI site, no stop	tataGCGGCCGCccACTGCATTTGCGTG
NetB 11	To amplify entire NetB, KpnI site	gcatGGTACCATGGTCAGAGCGA-CAGGGAC
NetB 1	To sequence NetB plasmids	CAAGAAGTACGAGCTGAC
NetB 2	To sequence NetB plasmids	GAATATGGCCAGCGAATC
NetB 3	To sequence NetB plasmids	GACTACAATCTGCAGGAC
NetB 4	To sequence NetB plasmids	CAAACTGACCATGACCTG
NetB 5	To sequence NetB plasmids	AACATGATTCAGGCCGAG
NetB 6	To sequence NetB plasmids	ATCTCATCCTTGGACGTG
cd8-cer V5 1	To amplify *Cerulean-cd8-V5* sequence, NotI site	gtatGCGGCCGCTCGCCTGTGATATTTA-CATC
cd8-cer-V5 2	To amplify *Cerulean-cd8-V5* sequence, XhoI site, stop	gagcCTCGAGTTAACCTGCAGTAGAATC
Primer V5 3	To create a V5 tag	5'PGGCCGCttGGTAAGCCTATCCCTAAC CCTCTCCTCGGTCTCGATTC-TACCTAGGtaaC
Primer V5 4	To create a V5 tag	5'PTCGAGttaCCTAGGTAGAATCGAGAC CGAGGAGAGGGTTAGGGATAGGCT TACCaaGC

2.4.4 Cloning of the *UAS-NetB* and *UAS-NetB^{cd8}* constructs into *pKC* vectors for the generation of transgenic flies

For the generation of *UAS-NetB* transgenic flies the *NetB^{V5}* construct was excised from the *pCR-Topo2.1* vector using KpnI and NotI restriction enzymes and cloned into *pKC26-MCS* vector containing a *UAS* sequence. To label the resulting *UAS-NetB* with a V5 tag single-stranded oligos of full-length V5 were generated by aligning primer V5 3 and 4 (10 ng) in 2.5 μl NaCl (5M), 03 μl Tris (1M), 0.45 μl $MgCl_2$ (1M) and H_2O. For the annealing of the single strands of the V5 sequence, the PCR reaction was performed for 10 minutes for each temperature, by step wise reducing the temperature from 95ºC – 75ºC – 65ºC – 60ºC – 55ºC – 25ºC.

For the generation of *UAS-NetB^{cd8}* transgenic flies, the *NetB^{cd8}* construct was excised from the *pMT-V5-NetB^{cd8}* vector using KpnI and XhoI restriction enzymes and sub-cloned into *pKC26-MCS* vector.

2.4.5 Cloning of the *Fra^{F1}* and *Fra^{ECD-HA}* constructs to use in cell based aggregation assays into *pMT-V5* vectors

Fra cDNA was amplified from the *pAWG-Fra* plasmid (provided by W. Joly) using standard PCR with the designed primers Fra1 containing a KpnI restriction site and Fra2 containing a NotI site and a stop signal. The fragment of 4125 bp was gel-purified (Qiagen) and subcloned into *pCR-Topo2.1* vector using the Topo TA cloning kit (Invitrogen). Sequence analysis using primers Fra6 - Fra11 confirmed the correct full-length sequence of Fra. For the truncated *Fra^{ECD-HA}* construct primers Fra1 and Fra3 containing a NotI site, a stop, and a 1x HA tag were used for the cloning into the *pCR-Topo2.1* vector.

KpnI and NotI restriction sites were used to excise and subsequently clone the *Fra*^{fl} or the *Fra*$^{ECD\text{-}HA}$ inserts into the *pMT-V5* vector (Ligation ratio of insert to vector 1:3, in a total volume of 10 μl using T4 DNA ligase (Roche) at 18°C for 2 hours) resulting in *pMT-V5-Fra*^{fl} and *pMT-V5-Fra*$^{ECD\text{-}HA}$ constructs.

Table 7: Primers used for sequence analysis and cloning of Fra constructs

Primer	Purpose	Sequence 5' – 3'
Fra1	To amplify Frafl, KpnI site	gatcGGTACCATGGCCATCACAACAAAC
Fra2	To amplify Frafl, NotI site, stop	gtatGCGGCCGCttaACACTCGAACTCGTTG
Fra3	To amplify Fra$^{ECD\text{-}HA}$, NotI site, stop, 1x HA tag	gtatGCGGCCGCttacgcatagtcagggacgtcgtatggg-taaccggtCTCGTTGTCGATTC
Fra4	To amplify Fra$^{ECD\text{-}HA}$ 1.1kb fragment 5' of EcoRV site	gagcGATATCGCACTTCAATTCCGGTTC
Fra5	To amplify Fra$^{ECD\text{-}HA}$, KpnI site	GAAGTGCGATATCTGGGGAAAGCCAAAG
Fra6	To sequence Fra plasmids	GACTTTGTGGAACTGGCT
Fra7	To sequence Fra plasmids	CACTTCGTCGATCTCCAG
Fra8	To sequence Fra plasmids	CAGCAATACGGTGGATTC
Fra9	To sequence Fra plasmids	GCACCGCAGGTCAAGAGT
Fra10	To sequence Fra plasmids	ATCGCGACTGGTCAGTTG
Fra11	To sequence Fra plasmids	CGAAACGGAATGGGTGAC
mCher-ryfw	To amplify mCherry 5', NotI site	tataGCGGCCGCtATGGTGAGCAAGGGCGAG
mCher-ryrev	To amplify mCherry 3', XhoI site, stop	TCGACTCGAGTTACTTGTA-CAGCTCGTCCATG
Fra33	To amplify Fra, NotI site, no stop	tataGCGGCCGCACACTCGAACTCGTTG
MTfor	To sequence Fra plasmids	CATCTCAGTGCAACTAAA
BGHrev	To sequence Fra plasmids	TAGAAGGCACAGTCGAGG

2.4.6 Cloning of the *Fra-mCherry* construct into the *pMT-V5* vector for use in cell based assays

To visualize Fra in cells, the *Fra-mCherry* construct was cloned. *mCherry* cDNA was amplified from the *pTRC-mCherry* plasmid (D. Hadjieconomou) using standard PCR with the designed primers mCherry fw containing a NotI restriction site and mCherry rev containing a XhoI site and a stop signal. A fragment of 719 bp was gel-purified (Qiagen) and subcloned into the *pMT-V5* vector. For this, an initial digestion of the *pMT-V5* vector with NotI over night was followed by a digestion with XhoI for 1.5 hours (this was necessary since the restriction sites are overlapping (GC^GGCCGC^TCGAG).

In parallel, *Fra* cDNA was amplified from the pAWG-Fra plasmid (W. Joly) using standard PCR with the designed primers Fra1 containing a KpnI restriction site and Fra33 containing a NotI site, but no stop signal. A fragment of 4125 bp was gel-purified (Qiagen) and subcloned into *pCR-Topo2.1* vector using the Topo TA cloning kit (Invitrogen). The KpnI and NotI restriction enzymes were used to excise and subclone the Fra^{fl} sequence into the *pMT-V5-m-Cherry* vector (Ligation ratio insert to vector 1:3, in a total volume of 10 μl using T4 DNA ligase (Roche) at 18°C for 2 hours) resulting in a *pMT-V5-*Fra^{fl}*-mCherry* construct. Sequence analysis using the primers MTfor, Fra8, Fra10 and BGHrev confirmed the correct sequence of *Fra-mCherry*.

2.5 Cell assays

2.5.1 S2 and S2R+ Schneider cell culture

The S2 cell line is a derivate of a formerly primary culture of a macrophage-like lineage of *Drosophila melanogaster* embryos (Schneider, 1972). These cells grow without special CO_2 adjustments at 25ºC as a semi-adherent monolayer or in suspension in Schneider's *Drosophila* Medium (containing 500ml Standard Schneider's Medium, 10% fetal calf serum (heat-inactivated), 50 μg/ml Penicillin/Streptomycin and 2mM L-glutamine). S2R+ cells are modified and are more strongly adherent to the substrate than other S2 cell lines (Yanagawa et al., 1998).

2.5.2 Transient transfection of S2 / S2R+ cells

For the transient DNA transfection of S2 and S2R+ cells the non-liposomal lipid Effectene transfection reagent (QIAGEN) was used. Cells were seeded on cover slips (Thermo scientific, 13 mm) in 3 ml medium in 6 well plates at a density of 0.5 x 10^5 /ml. After 2 hours, most cells adhere to the cover slips. 1 ml of the medium was removed from the cells. For the transfection, 1 μg DNA of *pMT-V5-NetB*^{V5} (or others) was mixed well with 150 μl Buffer EC and 8 μl Enhancer and incubated for 3 minutes at room temperature. After this step, 25 μl of Effectene reagent was added, mixed well and incubated for 6 minutes at RT. 825 μl of S2 Medium was added and the solution was spread carefully on the plated cells. The *pMT-V5* promoter is not constitutively active but is induced by 500 μM $CuSO_4$ (final concentration) 12-24 hours post-transfection.

2.5.3 Concentration of secreted NetB and Fra^{ECD-HA} proteins from conditioned medium

NetB and Fra proteins were enriched in the conditioned medium from transiently transfected *Drosophila S2* and *S2R+* cells, respectively. Cells were seeded on cover slips in 3 ml medium in 6 well plates at a density of 0.5 x 10^5 /ml and transfected as described above. After 3-4 days of incubation, the conditioned medium was collected and centrifuged at 1,500 rpm for 10 min to remove cell debris. Proteins were concentrated from the supernatant using CENTRIPREP® Centrifugal filter devices with a Nominal Molecular Weight Limit (NMWL) of 30,000 at 1,000 g in 3 subsequent centrifugations of 10 minutes, whereby after each step the flow-through was discarded.

2.5.4 Binding assays

Several individual binding assays were performed to test as to whether NetB and Fra can form a ternary complex. Fra-GFP positive R+ cells (construct provided by W. Joly) were incubated with the NetB containing conditioned medium in the presence of 50 μg/ml Heparin sodium salt (SIGMA) and incubated for 2 hours at room temperature. The NetB containing conditioned medium was removed, cells were washed 3x with *Drosophila* Schneider's medium and fixed with 4% PFA.

NetB^{cd8} positive R+ cells were incubated with the Fra^{ECD-HA} containing conditioned medium, both with and without 50 μg/ml Heparin sodium salt (SIGMA), and incubated for 2 hours at room temperature. As before, the Fra^{ECD-HA} containing conditioned medium was removed, the cells were washed 3x with *Drosophila* Schneider's medium and fixed with 4% PFA.

To identify a ternary complex of Fra, NetB and $Fra^{EDC\text{-}HA}$, Fra-GFP postive R+ cells were incubated with the NetB containing conditioned medium in the presence of 50 μg/ml Heparin and incubated for 2 hours at room temperature. The NetB containing conditioned medium was removed, the cells were washed 3x with *Drosophila* Schneider's medium and subsequently incubated with $Fra^{ECD\text{-}HA}$ containing conditioned medium for 2 hours at RT. Cells were washed 3x with *Drosophila* Schneider's medium and fixed with 4% PFA.

For the analysis for the duration that NetB is attached to Fra-GFP cells were maintained after washing in *Drosophila* Schneider's medium in separate wells and fixed at several different time points.

Alternatively, following pre-incubation of Fra-GFP positive cells with NetB containing conditioned medium, Fra-cherry positive cells were added and allowed to bind for 4-5 hours. Cells were washed 3x and fixed with 4% PFA.

2.5.5 Fixation and immunohistochemistry

Cells were fixed on cover slips with 4% PFA for 10 min at room temperature and then washed 1x with PBS. Cells were quenched with 50 mM NH_4Cl/PBS for 10 min at room temperature and permeabilized with 0.1% of Triton®X-100 in PBS (PBT) for 10 min at room temperature. The samples were pre-incubated in 10% normal goat serum (NGS) in PBS for 15 minutes and then incubated for 2 hours at room temperature with the primary antibody which was diluted in 10% NGS in PBS. Next, the samples were washed with PBS and incubated with the secondary antibody for 1 hour at room temperature. After the cells were washed twice in PBS, they were embedded in hardset ProLong®

Gold antifade reagent (Invitrogen). Images were acquired using a laser scanning Leica SP5 confocal microscope. Images were processed with Adobe Photoshop.

2.5.6 Western blot analysis

Western blot analysis was used to detect the proteins in the cell lysates and conditioned medium. Samples were prepared as follows: Cell lysates were obtained after washing cells with cold PBS and adding 0.5 ml TEB buffer and 5 μl Phosphatase Inhibitor Cocktail 2 (Sigma) and 5 μl protease inhibitors (Halt Protease Inhibitor Cocktail, PIERCE). After incubation for 10 minutes on ice, the cell mix was collected into an eppendorf tube and centrifuged for 10 minutes at 5000 rpm. The supernatant was collected into a new tube. To denaturate the protein, NuPAGE® LDS Sample Buffer 4X (Invitrogen) was added and samples were incubated at 95˚C for 3 minutes. Samples of conditioned medium were obtained by collecting the supernatant from the cell assay into an eppendorf tube and centrifuged for 5 minutes at 1,000 rpm, following by an additional centrifugation step for 5 minutes at 5,000 rpm. The supernatant was collected into a new tube. To denaturate the protein, NuPAGE® LDS Sample Buffer 4X (Invitrogen) was added and samples were incubated at 95˚C for 3 minutes.

A Gel Sodium Dodecyl Sulfate Polyacrylamide Gel Electrophoresis (SDS-PAGE) was performed to separate the denatured proteins by the length of the polypeptide. For that NuPAGE® 4-12% Bis-Tris Gels (Invitrogen) were used. For the electrophoresis, 40 ml NuPAGE® MOPS SDS Running Buffer and 740 ml distilled water were mixed and poured into the Western blot tank. The acrylamide gels in the gel holder were assembled and immersed into the tank. 100 μl NuPAGE® antioxidant was added to the inner chamber.

The electrophoresis was performed at 200 V for approximately 50 minutes. After completing SDS-PAGE, the proteins were then transferred to a nitrocellulose membrane in semi-dry electrophoretic transfer. For this the gel was first soaked in soaking buffer (consisting of 5 ml NuPAGE® MOPS SDS running buffer, 45 ml distilled water and 50 μl 20% SDS) for 10 min. Membranes were prepared by incubation in methanol for 30 seconds and then transferred into transfer buffer (10 ml NuPAGE® MOPS SDS running buffer, 80 ml distilled water, 10 ml methanol and 100 μl antioxidant). The transfer was performed at 14 V for 22 minutes for 1 gel or 40 minutes for 2 gels. After this, the membranes were hydrated in water and blocked in 5% non fat dry milk in PBS with 0.1% tween-20 (PBST) for 2 hours. The membrane was incubated with the primary antibody for 16 hours at 4˚C on a rotator. The next day the membrane was rinsed 3x for 15 minutes in 0.1% PBST and incubated with the secondary antibody for 1.5 hours at room temperature. The chemiluminscent reagents using BM Chemiluminescence western blotting substrate (ROCHE) were prepared and applied immediately on the samples. A film cassette with the appropriate film was prepared and the membrane placed carefully. Several exposure times were used before the development process in the FUJI X-Ray Imaging film processor.

Chapter 3

The role of the Frazzled guidance receptor in R8 axons

3.1 Introduction

During the development of neuronal circuits different neuron subtypes must establish specific connections by unambiguously selecting appropriate synaptic partners from a large number of different alternatives. The spatial organization of axonal and dendritic processes into defined regions allows reducing the range of possible synaptic contacts. Structurally, this is enabled through columnar or laminar organization of projections in the central nervous system (CNS). Many regions in the CNS, such as the cerebellum, cerebral cortex, the hippocampus and the visual system are organized into columns and layers (Huberman et al., 2010). In addition in the visual system, columns are essential units of a topographic map to maintain the spatial sensory information during signal processing in deeper brain regions. The organization of neuronal connections into layers is pivotal for sensory information processing of several functional pathways, such as motion detection and color vision (Clandinin and Feldheim, 2009; Hadjieconomou et al., 2011b). Despite their importance for the functionality of a nervous system, the molecules and mechanisms that control the establishment of layered structures are still poorly understood.

In the visual system of *Drosophila,* the medulla represents the most complex structure with a large number of different neuronal processes organized into 10 distinct layers (Fischbach and Dittrich, 1989; Takemura et al., 2008). Out of the eight photoreceptor subtypes (R-cells, R1-R8), R8 and R7 axons terminate in distinct layers in the medulla. In the adult, R8 and R7 axons innervate the layers M3 and M6, respectively. Layer-specific connectivity of R8 and R7 axons is achieved with great precision in a two-step layer selection process during pupal development (Ting et al., 2005). Initially, R8 and R7 axons terminate at temporary layers and then proceed to their final recipient layers during mid-pupal development. Several guidance determinants have been impli-

cated in regulating the targeting of R8 axons to the M3 layer through cell adhesion interactions with target neurons (Hakeda-Suzuki et al., 2011; Shinza-Kameda et al., 2006; Tomasi et al., 2008). However, it is not clear as to how R8 axons precisely target to the M3 layer among a total of 10 neuropil layers in the medulla.

In *Drosophila,* the Frazzled (Fra) guidance receptor is the homolog of DCC in vertebrates and Unc-40 in *C. elegans*. A significant amount of our knowledge of the function of Fra in axon guidance has derived from studies investigating midline pathfinding in *C. elegans,* vertebrates and *Drosophila*, where it is required for pathfinding mediated through the Netrin ligand (Fazeli et al., 1997; Ishii et al., 1992; Keino-Masu et al., 1996; Kolodziej et al., 1996).

In the 3rd instar larval optic lobe of *Drosophila,* the Fra / Netrin guidance system is required for correct axon bundle spacing, as misexpression of Netrins in R-cells leads to severe targeting defects including a stalling of R-cell axons in the optic stalk (Gong et al., 1999). However, it is not known as to whether Fra can play a role in mediating layer-specific axon targeting in the visual system. In this chapter, following up initial findings by W. Joly in our laboratory, I investigate the role of Fra in layer-specific axon targeting in the medulla during pupal development.

3.2 Results

3.2.1 Fra is expressed in the optic lobe during pupal development

To gain first insights into the role of the Fra guidance receptor in visual circuit assembly, expression of Fra was examined during optic lobe development (data generated and provided by W. Joly). For this purpose, a polyclonal antibody was used that was directed against a 278 amino acid long fragment in the Fra C-terminal domain (aa 1328 to 1606) (Kolodziej et al., 1996).

During pupal stages and in the adult, Fra is expressed broadly at low levels and strongly in distinct layers in the medulla neuropil (Figure 9A-D'). More precisely, at 42 hours APF Fra accumulates at the distal medulla neuropil border, where R8 axons temporarily pause before proceeding to their final layer during the second half of pupal development (Figure 9B, B'). Fra is also enriched in the lamina in R1-R6 axons at 42 hours APF pointing towards a possible role in lamina cartridge targeting. From mid-pupal stages (~ 55 hours APF), Fra protein is strongly expressed in the M3 layer (Figure 9C, C'). In addition, Fra is also expressed in glial subtypes in the lamina.

Taken together, these results indicate that the Fra receptor is expressed in medulla target neurons arborizing in the M3 layer at 55 hours APF and possibly in R8 axons.

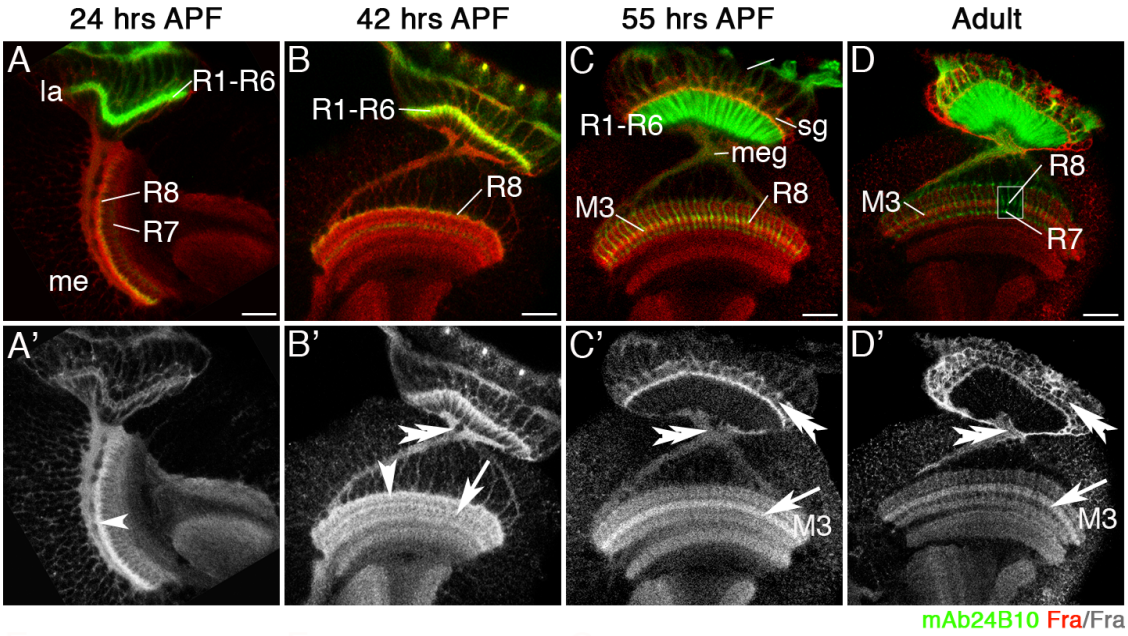

Figure 9. Fra expression in R-cells and the optic lobe during pupal development and in the adult. (A-B) Fra (red) is enriched in the temporary layer of R8 axons at 24 and 42 hours in the medulla neuropil (arrowheads in A' and B') and in the emerging M3 layer at 42 hours (arrows in B'). (C-D) Fra strongly accumulates in the final M3 layer at 55 hours and persists in adults (arrows in C' and D'). (B) In addition, Fra is enriched in the lamina in R1-R6 axons at 42 hours (asterisk in B'). (B-D) Fra is also expressed in glial subtypes in the lamina at 42 hours and 55 hours APF and in the adult. me, medulla, la, lamina, lo, lobula, lop, lobula plate, meg medulla epithelial glia, sg, satellite glia. Scale bars are 20 μm. Data provided by W. Joly.

3.2.2 Fra is expressed in R8 cells along the cell body membrane and in the developing rhabdomeres

Because of the wide expression of Fra in the medulla neuropil, it was not possible to determine as to whether Fra is also expressed in R-cells during pupal development. Therefore, to test as to whether Fra is expressed in R-cells, cross sections of the retina were analyzed at distinct time points during pupal development (Figure 10A-D'). The *capricious-Gal4* (*caps-Gal4)* insertion into the *caps* gene locus was used in conjunction with a *UAS-cd8GFP* reporter to specifically label R8 cells (Shinza-Kameda et al., 2006). I observed that Fra is expressed on R8 cell body membranes at 24 hours APF and subsequently at 42 hours and 55 hours APF in developing R8 rhabdomeres, the

light gathering organelle in the adult that contains visual pigment (Figure 10A, A', C, C', D, D'). Furthermore, Fra is expressed transiently in R1-R6 rhabdomeres around 42 hours APF (Figure 10B, B'), but not at 55 hours APF (Figure 10D, D'), suggesting a possible function of Fra in R1-R6 targeting and lamina cartridge formation during this discrete time.

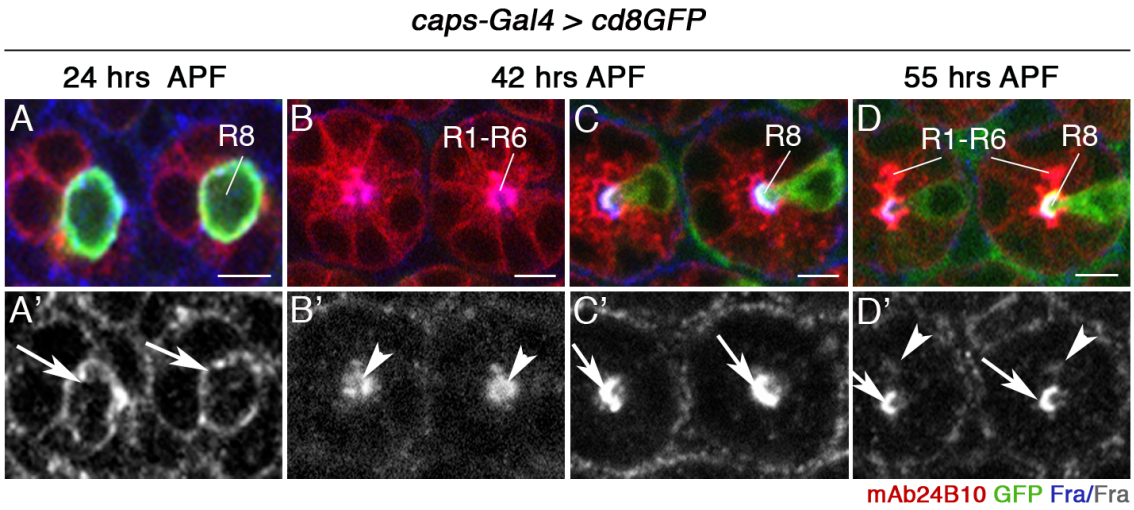

Figure 10. Fra is expressed on R8 cell bodies and in developing rhabdomeres. (A-D) Retina cross-sections of optic lobes at several developmental stages. Fra expression (blue/grey) is detected along the cell body membranes of R8 cells at 24 hours (arrows in A'), and in the rhabdomeres at 42 hours (arrows in C') and 55 hours APF (arrows in D'). Fra is also transiently detected in R1-R6 rhabdomeres at 42 hours APF (arrowheads in B'), but not at 55 hours APF (arrowheads in D'). R-cells are labeled with mAb24B10 (red), and R8 cells with *caps-Gal4* driving expression of *UAS-cd8GFP* (green). Scale bars are 10 μm.

3.2.3 Fra is localized to the growth cones of R8 axons

Next, I sought to test as to whether Fra also accumulates in the growth cones of R8 axons. This was complicated by the fact that Fra is expressed widely in the medulla neuropil. Therefore, to assay as to whether Fra accumulates at the growth cones of R8 axons, Fra was removed from neurons associated with the target area. In a knock-down experiment, RNA interference (RNAi) with the *UAS-fra*^{6RNAi} transgene was used in

combination with the *ey-FLP, act>>Gal4* FLPout (*ey-FLP*out) approach (Bazigou et al., 2007). This facilitates the knock-down of *fra* in the whole optic lobe including R-cells and the target area. However, in conjunction with early acting $ey^{3.5}$*-Gal80* (Chotard et al., 2005) and late acting *lGMR-Gal80* (kindly provided by C. Desplan) transgenes, RNAi activity is prevented in R-cells. This allows the visualization of Fra expression in R-cells. Therefore the remaining Fra protein staining can be attributed to the R8 growth cones. This showed that during pupal development at 24 hours and 42 hours APF, Fra is not only localized to R8 cell bodies, but also importantly to R8 growth cones (Figure 11A-B'). This finding suggests that Fra could have a role in mediating R8 axon targeting.

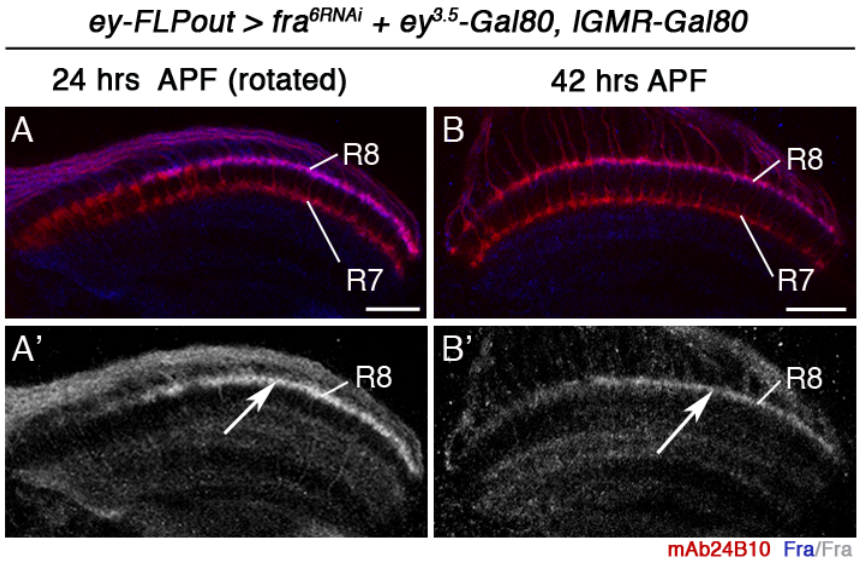

Figure 11. Fra is localized to the growth cones of R8 axons. (A-B) Optic lobes at 24 hours and 42 hours APF. Using the *ey-FLP, act>>Gal4* FLPout approach in combination with $ey^{3.5}$*-Gal80* and *lGMR-Gal80* to drive *UAS-*fra^{6RNAi} solely in the target area, reveals that Fra is localized to R8 growth cones at 24 hours and 42 hours APF (arrows in A', B'). R-cells are labeled with mAb24B10 (red). Scale bars are 20 μm.

3.2.4 *fra* is required for R8 axon targeting

To address the question as to whether Fra has a role in controlling R8 axon targeting, the $ey^{3.5}$*-FLP* approach (Bazigou et al., 2007) was used to generate mosaic *fra* mu-

tant animals, which specifically lack *fra* in the eye while maintaining activity in the target area (data was generated and provided by W. Joly). Two embryonic lethal *fra* null mutants - fra^3 and fra^4 -that were generated by ethyl methanesulfonate (EMS) mutagenesis, were available for our studies (Kolodziej et al., 1996). However, fra^4 showed rough eyes in mosaic mutant animals using the $ey^{3.5}$-*FLP* approach.

In addition, the mutation site in fra^4 has not been determined. Therefore, the well-characterized loss-of-function fra^3 allele was used, which contains a point mutation at amino acid position 1028 that causes a change of tryptophan (TGG) to a premature stop (TGA), thus resulting in a truncated protein (Kolodziej et al., 1996). With this allele, no general eye development errors, R8 cell-fate specification defects or abnormal proliferation and differentiation in the optic lobe was observed (data not shown, generated by I. Salecker).

Analysis of adult optic lobes revealed strong projection defects in 88.7% of fra^3 mutant R8 axons (Figure 12B, B', data generated by W. Joly). R8 axons were specifically labeled with the late genetic marker *Rh6-lacZ* which expresses ß-galactosidase under the control of the rhodopsin 6 (Rh6) promoter (Papatsenko et al., 2001). In detail, 56% of R8 axons stalled at the medulla neuropil border, while 33% terminated prematurely at the more distal layers M1/M2. To address as to whether Fra functions cell-autonomously, mosaic analysis with a repressible cell marker (MARCM) (Lee and Luo, 2001) was used to generate single *fra* mutant and GFP-positive R8 axons in otherwise heterozygous surroundings. This showed that *fra* is cell-autonomously required in R8 for layer-specific axon targeting (Figure 12C-D', data generated by W. Joly).

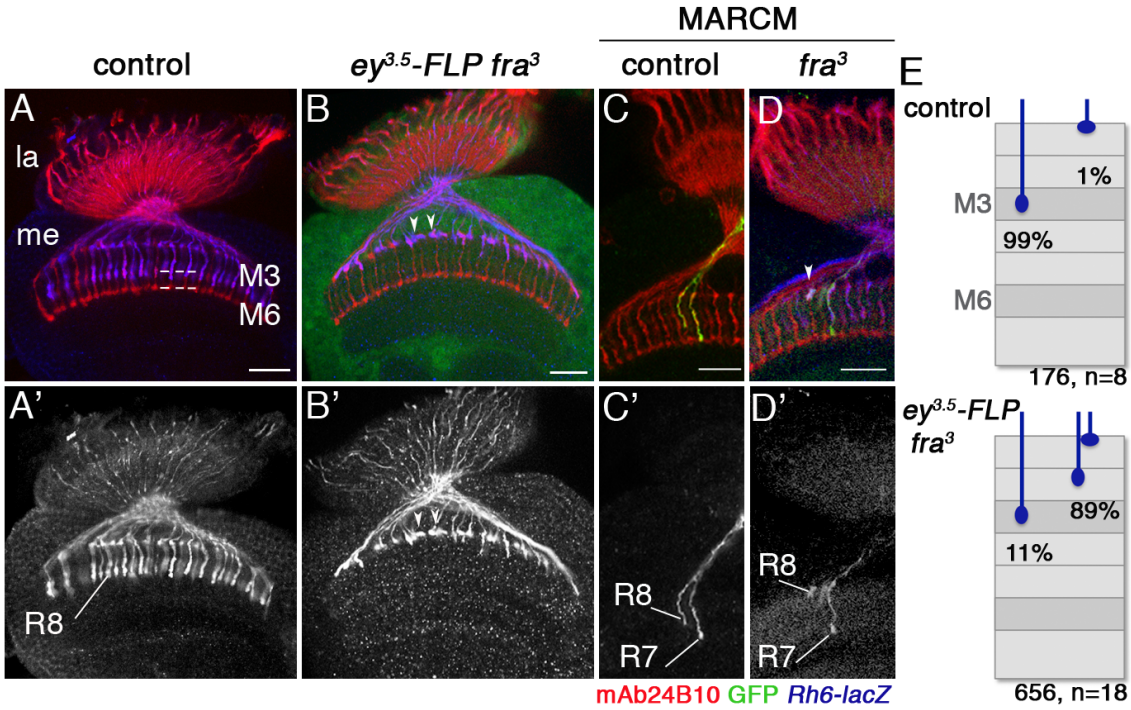

Figure 12. *fra* is required for R8 axon targeting to the M3 layer. (A, A') In controls, *Rh6-lacZ* positive R8 axons (blue) target to the M3 layer in the medulla (double-arrowhead in A'). (B, B') In *ey*$^{3.5}$*-FLP* mosaic animals lacking *fra* in R-cells, many R8 axons stall at the medulla neuropil border (arrows) or terminate incorrectly in the M1/M2 layers (arrowheads). (E) Quantification of phenotypes. (C-D') Compared to controls, a *fra* mutant, GFP-positive R8 axon in an otherwise heterozygous surroundings generated by MARCM terminates incorrectly in M1/M2 (arrowheads) showing that *fra* is cell-autonomously required in R8 for layer-specific axon targeting. me, medulla, la, lamina. Scale bars are 20 μm. Data provided by W. Joly.

3.2.5 *fra* is required in R8 axons for the targeting to the final layer M3

We next asked as to whether the aberrant targeting of R8 axons to the M3 layer in *fra* mutants is due to a requirement of *fra* in layer-specific targeting during development. Alternatively, it is conceivable that R8 axons initially correctly innervate the M3 layer but in later stages retract due to a missing stabilization of synaptic contacts. Using the *ey*$^{3.5}$*-FLP* approach to remove *fra* function in the eye, R8 axon targeting was assessed at 42 hours and 55 hours APF (Figure 13A-D'). R8 axons during early development were labeled with the *ato-τ-myc* marker (Senti et al., 2003). In control animals, at 42 hours APF all R8 axons remain at the medulla neuropil border (Figure 13A, A', total

of 235 R8 axons, n=7, data provided by W. Joly). In contrast, *fra* mutants show a mild targeting defect with 6% of a total of 324 *ato-τ-myc* positive R8 axons prematurely innervating deeper layers in the medulla (Figure 13B, B', n=8, W. Joly). At 55 hours APF in controls, R8 axons innervate the M3 layer (Figure 13C, C', 98% of 325 *ato-τ-myc* positive R8 axons, n=14). However, similar to the findings in the adult, about 91% of R8 axons fail to innervate the M3 layer (Figure 13D, D', total of 255 R8 axons, n=10).

This finding supports the conclusion, that Fra is required during development, and in particular during the second step of R8 axon targeting at mid-pupal stages, when R8 axons proceed to their final layer M3.

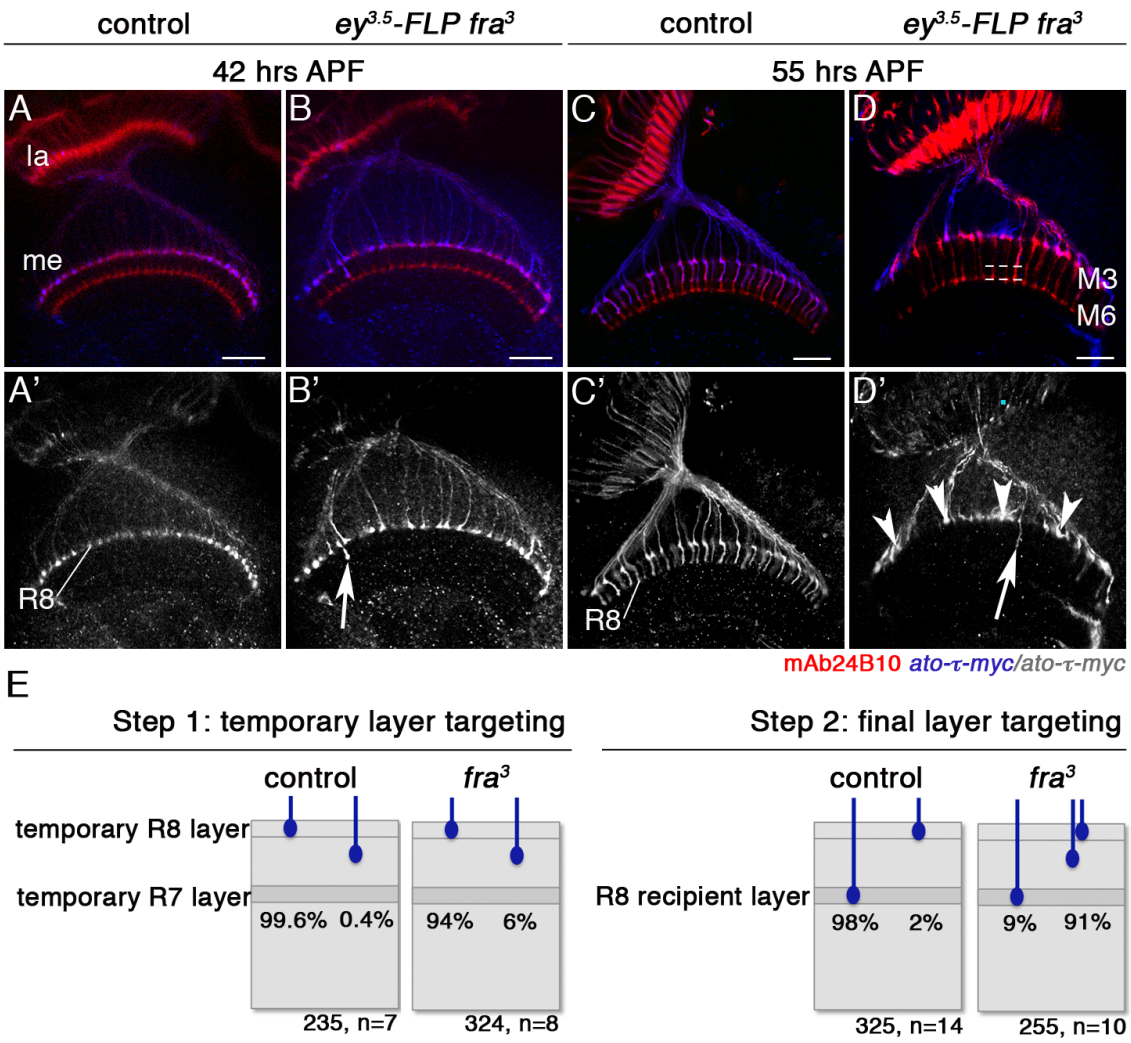

Figure 13. *fra* is required for R8 axon targeting to the M3 layer during pupal development. (A-D) The *ey*$^{3.5}$*-FLP* approach is used to remove *fra* function in the eye. (A, A') At 42 hours APF, all *ato-τ-myc* positive R8 axons (blue, 235 R8 axons, n=7) terminate in their temporary layer at the medulla neuropil border in controls. (B, B') In animals lacking *fra* in all R-cells, the majority of R8 axons pause correctly at the medulla neuropil border, while a small percentage (6% of 324 *ato-τ-myc* positive R8 axons, n=8) prematurely projects deeper (arrow in B'). (C, C') In wild type at 55 hours APF, all R8 axons project to the emerging M3 medulla layer. (D, D') In *fra* mutants, the majority of R8 axons (91% of 255 R8 axons, n=10) stalls at the border of the medulla neuropil (arrowheads in D') or terminate prematurely in the M1/M2 layers (arrow in D'). R-cells are labeled with mAb24B10. Scale bars are 20 μm. (E) Quantification of phenotypes. Data for panels A and B were provided by W. Joly.

3.2.6 Knock-down of *fra* using the RNAi approach leads to R8 axon targeting defects

Loss-of-function analysis of *ey$^{3.5}$-FLP* mosaic animals lacking *fra* in R-cells uncovered that *fra* is required in R8 axons for correct layer-specific targeting. For many genetic manipulations the RNAi approach is a very useful tool (Fire et al., 1998). However, one of the main drawbacks of RNAi is the secondary and unspecific effect through off-targets. This is mediated through sequence homology between the target dsRNA sequence and other genes (Perrimon and Mathey-Prevot, 2007). Hence it is of great importance to confirm observed phenotypes with independent RNAi transgenes. For that the *UAS-fra$^{29910\text{-}RNAi}$* transgene, available from the VDRC stock center, was expressed in R-cells using *lGMR-Gal4* as a driver. When knocking down *fra* specifically in R-cells, R8 axons show aberrant projections, such as stalling at the medulla neuropil border (91% of 195 R8 axons, n=9, Figure 14C-C'). Despite the fact that the driver is active in all R-cells, R1-6 ganglion specific targeting in the lamina and layer-specific R7 axon targeting in the medulla was not affected. This is consistent with findings from the *fra^{3}* mosaic analysis and the RNAi approach using *UAS-fra^{6RNAi}* (data provided by W. Joly, Figure 14B-B'). Hence, the results from both RNAi based approaches are reliable and this experimental paradigm can therefore be used for further genetic manipulations. For the further experiments, I focused on the *UAS-fra^{6RNAi}* transgene.

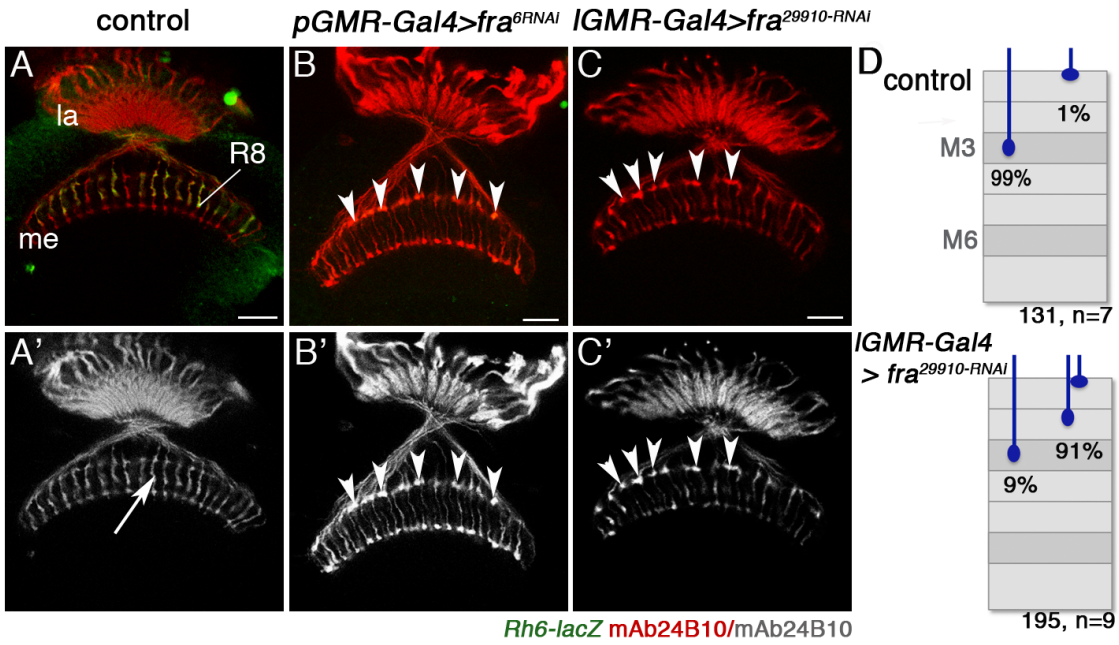

Figure 14. Knock-down of *fra* using RNAi. (A-C) Adult optic lobes. (A, A') In control optic lobes, R8 project normally to the M3 layer (arrow in A', 131 R8 axons, n=7). (B, B') In a RNAi knock-down approach *fra* was removed from the R-cells using *pGMR-Gal4* and *UAS-fra*^{6RNAi} (generated by W. Joly). R8 axons stall at the medulla neuropil border and fail to innervate the M3 layer (arrowheads in B, B'). (C, C') Using *lGMR-Gal4* to drive *UAS-Fra*$^{29910-RNAi}$ resulted in 91% of R8 axons terminating at the medulla neuropil border (arrowheads in C, C', total of 195 R8 axons, n=9). R-cells are labeled with mAb24B10 (red). la, lamina, me, medulla. Scale bars are 20 μm. (D) Quantification of phenotypes. Data for B, B' were provided by W. Joly.

3.2.7 Fra is not sufficient for layer-specific axon targeting

Next, to test as to whether *fra* is sufficient for axon targeting gain-of-function experiments were performed. Assuming that Fra is instructive for axon targeting to the M3 layer, it is conceivable that ectopic expression could lead to re-direction of for instance R7 axons, which normally do not express Fra, to the M3 layer. To test this possibility, the *UAS-fra* transgene was expressed in all R-cells using *lGMR-Gal4*. Prolonged ectopic expression of *UAS-fra* caused stalling of many R8 axons at the border of the medulla neuropil (Figure 15B, B', 32% of 210 *Rh6-eGFP* positive axons, *n*=9). Interestingly, this ectopic expression of *UAS-fra* was not sufficient to redirect R7 axons to the

M3 layer (Figure 15B). However, in rare instances R7 exhibit small finger-like protrusions into deeper medulla layers. The significance of these protrusions is unclear.

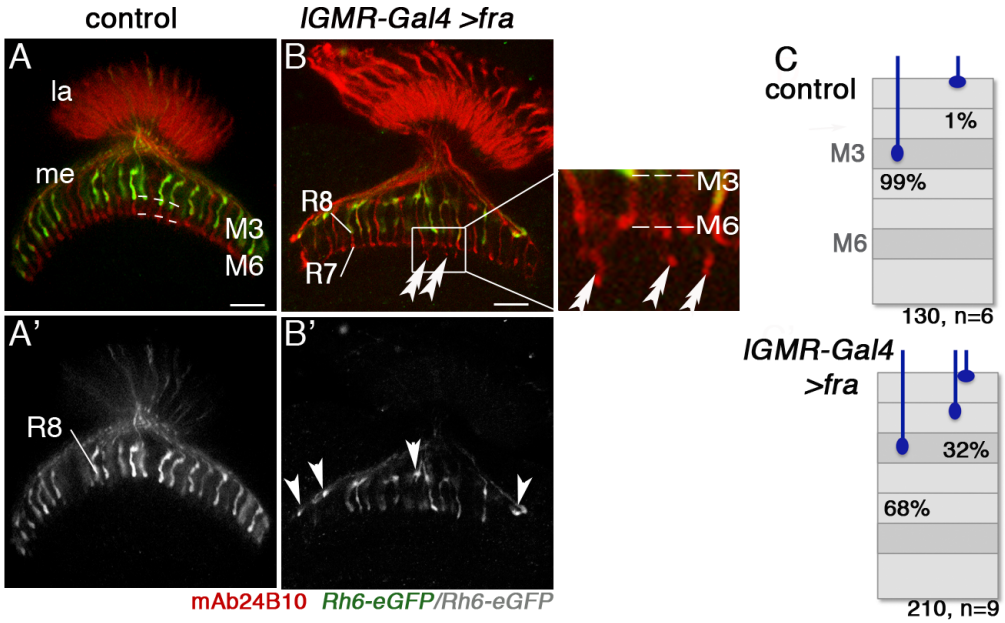

Figure 15. Prolonged ectopic expression of *fra* in all R-cells leads to aberrant targeting of R8 axons. (A, A') Control optic lobes show correct targeting of *Rh6-eGFP* positive R8 axons (green) to the M3 layer and R7 axons to the M6 layer in the medulla neuropil. (B-B') Over-expression of *fra* in R-cells causes stalling of R8 axons at the medulla neuropil border (arrowheads in B'). R7 axons are not re-targeted to the M3 layer, but show small extensions into deeper layers (double-arrow in B and in magnification). R-cells are labeled with mAb24B10 (red). Dashed lines indicate positions of the M3 and M6 layers. la, lamina, me, medulla. Scale bars are 20 μm. (C) Quantification of phenotypes.

3.3 Discussion

3.3.1 Fra is required for R8 axon targeting to the M3 layer

Our studies in the laboratory in collaboration with W. Joly established that the Fra guidance receptor is required in R8 axons to promote layer-specific axon targeting.

Fra is dynamically expressed in the optic lobe during development. In addition to a broad expression in target neurons and glial subtypes, Fra accumulates at the distal medulla neuropil border, where R8 axons temporarily pause during early pupal stages. From mid-pupal stages Fra protein is strongly expressed in the M3 layer, which timely coincides with R8 axons innervating this layer. However, as a result of the strong expression of Fra in the target neurons it was not clear as to whether Fra is expressed in R8 growth cones. To verify that Fra is present on R8 growth cones, the expression of Fra was reduced in target neurons using RNAi in combination with the *ey-FLP*out approach in conjunction with the *ey$^{3.5}$-Gal80* and *lGMR-Gal80* transgenes. Using this approach, I have shown that Fra localizes to the growth cones of R8 axons during 24 hours and 42 hours of pupal development.

Mutant analysis revealed that Fra is required for R8 axon targeting to the M3 layer. In *ey$^{3.5}$-FLP* mosaic animals lacking *fra* in most R-cells, while wild type activity was maintained in the target area, 89% of R8 axons fail to innervate the M3 layer. The high penetrance of this phenotype is striking and different to other guidance systems. Detailed analysis allowed to discriminate between two distinct phenotypes in *fra* mutants: 56% of R8 axons stalled at the medulla neuropil border, while 33% terminated prematurely at the more distal layers M1/M2. This might suggest that Fra has several functions during layer-specific R8 axon targeting, such as the coordination of the temporary and the final layer selection process.

To address as to whether *fra* is required for targeting to temporary layers during early pupal stages, or for the targeting to the final M3 layer, we assessed R8 axon targeting in *fra* mutants during pupal development. At 42 hours APF, similar to controls, the majority of R8 axons remain at the medulla neuropil border. However, a small percentage (6%) invades deeper into the medulla neuropil. This suggests that *fra* is required for targeting of R8 axons to their temporary layer. However, the low penetrance of this phenotype indicates that Fra might interact with other guidance determinants for its function during early pupal stages.

Notably, *fra* is required during mid-pupal stages in the second step of R8 axon targeting to the final layer M3, as in *fra* $ey^{3.5}$-FLP mosaics, 91% of R8 axons stall at the medulla neuropil border.

3.3.2 Fra is not sufficient to mediate layer-specificity

Prolonged expression of Fra in all R-cells leads to stalling of R8 axons at the medulla neuropil border. This suggests that precise temporal control of Fra levels in R8 axons is essential for the integration of guidance information.

Moreover, ectopic expression of Fra in other R-cells, such as R7 axons is not sufficient to redirect R7 axons from the M6 to the M3 layer. This is different from other guidance determinants studied in layer-specific targeting in the visual system. For instance, the leucine-rich repeat protein Capricious (Caps) is sufficient to promote homophilic cell adhesion between R8 axons and their recipient layer M3 (Shinza-Kameda et al., 2006). Caps is specifically expressed in R8 axons and in the target area in a broader domain including the R8 recipient layer M3, but not in R7 axons or their recipient layer M6. Interestingly, ectopic expression of *UAS-caps* in all R-cells redirects R7 axons to the Caps-positive R8 axon recipient layer M3.

Furthermore, the transmembrane receptor Golden Goal (Gogo) mediates repulsive axon-axon interactions between R8 axons and the target area in order to maintain correct columnar positions of R8 axons as they enter their temporary medulla neuropil layer (Tomasi et al., 2008). Interestingly, in *gogo* mutants loss of this repulsion results in stalling of R8 axons at the medulla neuropil border or a projection into deeper layers, while some R7 axons were re-directed to the M3 layer.

As for Fra, although it is not sufficient for M3 layer-specific targeting, interestingly Fra to some extent induces motility, as R7 axons extend filopodia-like protrusions deeper into the medulla neuropil. Nonetheless, it appears that either R7 cell-specific guidance determinants cannot be overwritten, or R7 cells lack essential cooperating receptors or downstream components of Fra signaling that are present in R8 cells allowing targeting to the M3 layer. Such R7 specific guidance determinants are for instance the cell adhesion molecule CadN, the receptor protein tyrosine phosphatases PTP69D and Lar, and the adapter protein Liprin-α (Hofmeyer et al., 2006; Lee et al., 2001; Maurel-Zaffran et al., 2001). Future studies will need to address as to how the Netrin/Fra guidance system cooperates with other guidance determinants in layer-specific axon targeting.

In conclusion, Fra is a R8 cell-specific guidance receptor crucial for layer-specific R8 axon targeting in the medulla neuropil.

Chapter 4

The role of Netrins in regulating layer-specific R8 axon targeting

4.1 Introduction

Netrins are the activating ligands for the Fra/DCC/Unc-40 receptor (Kennedy et al., 1994; Mitchell et al., 1996; Hedgecock et al., 1990). Much is known about the function of the Netrin family of secreted axon guidance molecules at the midline in the nervous system of vertebrates and invertebrates, where they play a fundamental role in orchestrating axon guidance (Harris et al., 1996; Hedgecock et al., 1990; Ishii et al., 1992; Kennedy et al., 1994; Serafini et al., 1994). Netrins are secreted by floor plate cells in the vertebrate spinal cord and analogously by midline cells in *Drosophila* in the CNS.

In *Drosophila,* two Netrins namely *Netrin-A* (*NetA*) and *Netrin-B* (*NetB*) are encoded by two adjacent genetic loci. Studies in midline pathfinding suggest that they act redundantly, as single mutants for either *NetA* or *NetB* do not display aberrant commissures, while loss of both *NetA* and *NetB* results in strong disruptions in commissure formation (Brankatschk and Dickson, 2006).

We observed that the Fra receptor is required for controlling layer-specific targeting of R8 axons to the medulla neuropil layer M3. This leads to the question as to whether Netrins function as the activating ligands in layer-specific axon targeting in the medulla. In particular, Netrins could provide layer-specific information through a gradient that the incoming Fra-expressing R8 axons use to navigate during the final step of axon targeting to the M3 layer. Alternatively, Netrins could be localized exclusively to the M3 layer and in that way provide positional information. Furthermore, if Netrins are required for Fra mediated R8 axon targeting, the prediction is that loss of *NetA* and *NetB* should display similar targeting defects as loss of the *fra* receptor.

This chapter focuses on the question as to whether Netrins play a role in mediating layer-specific R8 axon targeting during development.

4.2 Results

4.2.1 Netrin expressing neurons in the optic lobe

Our studies in the laboratory in collaboration with W. Joly and I. Salecker first set out to establish as to whether NetA and NetB are expressed in the *Drosophila* optic lobe. To gain insights, as to which neuron subtypes are potential sources for Netrins, enhancer trap *Gal4* P element insertions into or close to the *NetA* and *NetB* genomic loci were analyzed in the pupal and adult optic lobe. A total of nine lines are available from the Drosophila Genetic Resource Center (DGRC), of which eight are inserted into the *NetB* genomic locus and one is inserted close to *NetA* and *NetB*.

Detailed analysis was performed using two enhancer trap insertions, *NP0831-Gal4* and *NP4151-Gal4*, with the membrane-tethered *UAS-cd8GFP* reporter as a read-out for the identification of the arborization pattern and cell body positions of the Netrin producing neurons. When *UAS-cd8GFP* was expressed under the control of *NP4151-Gal4*, expression was detected in the cell bodies and processes of lamina neurons L3, as well as medulla neuron subtypes, with layer-specific arborizations in the M1/M2 and M3 layers (Figure 16A, A'). In contrast, *NP0831-Gal4* activity is mainly restricted to lamina neurons L3 that have cell bodies located above the lamina neuropil and processes terminating in the M3 layer (Figure 16B, B'). This suggests, that medulla neuron subtypes and lamina neurons L3 might be important as potential sources for Netrins.

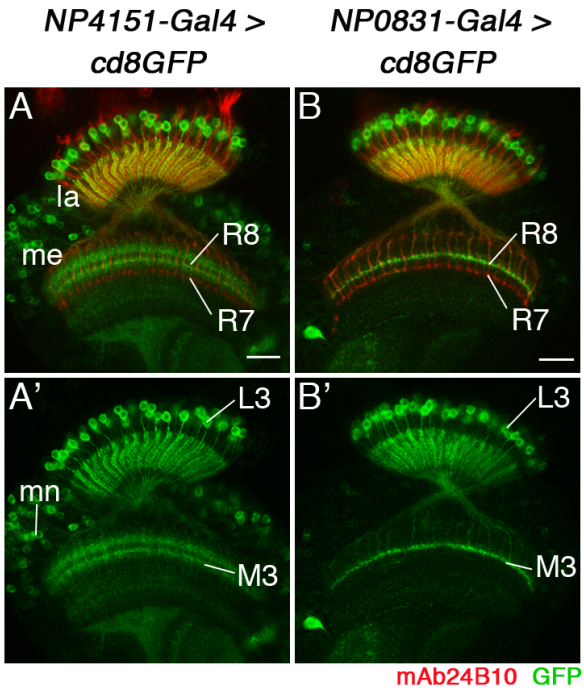

Figure 16. Analysis of the expression pattern of Netrin releasing neurons. (A-B) Expression of the *NP4151-Gal4* and *NP0831-Gal4* insertions in the adult optic lobe. (A, A') *NP4151-Gal4* drives GFP expression (green) in lamina neurons L3, which extend axonal terminals into the R8 recipient layer M3, and in medulla neuron subtypes (mn). (B, B') *NP0831-Gal4* is restricted to lamina neurons L3, which extend axonal terminals into the R8 recipient layer M3. R-cells are labeled with mAb24B10 (red). la, lamina, me, medulla. Scale bars are 20 μm.

4.2.2 NetB is dynamically expressed in the developing visual system with a strong localization to the emerging M3 layer

We next sought to determine where NetB protein is expressed within the optic lobe. Therefore wild type optic lobes were labeled with NetB antibody. This polyclonal antibody was directed against amino acids 294–312 of the NetB N-terminal domain (kindly provided by B. Altenhein) (Albrecht et al., 2011). As the NetB antisera were not available at the beginning of this project, the initial analysis of the NetB protein distribution was performed using Myc immunostaining in animals, in which *NetB* was replaced by C-terminal myc-epitope tagged *NetB* (*NetB*^{myc}, from Brankatschk and Dick-

son, 2006) (data generated by I. Salecker, not shown). These results were consistent with the following observations made using the NetB antibody.

Immunolabeling revealed a dynamic expression pattern during pupal development (Figure 17A-C') and low levels of expression in the adult (Figure 17D, D'). At 24 hours APF, NetB is expressed in the lobula (Figure 17A, A'). At 42 hours APF, R8 and R7 axons innervate their temporary layers in the medulla neuropil. NetB strongly accumulates in the emerging M3 layer between R8 and R7 axons (Figure 17B, B'). At 55 hours APF, NetB is highly enriched in the M3 layer (Figure 17C, C'). This coincides with the timing of R8 axon targeting to their final layer M3. Notably, NetB is in addition strongly expressed in the lobula from 24 hours APF and persists until 55 hours APF (Figure 17A-C'). Analysis of cross-sections of the retina revealed that NetB is not expressed on R-cell bodies or rhabdomeres, but in the surrounding pigment cells at 24 hours and 42 hours APF, but not at 55 hours (Figure 17E-G'). In contrast to the expression pattern observed using *NP4151-Gal4* insertion driving *UAS-cd8GFP* expression that labeled arborizations in the M1/M2 layers and the M3 layer, immunolabeling showed that the NetB protein mainly accumulated in the M3 layer.

Taken together, the endogenous NetB protein is temporally as well as spatially distributed in a way that is consistent with a role in guiding R8 axons to the M3 layer. More specifically these findings suggest that NetB could play a role in guiding R8 axons to the final recipient layer M3 during the second step of layer-specific axon targeting during pupal development.

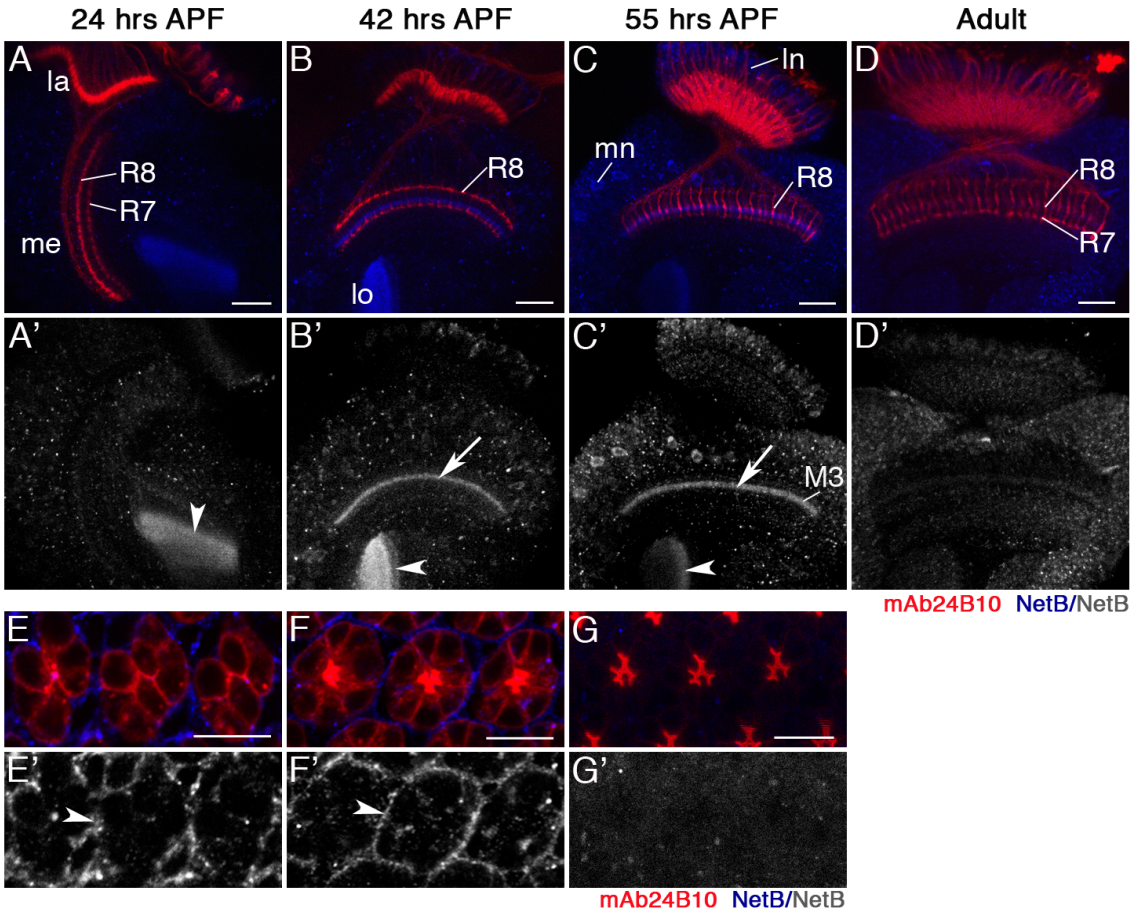

Figure 17. The secreted ligand NetB is localized in the M3 layer. (A-D) Wild type optic lobes at different pupal stages. Immunolabeling using a NetB antibody (blue) shows that this ligand is dynamically expressed in the medulla during pupal development. NetB is enriched in the emerging M3 layer at 42 and 55 hours after puparium formation (APF) (arrows in B' and C'). Lamina neurons (ln) and medulla neurons (mn) are producing the ligand (C). NetB is further expressed in the lobula at 24 hours, 42 hours and 55 hours APF (arrowheads in A', B', C'). R-cells are labeled with mAb24B10 (red). la, lamina, me, medulla, lo, lobula. (E-G) Cross-sections of the retina. NetB accumulates in pigment cells at 24 hours and 42 hours APF (arrowheads in E', F'). (E-G) NetB is not expressed on R-cell bodies or rhabdomeres during pupal development. Scale bars are 20 μm (A-D) and 10 μm (E-G).

4.2.3 NetA and NetB are expressed redundantly in a similar set of neurons

As a functional NetA antibody was not available, I next turned to the analysis of yellow fluorescent (YFP)-protein trap insertions to get insights into the expression of NetA (Ryder et al., 2009). These YFP-protein trap insertions were generated by insertion of an YFP exon flanked by a splice acceptor and a splice donor site into the coding sequence of NetA or NetB. Thus, the YFP is spliced into the mature mRNA resulting in potential NetA-YFP or NetB-YFP fusion proteins. As the expression is under the control of the endogenous promoter and enhancer elements, NetA and NetB expression patterns can be visualized.

This analysis revealed that both ligands are expressed in lamina neurons L3 and medulla neuron subtypes in likely overlapping patterns, with NetB more widely expressed than NetA (Figure 18A-H'). However, although YFP accumulation was detected in the cell bodies, it was not possible to visualize expression in the medulla neuropil layers. This is surprising, as one would expect that the *NetB-YFP* and *NetA-YFP* fusion proteins should be localized similarly as the endogenous protein that was visualized with the NetB antibody. Nevertheless, these findings show that NetA and NetB expression overlaps in L3 lamina neurons and medulla neurons. Therefore it is likely that these ligands act redundantly.

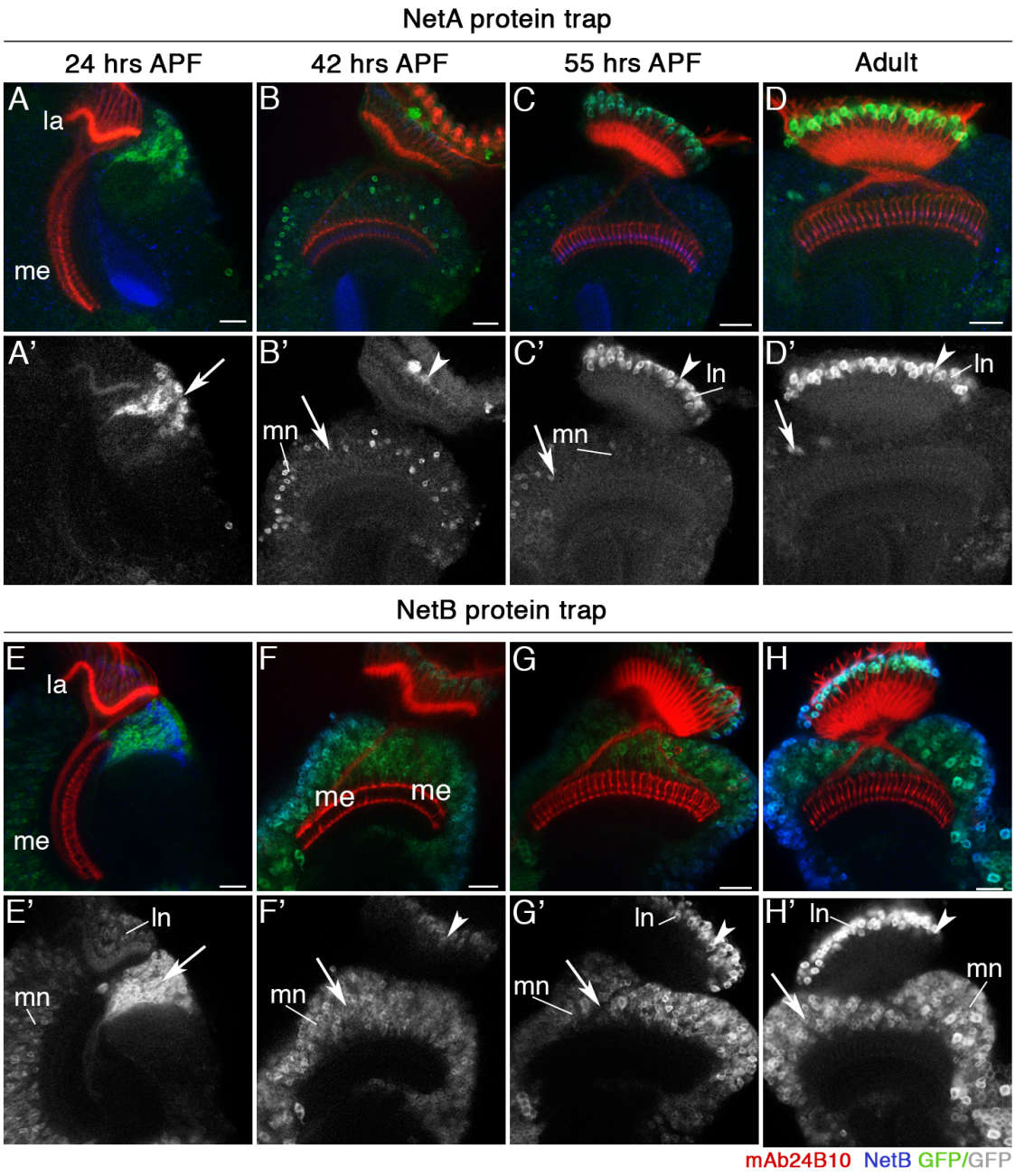

Figure 18. Analysis of YFP-protein traps show that NetA and NetB are expressed in a similar set of neurons. (A-D) NetA expression was analyzed using the protein trap transgenic fly line 115-271. NetA protein is expressed by lamina neurons (arrowheads in B', C') and medulla neuron subtypes (arrows in A', B', C'). (E-H) NetB expression was analyzed using the protein trap transgenic fly line 115-011. Similarly, NetB protein is expressed by lamina neurons (arrowheads in F', G') and medulla neuron subtypes (arrows in E', F', G'). la, lamina, me, medulla. Scale bars are 20 μm.

4.2.4 Netrins are required for R8 axon targeting to the M3 layer

If Netrins are required for M3 layer-specific targeting of R8 axons, loss of *NetA* and *NetB* should lead to similar defects as observed in R-cells mutant for *fra*. To test this possibility, $NetA^{\Delta}$ and $NetB^{\Delta}$ single, as well as $NetAB^{\Delta}$ double mutant adult flies were analyzed (data generated by W. Joly; Figures 19A-C'). *Rh6-lacZ* positive R8 axons targeted correctly to the M3 layer lacking either *NetA* or *NetB*, indicating that NetA and NetB act redundantly (Figure 19A-B'). In contrast, in hemizygous $NetAB^{\Delta}$ mutant males R8 axons aberrantly stalled at the medulla neuropil border (Figure 19C-C'). Detailed analysis of the phenotypes using the R8 cell specific marker *Rh6-lacZ* revealed that only a total of 47% of *Rh6-lacZ* positive R8 axons reach the M3 layer. 19.8% of R8 axons stall at the medulla neuropil border, 31.6% extend into the intermediate layers M1/M2 and 1.6% proceed to the R7 recipient layer M6. In conclusion, NetA and NetB are redundantly required for R8 axon targeting to the M3 layer.

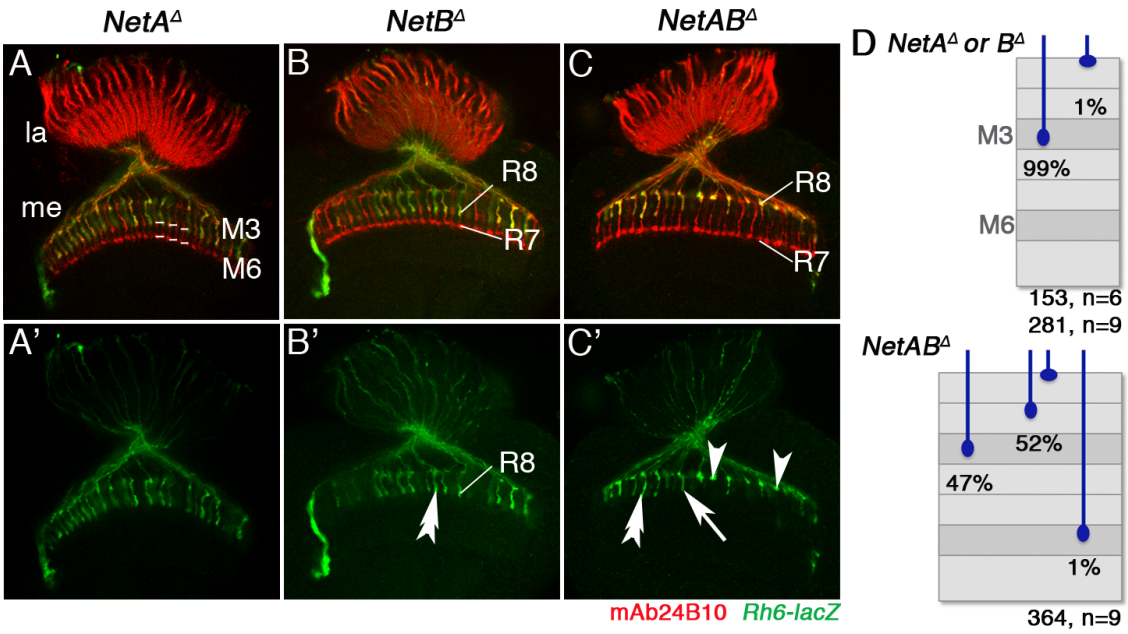

Figure 19. *NetA and NetB* are required for R8 axon targeting to the M3 layer. (A, B) In single mutants for *NetA*$^{\Delta}$ and *NetB*$^{\Delta}$, *Rh6-lacZ* positive R8 axons (green) target correctly to the M3 layer in the medulla neuropil (double-arrowheads). (C, C') In hemizygous *NetAB*$^{\Delta}$ males, R8 axons stall at the medulla neuropil border (arrowheads) or terminate prematurely in layers M1/M2 (arrows) instead of M3 (double-arrowheads). (D) Quantification of phenotypes. Scale bars are 20 μm. Data provided by W. Joly.

4.2.5 *NetA* and *NetB* are required in the target-associated neurons for layer-specific targeting

In mutants lacking *NetA* and *NetB* in the whole animal, R8 axons fail to innervate their target layer M3 and instead terminate at the medulla neuropil border or prematurely in the M1/M2 layers. Furthermore, the analysis of NetB protein expression strongly suggests a requirement in the target area for R8 axon targeting. To assess this, I performed loss-of-function studies of *NetA and NetB* using the RNAi and the *ey-FLP, act>>Gal4* FLPout approaches.

In RNAi knock-down experiments using *UAS-NetA*^{RNAi} and *UAS-NetB*^{RNAi}, NetA and NetB were removed either from (i) the eye, (ii) the eye and the target area, or (iii) the target area only by using variations of the *act>>Gal4* FLPout approach (Table 1,

Material and Methods) (Figure 20A-E'). *ey$^{3.5}$-FLP* activity is restricted to R-cells (Bazigou et al., 2007). In contrast, the *ey* enhancer is described to be active in the R-cells, as well as approximately 50% of the population of target neurons in the medulla (Morante and Desplan, 2008; Newsome et al., 2000). Furthermore, to restrict *ey* activity to target neurons only and prevent expression in R-cells, the *ey-FLP, act>>Gal4* FLPout approach was combined with the early active *ey$^{3.5}$-Gal80* and the late acting *lGMR-Gal80* transgenes that are expressed in R-cells thereby preventing *Gal4* activity in these cells.

As compared to controls (Figure 20A, A'), knock-down of *NetA* and *NetB* solely in the eye by using the *act>>Gal4* FLPout approach combined with the *ey$^{3.5}$-FLP* recombinase did not interfere with R8 axon targeting to the M3 layer (Figure 20B, B'). *Rh6-lacZ* labeled R8 axons target correctly to the M3 layer (Figure 20B, B', n=10).

In contrast, removal of *NetA* and *NetB* from the eye and target neurons using the *ey-FLP, act>>Gal4* FLP out approach (Figure 20D, D', n=8), or in the target area only using this approach in conjunction with *ey$^{3.5}$-Gal80* and *lGMR-Gal80* (Figure 20E, E', n=12), caused many R8 axons to remain at the border of the medulla neuropil.

This resembles the targeting defects observed in *NetAB$^{\Delta}$* double mutants. Thus, consistent with the expression pattern, *NetA* and *NetB* are functionally required in neurons in the medulla target area for layer-specific R8 axon targeting, but not in R8 axons themselves.

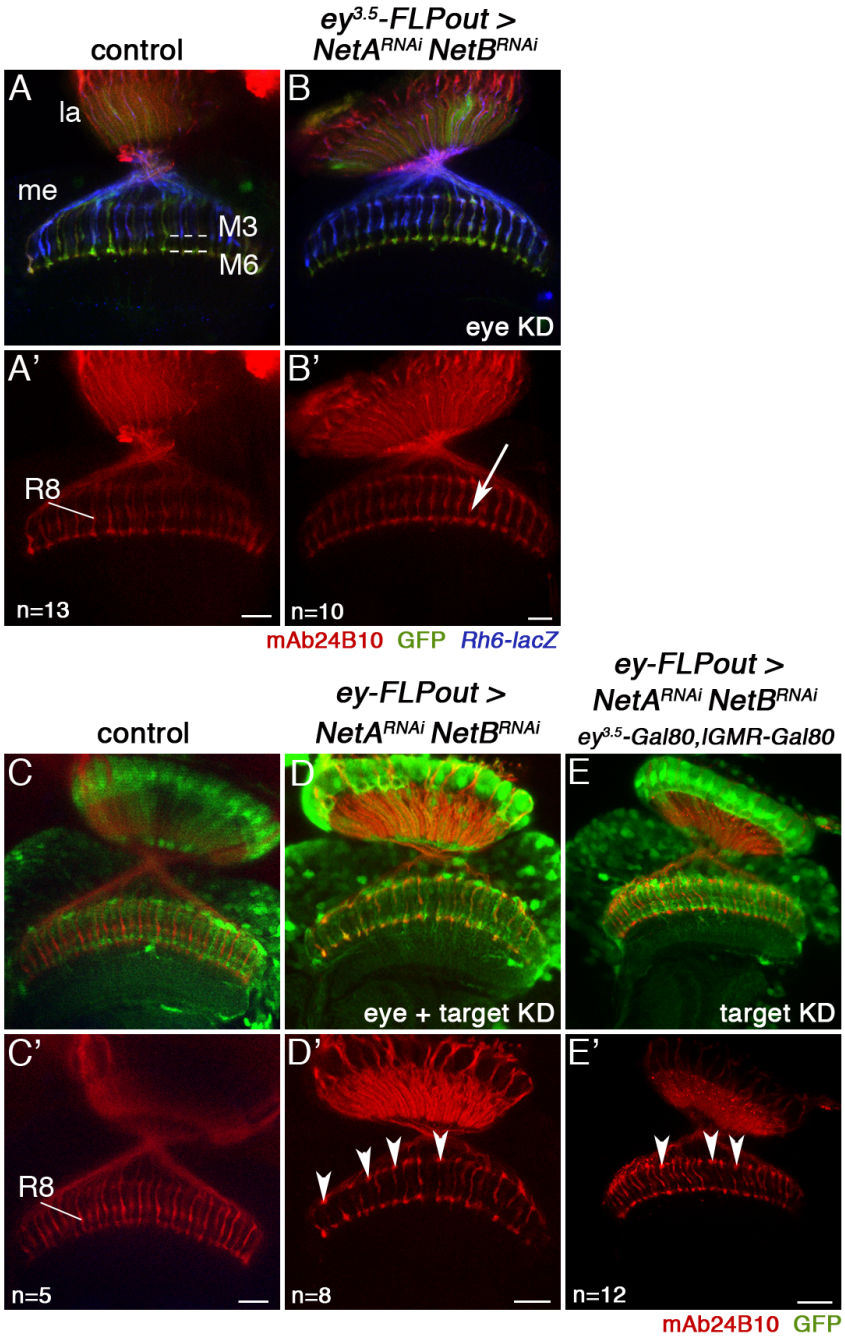

Figure 20. Knock-down of *NetA* and *NetB* in the eye and target neurons. (A-B) Adult optic lobes in wild type (A,A') and in a knock-down of *NetA* and *NetB* in the eye using *UAS-RNAi (UAS-NetA^{RNAi}* and *UAS-NetB^{IR})* and *ey$^{3.5}$-FLP, act>>Gal4* FLPout transgenes (B,B'). *Rh6-lacZ* positive R8 axons (blue) correctly target to the M3 layer (arrow in B'). GFP expression (green) indicates the areas of knock-down. la, lamina; me, medulla. R-cell axons are labeled with mAb24B10 (red). Dashed lines indicate the position of the M3 and M6 layers. (C-E) In animals, in which *NetA* and *NetB* have been knocked-down in the eye and the target area using *ey-FLP, act>>Gal4* FLPout, R8 axons stall at the medulla neuropil border (arrows in D,D') instead of terminating in the M3 layer as compared to wild type (C,C'). (E,E') Knock-down of *NetA* and *NetB* only in target neurons using the FLPout approach and *ey$^{3.5}$-Gal80* and *lGMR-Gal80* transgenes leads to comparable defects with R8 axons stalling at the medulla neuropil border (arrowheads in E,E'). Scale bars are 20 μm.

4.3 Discussion

4.3.1 Netrins are expressed in the M3 layer and mediate layer-specific R8 axon targeting

This chapter focused on the question as to whether Netrins are the functional ligands for Fra mediated R8 axon targeting to the M3 layer in the medulla. Netrins are expressed by lamina neurons L3 and medulla neuron subtypes in the optic lobe. As NetA and NetB likely function redundantly, in our studies the focus was on NetB due to the availability of the antibody that allowed visualizing NetB accumulation in several genetic backgrounds. NetB is dynamically expressed during the development of the optic lobe. More specifically, NetB is secreted by L3 lamina neurons and medulla neuron subtypes. Future studies need to determine the distribution of NetA protein in greater detail.

While the *NP4151-Gal4* and other enhancer trap P element insertions into the *NetB* genomic locus showed *UAS-cd8GFP* reporter expression in the M1/2 layers as well as the M3, analysis of the endogenous NetB protein using antibody revealed that it accumulates in the M3 layer. This raises the question, as to whether NetB is subcellularly localized and released in a precise way that would allow its accumulation in the M3 layer. This question will be addressed by experiments described in the next chapters.

Furthermore, we showed that *NetA* and *NetB* are redundantly required in the target neurons for correct layer-specific R8 axon targeting mediated through the Fra receptor. 53% of *Rh6-lacZ* positive R8 axons aberrantly stalled at the medulla neuropil border in $NetAB^{\Delta}$ homozygous mutant flies. Mutant analysis in studies at the midline in *Drosophila* have shown that despite the leading role of Netrins in commissural axon guidance, many commissural neurons are able to cross in the total absence of Netrins

(Brankatschk and Dickson, 2006; Evans and Bashaw, 2010). This argues for additional guidance systems possibly acting in parallel, which may also apply in the visual system of *Drosophila*.

Moreover, the penetrance of targeting defects observed in *NetAB*$^{\Delta}$ homozygous mutants is lower than that detected in mosaic animals lacking *fra* function in the R-cells, where 89% of *Rh6-lacZ* positive R8 axons terminated at the medulla neuropil border. This may point towards a role of Fra in regulating the activity of additional guidance determinants, as it was demonstrated in midline axon guidance in the embryonic CNS (Yang et al., 2009). In this study, Fra has been proposed to have two independent functions: (i) Netrin-mediated attraction towards the midline, and (ii) Netrin-independent transcriptional regulation of *comm*, which in turn prevents Robo localization in the growth cones thus inactivating Slit mediated repulsion (Yang et al., 2009). Therefore, Fra regulates an additional guidance system thus strengthening the attractive force by silencing repulsion. However, the ligand that is mediating this second function of Fra is not detected yet.

In the visual system, to date no such function for Fra has been uncovered. There is no evidence that *comm* is expressed or required for layer-specific targeting in the medulla neuropil. Alternatively, an additional ligand could mediate Fra attraction to the M3 layer. But there is no evidence so far that another ligand may exist. Therefore, identifying the downstream signaling mechanisms by which Fra induces attraction is important to be pursued in future experiments.

Chapter 5

Mechanisms of layer-specific Netrin localization

5.1 Introduction

The expression and precise localization of guidance cues is essential to enable growth cones to correctly navigate and target. In general, there are two possibilities as to how guidance cues convey information: at long-range in a gradient and at short-range when localized. Netrins are per se diffusible guidance cues providing guidance information by establishing a concentration gradient. *In vitro* growth cone turning assays provided substantial evidence that Netrins act in a graded fashion as axons turned towards the Netrin-1 cue several microns away from the source (Kennedy et al., 1994; Serafini et al., 1994). Recent studies provided further evidence that axons of commissural neurons within the embryonic spinal cord reach the ventral midline by following a gradient of Netrin-1 secreted by floor plate cells (Kennedy et al., 2006). In these studies, a graded distribution of Netrin-1 immunoreactivity was visualized *in vivo* in the embryonic chick spinal cord, further supporting the notion that Netrins act as long-range diffusible chemoattractants in axon guidance in the midline of vertebrates. In contrast, genetic analysis at the embryonic midline of *Drosophila* established that Netrins act as short-range attractants (Brankatschk and Dickson, 2006). In animals expressing a membrane-tethered NetB ($NetB^{TMmyc}$) instead of diffusible NetA and NetB, axon targeting was not affected. Therefore, NetB does not act in a graded fashion to guide commissural neurons at the *Drosophila* midline.

In the visual system, the mechanism that allows the secreted guidance cue Netrin to provide layer-specific information remains unclear. This leads to the question as to whether the target layer recognition of R8 axons depends on localized Netrins in the M3 layer or whether Netrins act in a graded fashion.

Our expression analysis showed that despite being a diffusible ligand, NetB is highly enriched in this narrow layer in the medulla neuropil. How can such localized

distribution be achieved? Studies in the embryonic CNS of *Drosophila* implicated Fra in capturing and re-localizing midline-derived Netrins along the dorso-lateral regions thus presenting localized Netrins to incoming axons (Hiramoto et al., 2000). Can target neuron derived Fra play a similar role in localizing Netrins in the M3 layer in the visual system?

Additionally, Netrins in the visual system might be released locally into the M3 layer, thus directly presenting layer-specific positional information. Our analysis of the Netrin expressing neuron population provided evidence that lamina neurons L3 and medulla neuron subtypes are the main source for Netrins in the medulla neuropil. Studies of the *NP4151-Gal4* and *NP0831-Gal4* insertions showed that Netrin-expressing neurons arborize in the M3 layer.

This chapter focuses on investigating the mechanisms that allow secreted NetB proteins to accumulate in the M3 layer. In particular, the experiments will address the question as to whether Fra in target-associated neurons is involved in the accumulation of NetB in the M3 layer and whether a local release by Netrin-positive target neurons can provide layer-specific positional information.

5.2 Results

5.2.1 Netrins act at short-range

Netrins are diffusible guidance cues that can act both at long-range in a gradient and at short-range when immobilized (Brankatschk and Dickson, 2006; Kennedy et al., 2006). To address as to whether the target layer recognition of R8 axons depends on localized NetB in the M3 layer, targeting was analyzed in flies, in which diffusible *NetB* was replaced by membrane-tethered *NetB* (*NetB*^{TMmyc}) at endogenous levels in a *NetA*$^{\Delta}$ mutant background using homologous recombination (Brankatschk and Dickson, 2006). R8 axon targeting is normal when solely *NetB*^{TMmyc} is available (Figure 21A-E, data generated by W. Joly, quantification by K. Timofeev). During initial targeting at 24 hours and 42 hours APF, a small percentage of R8 axons abnormally projected past the distal medulla neuropil border (Figure 21A, A', total of 162 R8 axons, n=6, and 21B, B', total of 164 R8 axons, n=6). At mid-pupal stages when R8 axons proceed to the final layer M3, projections were unaffected with 99% of R8 axons terminating correctly in the M3 layer (Figure 21C, C', n=5). Similarly in the adult, about 98% of R8 axons innervate the M3 layer (Figure 21D and E, total of 213 *Rh6-lacZ* positive R8 axons, n=9).

These findings are consistent with studies in the *Drosophila* embryo midline demonstrating that NetB in the visual system acts at short-range for providing target layer recognition of R8 axons.

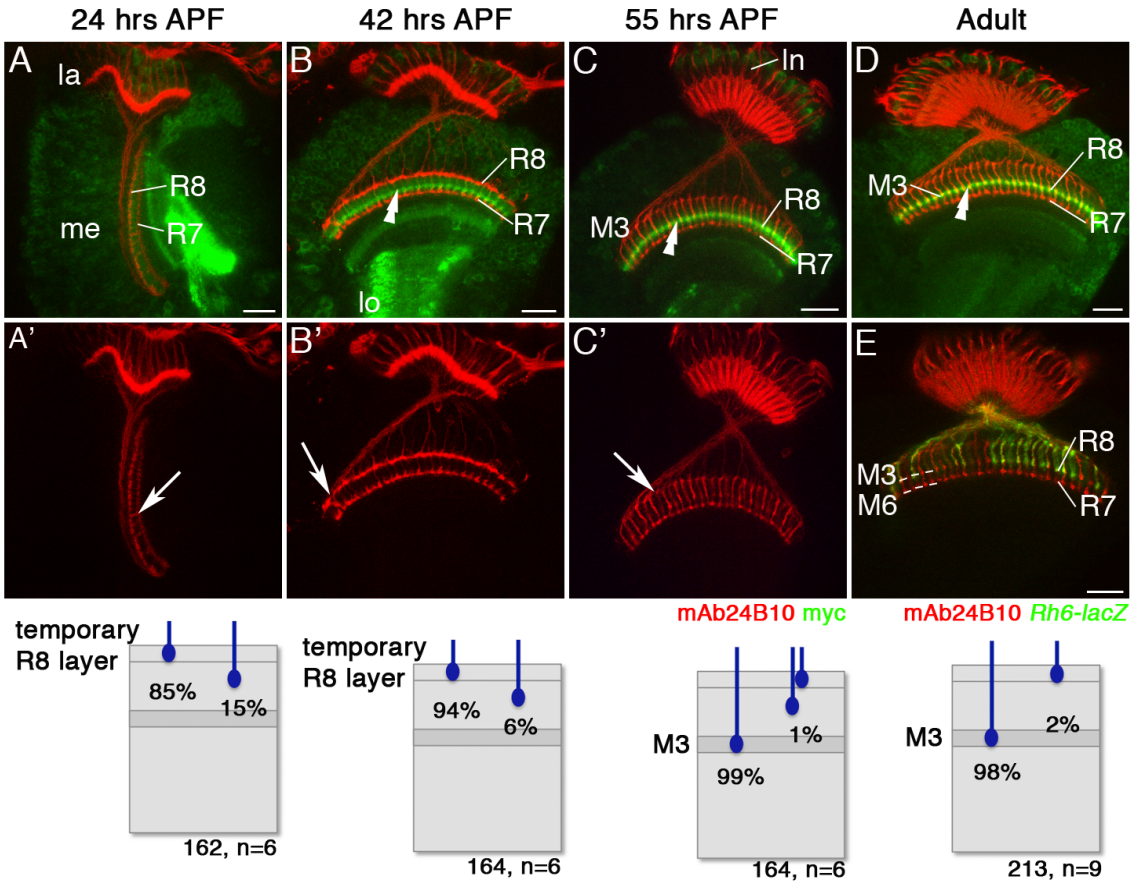

Figure 21. *NetB* acts at short-range. (A-D) Membrane-tethered myc-tagged *NetB* (green, $NetB^{TMmyc}$) replaces endogenous *NetB* in a $NetA^{\Delta}$ mutant background. $NetB^{TMmyc}$ is expressed by lamina neurons L3 and medulla neurons (mn), and enriched in the emerging and final M3 layer (asterisks in B,C,D). At 24 and 42 hr after puparium formation (APF), few R8 axons extend incorrectly past their temporary layer (arrows in A-B'). At 55 hr (C,C') and in adults (D-E'), R8 axons labeled with mAb2B10 (red) and *Rh6-lacZ* (green, E) correctly terminate in M3 (double-arrowheads, C-E'). Below are the quantifications of phenotypes. la, lamina; me, medulla; lo, lobula; lop, lobula plate. R-cells (red) are labeled with mAb24B10. Scale bars are 20 μm. Data provided by W. Joly.

However, considering that R8 axons terminate at the medulla neuropil border this poses the question as to how this distance to the NetB-positive layer M3 can be overcome to mediate short-range attraction. There are two possibilities one can imagine. Other guidance determinants guide R8 axons to the M3 layer independently, whereas the Fra/Net signaling provides a mechanism to maintain R8 axons in the M3 layer, once

they reached it. Alternatively, R8 axons could have the ability to bridge the distance. The question is as to how motile growth cone terminals of R8 axons are.

To assess the morphology of single R8 growth cones the Flybow *FB1.1* approach is a very useful multicolor cell-labeling tool (Hadjieconomou et al., 2011). This method facilitates single-cell labeling using the inducible modified FLP-FRT system and the Gal4/UAS binary system regulating the stochastic expression of one of four different membrane-tethered fluorescent proteins within one optic lobe. Using *FB1.1* in combination with the R-cell specific driver *pGMR-Gal4* allows visualizing R8 growth cone morphology with high resolution (Figure 22A-D, data generated by D. Hadjieconomou, I. Salecker). During pupal development at 42-44 hours APF, R8 growth cones are expanded along the distal medulla neuropil border as they pause in this temporary layer (Figure 22A). At 48-50 hours APF, they extend a single thin filopodium along the R7 axon shaft towards the NetB-positive emerging M3 layer (Figure 22B). From mid-pupal stages, R8 axons start extending to the final recipient layer M3. At 52-55 hours the part of growth cones at the medulla neuropil border decreased in size, while the filopodium increased in thickness to eventually develop into a mature axon terminal.

This observation that filopodial extensions of R8 axons can bridge the distance to the NetB-positive layer M3 provides a possible explanation as to how Netrins could mediate short-range interactions.

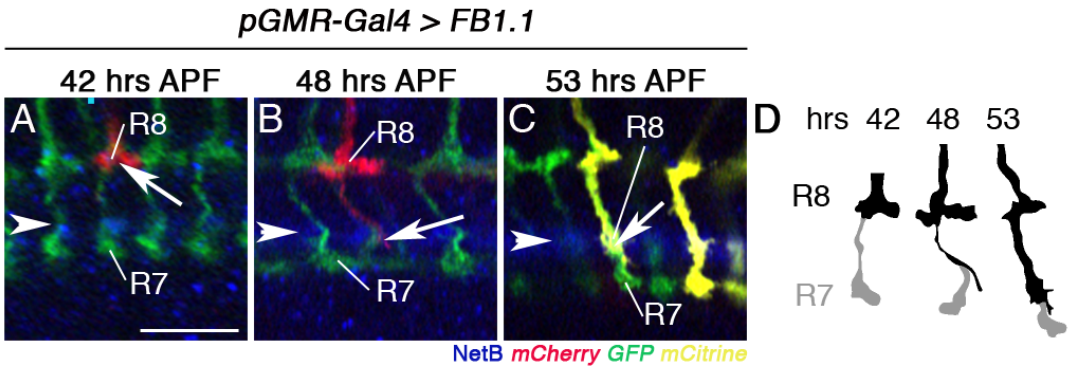

Figure 22. R8 axons bridge the distance to localized NetB in the M3 layer by extending filopodia. (A-C) R8 axons were labeled with *pGMR-Gal4* and *FB1.1* (red in A, B and yellow in C). NetB (blue) is accumulating in the emerging M3 layer (arrowheads). (A) At 42 hours APF, R8 growth cones terminate in the temporary layer at the medulla neuropil border (arrow). (B) At 48 hours APF, they extend a thin filopodium (arrow) along R7 axons towards the emerging M3 layer. (C) At 53 hours APF, R8 axons develop mature processes that innervate the M3 layer. Scale bars are 10 μm. (D) Drawing of R8 growth cone morphology during pupal development. Data and schematic provided by I. Salecker and D. Hadjieconomou.

5.2.2 Fra in target neurons localizes NetB in the M3 layer

Despite being a diffusible ligand, NetB accumulates in a very narrow layer in the wild type medulla neuropil. This leads to the question as to how such localized distribution can be achieved? Studies in the embryonic CNS of *Drosophila* implicated Fra in capturing and re-localizing Netrins (Hiramoto et al., 2000). Can Fra in target-associated neurons affect in the accumulation of NetB in the M3 layer in a similar way?

To visualize as to whether Fra can influence this accumulation of NetB, RNAi knock-down experiments using *UAS-fra*^{6RNAi} and the *act>>Gal4* FLP out approaches in combination with the *ey*$^{3.5}$*-FLP* or *ey-FLP* were performed (see Table 1, Material and Methods).

In these experimental approaches, NetB protein localization was visualized by labeling optic lobes at 55 hours APF using an antibody for NetB (Figure 23A-D). Immunofluorescence levels were determined using ImageJ and intensities of NetB staining

were represented with a heatmap (Figure 23A'-D'). Knock-down of *fra* solely in the eye by using the *act>>Gal4* FLP out approach under the control of the $ey^{3.5}$*-FLP* promotor did not interfere with the accumulation of NetB in the M3 layer (Figure 23B, B'). However, R8 axon targeting was severely affected with axons stalling at the medulla neuropil border (Figure 23B).

In contrast, when *fra* is removed from the eye and target neurons at the same time, using the *ey-FLP, act>>Gal4* FLP out approach, the NetB signal in M3 is decreased dramatically (Figure 23C, C'). Furthermore, knock-down of *fra* resulted in aberrant R8 axon targeting with R8 axons stalling at the medulla neuropil border. Therefore, the localization of NetB is likely due to Fra-positive neurons in the target area. However, one impediment is that Fra is also removed from the R-cells in this experimental paradigm which allows no conclusion about the requirement of target neuron associated Fra for layer-specific R8 axon targeting. To demonstrate that the reduction of NetB expression in the M3 layer is due to a requirement of *fra* in the target area, expression of the RNAi transgene *UAS-*fra^{6RNAi} in R-cells was prevented by using the *ey-FLP, act>>Gal4* FLP out approach in combination with $ey^{3.5}$*-Gal80* and *lGMR-Gal80*. As before the NetB signal is strongly decreased, but still present weakly in the M3 layer (Figure 23D, D'). Moreover, R8 axons target correctly to the M3 layer (Figure 23D).

This suggests that a Fra mediated ligand capture mechanism is likely to affect layer-specific accumulation of NetB.

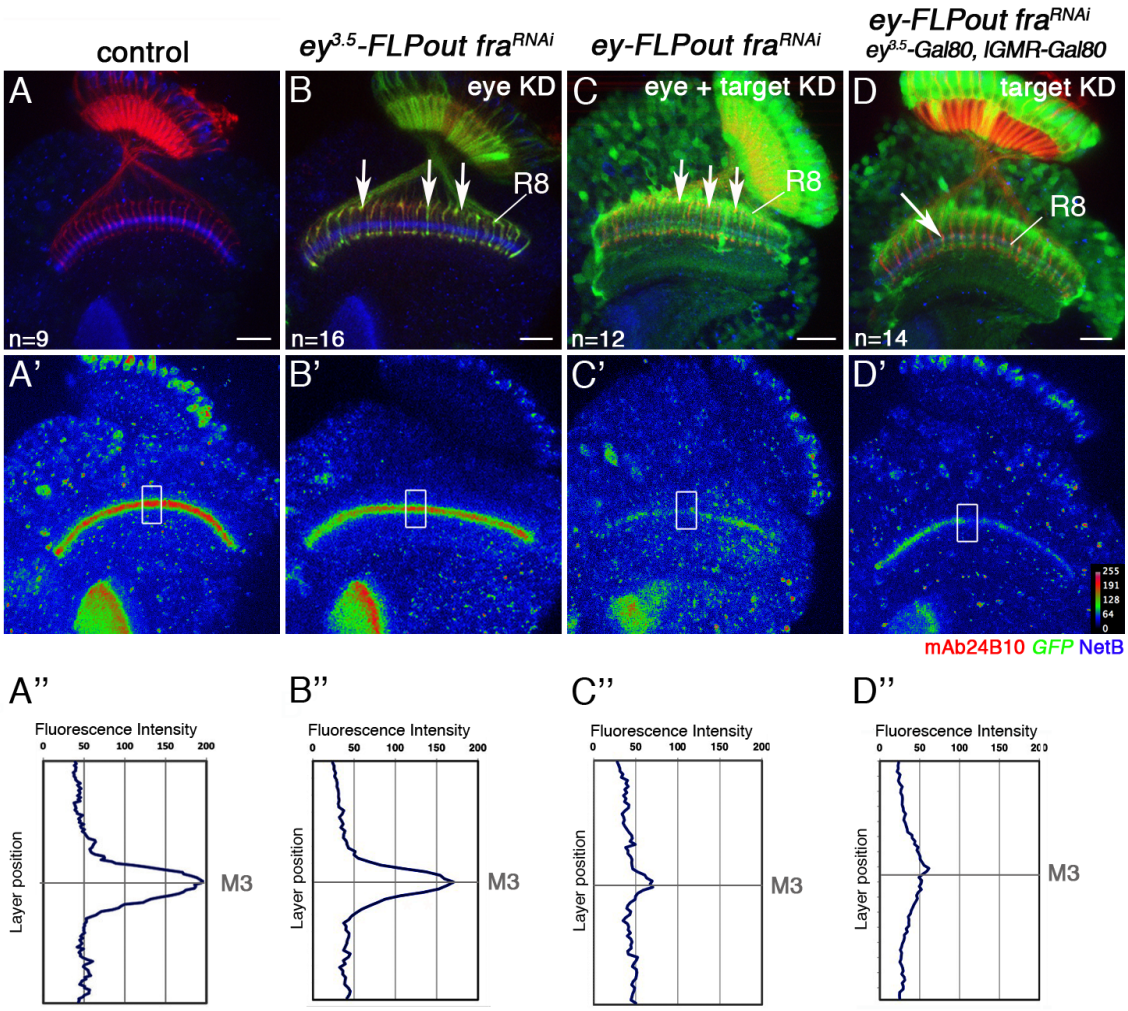

Figure 23. NetB localization in *fra* knock-down experiments. (A-D) Optic lobes at 55 hours APF. NetB is visualized using a polyclonal antibody. (A,A') In controls NetB is enriched in the M3 layer. R-cells are labeled with mAb24B10 (red). (A') NetB protein expression is shown in a heatmap plot based on intensities of NetB staining using ImageJ lookup table Rainbow RGB, with red indicating high levels of intensities to blue sindicating low levels (see scale for values). (A") Average NetB fluorescence intensities measured within indicated boxes (in A') are presented in the underlying graphs. (B,B') When knocking down *fra* in the eye using the *ey$^{3.5}$-FLP, act>>Gal4* FLPout approach, NetB is localized to the M3 layer. R8 axons show targeting defects and terminate at the border of the medulla neuropil (arrows in B). (C,C') In the *fra* knock-down in the eye and target area using the *ey-FLP, act>>Gal4* FLPout approach, the localization of NetB is dramatically decreased and R8 axons fail to innervate the M3 layer (arrows in C). (D,D') Using the *ey-FLP, act>>Gal4* FLPout approach in conjunction with *ey$^{3.5}$-Gal80* and *lGMR-Gal80* transgenes, *fra* was removed only in target neurons but remained in R-cells. The NetB signal is dramatically decreased. R8 axons target correctly to the M3 layer. Scale bars are 20 μm.

These data suggest that Fra, which is expressed by target neurons, prevents NetB from diffusion thus mediating its accumulation in the M3 layer. This was shown by experiments, in which *fra* was removed in target neurons. However, alternatively the diminished NetB signal could be due to a loss of the M3 layer, as *fra* mutant target neurons might not be able to innervate this layer.

To exclude this alternative possibility, I used an independent marker, the non classical cadherin Flamingo (Fmi) to label the M3 layer in optic lobes of flies, in which *fra* has been knocked-down in the eye or in the eye and in the target area. At 55 hours APF, in control optic lobes Fmi localizes to several layers in the medulla neuropil including the M3 layer (Figure 24A, A'). Knock-down of *fra* in the eye using the *act>>Gal4* FLP out approach under the control of the $ey^{3.5}$*-FLP* did not alter layer-specific Fmi expression or NetB localization to the M3 layer (Figure 24B-B"). In animals, in which *fra* has been knocked-down in the eye and the target area, Fmi expression in the M3 layer was unaffected, while the NetB signal was reduced as compared to control siblings (Figure 24A-A" and C-C"). This excludes the possibility that the layer-specific NetB accumulation is decreased because the M3 layer failed to form.

Moreover, Fmi also labels a layer in the lobula (Figure 24A). Interestingly, in the *fra* knock-down in the eye and target area, Fmi expression is in addition present in the lobula plate suggesting that targeting of higher-order neurons may be affected (Figure 24C).

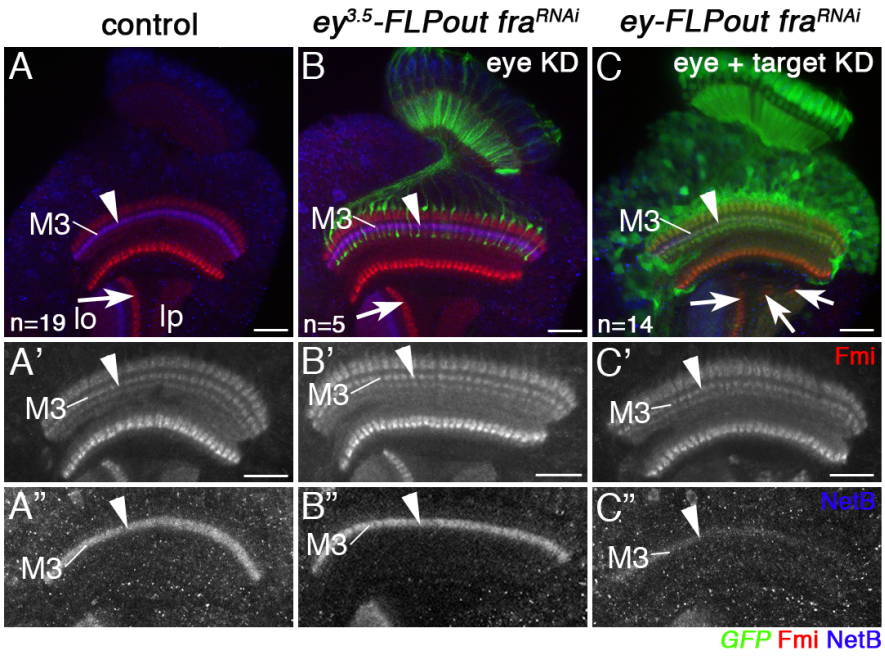

Figure 24. Fmi localization in *fra* knock-down experiments. (A-C) Optic lobes at 55 hours APF. Fmi and NetB are visualized using antisera. (A-A") In controls NetB is enriched in the M3 layer (arrowheads). The M3 layer is labeled independently using Fmi as a marker (red). (B-B") In flies, in which *fra* has been knocked-down in the eye using *ey$^{3.5}$-FLP, act>>Gal4* FLPout approach NetB and Fmi are expressed in the M3 layer (arrowheads). (C-C") In the *fra* knock-down in the eye and target area using the *ey-FLP, act>>Gal4* FLPout approach, the localization of NetB is dramatically decreased while co-labeling with Fmi confirms that the M3 layer (arrowhead) has formed normally. (A-B) Fmi is detected within a layer in the lobula (arrow in A, B). (C) Fmi expression is also present in the lobula plate (arrows). Scale bars are 20 μm.

As a second line of evidence, to show that Fra prevents the diffusion of NetB, I analyzed NetB localization in animals solely expressing membrane-tethered myc-tagged *NetB* (*NetB^{TMmyc}*), while *fra* has been knocked-down in the target. If Fra normally prevents diffusion, accumulation of *NetB^{TMmyc}* would not be affected in the target knock-down of *fra*. However, if in the absence of Fra in target neurons the M3 layer does not form, *NetB^{TMmyc}* would not be accumulated in the M3 layer.

As a control experiment, findings by W. Joly in our laboratory showed that using a diffusible *NetB^{myc}* transgene, NetB accumulation is decreased upon knock-down of *fra* using the *ey-FLP, act>>Gal4* FLPout approach. This was confirmed in the following

experiment showing that secreted NetB localization in the M3 layer is significantly decreased in the absence of Fra in R-cells and target neurons as compared to controls (Figure 25A-B").

Finally, using the *ey-FLP, act>>Gal4* FLPout approach in conjunction with $ey^{3.5}$-*Gal80* and *lGMR-Gal80* transgenes, *fra* was removed only in target neurons but remained in R-cells. Strikingly, the membrane-tethered $NetB^{TMmyc}$ is localized to the M3 layer despite the removal of *fra* in target neurons (Figure 25C, C'). Moreover, this shows that in the absence of Fra in target neurons, the M3 layer is able to form normally. R8 axons target correctly to the M3 layer. Consequently, Fra is required in target neurons to prevent the diffusion of NetB.

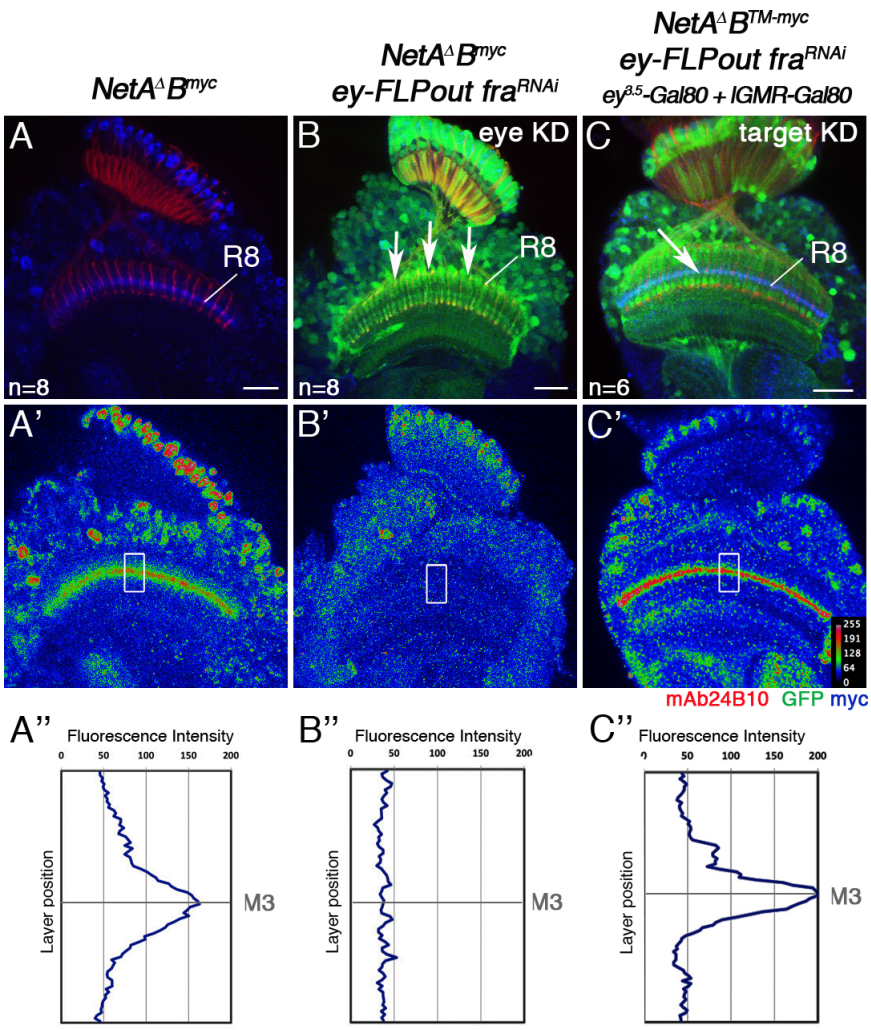

Figure 25. Membrane-tethered NetB^{TMmyc} localization in *fra* knock-down experiments. (A-B) Optic lobes at 55 hours APF. *NetA$^{\Delta}$B^{myc}* transgene is used to visualize NetB. (A, A') In controls *NetB^{myc}* is enriched in the M3 layer. R-cells are labeled with mAb24B10 (red). (A') NetB protein expression is shown in a heatmap plot (see scale for values). (A") Average NetB fluorescence intensities measured within indicated boxes (in A') are presented in the underlying graphs. (B, B') In the *fra* knock-down in the eye and target area using the *ey-FLP, act>>Gal4* FLPout approach, the localization of NetB is dramatically decreased and R8 axons fail to innervate the M3 layer (arrows in B). (C, C') Using the *ey-FLP, act>>Gal4* FLPout approach in conjunction with *ey$^{3.5}$-Gal80* and *lGMR-Gal80* transgenes, *fra* was removed only in target neurons but remained in R-cells. The membrane-tethered *NetB^{TMmyc}* is localized to the M3 layer despite the removal of *fra* in target neurons. R8 axons target correctly to the M3 layer. Scale bars are 20 μm.

Although layer-specific distribution of NetB was significantly reduced, it was not completely abolished. To assess the efficiency of the *fra* knock-down, Fra immunolabeling was used to analyze Fra protein expression (Figure 26A-B'). This showed that

fra is efficiently removed from the subpopulation of neurons that normally express it (Figure 26B'): levels of Fra in the medulla, including the M3 layer, are strongly decreased. Levels of Fra in glial cells in the lamina are not affected, as this *FLPout* approach is not effective in these cells.

Taken together, as *fra* is significantly removed in the target neurons, the data provided thus far support the notion that Fra plays a role in localizing NetB by preventing diffusion. However, in the *fra* knock-down in target neurons, while NetB signal is significantly diminished it is not completely abolished and still expressed in the M3 layer. This indicates that a second mechanism might be involved in localizing NetB in the M3 layer.

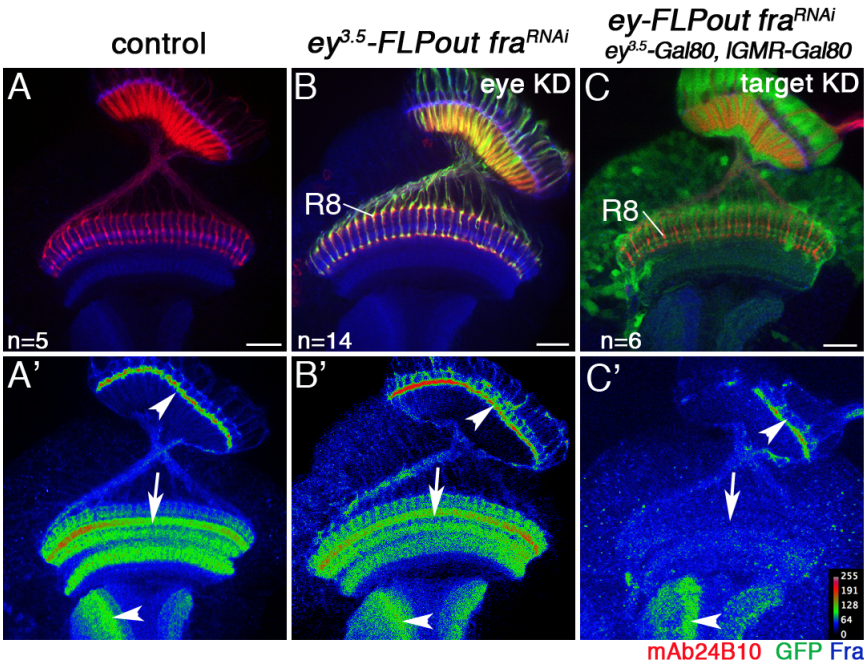

Figure 26. Expression of Fra in target neurons. (A-B) Optic lobes at 55 hours APF were analyzed for Fra expression using a polyclonal Fra antibody (blue). (A, A') In controls Fra is enriched in the M3 layer (arrow in A,A'). (A') Fra protein expression is shown in a heatmap plot (see scale for values). Fra expression is also detected in glia in the lamina and in arborizations in the lobula (arrowheads in A'). R-cells are labeled with mAb24B10 (red). (B, B') Using the *ey-FLP, act>>Gal4* FLP out approach in conjunction with *ey$^{3.5}$-Gal80* as well as *lGMR-Gal80*, *fra* was removed only in target neurons but remained in R-cells. Staining with a polyclonal Fra antibody indicated that *fra* in this genetic background is strongly reduced (arrow in B'). Expression is still detected in glia and also in arborization if the lobula (arrowheads in B'). Scale bars are 20 μm.

5.2.3 Cell-based binding assays to analyze Fra and Netrin in a ternary complex

So far our findings indicate that Fra has a dual function in mediating layer specific R8 axon targeting. It is (i) expressed and required in R8 cells and (ii) Fra is expressed in target associated medulla neuron subtypes and required to capture and localize NetB to the M3 layer. This raises the question as to how Fra can mediate both functions by binding to NetB. Therefore, to gain insights into the dynamics of Fra and NetB interactions, I turned to cell-based assays. I asked, as to whether Fra is required to prevent diffusion by a ternary complex or by a more dynamic mechanism, in which target derived Fra captures NetB temporally. Studies published so far showed interactions of these molecules in *in vitro* assays for the vertebrate counterparts Netrin-1 and DCC (Hong et al., 1999; Keino-Masu et al., 1996; Stein et al., 2001). However, these studies did not address as to whether DCC can bind Netrin-1 in trans in a ternary complex.

We therefore developed cell-based assays to gain insights into the binding properties of *Drosophila* Fra and NetB and to test whether these determinants can form a ternary complex in trans. To test as to whether two Fra molecules can bind one NetB molecule in trans, one has to use two differently labeled Fra molecules that together with NetB may allow visualizing a ternary complex. For that purpose, we used a full-length transmembrane Fra receptor that was expressed in cells and localized to the membrane. This can be detected using the Fra antibody that was directed against a 278 amino acid long fragment in the C-terminal domain of Fra (Kolodziej et al., 1996). To distinguish the interaction in cis and in trans, the second Fra molecule has been truncated lacking its intracellular and transmembrane domains. The extracellular domain of Fra is expected to be soluble in the conditioned medium. This fragment has been additionally tagged with HA as a marker. The prediction is that when NetB is added to the

Fra-expressing cells it should bind to its receptor. The truncated Fra molecule should then bind to NetB if a ternary complex is formed.

To conduct these experiments, we generated the following *Drosophila* Fra and NetB constructs: Fra^{Fl} is the construct of the full-length Fra transmembrane receptor (Figure 27A). The secreted $NetB^{V5}$ construct was tagged using V5 at the C-terminus, as the antibody for NetB was initially not available (Figure 27A). The secreted $Fra^{ECD\text{-}HA}$ construct was generated by deletion of the membrane and intracellular region and tagged with HA (Figure 27A). To test as to whether the truncated $Fra^{ECD\text{-}HA}$ is functional and able to bind NetB, a membrane-tethered $NetB^{cd8}$ was generated and tested in binding assays with $Fra^{ECD\text{-}HA}$. Membrane-tethered $NetB^{cd8}$ was tagged using V5 at the C-terminus and contained an additional *Cerulean* sequence between the *cd8* membrane tag and the V5 tag as a spacer (Figure 27A, the *cd8-Cerulean-V5* construct was provided by D. Hadjieconomou).

To enable the expression of the above described proteins in *Drosophila* S2 or S2R+ Schneiders cells these fragments were subcloned into inducible *pMT* vectors. Western Blot analyses confirmed their expression (Figure 27B, C). Specific antibodies for the V5 and HA tags or the Fra antibody, that recognizes Fra^{Fl} only, were used. Cell lysates of S2R+ were used to detect the molecules that are localized in the membrane. The transmembrane constructs of $NetB^{cd8}$ and Fra^{Fl} were correctly present in the cell lysates. Secreted $NetB^{V5}$ accumulated also in the cell lysate (Figure 27B). In addition, conditioned medium was collected to test the fraction containing the molecules that are secreted. This showed that NetB and $Fra^{ECD\text{-}HA}$ were indeed secreted into the conditioned medium (Figure 27C). Unexpectedly, Fra^{Fl} was also found in the conditioned medium (Figure 27C). However, as this experiment was not repeated this could be an artifact possibly due to that the fractions were not properly purified before the Western

Blot analysis. Nevertheless, this analysis showed that the different constructs are expressed in S2 and S2R+ cells and can be detected using specific antibodies.

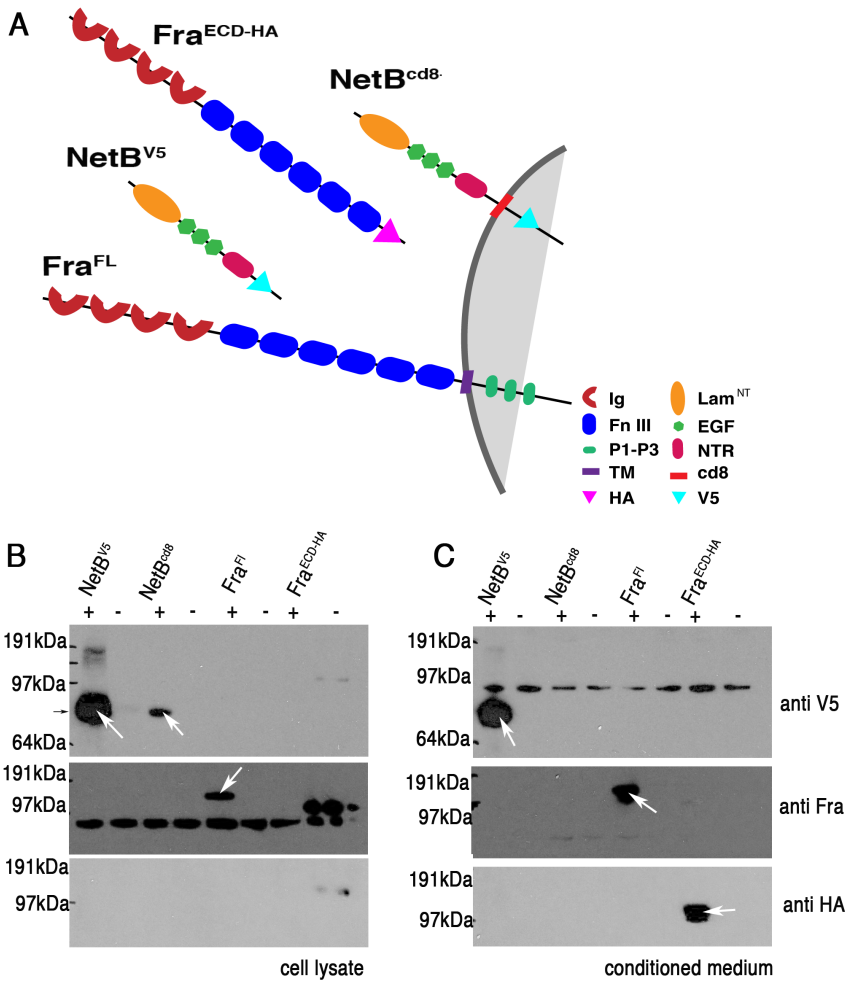

Figure 27. *NetB*^{V5}, *NetB*^{cd8} and *Fra*$^{ECD-HA}$ and *Fra*^{Fl} constructs used in cell-based assays. (A) Schematic of the constructs cloned and used in cell-based assays. Ig, Immunoglobulin domain, Fn III, Fibronectin type III domain, P1-P3, P1-P3 domains, TM, transmembrane domain, HA, HA tag, Lam^{NT}, laminin N-terminal domain, EGF, epidermal growth factor domain, NTR, C-terminal Netrin-like domain, cd8, cd8 transmembrane domain, V5, V5 tag. (B-C) Western blot analyses of S2R+ cells transfected with *NetB*^{V5}, *NetB*^{cd8} and *Fra*$^{ECD-HA}$ and *Fra*^{Fl} constructs. (B) Cell lysates. Secreted *NetB*^{V5} (arrow in B, a correct band is detected with the anti-V5 antibody at 87 kDa). The transmembrane constructs of *NetB*^{cd8} and *Fra*^{Fl} are correctly present in the cell lysates. Fra is detected with a polyclonal antibody (arrow in B, band at 152 kDa). (C) Conditioned medium. NetB (arrow in C, band at 87 kDa) and truncated *Fra*$^{ECD-HA}$ (arrow in C, using the anti-HA antibody a band at 124 kDa was detected) are present in the conditioned medium. *Fra*^{Fl} is also found in the conditioned medium (arrow in C, band at 152 kDa).

In a cell-based binding assay, I next analyzed as to whether secreted NetB can bind Fra expressed in R+ Schneider cells. NetB protein was collected and concentrated from the conditioned medium of S2 cells transfected with the *NetB*^{V5} construct. The binding abilities were examined over a period of 8 hours after an initial binding period (see Material and Methods) and visualized by specific antibodies. However, although *NetB*^{V5} can be detected in Western blot analysis using the V5 antibody, visualization in cells was unsuccessful. Therefore, *NetB* was subsequently detected using a polyclonal antibody raised against the N-terminus of NetB (Albrecht et al., 2011). As both NetB and Fra antibodies are raised in rabbits, it was initially not possible to visualize Fra and NetB positive cells simultaneously (data not shown). I therefore turned to the *Fra-GFP* construct (generated by W. Joly) for the binding assays. This binding assay was performed in the presence of Heparin, which reduces background binding of NetB as described in previous studies (Keino-Masu et al., 1996).

For the assay, NetB was allowed to bind to full-length *Fra-GFP* expressed in R+ cells for 2 hours and then cells were washed 3x with *Drosophila* Schneider's medium to remove remaining NetB that is not bound to Fra. Cells were maintained after washing in the medium in separate wells and fixed at several different time points. I observed that *Fra-GFP* is localized to the cell membrane of transfected cells and expression persists for the duration of the experiment (Figure 28A-E"). I observed that *Drosophila* Fra binds efficiently to NetB that was concentrated from conditioned medium as represented by the time point '0 hours' that shows a binding of NetB to Fra immediately after the 2 hours binding period (Figure 28A', A"). For the different time points, images of cells were collected using confocal microscopy and the fluorescence intensities of *Fra-GFP* and NetB signals were measured using ImageJ, whereby 10 different filopodial extensions of 10 cells were measured and averaged per time point. This experiment

showed that NetB is firmly bound to Fra for at least 4 hours (Figure 28B'-C' and B"-C"). 6 to 8 hours after binding, the NetB fluorescent signal is reduced indicating that NetB binding is decreased (Figure 28D'-E' and D"-E"). This showed that *Drosophila* NetB can bind the Fra receptor in cell based assays and the binding persist for several hours.

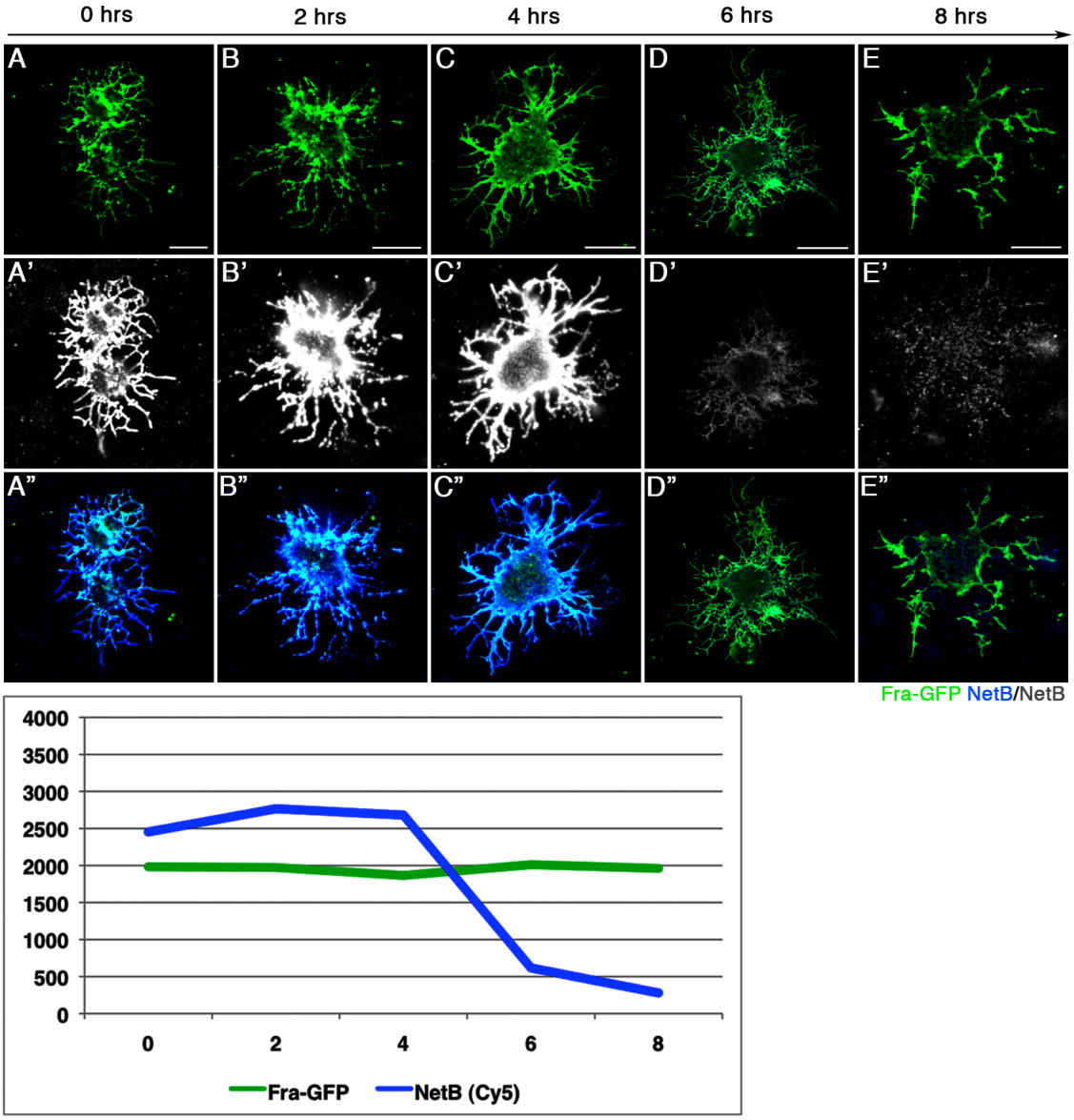

Figure 28. Cell assays to demonstrate binding of Fra and NetB. (A-E") Confocal images of S2R+ cells expressing *Fra-GFP* that have $NetB^{V5}$ bound on the cell surface. $NetB^{V5}$ signal is detected using a polyclonal antibody raised against NetB and a secondary antibody conjugated with Cy5 fluorescent dye. *Drosophila Fra-GFP* can bind $NetB^{V5}$ concentrated from conditioned medium (CM) in the presence of 50 μg/ml Heparin. After an initial binding for 2 hours, cells were washed and cells in different wells were

fixed at several time points. Experiments were performed over a period of 8 hours after initial binding. Scale bars are 10 μm.

Next, to test as to whether a stable ternary complex in trans may be formed, R+ cells were transfected with transmembrane *Fra-GFP* and exposed to secreted $NetB^{V5}$ and secreted $Fra^{ECD\text{-}HA}$ collected from conditioned medium of transfected S2 cells. The idea was that a full-length Fra receptor captures NetB from the conditioned medium, which in turn could bind $Fra^{ECD\text{-}HA}$.

Although I observed that Fra-GFP can efficiently bind NetB in conditioned medium in the presence of Heparin (Figure 29A, C), a binding of $Fra^{ECD\text{-}HA}$ was not detectable above background levels when compared to untransfected control cells (Figure 29D).

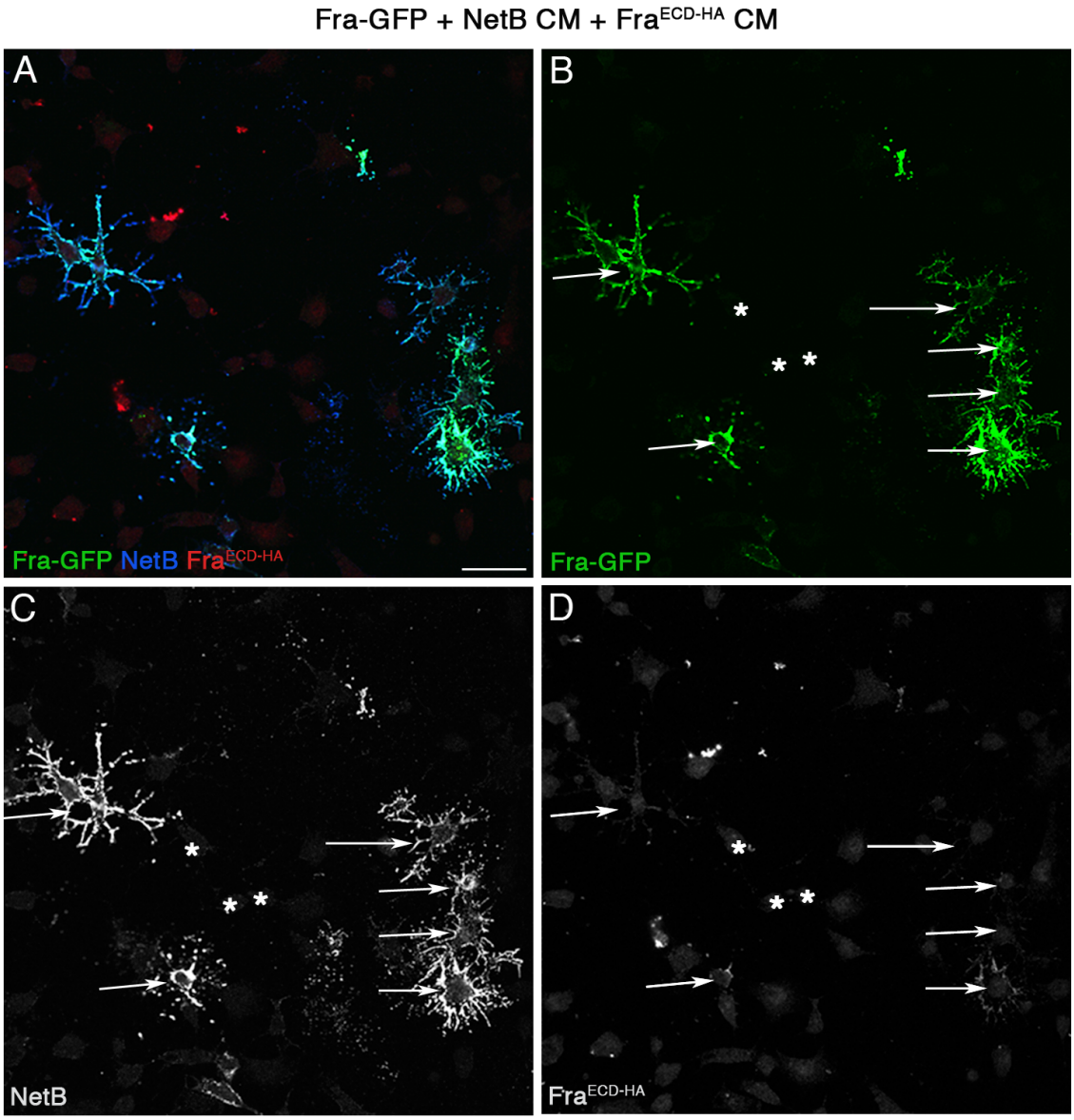

Figure 29. Cell assays to demonstrate a binding of *Fra-GFP* to *NetB^{V5}* and *Fra^{ECD-HA}*. (A,B) Confocal images of S2R+ cells expressing *Fra-GFP*. (A, C) *NetB^{V5}* was collected from CM, and applied to *Fra-GFP* expressing cells. *NetB^{V5}* signal is clearly detected using a polyclonal antibody (arrow in C). (B-D) Asterisks indicate untransfected Fra-negative cells and serve as controls. (A, D) *Fra^{ECD-HA}* was collected from CM, and applied. *Fra^{ECD-HA}* was detected using an antibody against HA tag. *Fra^{ECD-HA}* is not able to bind in a ternary complex above background levels (arrows in D). Experiment was repeated 7 times, with a total number of 294 cells analyzed. Scale bars are 20 μm.

Therefore, to verify the binding abilities of *Fra^{ECD-HA}*, membrane-tethered *NetB^{cd8}* was expressed in R+ cells. These were subsequently exposed to concentrated conditioned medium from S2 cells transfected with *Fra^{ECD-HA}* either in the presence or ab-

sence of Heparin. Again, *Fra*$^{ECD\text{-}HA}$ was not able to bind *NetB*^{cd8}. No signal was detected above background levels (Figure 30A-A"). As a control, *Fra*$^{ECD\text{-}HA}$-positive S2 cells were fixed and analyzed under the same conditions (Figure 30B-B'). *Fra*$^{ECD\text{-}HA}$ expression can be specifically detected in *Fra*$^{ECD\text{-}HA}$-positive cells, when compared to untransfected cells (Figure 30B'). This indicates that the truncated *Fra*$^{ECD\text{-}HA}$ is generated by cells, but unable to bind to NetB when it is concentrated from the conditioned medium.

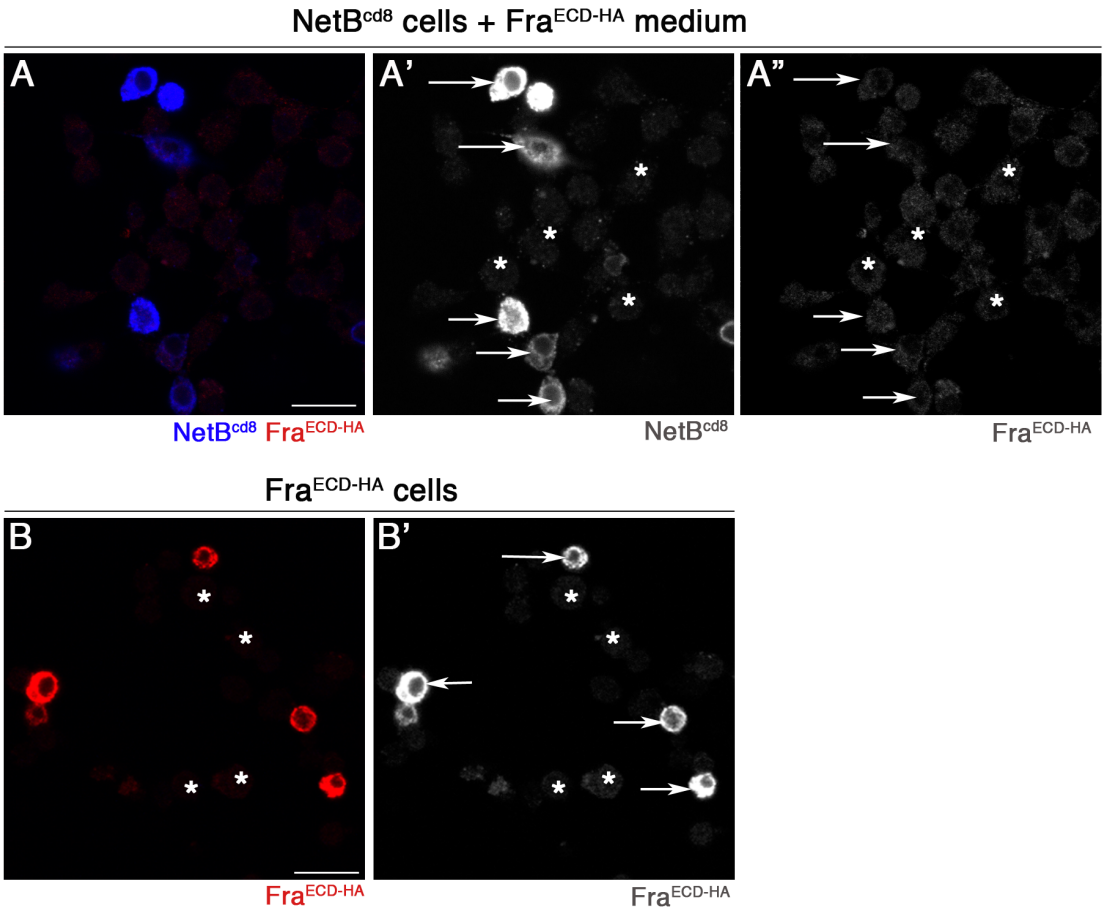

Figure 30. Cell assays to demonstrate binding of *Fra*$^{ECD\text{-}HA}$ and *NetB*^{cd8}. (A,A') Confocal images of S2R+ cells expressing *NetB*^{cd8}. *NetB* signal is clearly detected using a polyclonal antibody (A,A") *Fra*$^{ECD\text{-}HA}$ was collected from CM, and applied to *NetB*^{cd8} expressing cells. *Fra*$^{ECD\text{-}HA}$ does not bind *NetB*^{cd8} above background levels (arrows in A' indicate *NetB*^{cd8} positive cells, asterisks mark untransfected control cells). The experiment was repeated 8 times, with a total number of 310 cells analyzed. (B, B') Confocal images of S2 cells expressing *Fra*$^{ECD\text{-}HA}$ (arrows in B' mark *Fra*$^{ECD\text{-}HA}$ positive cells, asterisks mark untransfected control cells). Scale bars are 20 μm.

The data so far showed that full-length Fra is able to bind NetB from conditioned medium. Unfortunately, it was not possible to visualize a ternary complex, likely because of the inability of $Fra^{ECD\text{-}HA}$ to bind to NetB. In an alternative approach, I tried to determine as to whether two different populations of cells expressing full-length Fra are able to attract each other in the presence of NetB. For this purpose, a new full-length Fra construct was generated, in which Fra was tagged with the fluorescent marker *Cherry*, for *Fra-Cherry* expression in R+ cells. In this assay, Fra-GFP positive cells were exposed to NetB in the conditioned medium for 2 hours (as described before) and washed with medium. Subsequently, 'naïve' Fra-Cherry cells were added and allowed to interact for 4-5 hours. Fixed samples were then monitored for clusters between Fra-Cherry cells with Fra-GFP cells. I observed that Fra-GFP and Fra-Cherry cells form clusters in both, the absence and presence of NetB (Figure 34 A and B). The experiment was repeated with sparsely plated cells at a density of 0.25 x 10^5 /ml instead of the usual 0.5 x 10^5 /ml, expecting that if NetB, which is bound on Fra-GFP at the cell surface has an instructive role for attracting cells, Fra-Cherry cells should migrate specifically to this source. However, I could not detect increased clustering or strongly overlapping filopodia as compared to the control. Therefore, I cannot exclude that Fra-GFP and Fra-Cherry cells randomly clustered because they were in close proximity from the onset of the experiment. Preliminary analysis using DeltaVision microscopy for live cell imaging suggested that although S2R+ cells motile, they are not actively migrating (data not shown).

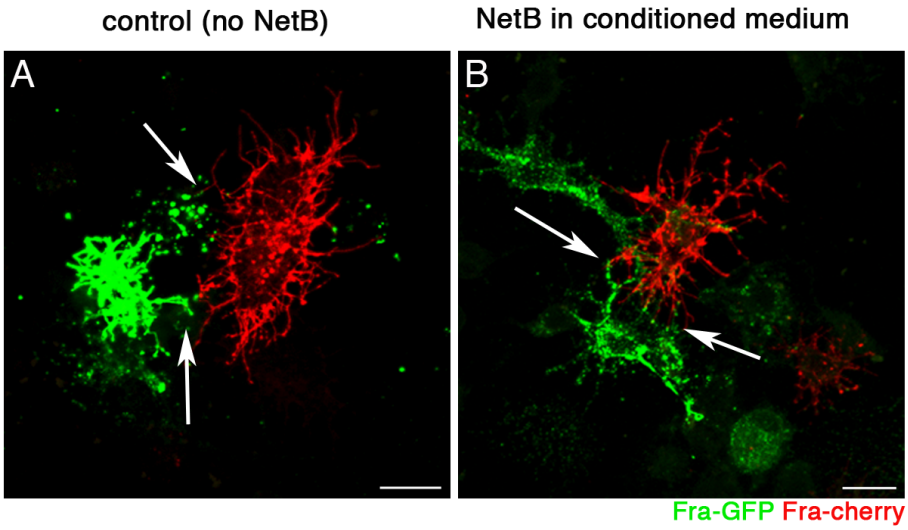

Figure 31. Clustering Fra-GFP R+ cells and Fra-Cherry R+ cells. (A) Clustering of Fra-GFP and Fra-Cherry cells were detected in the absence of NetB. Moreover, cells appear to form contacts (arrows in A, the experiment was repeated 6 times, with 22 couples analyzed). (B) Fra-GFP cells were predisposed with NetB concentrated from conditioned medium. 'Naïve' Fra-Cherry cells were added. After 4-5 hours clustering was analyzed on fixed samples using the confocal microscope. Fra-GFP and Fra-Cherry cells form contacts (arrows in B). The experiment was repeated 6 times, with 27 couples analyzed. Scale bars are 10 μm.

5.2.4 Layer-specific targeting is mediated by local axonal release of NetB

Our genetic analyses *in vivo* provided evidence that Fra prevents NetB diffusion, thus mediating the accumulation of NetB in the M3 layer. However, despite the efficient *fra* knock-down in the target area, NetB accumulation and expression in a layer was not completely abolished. This points towards the possibility that a second mechanism is likely acting in parallel, whereby NetB could be locally released into the M3 layer by for instance target neurons, such as L3 lamina neurons and medulla neuron subtypes. This leads to the question as to how complex neurons release Netrins into the M3 layer. More specifically, as to whether Netrins are preferentially released from axons or dendrites.

To gain further insights as to where target neurons release NetB in the medulla, enhancer trap *Gal4* P element insertions into or close to the *NetA and NetB* genomic loci were assessed (Figure 32A-B'). To allow conclusions about the release sites of the NetB expressing neurons in the medulla neuropil, I turned to the *UAS-syt^{HA}* reporter, which labels presynaptic sites in axon terminals of neurons. Two enhancer trap *Gal4* P-element insertions were analyzed in detail (Figure 32A-B'). *NP4151-Gal4* shows a broader expression in lamina neurons L3 and several medulla neuron subtypes and *NP0831-Gal4* is limited to lamina neurons L3. Although *NP4151-Gal4* shows expression in several medulla layers when using the *UAS-cd8GFP* reporter, *UAS-syt^{HA}* is strongly enriched in the M3 layer in the medulla neuropil (Figure 32A, A'). Similarly, when *UAS-syt^{HA}* is expressed under the control of *NP0831-Gal4,* high levels are detected the M3 layer (Figure 32B, B'). These findings suggest, that NetB is locally released likely form axonal terminals into the M3 layer from L3 lamina neurons and possibly medulla neuron subtypes.

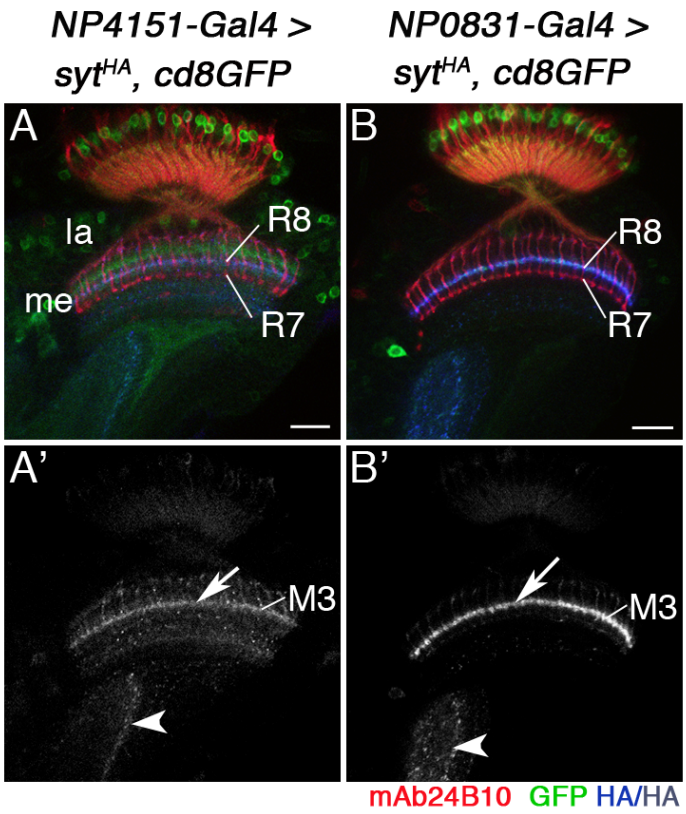

Figure 32. Analysis of *NP4151-*, and *NP0831-Gal4* insertions adjacent to *NetB* and *NetA* loci. (A-B) Adult optic lobes. (A) *NP4151-Gal4* drives GFP expression (green) in lamina neurons L3, which extend axonal terminals into the R8 recipient layer M3, and in medulla neuron subtypes that arborize in several layers in the medulla neuropil. (B) *NP0831-Gal4* is restricted to lamina neurons L3. (A',B') The *UAS-syt^{HA}* reporter revealed the M3 layer as the axonal release site of Netrin expressing neurons (arrows in A' and B'). Furthermore, axonal release sites are detected in the lobula (arrowheads in A' and B'). la, lamina, me, medulla. Scale bars are 20 μm.

5.2.5 Cell-type specific RNAi knock-down of *NetA* and *NetB*

To pinpoint, which target neurons play a crucial role in providing Netrins as guidance cues in the M3 layer for R8 axon targeting, I performed knock-down experiments of *NetA* and *NetB* using the RNAi approach in conjunction with Gal4 drivers that have preferentially restricted activity in neurons arborizing in the M3 layer. I expected that this would allow me to narrow down the target neuron subtypes that release NetB into the M3 layer and are therefore required for layer-specific targeting of R8 axons.

In RNAi knock-down experiments using *UAS-NetA^{RNAi} and UAS-NetB^{RNAi}*, *NetA* and *NetB* were removed from target neurons using the *NP4151-*, and *NP0831-Gal4* insertions adjacent to *NetB* and *NetA* loci. Expression of the *UAS-cd8GFP* reporter under the control of *NP4151-Gal4* showed activity of this driver in lamina neurons L3, as well as medulla neuron subtypes with layer-specific arborizations in the M1/M2 and M3 layers, while *NP0831-Gal4* activity is restricted to lamina neurons L3, whose processes terminate in the M3 layer (see Chapter 4, Figure 16). Subsequent analysis assessed R8 axon targeting in the adult optic lobe (Figure 33A-B). Removal of *NetA* and *NetB* with these drivers was not sufficient to affect R8 axon targeting, as R8 axons terminated correctly in the M3 layer.

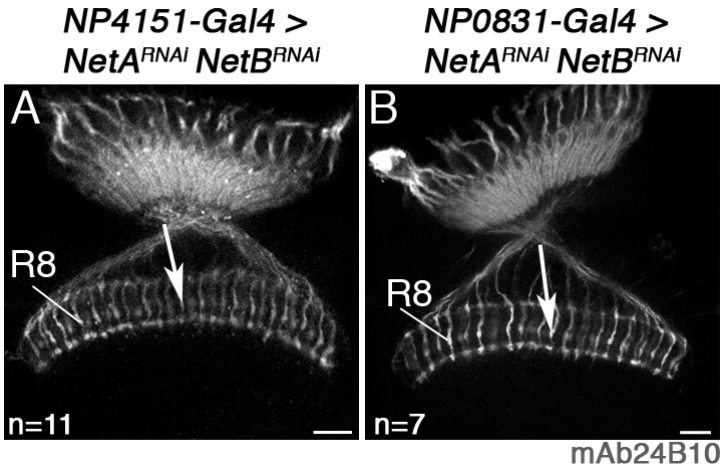

Figure 33. Knock-down of *NetA* and *NetB* using *NP4151-Gal4* and *NP0831-Gal4*. (A-D) Adult optic lobes. (A-B) *NP4151-Gal4* drives expression in lamina neurons L3, and in medulla neuron subtypes (A). Combination with *UAS-NetA^{RNAi}, UAS-NetB^{RNAi}* to knock-down Netrin function did not result in aberrant R8 axon targeting (n=11, arrow in B). (C-D) *NP0831-Gal4* is restricted to lamina neurons L3 (C). Removal of *NetA* and *NetB* using this driver did not affect normal R8 axon projections to the M3 layer (n=7, arrow in D). R-cells are labeled with mAb24B10. Scale bars are 20 μm.

I next turned to *MH56-Gal4* (identified in an enhancer trap Gal4 screen in our laboratory by L. Ferreira), *MH936-Gal4* (identified by W. Joly) and *9.9-Gal4* insertions (kindly provided by L. Zipursky) to knock-down *NetA* and *NetB*. *MH56-Gal4* is expressed in L3 lamina neurons in the adult, whereas *MH936-Gal4* and *9.9-Gal4* are expressed in lamina neurons L3, as well as medulla neuron subtypes with stronger localization in the M3 layer among other layers in the medulla neuropil (Figure 34A, C, E). *UAS-NetA^{RNAi}* and *UAS-NetB^{RNAi}* were expressed under the control of *MH56-Gal4* in lamina neurons L3 (Figure 34B). However, when examining R8 axon projections I could not detect targeting defects. Equally, a knock-down of *NetA* and *NetB* using the more widely expressed Gal4 drivers *MH936-Gal4* and *9.9-Gal4* did not result in aberrant R8 axon targeting (Figure 34D, F).

There are three possible explanations for these unexpected results, that R8 axons target correctly to the M3 layer in these different knock-down approaches. Firstly, the *UAS-NetA^{RNAi} and UAS-NetB^{RNAi}* constructs may not be effective. However, this possibility can be excluded, as we could demonstrate that the RNAi approach efficiently knocks down *NetA* and *NetB* in the target area using the *ey-FLP, act>>Gal4* FLPout approach, resulting in R8 axon targeting defects (compare Chapter 4, Figure 20). Secondly, the knock-down in restricted *NetA* and *NetB* expressing neuron subtypes may be insufficient, as other medulla neuron subtypes that are not affected by the knock-down may compensate by providing the ligand. Thirdly, the *Gal4* drivers were most likely not expressed in a timely fashion and at not high enough level for efficiently knocking-down *NetA* and *NetB* in target neuron subtypes.

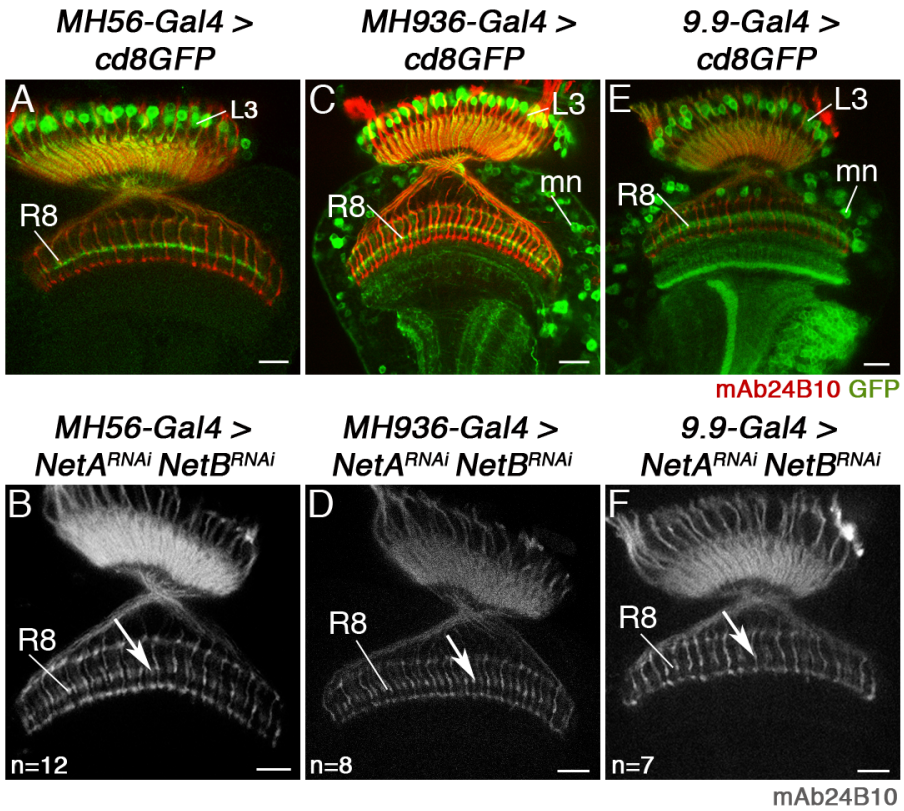

Figure 34. Knock-down using *UAS-NetA^{RNAi}, UAS-NetB^{RNAi}* in target neuron subtypes. (A-F) Adult optic lobes. (A,B) *MH56-Gal4* is active in lamina neurons L3 (A). *MH56-Gal4* driving expression of *UAS-NetA^{RNAi}, UAS-NetB^{RNAi}* did not result in aberrant R8 axon targeting (n=12 optic lobes, arrow in B). (C,D) *MH936-Gal4* is expressed in L3 neurons and medulla neuron subtypes (C). Using *MH936-Gal4* in this knock-down R8 axons targeted correctly to the M3 layer (n=8, arrow in D). (E,F) *9.9-Gal4* is strongly expressed in L3 neurons and medulla and lobula plate neuron subtypes (E). In conjunction with *UAS-NetA^{RNAi}, UAS-NetB^{RNAi}* this did not result in aberrant R8 axon targeting (n=7, arrow in F). R-cells are labeled with mAb24B10. Scale bars are 20 μm.

5.2.6 Rescue of aberrant R8 axon targeting in *NetAB*$^{\Delta}$ mutants

The question, as to which neurons in the target area provide NetB and are therefore required for correct R8 axon targeting remained unanswered. Due to the inconclusive results of the *NetA* and *NetB* knock-down in lamina neurons, I therefore turned next to rescue experiments. As established previously, Netrins are expressed by numerous neuron subtypes. However, they are likely released primarily from axonal terminals into the M3 layer, as suggested by studies of enhancer trap *Gal4* P element insertions in combination with *UAS-syt*^{HA} reporter (Figure 32). Many Netrin-positive medulla neuron subtypes have mostly dendritic arbors in the medulla and axon terminals in the lobula and might not be crucial for releasing NetB into the M3 layer. I therefore focused on lamina neurons L3, as they have axonal terminals in the M3 layer and consequently might represent the main NetB releasing neuron population. I used the enhancer trap Gal4 line *MH56-Gal4* to specifically express NetB in lamina neurons L3 in a *NetAB*$^{\Delta}$ mutant background.

For this purpose, first the expression pattern of *MH56-Gal4* was analyzed during pupal development and in the adult optic lobe in detail. *MH56-Gal4* drives expression strongly in lamina neurons L3 throughout pupal development and at moderate levels in L1 neurons during late pupal development and in the adult, as shown with *UAS-cd8GFP* as a reporter read-out (Figure 35A-D'). It is not expressed in R-cells as shown in the analysis of cross-sections of the retina at 24 hours, 42 hours or 55 hours APF (Figure 35E-G'). Therefore, *MH56-Gal4* is suitable to be used for expressing *UAS-NetB* in lamina neurons L3 in a *NetAB*$^{\Delta}$ mutant background.

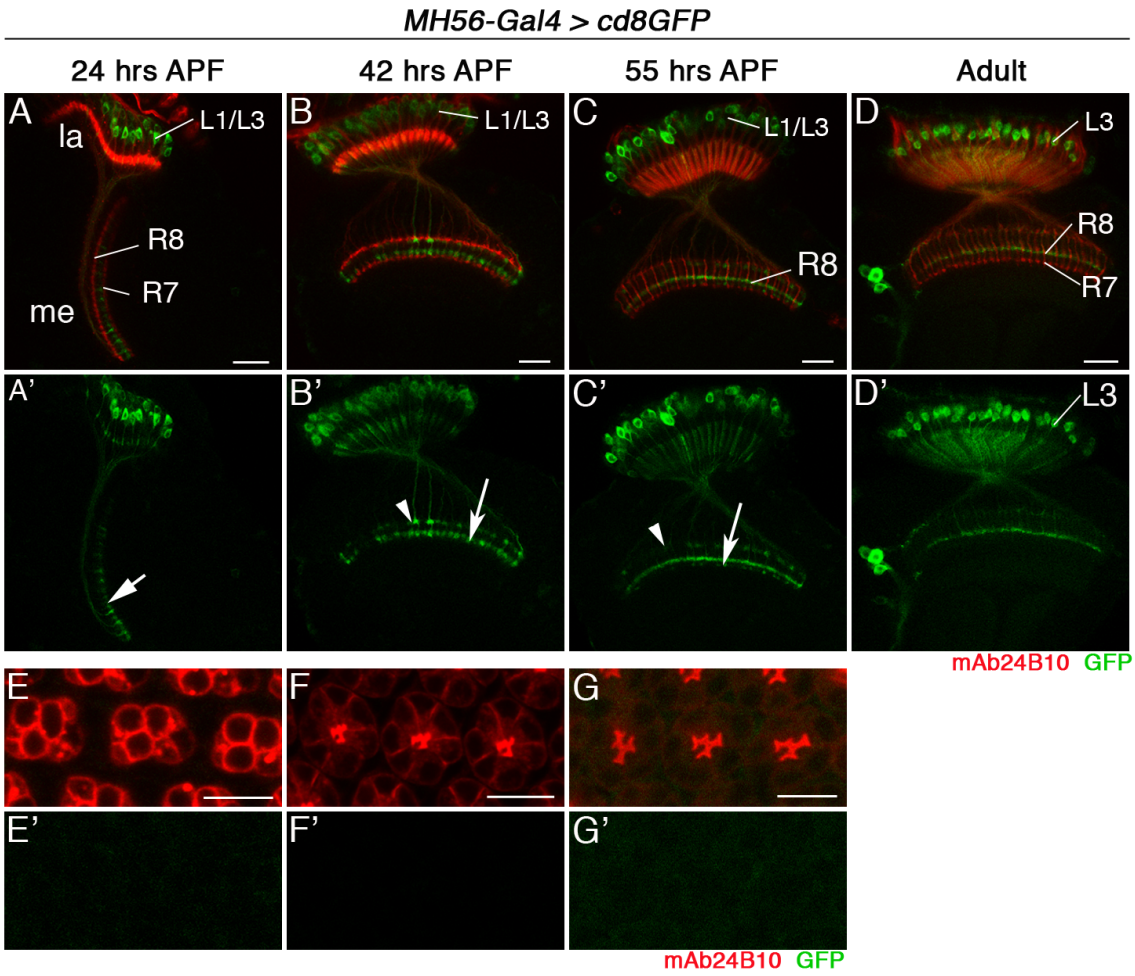

Figure 35. Analysis of the enhancer trap *MH56-Gal4* expression pattern. (A-D) Throughout pupal development and in adults, *MH56-Gal4* drives strong expression in lamina neurons L3 extending axonal arbors into the emerging and final M3 layer (arrows in A'-C'). At 24, 42 and 55 hours APF *MH56-Gal4* drives moderate GFP expression (green) in lamina neurons L1 extending axonal arbors into layers M1 and M5 (arrowheads in B', C'). (E-G) Cross-sections of the retina during development confirm that *MH56-Gal4* is not expressed in R-cells. R-cell axons are labeled with mAb24B10 (red). la, lamina, me, medulla. Scale bars are 20 μm (A-D) and 10 μm (E-G).

In addition, using *MH56-Gal4* together with the *UAS-syt*^{HA} reporter showed that the presynaptic release sites of these neurons are localized to the M3 layer (Figure 36A, A'). Importantly, ectopic expression of *UAS-NetB* under the control of *MH56-Gal4* confirmed that NetB is released into the M3 layer as detected using antibody labeling for NetB (Figure 36B, B'). Therefore this driver is suitable for the correct spatio-temporal release of NetB into the M3 layer in subsequent rescue experiments.

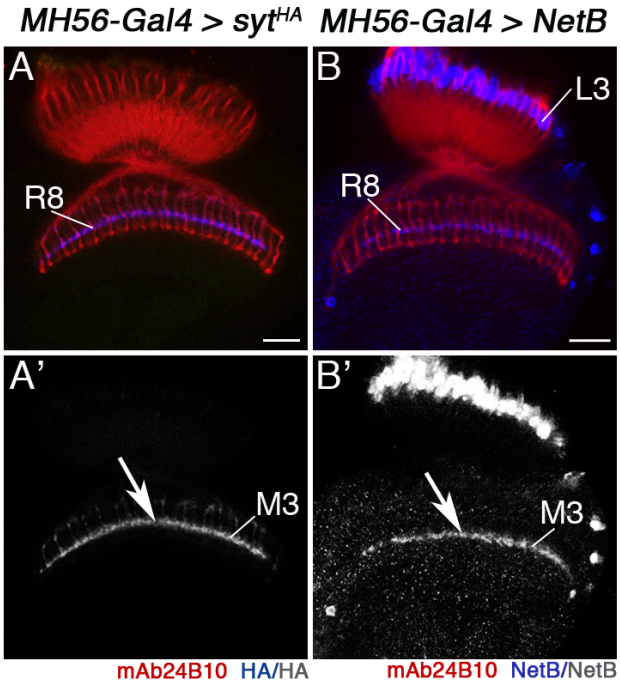

Figure 36. *MH56-Gal4* ectopically releases NetB into the M3 layer. (A-B) Adult optic lobes. (A, A') Expression of *UAS-syt*^{HA} with *MH56-Gal4* confirms that the M3 layer represents the output area of this neuron population (arrow in A'). (B, B') *MH56-Gal4* is active in lamina neurons releasing NetB into the M3 layer in the medulla neuropil (arrow in B'). R8 axons target normally to the M3 layer in this situation. R-cell axons are labeled with mAb24B10 (red). Scale bars are 20 μm.

To test as to whether L3 lamina neurons are critical for provision of NetB in the M3 layer, I performed rescue experiments using above described reagents. In control animals using the *MH56-Gal4* insertion, *UAS-NetB* was over-expressed in an otherwise wild type background. Over-expression of NetB did not result in aberrant R8 axon targeting (Figure 37A, A', n=11, 99% of 209 *Rh6-lacZ* labeled R8 axons terminated correctly in the M3 layer). Homozygous mutants for *NetA* and *NetB* showed aberrant targeting with R8 axons stalling at the medulla neuropil border (Figure 37B, B', n=5, 61% of 91 *Rh6-lacZ* labeled R8 axons). Strikingly, R8 axon targeting defects in *NetAB*$^{\Delta}$ mutants were rescued by re-introducing NetB in lamina neurons projecting to the M3 layer, as 92% of *Rh6-lacZ* labeled R8 axons terminated correctly in the M3 layer (Figure 37C, C', n=12, 248 R8 axons).

This suggests that, while a contribution of other neuron subtypes cannot be excluded, provision of NetB in lamina neurons L3 is sufficient to correctly guide R8 axons to the M3 layer.

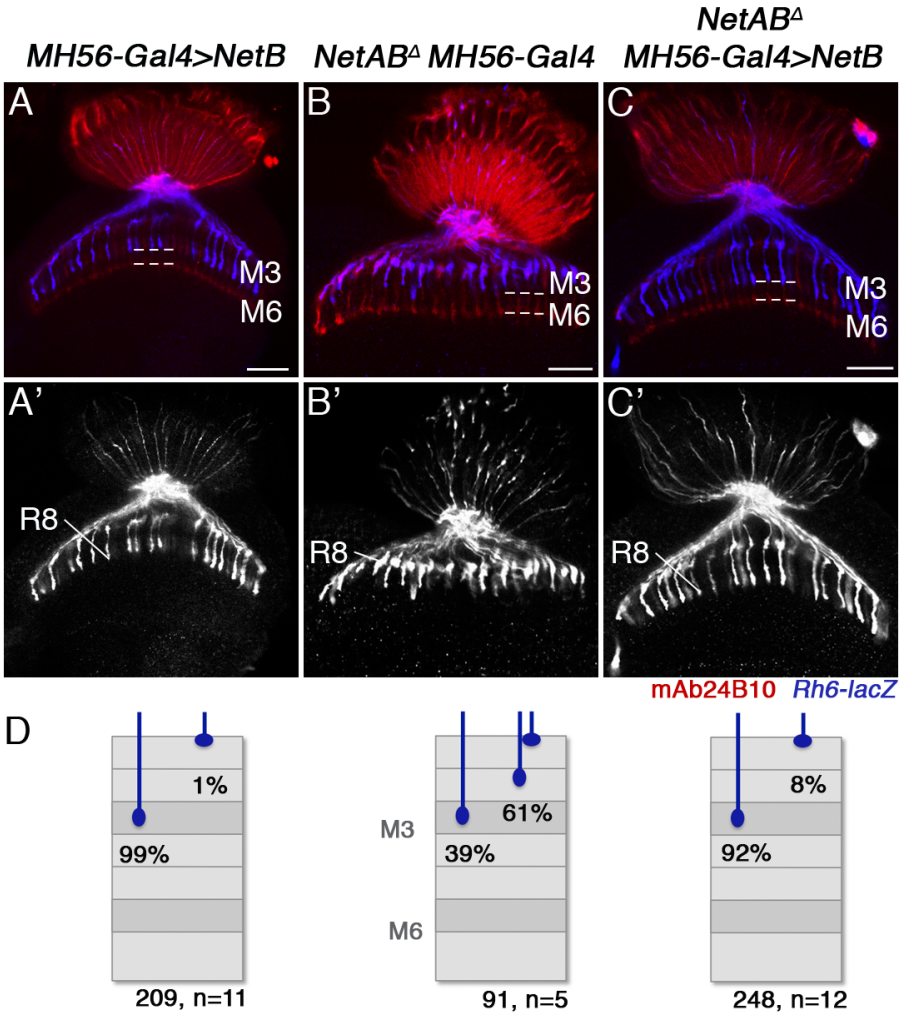

Figure 37. M3 layer-specific expression of *UAS-NetB* rescues R8 axon targeting defects. (A-C) Adult optic lobes. (A, A') Over-expression of *UAS-NetB* with *MH56-Gal4* did not interfere with R8 axon targeting. (B, B') In hemizygous *NetAB*$^{\Delta}$ mutant males, *Rh6-lacZ* positive R8 axons (blue) prematurely terminated at the medulla neuropil border or in the M1/M2 layers. (C, C') Expression of *UAS-NetB* in lamina neurons L3 rescued R8 axon targeting defects in *NetAB*$^{\Delta}$ mutant animals. *Rh6-lacZ* positive R8 axons are labeled in blue. R-cells are labeled with mAb24B10 (red). Scale bars are 20 μm. (D) Quantification of phenotypes.

5.3 Discussion

5.3.1 NetB mediates short-range attraction of R8 axons to the M3 layer

Layer-specific targeting of R8 axons is achieved in two subsequent steps during pupal development (Ting et al., 2005). Initially R8 axons terminate at the temporary layers at the medulla neuropil border. From mid-pupal stages R8 axons regain motility and proceed to their final layer M3. Our studies have shown that NetB accumulates in the M3 layer in the medulla neuropil, thus likely providing positional information for Fra-positive incoming R8 axons. Consistent with studies examining the *Drosophila* embryo midline pathfinding (Brankatschk and Dickson, 2006), NetB in the visual system acts at short-range, as R8 axon targeting is normal when solely membrane-tethered NetB is available at near endogenous levels.

However, this raises the question as to how R8 axons can be attracted to localized NetB in the M3 layer, when they are situated several microns away at the medulla neuropil border. Our findings suggest that to bridge the distance, R8 axons extend a fine filopodium that might allow searching for the NetB positive layer. Upon contact they establish thick processes into the M3 layer. This means that NetB does not require to form a gradient for attraction of R8 axons into the M3 layer during the final target layer selection step. Yet Netrins are per se diffusible, raising the question as to which mechanism allows NetB to be localized in this distinct layer.

5.3.2 Role of Fra in target neurons in the localization of NetB to the M3 layer

To address as to whether Fra in target neurons can capture and localize NetB to the M3 layer, RNAi knock-down experiments were performed. The loss of *fra* in R-cells does not affect NetB accumulation in the M3 layer. However, it results in a non-

responsiveness of R8 axons to the Netrin source in the target area, causing R8 axons to stop prematurely at the medulla neuropil border. In contrast, when *fra* is removed from R-cells and target neurons or target neurons only, this leads to decreased NetB accumulation in the M3 layer. An essential point was to demonstrate that the loss of NetB signal observed in *fra* knock-down is due to the diffusion of NetB rather than to the loss of the M3 layer. In addition, it is important to examine as to whether the M3 layer is maintained in the absence of R8 axon innervation, as in the *fra* knock-down in the target area, R8 axons stall at the medulla neuropil border.

Several lines of evidence support the notion that the decreased NetB signal is due to the loss of Fra-mediated capture of NetB in the target neurons, as M3 layer assembly in the medulla neuropil is not affected. This was tested using the independent marker Fmi to label the M3 layer in optic lobes of flies, in which *fra* has been knocked-down in the eye and in the target area. At 55 hours APF, Fmi expression in the M3 layer was unaffected, while the NetB signal was diminished. Furthermore, the membrane-tethered NetB ($NetB^{TMmyc}$) is localized to the M3 layer despite the removal of *fra* in target neurons demonstrating that in the absence of Fra in target neurons, the M3 layer is able to form normally and Fra is required in the target neurons to prevent the diffusion of NetB. Despite the use of multiple genetic approaches to manipulate Fra levels exclusively in target neurons, R8 axon targeting was not affected. It could be attributed to the technical limitation, that the knock-down of *fra* in the target area is incomplete, due to that the *ey* enhancer is only active in about 50% of medulla neurons (Morante and Desplan, 2008). Thus remaining low levels of Fra activity in the target neurons suffice to keep NetB in place to guide fully responsive incoming R8 axons. Unfortunately, a target specific removal of *fra* using mutant mosaics in all neurons in the target area is genetically not feasible. However, to sensitize R8 axons, I repeated this experiment in a *fra* heterozy-

gous genetic background. Although this may have led to less responsive R8 axons, it did not result in targeting defects of R8 axons (data not shown). This leads to the possibility that additional guidance systems may act in parallel.

Importantly, as lamina neurons L3 continue to locally release Netrins in a *fra* knock-down, it is not possible to completely remove the ligands, and remaining Netrins within the M3 layer may be sufficient to guide fully responsive R8 axons to their target layer.

Generally regarding the role for Fra in R8 axon targeting, the findings presented in this thesis thus far lead to the interpretation that Fra has a dual function of (i) guiding R8 axons to the NetB source in the M3 layer, and in addition (ii) of locally capturing and presenting NetB to the incoming R8 axons, by employing target neurons. Because of the complexity of the fly visual system, it is not possible to analyze the binding dynamics of the Netrin/Fra guidance system *in vivo*. Our genetic data raised the central question as to whether NetB captured by Fra-positive target neurons may either be presented to Fra-expressing R8 axons in a dynamic fashion, or R-cell and target neuron-derived Fra interact with NetB in a stable ternary complex in *trans*. Previous studies showed that for the vertebrate counterpart Netrin-1 has a high binding affinity for DCC ($K_d = 10^{-8}M$) (Keino-Masu et al., 1996). Further support for a complex of multiple molecules comes from studies that showed that DCC can bind Netrins with multiple domains (see Introduction) (Geisbrecht et al., 2003; Kruger et al., 2004). In addition, Netrins can bind and aggregate multiple DCC ectodomain molecules in *cis* (Stein et al., 2001). I therefore turned to address the question as to whether Fra and NetB form a ternary complex using cell-based *in vitro* studies. I could show, that *Drosophila* Fra is able to bind NetB in a stable complex for up to 4 hours. To test the possibility as to whether

a stable ternary complex forms between two Fra molecules and one NetB molecule in trans, I used two differently labeled Fra molecules. Cells expressing full-length Fra were exposed to NetB and a truncated version of Fra ($Fra^{ECD\text{-}HA}$). $Fra^{ECD\text{-}HA}$ did neither bind to NetB in this experiment nor in the control. The suggestion that soluble DCC is not able to bind Netrin-1 when the transmembrane domains is removed were made for the vertebrate counterpart (Stein et al., 2001). To overcome this issue in the future, soluble $Fra^{ECD\text{-}HA}$ could be stabilized using beads or larger protein domains such as Ig (Immunoglobulin) domains.

Furthermore, I used aggregation assays, in which two different cell populations were transfected with either *Fra-GFP* or *Fra-Cherry*. Fra-GFP labeled cells were treated with NetB, washed and left to adhere in cell culture dishes. After the addition of 'naïve' Fra-Cherry cells, it was expected that Fra-GFP and Fra-Cherry cells cluster or at least show overlapping filopodia, indicative of the attraction to NetB bound by Fra-GFP. However, no specific clustering was observed. These findings could be explained by the fact that NetB functions at short-range and is immobilized by Fra. Therefore, Fra-Cherry cells likely cannot be attracted over long distances. Rather, if both cell types are in close proximity by chance, they will interact. Therefore, the so far tested cell-based approaches were not conclusive to gain insights into the binding properties of Netrins and Fra.

In summary, the results of the experiments performed thus far suggest that the secreted guidance cue NetB exerts layer-specific information not in a graded manner, but is localized through Fra associated with target neurons. However, it remains to be elucidated as to whether Fra can interact with NetB in a ternary complex in *trans* or in a dynamic fashion.

5.3.3 Role for L3 lamina neurons in local release of NetB into the M3 layer

In addition to Fra preventing NetB diffusion, thus mediating its accumulation in the M3 layer, a second mechanism of local ligand release by neurons arborizing in the M3 layer possibly acts in parallel. In neurons, proteins are differentially distributed to axons and dendrites based on the opposite polarity of microtubules in axons and dendrites whereby dynein mediates transport into dendrites, and kinesins into axons (Rolls, 2011). It is possible that guidance cues use the same machinery to be differentially distributed as synaptic proteins. Recent findings in *C. elegans* further provided evidence that Netrins are released from axonal terminals. Indeed they showed that proteins that are involved in motor cargo assembly, axonal transport and exocytosis are also essential for Netrin localization and secretion (Asakura et al., 2010). For instance, loss of the *unc-104/Kinesin superfamily protein 1A (KIF1A)* leads to failure of Netrin to be localized to the axon. As to how Netrins are localized and released in the *Drosophila* visual system remains to be addressed in future studies.

Although Netrins are expressed by numerous neuron subtypes, our subsequent studies focused primarily on lamina neurons L3, as these represent the main neuron subtype within the NetB expressing neuron population with axon terminals in layer M3. Whereas medulla neuron subtypes have mostly dendritic arbors in the medulla and axon terminals in the lobula (Takemura et al., 2008). Thus, lamina neurons L3 are very good candidates for releasing Netrins in layer M3. To gain evidence for the function of L3 lamina neurons in providing NetB for M3 layer-specific R8 axon targeting, knock-down experiments using several Gal4 drivers which are active either in L3 lamina neurons and medulla neuron subtypes, or Gal4 enhancer trap insertions adjacent to *NetA* and *NetB* genetic loci were carried out. Removal of *NetA* and *NetB* in restricted subtypes of the Netrin producing neuron population was likely insufficient, as other target neurons

might provide this guidance cue in sufficient levels for R8 axons during M3 layer-specific targeting. Alternatively, as knock-down of *NetA* and *NetB* with neither of these drivers resulted in aberrant R8 axon targeting, this suggests that they are spatially and temporally not efficient to remove *NetA* and *NetB* sufficiently. As these results were inconclusive, I turned to rescue experiments. R8 axon targeting defects in flies lacking *NetA* and *NetB* were rescued by re-introducing NetB in lamina neurons L3 projecting to the M3 layer. This indicates that indeed L3 lamina neurons are crucial for providing NetB in the M3 layer for R8 axon targeting.

Collectively these data demonstrate, that two mechanisms contribute to layer-specific accumulation of NetB in the M3 layer: (i) local release by lamina neuron L3 axon terminals, and (ii) capture by Fra in target neurons.

Chapter 6

The role of ectopic NetB in R8 axon targeting

6.1 Introduction

The data presented so far demonstrate that NetB is essential for layer-specific R8 axon targeting. It accumulates in the M3 layer through local release by L3 lamina neurons and possibly medulla neuron subtypes, and a capturing mechanism through Fra-positive medulla neurons in the target area. However, the question remains as to whether the localization of NetB to a distinct layer in the medulla is instructive for R8 axon targeting. In particular, as to whether R8 axons can be redirected to an ectopic NetB-positive layer in the medulla neuropil.

For establishing an ectopic NetB layer, several issues have to been considered. Firstly, as previously described NetB is primarily released from axon terminals into the M3 layer. Therefore a suitable driver must be chosen, that allows the release of NetB into the ectopic layer by axon terminals. Secondly, spatiotemporal activity of the driver must be appropriate to allow correct expression of NetB at appropriate levels during pupal development. Thirdly, diffusible NetB must be localized in the ectopic layer by preventing diffusion, as this is usually achieved in the M3 layer by Fra-associated with target neurons. To provide localized NetB in an ectopic layer, one can use two strategies: either NetB and Fra are co-expressed to prevent diffusion or a membrane-tethered NetB variant can be directly expressed in suitable cell populations.

In this chapter, these strategies were tested to determine as to whether NetB is sufficient to redirect R8 axons, when it is expressed ectopically in a different layer.

6.2 Results

6.2.1 Co-expression of NetB and Fra in ectopic layers

Experiments described in Chapter 5 showed that Fra actively localizes NetB in the M3 layer in the medulla. To show that layer-specific localization of NetB is sufficient for R8 axon targeting, I therefore aimed at developing a genetic approach enabling to over-express NetB together with Fra to create a 'new' ectopic NetB-positive layer in an otherwise wild type background.

Several enhancer trap *Gal4* lines were used, which were identified in a screen in our laboratory by H. Apitz and W. Joly. These are active in target neurons arborizing in the medulla layers M1/M2 in the adult when crossed to a *UAS-cd8GFP* reporter. *MH728-Gal4* is active in lamina neurons L1 and L2, and weakly in L3. *MH919-Gal4* is expressed in L2 lamina neurons as well as in glial subtypes (Figure 38A, B). However, expression of the secreted *UAS-NetB* and the full-length *UAS-Fra* transgenes in this experimental paradigm did not result in a redirection of R8 axons (Figure 38C, D). R8 axons target correctly to the M3 layer, which provides endogenous NetB.

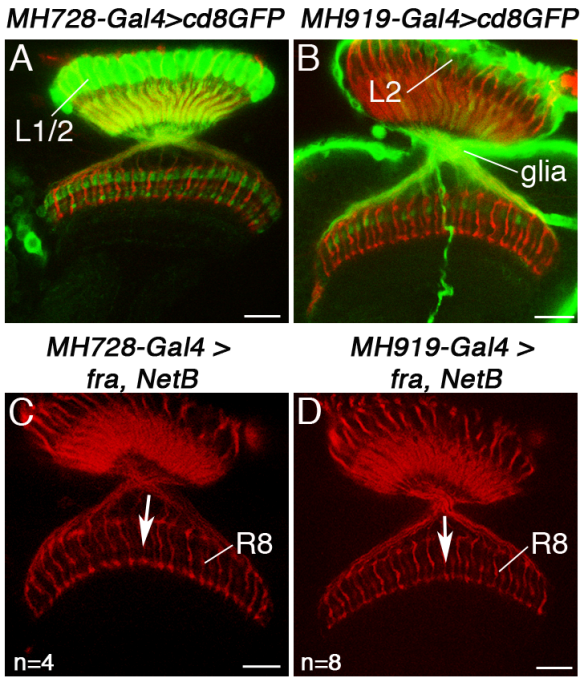

Figure 38. *MH728-Gal4* and *MH919-Gal4* drivers were used to co-express *UAS-fra* and *UAS-NetB*. (A-D) Adult optic lobes. (A-B) Analysis of *UAS-cd8GFP* reporter driven by *MH728-Gal4* revealed activity in lamina neurons L1 and L2, and weakly in L3. *MH919-Gal4* is expressed in L2 lamina neurons as well as glial subtypes. (C-D) R8 axons were not redirected to the M1/2 layers with either of the drivers (arrows in C, D). R-cells are labeled with mAb24B10. Scale bars are 20 μm.

Another Gal4 driver, *MH939-Gal4,* is expressed exclusively in T1 medulla neurons in the adult, as shown by using *UAS-cd8GFP* as read-out (Figure 39A). These T1 neurons have dendritic arbors in the M2 layer and axonal branches in the lamina (Fischbach and Dittrich, 1989). When *MH939-Gal4* was used to express *UAS-NetB* and full-length *UAS-fra* in T1 medulla neurons, R8 axons are not redirected to the ectopic M2 layer but innervate the target layer M3, which endogenously expresses NetB (Figure 39B). However, interestingly arborizations of these T1 neurons were redirected to the M3 layer because their processes are now responsive to the endogenous NetB layer, as they also ectopically express Fra (Figure 39C). This indicates that ectopically expressed Fra is able to guide dendritic processes to Netrin-positive layers. Therefore, the full-

length *UAS-fra* transgene is not suitable for ectopic localization of NetB in target neurons.

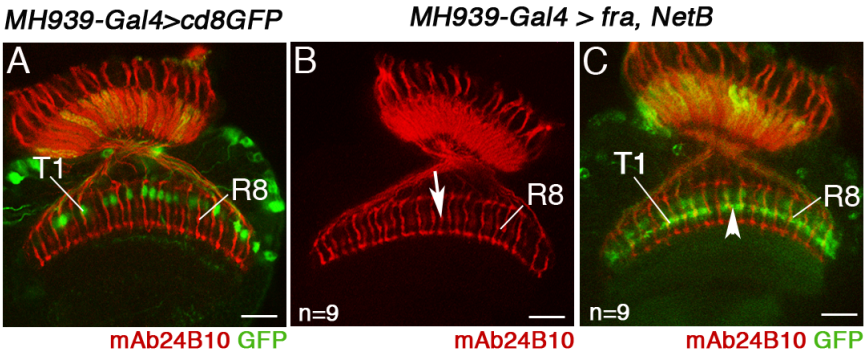

Figure 39. *MH939-Gal4* is used to co-express of *UAS-fra* and *UAS-NetB*. (A-C) Adult optic lobes. *MH939-Gal4* is expressed exclusively in T1 medulla neurons. (B) R8 axons were not redirected to the M1/2 layer but normally innervate the M3 layer (arrow in B, n=9). R-cells are labeled with mAb24B10. (C) T1 medulla neurons ectopically expressing *UAS-fra* and *UAS-NetB* are redirected to the endogenous NetB accumulating in the M3 layer (arrowhead in C, n=9). Scale bars are 20 μm.

6.2.2 Ectopic expression of NetB with truncated Fra in the M1/M2 layers

In the previous experiment, T1 neuron arborizations were redirected when *UAS-NetB* and full-length *UAS-fra* transgenes were co-expressed in target neurons. To circumvent this by separating the signaling and localization function of Fra, I turned to a truncated *UAS-fra*$^{\Delta Cmyc}$ transgene. This transgene lacks the intracellular part of the protein, while the truncated transmembrane Fra protein still can bind Net, but is unable to signal (Hiramoto et al., 2000). The previously described enhancer trap insertions *MH919-Gal4* and *MH939-Gal4*, which are expressed in neurons arborizing in the M1/M2 layers were used in this set of experiments. Co-expression of *UAS-fra*$^{\Delta Cmyc}$ and *UAS-NetB* under the control of either of these drivers neither redirected R8 axons to the M1/M2 layers (Figure 40A, B), nor affected the targeting of T1 neurons in the medulla (Figure 40B'). This shows that processes of Fra-positive neurons, such as T1 neurons, in these experimental conditions can be targeted to a Netrin-expressing layer. However,

the conditions were not effective to target R8 axons to the ectopic M2 layer. This is possibly due to the fact that the drivers used thus far are timely and spatially not expressed correctly to provide NetB ectopically at correct levels.

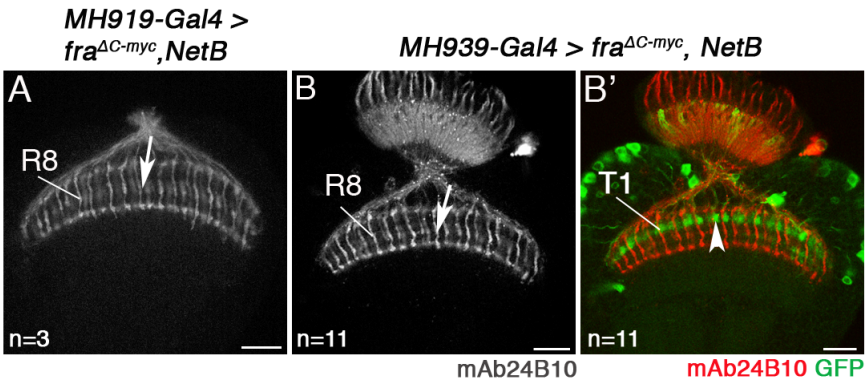

Figure 40. Ectopic layer of NetB is created by co-expression of *UAS-fra$^{\Delta Cmyc}$* and *UAS-NetB*. (A-B) Adult optic lobes. When using *MH919-Gal4* or *MH939-Gal4* to ectopically express *UAS-fra$^{\Delta Cmyc}$* and *UAS-NetB*, R8 axons were not redirected to the M1/2 layers but targeted correctly to the M3 layer (arrows in A, n=3, B, n=11). (B') T1 neurons were not redirected to the endogenous NetB layer in M3 as they express the truncated *UAS-fra$^{\Delta Cmyc}$* construct (arrowhead in B', n=11). R-cells are labeled with mAb24B10. Scale bars are 20 μm.

Next, I used the *MH502-Gal4* enhancer trap insertion, which drives GFP reporter expression in neurons arborizing in the M1/M2 layers during pupal development and in the adult (Figure 41A-D'). It is expressed in L1-L2 lamina neurons, T1 medulla neurons and C2/C3 neurons. In addition, when analyzing cross-sections of the retina at 24 hours, 42 hours and 55 hours APF, strong expression of the GFP reporter was detected in R-cells (Figure 41E-G').

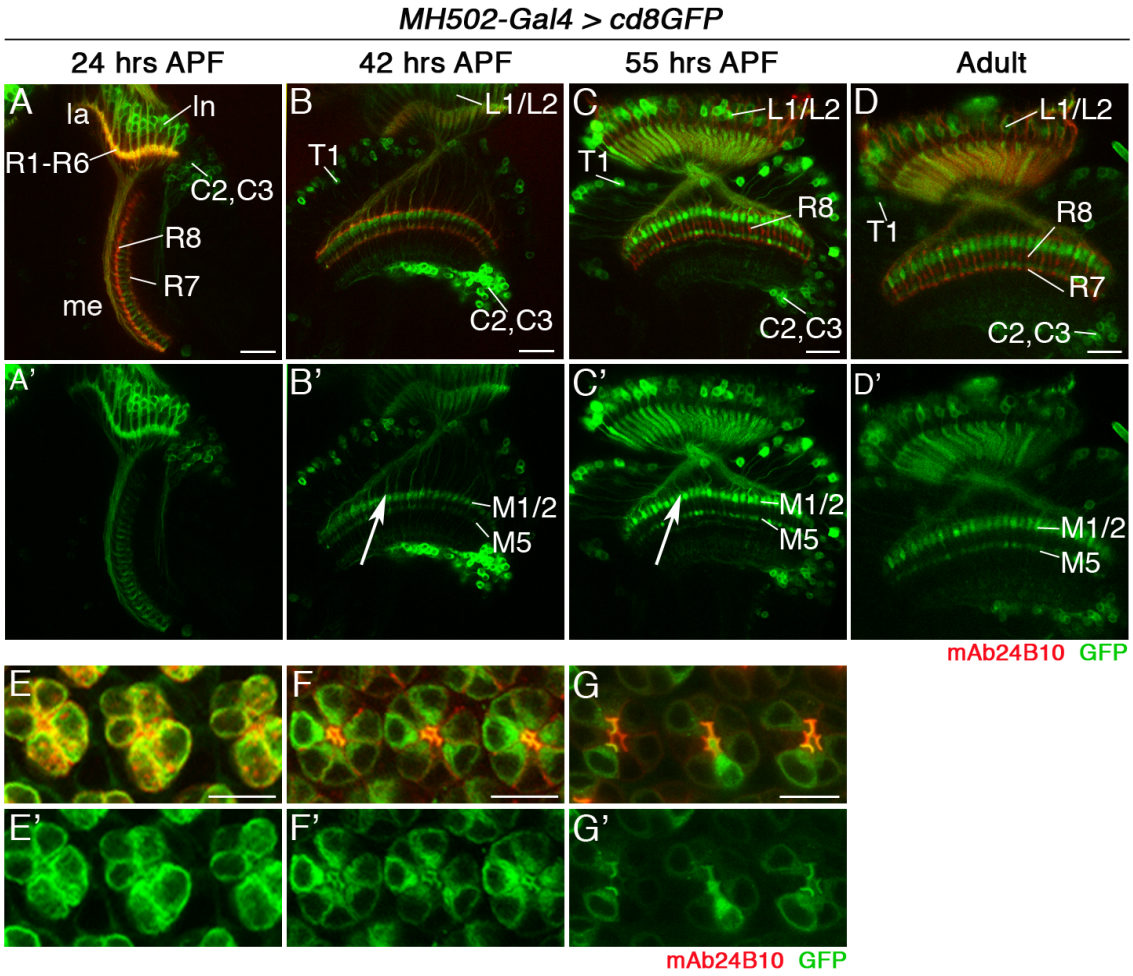

Figure 41. Analysis of the *MH502-Gal4* expression pattern during development. (A-D) Throughout development and in adults, *MH502-Gal4* is active in R-cells, lamina neurons L1 and L2, and ascending T1 medulla neurons, as well as C2/C3 neurons projecting into the M1/M2 and M5 layers within the distal medulla neuropil (arrows in B', C' point out GFP reporter expression in the M1/M2 layers at 42 and 55 hours APF). (E-G) Cross-sections through the retina at 24 hours, 42 hours and 55 hours APF. Strong expression is found in ommatidial clusters in the retina. R-cell axons are labeled with mAb24B10 (red). la, lamina; me, medulla. Scale bars, 20 μm.

To assess as to whether R8 axons can be redirected to the M1/M2 layers, *UAS-fra$^{\Delta Cmyc}$* and *UAS-NetB* were co-expressed in a wild type background using *MH502-Gal4* (Figure 42C, C'). Surprisingly, R8 axons terminated at the border of the medulla neuropil just prior to this Fra and NetB ectopic layer. This is not due to *fra$^{\Delta Cmyc}$*; as in a control experiment when only *UAS-fra$^{\Delta Cmyc}$* is expressed with *MH502-Gal4*, R8 axon targeting was not affected (Figure 42B, B'). However, when *UAS-NetB* was expressed

with *MH502-Gal4*, R8 axon targeting defects were observed with axons stalling at the medulla neuropil border (Figure 42A, A'). This raises the question as to whether ectopic NetB expression in R-cells can affect axon targeting.

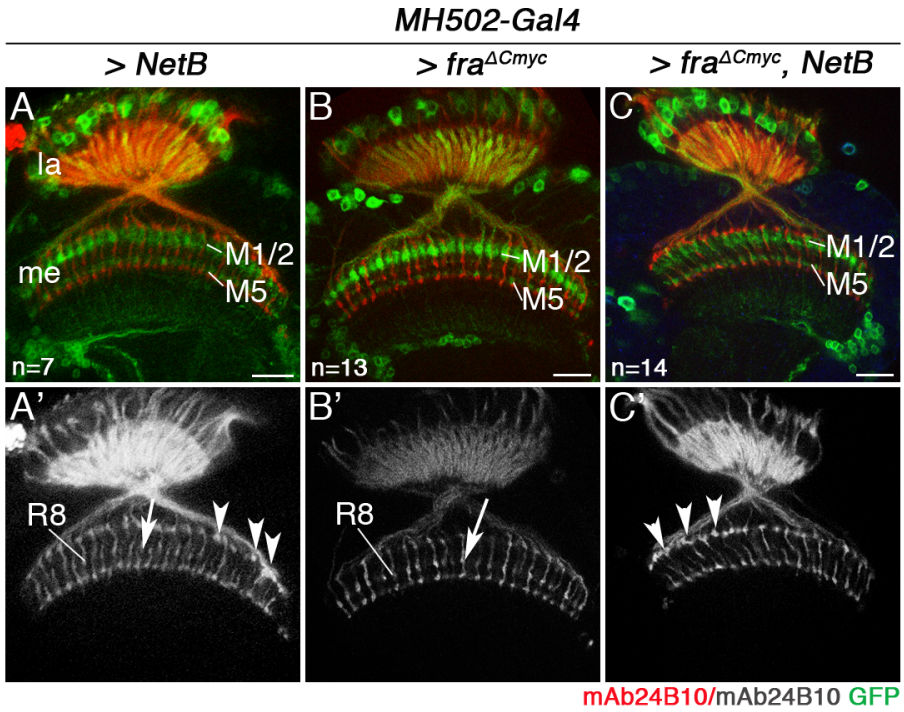

Figure 42. Truncated *UAS-fra$^{\Delta Cmyc}$* was co-expressed with *UAS-NetB* using *MH502-Gal4*. (A-C) Adult optic lobes. *MH502-Gal4* shows expression of *UAS-cd8GFP* reporter in the M1/2 layers. (A,A') In controls *UAS-NetB* was expressed using *MH502-Gal4*. A small percentage of R8 axons were not redirected but stall at the medulla neuropil border (arrowheads in A', n=7). (B,B') Ectopic expression of *UAS-fra$^{\Delta Cmyc}$* did not result in aberrant R8 axon targeting (arrow in B', n=13). (C,C') Co-expression of *UAS-NetB* and *UAS-fra$^{\Delta Cmyc}$* leads to stalling of R8 axons at the medulla neuropil border (arrowheads in C', n=14). Scale bars are 20 μm.

6.2.3 Misexpression of NetB in R-cells

To address as to how ectopic expression of NetB in R-cells can alter targeting, the *UAS-NetB* transgene was expressed in all R-cells using the late acting driver *lGMR-Gal4*. In this experiment, R8 axons show a strong phenotype with 91% of 90 *Rh6-eGFP* positive axons remaining at the border of the medulla neuropil (Figure 43B, B', n=5).

However, R7 axons were not affected despite the ectopic expression of NetB. This suggests that R8 axons are likely more susceptible due to their endogenous Fra expression, which can interact with NetB. Thus, expression of NetB in R-cells leads to aberrant R8 axon stalling at the border of the medulla neuropil.

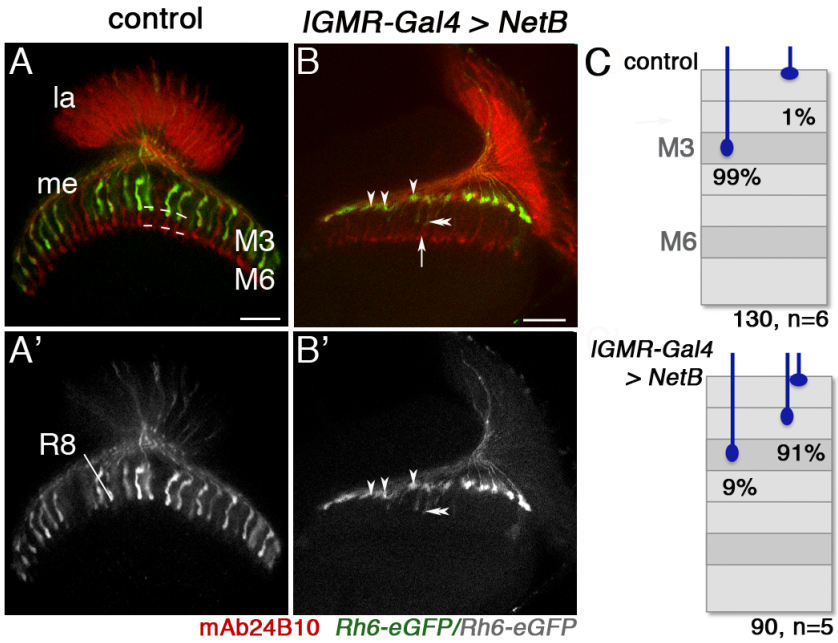

Figure 43. Ectopic expression of NetB in R-cells leads to stalling at the medulla neuropil border. (A-B) Adult optic lobes. (A, A') In controls, Rh6-eGFP positive R8 axons terminate in the M3 layer (99% of 130 R8 axons, n=6). (B-B') Prolonged ectopic expression of *UAS-NetB* in R-cells using *lGMR-Gal4* resulted in stalling of 91% of Rh6-eGFP positive R8 axons at the medulla neuropil border (arrowheads in B,B', n=90) or correct projections into the M3 layer (9%, double-arrowheads). R7 axon targeting was not affected (arrow in B). la, lamina; me, medulla. R-cell axons are labeled with mAb24B10 (red). Dashed lines indicate the position of the M3 and M6 layers. Scale bars are 20 μm. (C) Quantification of phenotypes.

6.2.4 Ectopic expression of membrane-tethered NetB^{cd8}

As the parallel experimental approach to localize NetB with the truncated *UAS-fra$^{\Delta CHA}$* transgene was not successful, I generated flies containing a *UAS-NetB^{cd8}* transgene (see Material and Methods). This made it possible to bypass the role of Fra in localizing NetB, as the ligand was directly tethered to the cell membrane to prevent diffusion.

Different Gal4 drivers such as *MH728-Gal4*, *MH919-Gal4*, *MH939-Gal4* and *NP1086-Gal4* were used to ectopically localize NetB (Figure 44A-D). However, none of these drivers could redirect R8 axons to ectopic layers (Figure 44A'-D'). How can this be explained? I initially assumed that *MH939-Gal4* and *NP1086-Gal4* would be the most suitable, as they are expressed exclusively in T1 neurons arborizing in the M2 layer, when using *UAS-cd8GFP* as read-out. However, when visualizing NetB^{cd8} accumulation, I observed that with these drivers NetB is not localized in the M2 layer. T1 neurons have dendritic arbors in the medulla and ascending axon terminals in the lamina (Fischbach and Dittrich, 1989). Thus, NetB expression is likely not detectable in the medulla, because it cannot be released by dendritic arborizations but only by axon terminals.

Consistently, when *NP1086-Gal4* was used to express *UAS-NetB^{cd8}* specifically in T1 neurons, NetB^{cd8} accumulation was not detected in the M2 layer, but in the lamina cartridges (Figure 44D"). Hence, NetB^{cd8} cannot be localized to the M2 layer in the medulla when using a T1 neuron specific driver, and layer-specific targeting of R8 axons is not affected (Figure 44C' and D').

Finally, when *UAS-NetB^{cd8}* was expressed under the control of *MH728-Gal4*, strong localization was detected in the M1/2 and M4 layers in the adult (Figure 44A"). This shows that in principle *NetB^{cd8}* can be accumulated in ectopic layers in the medulla

neuropil. However, this still did not redirect R8 axons to the ectopic layers, likely due to that the driver is not suitable to timely express NetB in these layers during development (Figure 44A'). Therefore, none of the used Gal4 drivers were suitable for redirecting R8 axons to ectopic layers in the medulla neuropil using the membrane-tethered *NetB*^{cd8}.

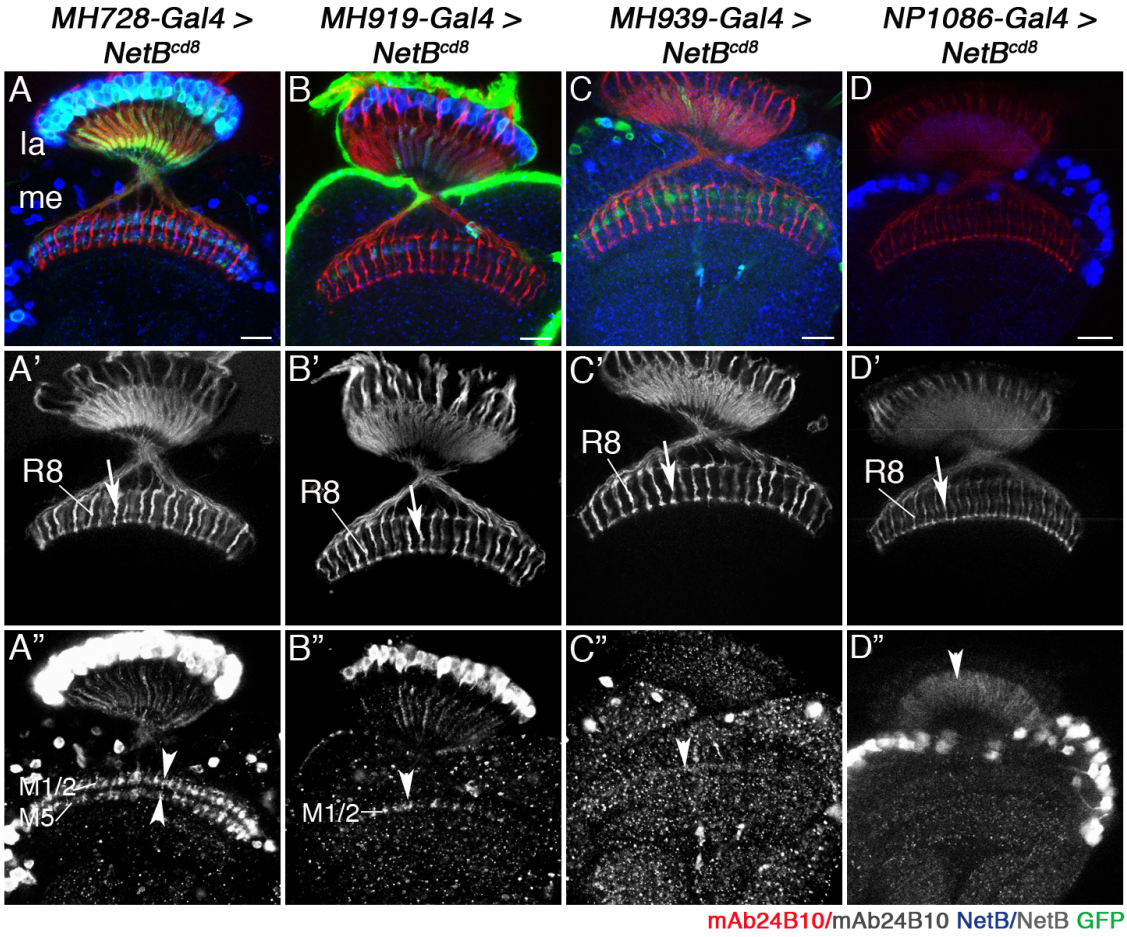

Figure 44. Ectopic expression of *UAS-NetB*^{cd8} in the M1/2 layers. (A-D) Adult optic lobes. (A-A") *MH728-Gal4* is strongly expressed in lamina neurons L1 and L2, and weakly in L3. It localizes NetB^{cd8} in the M1/2 and M4 layers (arrowheads in A"). R8 axons are not redirected (arrow in A'). (B-B") *MH919-Gal4* is expressed in L2 lamina neurons as well as glial subtypes, and localizes NetB^{cd8} to the M1/2 layers (arrowhead in B"). R8 axon targeting is not altered by the ectopic NetB layer. (C-C") *MH939-Gal4* is expressed in T1 medulla neurons. The expression is weak and ectopic NetB is hardly noticeable (arrowhead in C"). R8 axons target normally to the M3 layer (arrow in C'). (D-D") *NP1086-Gal4* is exclusively expressed in T1 neurons arborizing in the M1/2 layers. When it is used to drive *UAS-NetB*^{cd8} NetB is not detected there, but in the lamina (arrowhead in D"). This indicates that axons are release sites for NetB and T1 axonal release sites are following from that located in the lamina cartridges. R8 layer specific targeting is not affected (arrow in A'). R-cells are labeled with mAb24B10. la, lamina, me, medulla. Scale bars are 20 μm.

As the Gal4 drivers used for ectopic localization of NetB did not have any effect on R8 axon targeting, I returned to the *MH502-Gal4* driver. Except for expression in R-cells, the *MH502-Gal4* driver is a very useful tool for ectopically localizing NetB, because it is strongly expressed in the M1/M2 and M5 layers during development. Therefore this driver was combined with the $ey^{3.5}$*-Gal80* and *lGMR-Gal80* transgenes to prevent its activity in R-cells (Figure 45A-G'). Importantly, expression in L1-L2 lamina neurons, T1 medulla neurons and C2/C3 neurons remained (Figure 45A-D'). Furthermore, using *UAS-*syt^{HA} as a reporter for axonal release sites under the control of *MH502-Gal4,* confirmed that layers M1/M2 and M5 represent the output area of this neuron population within the medulla (Figure 45H). Thus, this driver is likely suitable for spatially and timely release of NetB in ectopic layers.

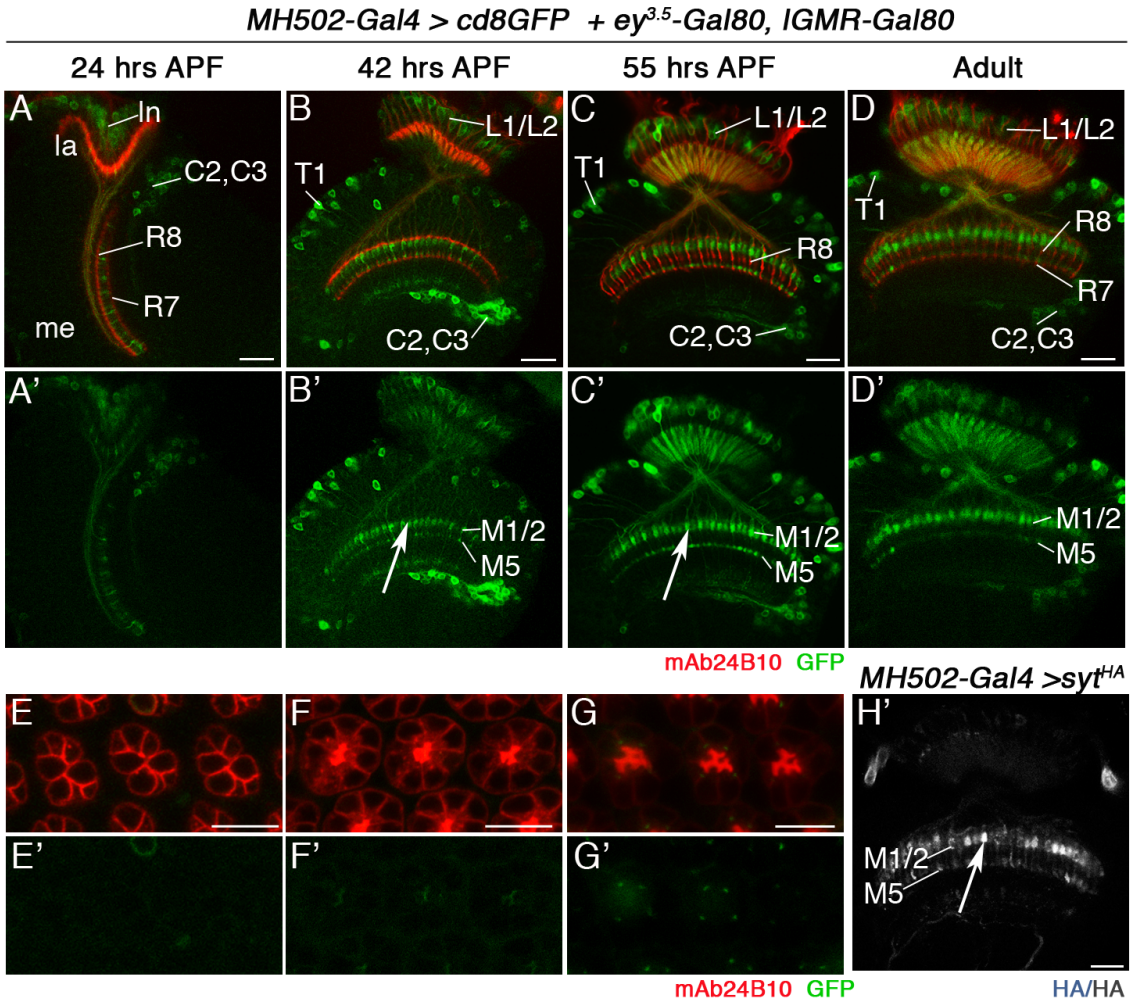

Figure 45. GFP-reporter expression under the control of *MH502-Gal4* with suppressed expression in R-cells. (A-D) Co-expression of *ey$^{3.5}$-Gal80* and *lGMR-Gal80* suppresses *MH502-Gal4* activity in R-cells. *MH502-Gal4* is still active in lamina neurons L1/L2, T1 medulla neurons, as well as C2/C3 neurons projecting into the M1/M2 and M5 layers within the distal medulla neuropil. (F-H) Cross-sections through the retina at 24 hours, 42 hours and 55 hours APF. GFP expression is strongly reduced in R-cells in the retina. (E,E') Expression of *UAS-syt^{HA}* with *MH502-Gal4* confirms that layers M1/M2 and M5 represent the principal output area of this neuron population within the medulla. R-cell axons are labeled with mAb24B10 (red). la, lamina, me, medulla. Scale bars are 20 μm.

When *UAS-NetB*^{cd8} is expressed under the control of *MH502-Gal4* combined with *ey*$^{3.5}$*-Gal80* and *lGMR-Gal80*, high levels of NetB protein are present in layers M1/M2 and M5 at 55 hours APF (Figure 46A-A'). This is critical as from mid-pupal stages R8 axons target to their final layers. In this genetic background, endogenous NetB accumulates in the M3 layer although at lower levels compared to the ectopic layer expression. Therefore, this experimental setup is suitable for ectopic localization of NetB$^{cd8.}$

I next analyzed in adults as to whether R8 axons responded to this ectopic layers of NetB^{cd8}. In controls, R8 axons terminated in the M3 layer in the adult (Figure 46B, B'). Strikingly, I observed that R8 axons are redirected to the M1/2 layers (Figure 46C-C"). More precisely, 19% of *Rh6-lacZ* labeled R8 axons stopped in the NetB positive M1/2 layers, while 32% stalled at the medulla neuropil border and 49% targeted to the M3 layer (Figure 46C-C", total of 227 *Rh6-lacZ* positive R8 axons, n=12). This percentage of redirected R8 axons to the M3 layer suggests that ectopically localized NetB is able to provide layer-specific positional information.

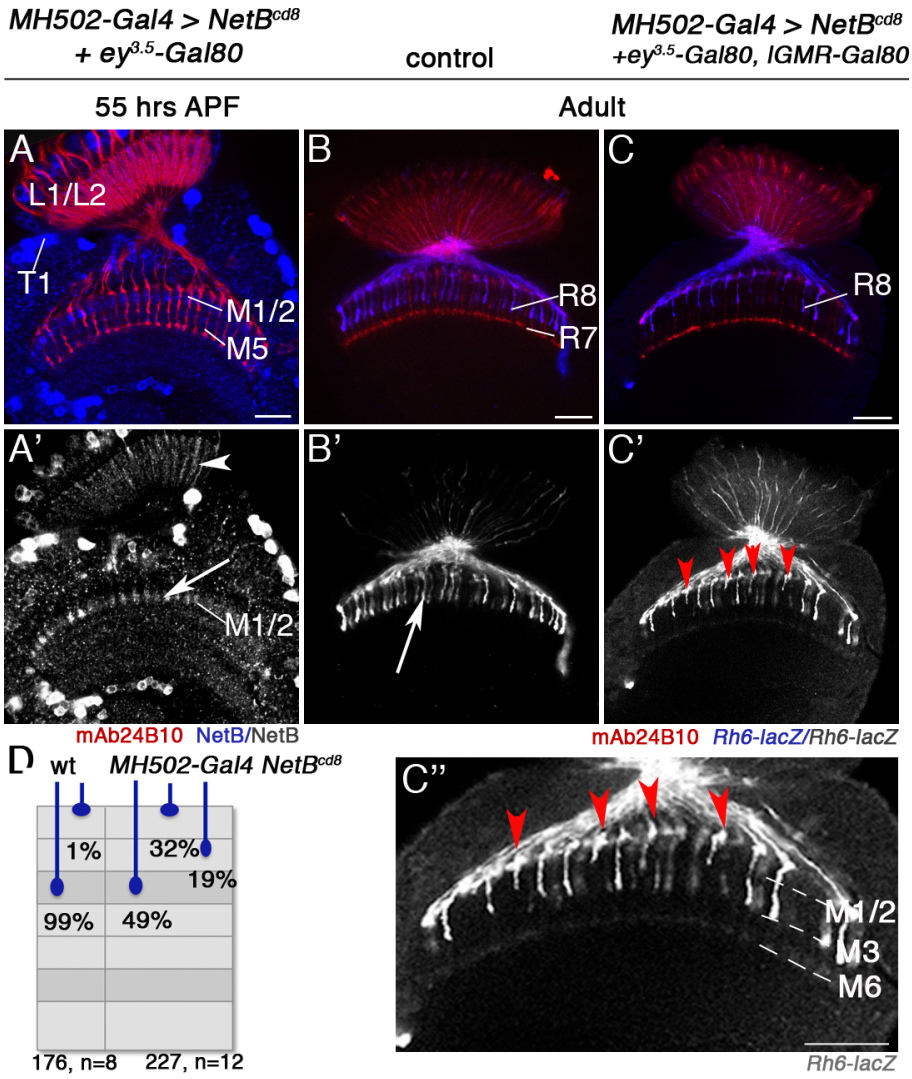

Figure 46. Ectopic expression of *UAS-NetB^{cd8}* using *MH502-Gal4*. (A-A') *MH502-Gal4* active in L1/L2, T1 medulla neurons and C2/C3 neurons. At 55 hours APF, NetB^{cd8} strongly localizes to the layers M1/M2 and M5 (arrow in A') and also in the lamina (arrowhead in A'). (B-C) Adult optic lobes. Analysis of R8 axon targeting to ectopic NetB accumulating layers. (B-B') In controls, all *Rh6-lacZ* positive R8 axons target normally to the M3 layer (arrow in B'). (C-C') In optic lobes where NetB is provided ectopically, 19% of R8 axons are redirected to the new NetB positive layer (arrowheads in C' and C''). 32% stalled at the border, while 49% terminate in the M3 layer. R-cells are labeled with mAb24B10 (red). (D) Quantification of phenotypes. Scale bars, 20 μm.

To further validate these findings, membrane-tethered NetB was widely expressed in medulla neuropil layers. This experiment used the *apterous-Gal4* (*ap-Gal4*) driver that has been described to be active in lamina neurons L4 and in 40% of medulla neurons and is widely expressed in medulla neuropil layers (Morante and Desplan, 2008). Furthermore, *ap-Gal4* is not expressed in R-cells. The expression of *ap-Gal4* was analyzed during pupal development and in the adult using the *UAS-cd8GFP* reporter (Figure 47A-D).

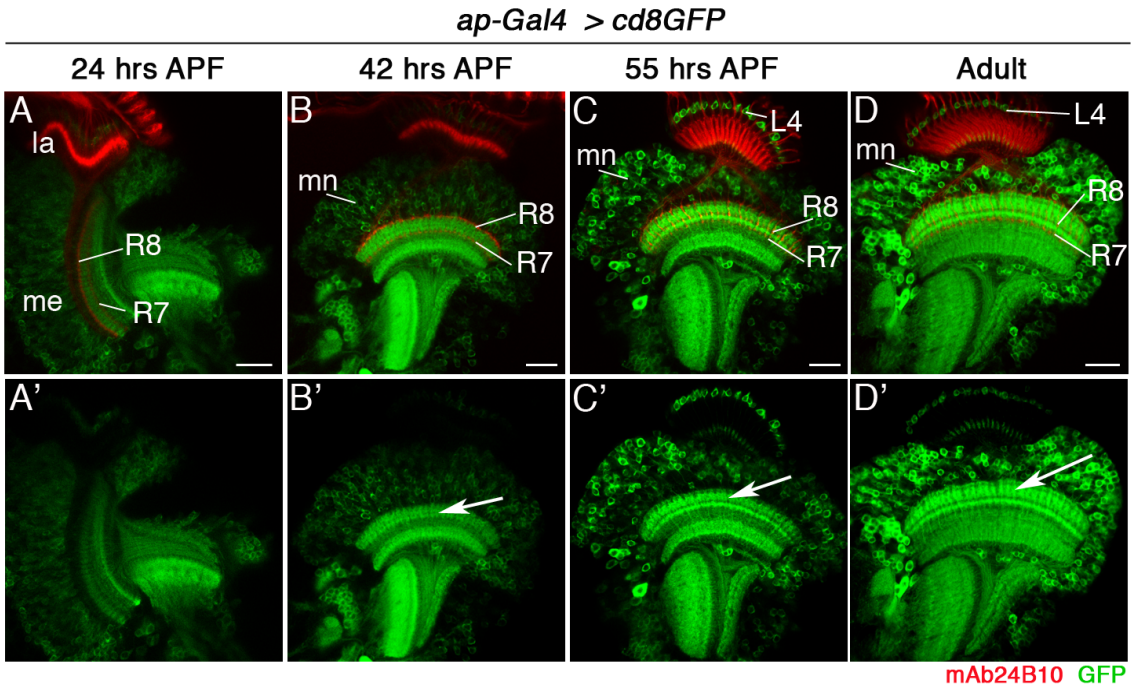

Figure 47. *ap-Gal4* expression during pupal development and in the adult. (A-D) Throughout pupal development and in adults, *ap-Gal4* drives strong expression of the *UAS-cd8GFP* reporter in cell bodies and processes of lamina neurons L4 and in 40% of medulla neurons and is localized in several medulla neuropil layers (arrows in B', C'). *ap-Gal4* is not expressed in R-cells. R-cell axons are labeled with mAb24B10 (red). la, lamina, me, medulla. Scale bars are 20 μm.

When membrane-tethered *UAS-NetB^{cd8}* was expressed under the control of *ap-Gal4*, NetB^{cd8} was widely localized in several medulla neuropil layers (Figure 48A, A'). In this experiment, R8 axon targeting is affected (Figure 48C-C"). 65% of *Rh6-lacZ* labeled R8 axons terminated correctly in the M3 layer and 27% of R8 axons stalled at the medulla neuropil border (total of 265 *Rh6-lacZ* positive R8 axons, n=13). Importantly, only 8% extended fine processes in to the M1/2 layers (Figure 48C-C"). Thus, when *NetB^{cd8}* is localized widely in the medulla neuropil, R8 axons seem to lose the positional information this guidance cue normally provides and stall at the medulla neuropil border or extend into the M1/M2 layers in the medulla.

Taken together, when *UAS-NetB^{cd8}* is expressed under the control of *MH502-Gal4* combined with *ey$^{3.5}$-Gal80* and *lGMR-Gal80,* this M1/M2 layer-specific localization of NetB^{cd8} allows 19% of R8 axons to retarget to the M1/M2 layers as compared to 8% when using the *ap-Gal4* driver. These findings indicate that for correct layer-specific R8 axon targeting, NetB is required to be localized in a precise layer. This is pivotal to provide positional information. Moreover, these experiments support the notion that NetB is instructive for layer-specific axon targeting.

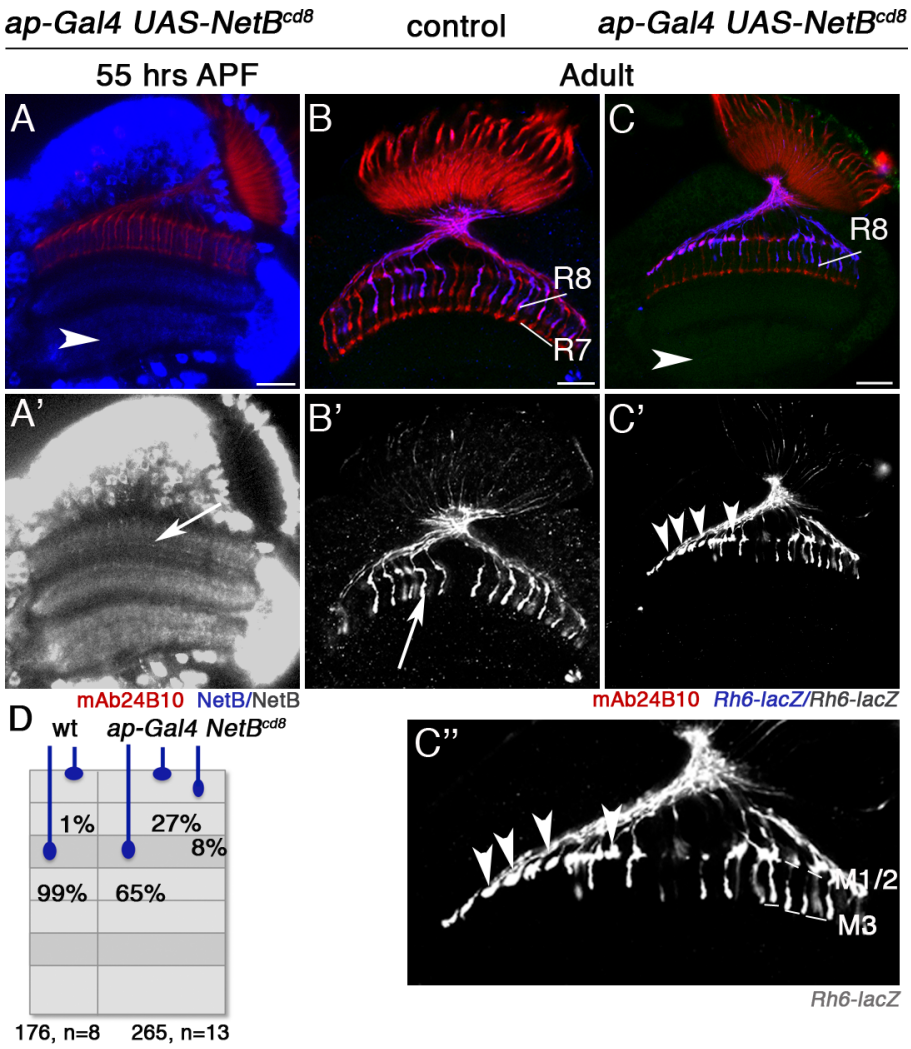

Figure 48. *UAS-NetB^{cd8}* over-expression broadly in the target neurons in the medulla using *ap-Gal4*. (A-A') Expression of *UAS-NetB^{cd8}* under the control of *ap-Gal4*. At 55 hours APF, NetB is detected in cell bodies and arborizations of lamina neurons L4 and medulla neurons. NetB^{cd8} accumulates widely in layers in the medulla neuropil (arrow in A'). The assembly of the lobula and lobula plate is affected (arrowheads in A and C). (B-C) Adult optic lobes. Analysis of R8 axon targeting to ectopically expressed NetB. (B-B') In controls, *Rh6-lacZ* positive R8 axons target normally to the M3 layer (arrow in B', 176 R8 axons, n=8). (C-C") In optic lobes, in which NetB is provided widely in several layers in the medulla neuropil, 27% of *Rh6-lacZ* positive R8 axons stall at the medulla neuropil border (arrowheads in C' and C", 265 R8 axons, n=13). 8% of R8 axons grow towards the M1/M2 layers. R-cells are labeled with mAb24B10 (red). (D) Quantification of phenotypes. Scale bars are 20 μm.

6.3 Discussion

6.3.1 Layer-specific localization of NetB is sufficient to target R8 axons

The overall aim of the experiments described in this chapter was to create an ectopic NetB accumulating layer to demonstrate that NetB has an instructive role in R8 axon targeting. This was proven not to be straightforward for several reasons: Firstly, NetB is released from axonal terminals into the M3 layer. Therefore a suitable driver must be chosen, that allows releasing NetB into the ectopic layer. Secondly, spatiotemporal activity of the driver must be appropriate to allow correct expression of NetB. Thirdly, diffusible NetB must be localized in the ectopic layer by preventing diffusion. For this purpose, in two independent approaches, NetB and Fra were either co-expressed or NetB was tethered to the membrane by introducing a *cd8* membrane tag into the *UAS-NetB* transgene.

However, as Fra is a guidance receptor, introducing it in cell types that usually do not express Fra can make those cells equally responsive to endogenous NetB (as shown with T1 neurons expressing *UAS-Fra*^{fl}*)*. This initial caveat was overcome by introducing a truncated transmembrane Fra receptor (*UAS-fra*$^{\Delta Cmyc}$) that still binds NetB, but is unable to signal. However, when this construct was expressed together with *UAS-NetB* under the control of enhancer trap Gal4 lines that have arborizations in the M1/M2 layers, this did not lead to re-targeting of R8 axons. It is conceivable that this is due to too weak or timely incorrect expression of the drivers. In addition, ectopically introducing Fra and NetB in cells, which normally do not express these proteins, does not ensure that they will be correctly sub-cellularly localized or released. Unfortunately, during the initial stage of the experiments it was not possible to assess the localization of NetB protein, because the antibody was not available to us. Therefore, it remains

open as to whether NetB was correctly localized in the ectopic layers M1/M2 by *UAS-fra*$^{\Delta Cmyc}$.

In subsequent experiments a membrane-tethered construct of NetB (*UAS-NetB*^{cd8}) was generated. However, also when using this strategy, NetB is required to be localized sub-cellularly and correctly released. Indeed, when drivers were used that are active in T1 neurons, the *UAS-cd8GFP* reporter expression revealed arborizations in the M1/M2 layers. However, NetB was not localized in the medulla but in the lamina. T1 neurons have their axonal terminals in the lamina and dendritic branches in the medulla. Thus, this further strengthens the notion, that the guidance molecule NetB is released from axon terminals. Moreover, ectopic expression of full-length *Fra* leads to re-targeting of dendrites of T1 neurons to the endogenous NetB in the M3 layer. This is in line with the hypothesis that pre- and postsynaptic partner neurons use the same guidance cue as positional information to find the same layer, likely mediated through their respective expression of the guidance receptor Fra. This also suggests that while NetB is primarily released by axons, Fra is likely localized to axons and dendrites.

Finally, NetB was successfully localized to the M1/M2 layer using membrane-tethered *UAS-NetB*^{cd8} under the control of *MH502-Gal4*. Under this condition a significant number of R8 axons innervated the M1/M2 layers. This driver is active in L1 and L2 lamina neurons, C2/C3 neurons and T1 neurons. Consistent with the idea that axon terminals are the primary source of NetB, this ectopic ligand accumulation using *MH502-Gal4* can be mainly attributed to lamina neurons L1 and L2. To further verify the findings of retargeting R8 axons to a layer-specific NetB source, these effects were compared to a more globally expressed *NetB*^{cd8}. The increased percentage of redirected axons to defined NetB expressing layers using *MH502-Gal4* compared to the effects of

wide ectopic expression using *ap-Gal4* supports the model that layer-specific localization of NetB is instructive for R8 axon targeting.

Taken together, layer-specific localization of NetB is sufficient to target R8 axons. However, the penetrance of retargeted R8 axons to the ectopically accumulating NetB in the M1/2 layers is 19% of *Rh6-lacZ* positive R8 axons, while 32% stall at the medulla neuropil border and 49% correctly innervate the M3 layer. The latter is likely due to endogenous NetB present in the M3 layer. In addition, other guidance forces might be active that prevent R8 axons from innervating inappropriate layers. One possibility that will be explored in the next chapter is therefore as to whether repulsive forces play a role in layer-specific R8 axon targeting.

Chapter 7

The role of Unc-5 in R8 axon targeting

7.1 Introduction

Axon guidance, target recognition and synapse formation involve both, positive and negative regulation. Therefore, a guidance cue such as Netrin can be interpreted by an axon in different ways, depending on the receptors it expresses.

So far, we have demonstrated that the Fra/NetB guidance system is required and instructive for the targeting of R8 axons to their final layer M3 at mid-pupal stages. However, during early pupal development, R8 axons remain and pause at the neuropil border, although NetB is already localized in the emerging M3 layer from 42 hours APF (see Figure 17, Chapter 4), at which time also Fra is expressed in R8 axons (Figure 11 in Chapter 3). In principle, if all that is required for targeting is the attractive force mediated through Fra and NetB, R8 axons should proceed to their final layer as early as that. However, they remain at the medulla neuropil border. This may be essential to synchronize R8 axons, as they arrive gradually in the medulla during larval and early pupal stages and become located at the medulla neuropil border. Moreover, this may provide a mechanism that allows the coordination of target neuron and R-cell development during the assembly of the medulla neuropil.

During the second step of R8 axon targeting, R8 axons are released from the medulla neuropil border and proceed to their final layer. This raises the question as to which mechanisms can keep R8 axons at their temporary layer at the medulla neuropil border and subsequently lead to their release. Therefore, I tested next as to whether repulsion can affect layer-specific R8 axon targeting during early pupal development. If *unc-5* fulfills the role in keeping R8 axons at the medulla neuropil border, loss of it in R-cells should lead to premature ingrowth of R8 axons towards the NetB-positive layer.

In this chapter, I investigated as to whether the repellent receptor Unc-5 has a function in layer-specific targeting of R8 axons.

7.2 Results

7.2.1 Unc-5 is expressed in the optic lobe during pupal development

To gain insights into the role of the Unc-5 guidance receptor in visual circuit assembly, expression of Unc-5 was examined during optic lobe development and in the adult. For this purpose we have generated antisera raised against a non-conserved sequence stretch downstream of the signal peptide and upstream of the fifth Ig-like domain of Unc-5 (see Material and Methods). In the optic lobe, Unc-5 is expressed dynamically during development. At early pupal stages, at 24 hours and 42 hours APF, Unc-5 is expressed at the medulla neuropil border corresponding to the temporary R8 layer (Figure 49A-B'). This suggests that Unc-5 may also be expressed in R8 axons during these developmental stages. Moreover, Unc-5 is co-expressed in the same layer as Fra.

From mid-pupal stages, during the final target layer selection process, Unc-5 is expressed in a largely complementary pattern to the expression domains of Fra and NetB (Figure 49C, C'). In particular, Unc-5 is expressed in the M1/2 layers and additionally in the layer M5. It is likely not expressed in R8 axons during mid-pupal development. This expression persists in the adult fly (Figure 49D, D'). In addition, Unc-5 expression in detected in the lobula plate at 42 hours APF, 55 hours APF and in the adult (Figure 49B-D').

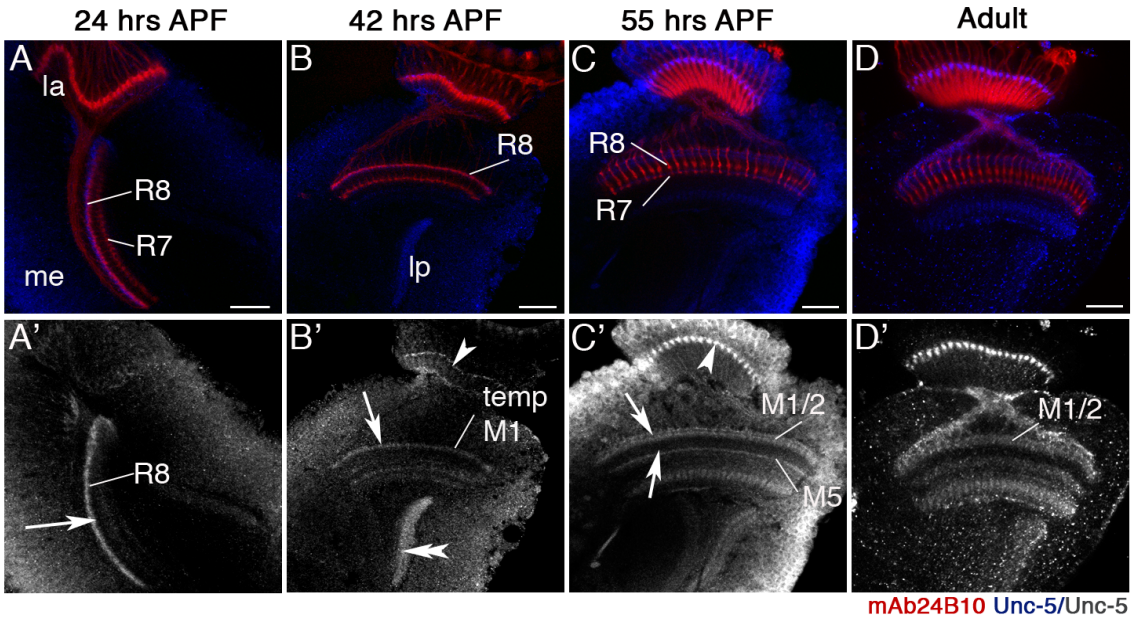

Figure 49. The guidance receptor Unc-5 is dynamically expressed in the visual system. (A-D) A newly generated polyclonal antibody reveals expression of Unc-5 (blue) throughout development in wild type optic lobes. (A, B) At 24 and 42 hours APF, Unc-5 is expressed in the temporary layer of R8 axons at the border of the medulla neuropil and co-localizes with R8 growth cones (arrows, A', B'). Unc-5 is strongly expressed in the lobula plate (lp) at 42 hours APF (double-arrowhead in B'). Unc-5 staining is further detected in the lamina (arrowhead in B'). (C-D) At 55 hours APF and in the adult, Unc-5 is expressed in the M1/M2 and M5 layers (arrows in C'), but not in the R8 recipient layer M3. In the lamina Unc-5 is detected in glia cells (arrowhead in C'). R-cells are labeled with mAb24B10. la, lamina, me, medulla, lp, lobula plate. Scale bars are 20 μm.

7.2.2 *unc-5* is required for layer-specific targeting of R8 axons

This expression pattern raised the question as to whether *unc-5* could play a role in layer-specific targeting in the visual system. To determine the requirement of *unc-5*, the *unc-5*^{8} null mutant EMS allele was analyzed in detail (Labrador et al., 2005). This allele contains a P{GS} element, as it was originally generated in a gain-of-function suppressor screen. To avoid unspecific effects of the P{GS} element, I used a P-element excision strategy to remove this P-element and obtained the new allele *unc-5*$^{8\text{-}2a}$. PCR and sequence analysis confirmed the removal of the P insertion and the point mutation at Glutamine$_{19}$ leading to a base pair change from CAG to TAG and thus a premature

stop. For further mosaic analysis, *unc-5*$^{8\text{-}2a}$ was recombined on a FRT42D site containing chromosome. Functional studies were carried out using the *ey*$^{3.5}$*-FLP* system based mosaic analysis approach to determine its potential role in R-cells. R8 axons were specifically labeled with the late genetic marker *Rh6-lacZ*. This revealed, that 45% of R8 axons lacking *unc-5* remained at the border of the medulla neuropil, while R7 axons were not affected (Figure 50B, B', total of 185 R8 axons, n=10). In controls R8 axons target normally to the M3 layer (Figure 50A, A', total of 176 axons, n=8).

Thus, *unc-5* is required in R8 for layer-specific targeting in the medulla. Surprisingly, this phenotype strongly resembles the loss-of-function phenotype observed with the attractant receptor *fra*.

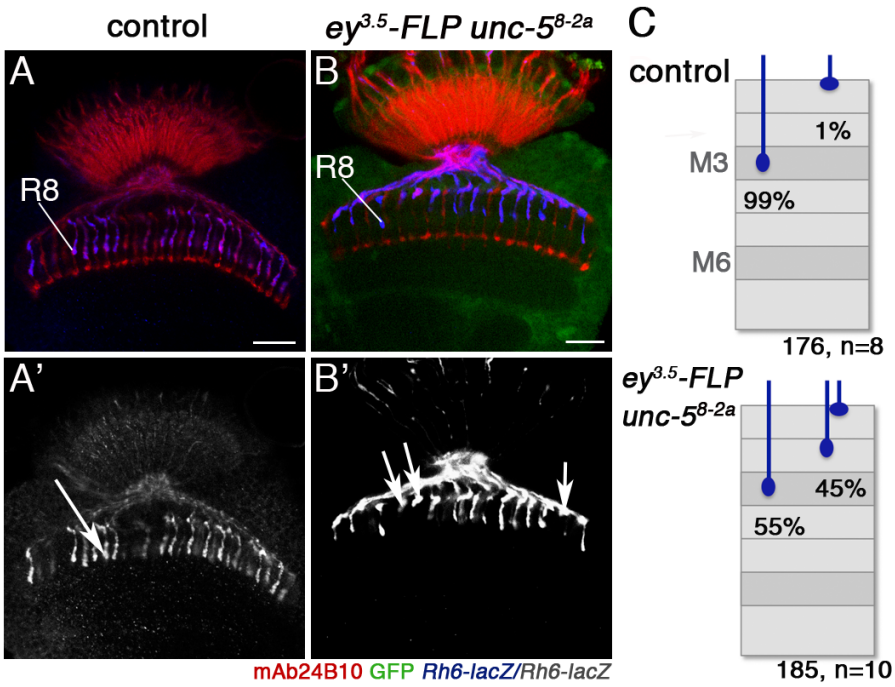

Figure 50. *unc-5* is required for R8 axon targeting. (A, A') In wild type adult flies, R8 axons terminate in their target layer M3 in the medulla (arrow in A'). (B, B') The *ey*$^{3.5}$*-FLP* approach is used to remove *unc-5* function in the eye. Analysis of the modified *unc-5*$^{8\text{-}2a}$ allele revealed that R8 axons terminated at the medulla neuropil border. In animals lacking *unc-5* in all R-cells, 45 % of *Rh6-lacZ* positive R8 axons stall at the border of the medulla neuropil (total of 185 R8 axons, n=10, arrows in B'). Mutant R-cells were generated using the *ey*$^{3.5}$*-FLP* system. R-cells are labeled with mAb24B10. Scale bars are 20 μm. (C) Quantification of R8 axon targeting phenotypes.

7.2.3 *unc-5* is required to maintain R8 axons at the medulla neuropil border during the first half of pupal development

To gain further insights into the role of Unc-5, I next tested as to whether the aberrant targeting of R8 axons to the M3 layer in *unc-5* mutants is due to a requirement of *unc-5* in layer specific targeting during development. Using the *ey$^{3.5}$-FLP* approach to remove *unc-5* in the eye, I observed that R8 axons prematurely extend deeper into the medulla neuropil as early as 24 hours APF (Figure 51B, B', 29% of 262 *ato-τ-myc* positive R8 axons, n=9), when compared to wild type controls (Figure 51A, A', 1% of 201 *ato-τ-myc* positive R8 axons, n=7). These defects persisted at 42 hours APF (Figure 51D, D', 23% of 134 *ato-τ-myc* positive R8 axons, n=5). In controls at 42 hours APF, R8 axons terminate correctly at the medulla neuropil border (Figure 51C, C', 27 *ato-τ-myc* positive R8 axons, n=2).

This suggests that *unc-5* could play a role in preventing R8 axons from premature entry into deeper medulla layers, thus keeping R8 axons at the medulla neuropil border. However, as to whether layer-specific R8 axon target at later pupal stages at 55 hours APF requires *unc-5* was not tested yet and will need to be addressed in future studies.

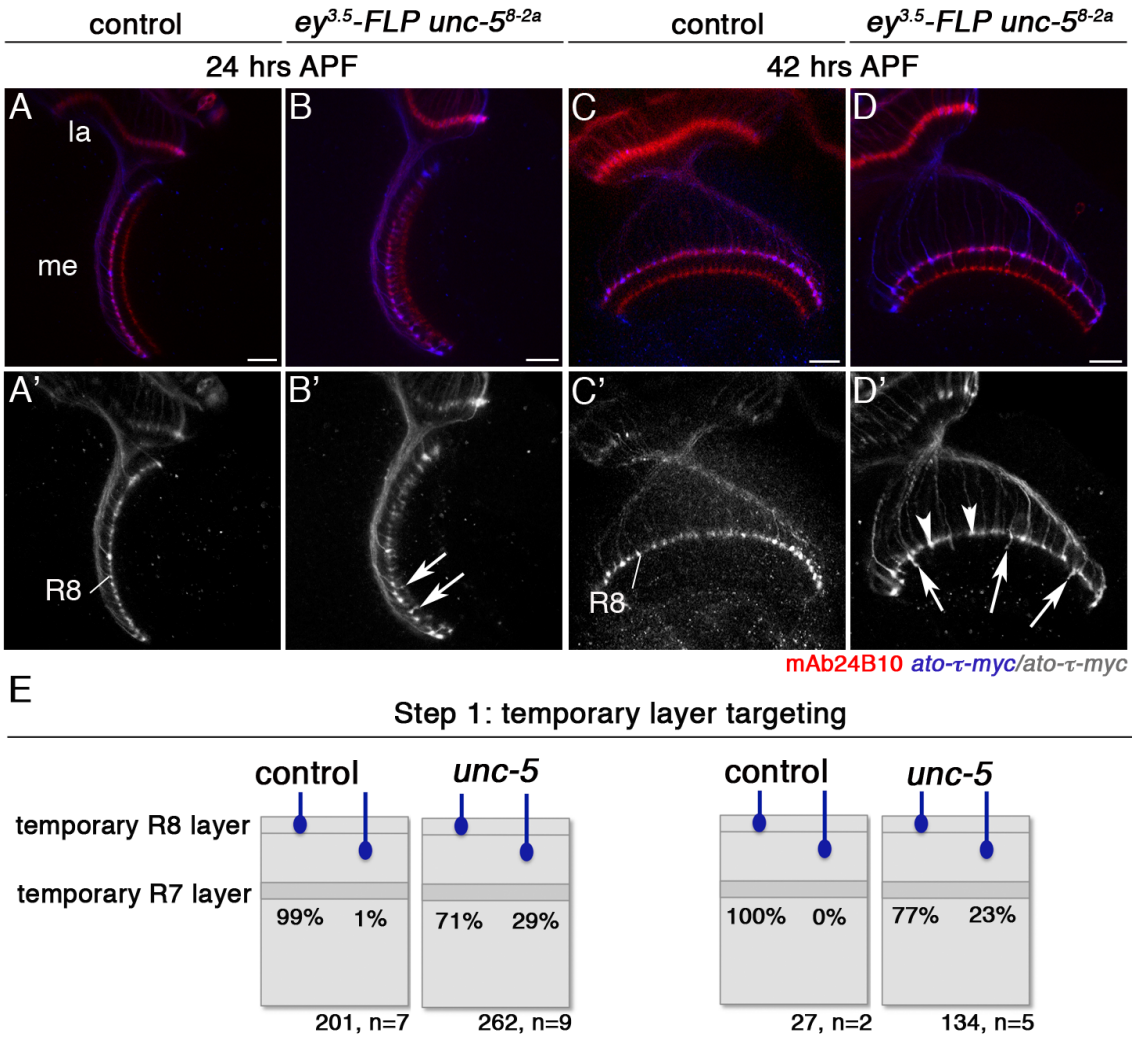

Figure 51. *unc-5* is required during early pupal development. (A-D) At early stages of pupal development, *unc-5* requirement was assessed in *ey*$^{3.5}$*-FLP* mutant clones using the *unc-5*$^{8-2a}$ allele or in controls, in combination with the early R8 axon marker *ato-τ-myc*. (A, A') At 24 hours APF all *ato-τ-myc* positive R8 axons (blue, 201 R8 axons, n=7) terminate in their temporary layer at the medulla neuropil border in controls. (B, B') In animals lacking *unc-5* in all R-cells, 71% of R8 axons pause correctly at the medulla neuropil border, while 29 % of 262 *ato-τ-myc* positive R8 axons prematurely project deeper (n=9, arrows in B'). (C, C') In wild type at 42 hours APF, all R8 axons project to the emerging M3 medulla layer (n=2). (D, D') In *unc-5* mutants, a large number of R8 axons (77% of 134 R8 axons, n=5) stayed at the border of the medulla neuropil (arrowheads in D'). However, 23% of R8 axons terminated prematurely in the M1/M2 layers (arrows in D'). Scale bars are 20 μm. (E) Quantification of phenotypes.

7.2.4 Ectopic expression of *unc-5* in R-cells prevents targeting to the lamina and medulla neuropils

In addition to the loss-of-function studies, I performed over-expression analyses using an available *UAS-HA-unc-5* transgene (Keleman and Dickson, 2001). In control adult optic lobes, R8 axons terminated in M3 layer, while R7 axons innervated the layer M6 (Figure 52A, A', n=7). Expression of *UAS-HA-unc-5* with the R-cell specific *lGMR-Gal4* driver resulted in a strong phenotype: both R8 and R7 axons stalled at the medulla neuropil border. Moreover, lamina cartridge assembly was severely affected (Figure 52B, B', n=6). This lack of innervation by R-cells did not affect the general development of the medulla neuropil, as the overall shape of the medulla, lobula and lobula plate appear to be unaltered (Figure 52C, n=5).

These findings reveal that *unc-5* is a generally strong repulsive receptor. It affects targeting of all R-cells that ectopically express *unc-5*. Thus, the expression of Unc-5 must be under a tight spatial and temporal control.

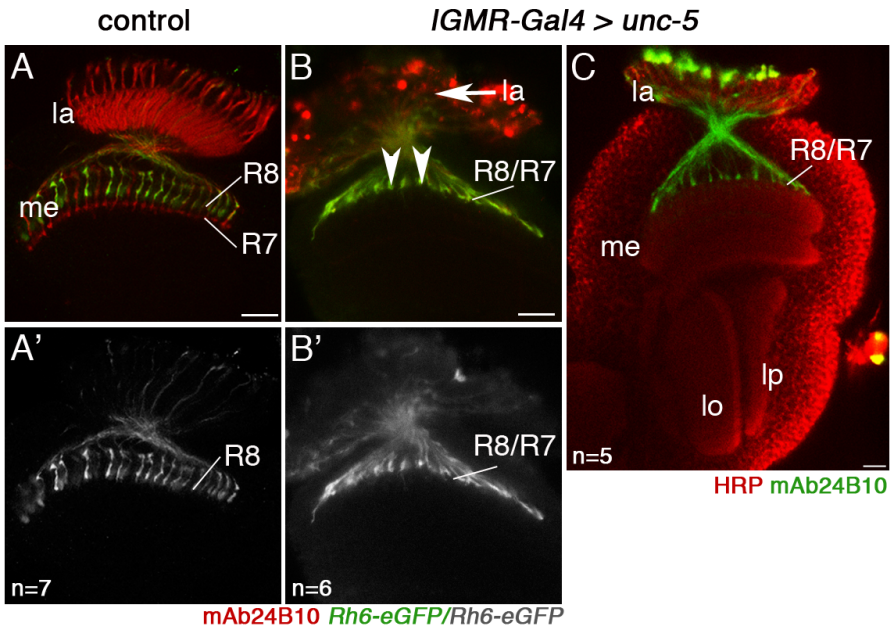

Figure 52. Unc-5 acts as a repellent receptor when expressed ectopically in R-cells. (A-C) Adult optic lobes. (A, A') Control optic lobes show correct targeting of *Rh6-eGFP* positive R8 axons (green) to the M3 layer and R7 axons to the M6 layer in the medulla neuropil. R-cells are labeled with mAb24B10 (red). (B-C) Over-expression of *UAS-unc-5* using the R-cell driver *lGMR-Gal4* resulted in a general repulsion of R-cell axons with all R-cell axons stalling at the medulla neuropil border (arrows in B'). Lamina cartridges are severely disrupted (arrowhead in B'). (C) Labeling of the neuropils in the optic lobe using horse radish peroxidase (HRP) displays no obvious structural defects in the assembly of the medulla (me), lobula (lo) and lobula plate (lp) neuropils. Scale bars are 20 μm.

7.3 Discussion

7.3.1 *unc-5* is required for R8 axon targeting during early pupal development

In addition to attraction, the action of repellent guidance cues is an equally strong force in layer-specific targeting through signals that drive axons away from improper synaptic layers. Previous studies have identified Unc-5 as the repulsive Netrin receptor in *C. elegans, Drosophila* and in vertebrates (Hedgecock et al., 1990; Keleman and Dickson, 2001; Leonardo et al., 1997). In this part of my PhD studies, the role of Unc-5 was determined in the context of layer-specific targeting in the visual system.

Results presented thus far uncovered, that Unc-5 is expressed dynamically in the optic lobe. During initial R8 axon targeting, it is co-expressed with Fra in the same layer at the medulla neuropil border. In contrast, at later stages during the final target layer selection process, there is a striking complementarity between the expression pattern of Unc-5, as well as Netrin and Fra.

Functional studies using the *ey$^{3.5}$-FLP* mosaic approach determined the role of Unc-5 in R-cell targeting. In adults, removal of *unc-5* in R-cells leads to severe R8 axon targeting defects. R8 axons fail to innervate their correct target layer, but remain at the border of the medulla neuropil. To gain further insights into the function of *unc-5*, I analyzed R8 axon targeting during development. During early pupal stages, loss of *unc-5* in R-cells leads to premature ingrowth of R8 axons into the medulla neuropil. The premature ingrowth due to the loss of repulsion is consistent with the findings that during early pupal development Fra is expressed in R8 cells and NetB starts to accumulate in the emerging M3 layer. This suggests that R8 axons are able to target to this layer, but are initially held at the medulla neuropil border. Moreover, this may allow the coordination of the development of R-cells and target neurons during medulla neuropil assembly.

7.3.2 Unc-5 likely interacts with Fra in the Netrin mediated R8 axon targeting to the M3 layer

Interestingly, the loss of *NetA* and *NetB, fra* and *unc-5* results in a similar phenotype in the adult. How can this be explained? It is conceivable that Unc-5 provides a mechanism to keep R8 axons at the medulla neuropil border until the appropriate time for ingrowth, thus orchestrating the release of R8 axons and enabling them to grow towards their final target layer during mid-pupal development. As in *unc-5* mutants, R8 axons invade the medulla neuropil at an inappropriate time, they might fail to stabilize in the target layer and instead retract to the medulla neuropil border. This can explain the R8 axon targeting defects observed in the adult *unc-5* mutants. This is similar to findings in *caps* mutants in R8 axon targeting (Shinza-Kameda et al., 2006). These studies demonstrated, that *caps* mutant R8 axons initially reach the M3 layer in the medulla correctly. However, they then fail to establish stable connections with the target neurons and instead extend abnormally to neighboring columns or layers in the medulla neuropil. However, a crucial experiment will be to determine the *unc-5* loss-of-function phenotype at 55 hours APF.

Moreover, the question remains to be elucidated as to how Fra and Unc-5 are regulated to enable the coordination of attractive and repulsive responses to NetB during layer-specific R8 axon targeting. During the first half of pupal development, Fra and Unc-5 are initially co-expressed. This leads to the question as to how repulsion can be the outcome in this situation. From mid-pupal stages, Unc-5 is likely not expressed in R8 axons, thus likely allowing Fra-positive R8 axons to target to the NetB-positive M3 layer. Several findings suggest a hypothesis, by which Fra and Unc-5 could act in concert to mediate R8 axons targeting within the medulla neuropil in two steps. During initial targeting to the temporary layer at 24 and 42 hours APF, R8 axons are further away

from the accumulating NetB source in the emerging M3 layer. In addition to a role as a short-range chemo-attractant, NetB may act as a long-range cue during the first half of pupal development: Firstly, in flies in which diffusible NetB was replaced by membrane-tethered NetB ($NetB^{TMmyc}$) at endogenous levels in *NetA* mutants, R8 axons show aberrant R8 axon targeting, with 12% of R8 axons at 24 hours APF and 6% at 42 hours APF abnormally projecting past the distal medulla neuropil border (see Figure 21, Chapter 5). Secondly, it is not known as to whether the Fra-positive target neurons are able to localize and present NetB during early pupal stages, for instance at 24 hours APF. Therefore, one can imagine that the initial NetB concentration is low, as well as graded, and Unc-5 may prevent R8 axons to target towards the emerging M3 layer during early stages.

However, one problem is that Fra is also expressed in R8 cells. How can an attractive response be overwritten? Studies in *C. elegans* provided evidence that Unc-5 and Unc-40 are required to form a complex when concentrations of Netrins are low (Hedgecock 1990). Furthermore, studies in *Xenopus* demonstrated that in the presence of Netrin, Unc-5 undergoes conformational changes and is able to interact intracellularly with Unc-40 (Hong et al., 1999). This Unc-40/Unc-5 complex is suggested to have a higher sensitivity to Netrin than the Unc-5 receptor alone. Moreover, attraction through Unc-40 is silenced by Unc-5 mediated repulsion, which requires the cytoplasmic domain of Unc-5 (Hong et al., 1999).

In our studies, during early pupal stages Unc-5 and Fra are initially co-expressed. This may suggest that Unc-5 possibly together with Fra, prevents R8 axons from leaving their temporary layer. It will be interesting to test as to whether in *Drosophila*, Unc-5 and Fra can form a receptor complex to exert repulsion during the targeting to the temporary layers at the medulla neuropil border.

During R8 axon targeting to the final layer M3 at 55 hours APF, Fra executes attraction. *fra* mutant R8 axons fail to innervate the M3 layer and this phenotype persists in the adult. Unc-5 is likely not expressed and possibly not required in the R8 axons at this stage. Thus, the coordination of both, repulsion at early pupal stages and attraction at later stages, could allow the coordination of the two-step targeting process of R8 axons during development.

In addition, the dynamic expression pattern of Unc-5 indicates that it may have two separate functions. Firstly, Unc-5 plays a role in R8 axon targeting during the first half of pupal development. Secondly, at later stages, Unc-5 is likely not expressed R8 axons, but in dendritic and axonal branches of target neurons. This suggests that Unc-5 may be involved in shaping layer-specific branching of target neurons innervating the layers M1/2 and M5 at the same time. This could allow neurons that are expressing the repulsive receptor Unc-5 to restrict their arborizations away from the Netrin-expressing M3 layer, and explain how neurons can form branches in more than one layer. Future studies in our laboratory will address this role of Unc-5 in organizing the target field.

Chapter 8

Concluding remarks and future work

8.1 Strategies to form synaptic layers in the visual system

To understand as to how functional neuronal circuits are established, it is pivotal to uncover the mechanisms, which enable axons and dendrites of synaptic partners to form specific contacts among a great number of possible candidates. To limit possibilities, axons and dendrites of partner neurons have to be organized in spatial proximity. One way is to form synaptic columns or layers. Synaptic layers are omnipresent in the nervous system and form the structural basis for information processing in many anatomical structures of the nervous system such as the cortex, the hippocampus or the visual system (Holt and Harris, 1998; Huberman et al., 2010).

Several mechanisms have been identified that direct the formation of layer-specific connections. These include (i) the expression of a combinatorial code of cell adhesion molecules, (ii) temporal control of responsiveness to ubiquitous adhesion molecules and (iii) repulsion from inappropriate layers (Matsuoka et al., 2011; Petrovic and Hummel, 2008; Yamagata and Sanes, 2008). However it remains unclear, how these partner neurons find their precise position in a wider laminated brain area.

The work presented in here describes a different strategy to provide layer-specific positional information in the visual system of *Drosophila*. This is mediated by a localized guidance cue that defines a layer, thus providing precise positional information required for layer-specific axon targeting.

8.2 NetB regulates R8 axon targeting through both Fra and Unc-5 receptors

Axon targeting to medulla layers relies on several coordinated consecutive steps. Starting from the 3rd instar larval stage and during early pupal development, upon arri-

val at the medulla neuropil border R8 axons have to select the correct retinotopic column and pause at their temporary layer to orchestrate the incoming of all R8 axons. Recent findings have suggested interactions of the transmembrane Gogo receptor and the protocadherin cell adhesion molecule Fmi to mediate R8 inter-axonal repulsion enabling R8 axons to find their correct columnar position in the medulla (Hakeda-Suzuki et al., 2011; Tomasi et al., 2008). Fmi is further expressed broadly in the medulla, suggesting a role in targeting of afferent and target neuron axons through homophilic interactions (Hakeda-Suzuki et al., 2011; Mann et al., 2012). Fmi expression likely contributes to the timely release of R8 growth cones from their temporary layer, and consequently enables correct targeting to the M3 layer.

However, in addition a strategy is conceivable, by which timely regulation of repulsion can prevent R8 axons from extending into the medulla neuropil. In this study, we propose that Unc-5 provides a mechanism to keep R8 axons at the medulla neuropil border through repulsion from accumulating Netrin in the target area. However, during early pupal development, the repulsive Unc-5 and the attractive Fra receptor are initially co-expressed. Furthermore, at 42 hours APF, 23% of *unc-5* mutant R8 axons fail to stay at the temporary layer but invade deeper into the medulla neuropil. Similarly, the majority of *fra* deficient R8 axons pause correctly at the medulla neuropil border, while a small percentage (6%) prematurely projects deeper at this stage. This indicates that both Unc-5 and Fra are required to mediate short-range repulsion during early pupal stages for temporary layer targeting. This raises the question as to how this can be achieved. Findings in *C. elegans* and *Xenopus* showed that Fra and Unc-5 form complexes to allow higher sensitivity to Netrin when the concentrations are low (Hong et al., 1999; Hedgecock 1990). This is similar to the situation during initial targeting in the *Drosophila* visual system, when presumably graded NetB concentrations are low at the me-

dulla neuropil border. Recent studies have demonstrated that attraction through Unc-40 is silenced, when both receptors are co-expressed resulting in Unc-5 executing repulsion (Hong et al., 1999). This could be mediated through the integration of downstream signaling mechanisms. However, it remains to be elucidated in future studies, how Fra and Unc-5 regulate attraction versus repulsion in the *Drosophila* visual system.

From mid-pupal stages, R8 axons are released from this block possibly due to a down-regulation of Unc-5 as well as other guidance mechanisms, and proceed to their final target layer M3. They then have to pass by incorrect layers as well as inappropriate synaptic partners, and correctly identify their precise target layer position. The cell adhesion molecule Caps is suggested to specifically promote cell-cell recognition and stabilize interactions between R8 axons and synaptic partner within their correct column and target layer (Shinza-Kameda et al., 2006). However, Caps is expressed in a wider domain in the target area including layers M2 – M4. How do R8 axons find their precise position in the M3 layer? This can be mediated through the use of a localized short-range guidance cue to one positionally defined target layer. Our study demonstrated that Fra is expressed and cell-autonomously required in R8 axons for correct targeting to the M3 medulla neuropil layer. Localization of Netrin to a specific layer is both essential and instructive for layer-specific R8 axon targeting. Accumulation of NetB in the M3 layer is mediated by two mechanisms, local release by lamina neurons and capture by Fra-positive medulla neurons. Future studies will need to address, as to whether in addition a positive feedback loop mediated through asymmetrical accumulation of the Fra receptor may in turn increase NetB localization. Netrins have previously been shown to promote exocytosis and recruitment of Unc-40 to distinct subcellular locations along the axon, thus increasing the amount of Unc-40 at the cell surface (Adler et al., 2006; Cotrufo et al., 2011; Matsumoto and Nagashima, 2010). Similarly, in the visual system,

Netrins could increasingly attract processes of Fra-positive target neurons into the M3 layer, which in turn could promote further ligand accumulation. Thus, additional feedback loops may contribute to the specific enrichment of both Netrins and Fra in the M3 layer.

8.3 L3 lamina neurons function as intermediate targets for R8 axons

During pathfinding axons can use intermediate target cells along their trajectory to guide them towards their target areas. Also within the target area intermediate targets can bring putative synaptic partners into close vicinity (Sanes and Yamagata, 2009). Our findings investigating layer-specific R8 axon targeting indicate that lamina neurons L3 could play a role as intermediate targets in the visual system. R8 axons and lamina neurons L3 terminate closely adjacent to each other in the M3 layer. Moreover, studies using serial transmission electron microscopy revealed that L3 axons arborize in the proximal region of the M3 medulla layer in close proximity to R8 axons (Takemura et al., 2008). Although R8 axons and lamina neurons L3 do not form synaptic contacts with each other, they have been reported to connect with the same postsynaptic neuron subtypes, such as the transmedullary neuron Tm9 (Gao et al., 2008; Takemura et al., 2008). In their role as intermediate target neurons, lamina neurons L3 likely guide R8 axons into their recipient layer M3. Consistently, lamina neurons L3 project towards and form the emerging M3 layer during early pupal development before R8 axons terminate in this final recipient layer. Moreover, cell adhesion molecules such as CadN independently control L3 targeting (Nern et al., 2008). Strikingly, expression of NetB by lamina neurons L3 in a $NetAB^{\Delta}$ background significantly rescued R8 axon targeting defects. In conclusion, although a contribution of other neurons subtypes such as me-

dulla neurons cannot be excluded, these findings indicate that NetB provided by lamina neurons L3 is sufficient to control layer-specific targeting of R8 axons.

Moreover, the use of intermediate targets is essential, if guidance cues can only be released from axonal terminals. The release of guidance cues preferentially by axon terminals of intermediate target neurons allows positioning of other afferent axons into a defined layer. Subsequently, target neurons that express the receptor could be guided to the same layer in vicinity of their pre-synaptic partners. However, as to whether target neurons employ this mechanism remains to be elucidated in future studies focusing on dendritic targeting of medulla neurons subtypes expressing the Fra receptor.

8.4 Hierarchy in the neuropils: Top-down control to connect synaptic neuropils

Visual information is transmitted from the retina through the lamina and medulla, to eventually be processed in the lobula complex. To date it is not known as to which mechanisms regulate the interconnection of the individual synaptic neuropils. One interesting concept is that one guidance system is used several times thus connecting neurons in subsequent neuropils in a top-down manner. Our findings presented thus far suggest the hypothesis that Netrin guidance cues could mediate this process through their receptors Fra and Unc-5.

NetB is expressed by lamina neurons L3 with dendritic projections in the lamina and axonal terminals in the medulla, with which it provides guidance to the M3 layer. Besides R8 axons, Fra-positive medulla neurons subtypes could use NetB for the targeting of their dendritic processes to this layer. In addition, NetB is also expressed in the lobula. Therefore axonal projections of these Fra-positive target neurons can be guided

to this next neuropil, thus connecting it with the medulla. Neuron subtypes that connect the distal medulla and the lobula are for instance transmedullary (Tm) neurons (Fischbach and Dittrich, 1989). However, it is not known as to which neurons express and require the Fra guidance receptor, therefore future studies will need to characterize the Fra-positive neuron population.

The notion that projections of target neurons could be guided to the lobula using the Netrin/Fra guidance system is consistent with observations that in knock-down of *fra* in the eye and target neurons, the expression of the independent marker Fmi was also present in the lobula plate, as compared to controls were Fmi is only detected within a layer in the lobula (Figure 24 in Chapter 5). This suggests that loss of *fra* in target neurons leads to abnormal projections.

In contrast, Unc-5 is expressed in the lobula plate, suggesting that axons of target neurons may be repelled by Netrins in the lobula, but grow into the permissive lobula plate target area. Consequently, expression of either the attractive Fra receptor or the repellent Unc-5 receptor, or a combination of both, could allow target neurons to make a binary choice between the NetB-positive lobula versus the NetB-negative lobula plate. Future studies in our laboratory aim at elucidating if and which target neurons use the Netrin/Fra/Unc-5 guidance system to make decisions at binary choice points, such as innervation of the lobula versus lobula plate. Furthermore, subsequent studies will address the question as to whether target neurons use this guidance system to establish layer-specific connections in the *Drosophila* visual system.

References

Aberle, H. (2009). No sidesteps on a beaten track: motor axons follow a labeled substrate pathway. Cell adhesion & migration, pp. 358-360.

Adams, R.H., and Eichmann, A. (2010). Axon guidance molecules in vascular patterning. Cold Spring Harbor Perspectives in Biology, pp. 1875.

Adler, C.E., Fetter, R.D., and Bargmann, C.I. (2006). UNC-6/Netrin induces neuronal asymmetry and defines the site of axon formation. In Nat Neurosci, pp. 511-518.

Albrecht, S., Altenhein, B., and Paululat, A. (2011). The transmembrane receptor Uncoordinated5 (Unc5) is essential for heart lumen formation in Drosophila melanogaster. Developmental Biology, pp. 89-100.

Andrews, G.L., Tanglao, S., Farmer, W.T., Morin, S., Brotman, S., Berberoglu, M.A., Price, H., Fernandez, G.C., Mastick, G.S., Charron, F., *et al*. (2008). Dscam guides embryonic axons by Netrin-dependent and -independent functions. Development, pp. 3839-3848.

Antoine-Bertrand, J., Ghogha, A., Luangrath, V., Bedford, F.K., and Lamarche-Vane, N. (2011). The activation of ezrin-radixin-moesin proteins is regulated by netrin-1 through Src kinase and RhoA/Rho kinase activities and mediates netrin-1-induced axon outgrowth. Molecular Biology of the Cell, pp. 3734-3746.

Asakura, T., Waga, N., Ogura, K., and Goshima, Y. (2010). Genes required for cellular UNC-6/netrin localization in Caenorhabditis elegans. Genetics *185*, 573-585.

Bányai, L., and Patthy, L. (1999). The NTR module: domains of netrins, secreted frizzled related proteins, and type I procollagen C-proteinase enhancer protein are homologous with tissue inhibitors of metalloproteases. Protein Sci *8*, 1636-1642.

Barallobre, M.J., Pascual, M., Del Rio, J.A., and Soriano, E. (2005). The Netrin family of guidance factors: emphasis on Netrin-1 signalling. Brain Res Brain Res Rev *49*, 22-47.

Bashaw, G.J., and Klein, R. (2010). Signaling from axon guidance receptors. Cold Spring Harbor Perspectives in Biology, pp. 1941.

Bate, C.M. (1976). Pioneer neurones in an insect embryo. Nature, pp. 54-56.

Bazigou, E., Apitz, H., Johansson, J., Lorén, C.E., Hirst, E.M.A., Chen, P.-L., Palmer, R.H., and Salecker, I. (2007). Anterograde Jelly belly and Alk receptor tyrosine kinase signaling mediates retinal axon targeting in Drosophila. Cell, pp. 961-975.

Bentley, D., and Caudy, M. (1983). Navigational substrates for peripheral pioneer growth cones: limb-axis polarity cues, limb-segment boundaries, and guidepost neurons. Cold Spring Harb Symp Quant Biol *48 Pt 2*, 573-585.

Bonhoeffer, T., and Yuste, R. (2002). Spine motility. Phenomenology, mechanisms, and function. Neuron, pp. 1019-1027.

Borod, E.R., and Heberlein, U. (1998). Mutual regulation of decapentaplegic and hedgehog during the initiation of differentiation in the Drosophila retina. Dev Biol *197*, pp. 187-197.

Borst, A., and Euler, T. (2011). Seeing things in motion: models, circuits, and mechanisms. Neuron, pp. 974-994.

Bradford, D., Cole, S.J., and Cooper, H.M. (2009). Netrin-1: diversity in development. Int J Biochem Cell Biol, pp. 487-493.

Brenner, S. (1974). The genetics of *Caenorhabditis elegans*. Genetics 77, pp. 71-94.

Brierley, D.J., Blanc, E., Reddy, O.V., Vijayraghavan, K., and Williams, D.W. (2009). Dendritic targeting in the leg neuropil of Drosophila: the role of midline signalling molecules in generating a myotopic map. PLoS Biol, pp. e1000199.

Brittis, P.A., Lu, Q., and Flanagan, J.G. (2002). Axonal protein synthesis provides a mechanism for localized regulation at an intermediate target. Cell *110*, pp. 223-235.

Brose, K., Bland, K.S., Wang, K.H., Arnott, D., Henzel, W., Goodman, C.S., Tessier-Lavigne, M., and Kidd, T. (1999). Slit proteins bind Robo receptors and have an evolutionarily conserved role in repulsive axon guidance. Cell, pp. 795-806.

Bukalo, O., Fentrop, N., Lee, A.Y.W., Salmen, B., Law, J.W.S., Wotjak, C.T., Schweizer, M., Dityatev, A., and Schachner, M. (2004). Conditional ablation of the neural cell adhesion molecule reduces precision of spatial learning, long-term potentiation, and depression in the CA1 subfield of mouse hippocampus. J Neurosci, pp. 1565-1577.

Cajal, S.R. y. 1890. À quelle époque apparaissent les expansions des cellules nerveuses de la moëlle épinière du poulet? Anatomischer Anzeiger 21-22, pp. 609-639.

Campbell, D.S., and Holt, C.E. (2001). Chemotropic responses of retinal growth cones mediated by rapid local protein synthesis and degradation. Neuron, pp. 1013-1026.

Camurri, L., Mambetisaeva, E., and Sundaresan, V. (2004). Rig-1 a new member of Robo family genes exhibits distinct pattern of expression during mouse development. Gene Expr Patterns *4*, 99-103.

Chan, S.S., Zheng, H., Su, M.W., Wilk, R., Killeen, M.T., Hedgecock, E.M., and Culotti, J.G. (1996). UNC-40, a C. elegans homolog of DCC (Deleted in Colorectal Cancer), is required in motile cells responding to UNC-6 netrin cues. Cell *87*, 187-195.

Chao, D.L., Ma, L., and Shen, K. (2009). Transient cell-cell interactions in neural circuit formation. Nat Rev Neurosci *10*, 262-271.

Chédotal, A., and Richards, L.J. (2010). Wiring the brain: the biology of neuronal guidance. Cold Spring Harbor Perspectives in Biology, pp. 1917.

Chen, P.-L., and Clandinin, T.R. (2008). The cadherin Flamingo mediates level-dependent interactions that guide photoreceptor target choice in Drosophila. Neuron, pp. 26-33.

Cheng, H.J., and Flanagan, J.G. (1994). Identification and cloning of ELF-1, a developmentally expressed ligand for the Mek4 and Sek receptor tyrosine kinases. Cell *79*, 157-168.

Cheng, Y., Endo, K., Wu, K., Rodan, A.R., Heberlein, U., and Davis, R.L. (2001). Drosophila fasciclinII is required for the formation of odor memories and for normal sensitivity to alcohol. Cell, pp. 757-768.

Choe, K.-M., Prakash, S., Bright, A., and Clandinin, T.R. (2006). Liprin-alpha is required for photoreceptor target selection in Drosophila. Proc Natl Acad Sci USA, pp. 11601-11606.

Chotard, C., Leung, W., and Salecker, I. (2005). glial cells missing and gcm2 cell autonomously regulate both glial and neuronal development in the visual system of Drosophila. Neuron, pp. 237-251.

Chou, Y.H., Spletter, M.L., Yaksi, E., Leong, J.C., Wilson, R.I., and Luo, L. (2010). Diversity and wiring variability of olfactory local interneurons in the Drosophila antennal lobe. Nat Neurosci *13*, 439-449.

Cirulli, V., and Yebra, M. (2007). Netrins: beyond the brain. Nat Rev Mol Cell Biol, pp. 296-306.

Clandinin, T.R., and Feldheim, D.A. (2009). Making a visual map: mechanisms and molecules. Curr Opin Neurobiol *19*, 174-180.

Clandinin, T.R., and Zipursky, S.L. (2000). Afferent growth cone interactions control synaptic specificity in the Drosophila visual system. Neuron, pp. 427-436.

Clandinin, T.R., and Zipursky, S.L. (2002). Making connections in the fly visual system. Neuron *35*, 827-841.

Cotrufo, T., Pérez-Brangulí, F., Muhaisen, A., Ros, O., Andrés, R., Baeriswyl, T., Fuschini, G., Tarrago, T., Pascual, M., Ureña, J., *et al*. (2011). A Signaling Mechanism Coupling Netrin-1/Deleted in Colorectal Cancer Chemoattraction to SNARE-Mediated Exocytosis in Axonal Growth Cones. In J Neurosci, pp. 14463-14480.

de la Torre, J.R., Hopker, V.H., Ming, G.L., Poo, M.M., Tessier-Lavigne, M., Hemmati-Brivanlou, A., and Holt, C.E. (1997). Turning of retinal growth cones in a netrin-1 gradient mediated by the netrin receptor DCC. Neuron *19*, pp. 1211-1224.

Deiner, M.S., Kennedy, T.E., Fazeli, A., Serafini, T., Tessier-Lavigne, M., and Sretavan, D.W. (1997). Netrin-1 and DCC mediate axon guidance locally at the optic disc: loss of function leads to optic nerve hypoplasia. Neuron *19*, pp. 575-589.

Dent, E.W., Gupton, S.L., and Gertler, F.B. (2011). The growth cone cytoskeleton in axon outgrowth and guidance. Cold Spring Harbor Perspectives in Biology.

Desai, C.J., Krueger, N.X., Saito, H., and Zinn, K. (1997). Competition and cooperation among receptor tyrosine phosphatases control motoneuron growth cone guidance in Drosophila. Development, pp. 1941-1952.

Dickson, B.J. (2002). Molecular mechanisms of axon guidance. Science *298*, pp. 1959-1964.

Dobritsa, A.A., van der Goes van Naters, W., Warr, C.G., Steinbrecht, R.A., and Carlson, J.R. (2003). Integrating the molecular and cellular basis of odor coding in the Drosophila antenna. Neuron *37*, 827-841.

Dominguez, M., and Hafen, E. (1997). Hedgehog directly controls initiation and propagation of retinal differentiation in the Drosophila eye. Genes Dev *11*, 3254-3264.

Drescher, U. (1997). The Eph family in the patterning of neural development. Curr Biol *7*, pp. 799-807.

Drescher, U., Kremoser, C., Handwerker, C., Loschinger, J., Noda, M., and Bonhoeffer, F. (1995). In vitro guidance of retinal ganglion cell axons by RAGS, a 25 kDa tectal protein related to ligands for Eph. Cell *82*, 359-370.

Erskine, L., and Herrera, E. (2007). The retinal ganglion cell axon's journey: insights into molecular mechanisms of axon guidance. Developmental Biology, pp. 1-14.

Erskine, L., Williams, S.E., Brose, K., Kidd, T., Rachel, R.A., Goodman, C.S., Tessier-Lavigne, M., and Mason, C.A. (2000). Retinal ganglion cell axon guidance in the mouse optic chiasm: expression and function of robos and slits. J Neurosci, pp. 4975-4982.

Evans, T.A., and Bashaw, G.J. (2010). Axon guidance at the midline: of mice and flies. Current Opinion in Neurobiology, pp. 79-85.

Fazeli, A., Dickinson, S.L., Hermiston, M.L., Tighe, R.V., Steen, R.G., Small, C.G., Stoeckli, E.T., Keino-Masu, K., Masu, M., Rayburn, H., *et al*. (1997). Phenotype of mice lacking functional Deleted in colorectal cancer (Dcc) gene. Nature *386*, pp. 796-804.

Feinstein, P., and Mombaerts, P. (2004). A contextual model for axonal sorting into glomeruli in the mouse olfactory system. Cell *117*, pp. 817-831.

Feldheim, D.A., Kim, Y.I., Bergemann, A.D., Frisen, J., Barbacid, M., and Flanagan, J.G. (2000). Genetic analysis of ephrin-A2 and ephrin-A5 shows their requirement in multiple aspects of retinocollicular mapping. Neuron *25*, 563-574.

Feldheim, D.A., and O'Leary, D.D.M. (2010). Visual map development: bidirectional signaling, bifunctional guidance molecules, and competition. Cold Spring Harbor Perspectives in Biology, pp. 1768.

Ferguson, K., Long, H., Cameron, S., Chang, W.-T., and Rao, Y. (2009). The conserved Ig superfamily member Turtle mediates axonal tiling in Drosophila. J Neurosci, pp. 14151-14159.

Fire, A., Xu, S., Montgomery, M.K., Kostas, S.A., Driver, S.E., and Mello, C.C. (1998). Potent and specific genetic interference by double-stranded RNA in Caenorhabditis elegans. Nature *391*, 806-811.

Fischbach, K.F., and Dittrich, A. (1989). The optic lobe of Drosophila melanogaster. 1. A golgi analysis of wild-type structure, pp. 35.

Fischbach, K.F., and Hiesinger, P.R. (2008). Optic lobe development. Adv Exp Med Biol *628*, pp. 115-136.

Forcet, C., Stein, E., Pays, L., Corset, V., Llambi, F., Tessier-Lavigne, M., and Mehlen, P. (2002). Netrin-1-mediated axon outgrowth requires deleted in colorectal cancer-dependent MAPK activation. Nature *417*, pp. 443-447.

Furrer, M.P., Kim, S., Wolf, B., and Chiba, A. (2003). Robo and Frazzled/DCC mediate dendritic guidance at the CNS midline. Nat Neurosci *6*, pp. 223-230.

Gallo, G., and Letourneau, P.C. (2004). Regulation of growth cone actin filaments by guidance cues. J Neurobiol *58*, 92-102.

Gao, S., Takemura, S.Y., Ting, C.Y., Huang, S., Lu, Z., Luan, H., Rister, J., Thum, A.S., Yang, M., Hong, S.T., *et al*. (2008). The neural substrate of spectral preference in Drosophila. Neuron *60*, pp. 328-342.

Garbe, D.S., and Bashaw, G.J. (2004). Axon guidance at the midline: from mutants to mechanisms. Crit Rev Biochem Mol Biol, pp. 319-341.

Garrity, P.A., Lee, C.H., Salecker, I., Robertson, H.C., Desai, C.J., Zinn, K., and Zipursky, S.L. (1999). Retinal axon target selection in Drosophila is regulated by a receptor protein tyrosine phosphatase. Neuron *22*, pp. 707-717.

Geisbrecht, B.V., Dowd, K.A., Barfield, R.W., Longo, P.A., and Leahy, D.J. (2003). Netrin binds discrete subdomains of DCC and UNC5 and mediates interactions between DCC and heparin. J Biol Chem *278*, 32561-32568.

Georgiou, M., and Tear, G. (2002). Commissureless is required both in commissural neurones and midline cells for axon guidance across the midline. Development *129*, pp. 2947-2956.

Geraldo, S., and Gordon-Weeks, P.R. (2009). Cytoskeletal dynamics in growth-cone steering. J Cell Sci, pp. 3595-3604.

Gong, Q., Rangarajan, R., Seeger, M., and Gaul, U. (1999). The netrin receptor frazzled is required in the target for establishment of retinal projections in the Drosophila visual system. Development *126*, pp. 1451-1456.

Hadjieconomou, D., Rotkopf, S., Alexandre, C., Bell, D.M., Dickson, B.J., and Salecker, I. (2011a). Flybow: genetic multicolor cell labeling for neural circuit analysis in Drosophila melanogaster. In Nat Methods, pp. 260-266.

Hadjieconomou, D., Timofeev, K., and Salecker, I. (2011b). A step-by-step guide to visual circuit assembly in Drosophila. Current Opinion in Neurobiology, pp. 76-84.

Hakeda-Suzuki, S., Berger-Müller, S., Tomasi, T., Usui, T., Horiuchi, S.-y., Uemura, T., and Suzuki, T. (2011). Golden Goal collaborates with Flamingo in conferring synaptic-layer specificity in the visual system. Nat Neurosci, pp. 314-323.

Harris, R., Sabatelli, L.M., and Seeger, M.A. (1996). Guidance cues at the Drosophila CNS midline: identification and characterization of two Drosophila Netrin/UNC-6 homologs. Neuron *17*, pp. 217-228.

Heberlein, U., Wolff, T., and Rubin, G.M. (1993). The TGF beta homolog dpp and the segment polarity gene hedgehog are required for propagation of a morphogenetic wave in the Drosophila retina. Cell *75*, pp. 913-926.

Hedgecock, E.M., Culotti, J.G., and Hall, D.H. (1990). The unc-5, unc-6, and unc-40 genes guide circumferential migrations of pioneer axons and mesodermal cells on the epidermis in C. elegans. Neuron *4*, pp. 61-85.

Hengst, U., Deglincerti, A., Kim, H.J., Jeon, N.L., and Jaffrey, S.R. (2009). Axonal elongation triggered by stimulus-induced local translation of a polarity complex protein. Nat Cell Biol *11*, pp. 1024-1030.

Herbert, T., Tee, A., and Proud, C. (2002). The extracellular signal-regulated kinase pathway regulates the phosphorylation of 4E-BP1 at multiple sites. J Biol Chem *13*, pp. 11591-11596.

Hidalgo, A., and Brand, A.H. (1997). Targeted neuronal ablation: the role of pioneer neurons in guidance and fasciculation in the CNS of Drosophila. Development, pp. 3253-3262.

Hiesinger, P.R., Zhai, R.G., Zhou, Y., Koh, T.W., Mehta, S.Q., Schulze, K.L., Cao, Y., Verstreken, P., Clandinin, T.R., Fischbach, K.F., *et al*. (2006). Activity-independent prespecification of synaptic partners in the visual map of Drosophila. Curr Biol *16*, pp. 1835-1843.

Hiramoto, M., Hiromi, Y., Giniger, E., and Hotta, Y. (2000). The Drosophila Netrin receptor Frazzled guides axons by controlling Netrin distribution. Nature, pp. 886-889.

Hofmeyer, K., Maurel-Zaffran, C., Sink, H., and Treisman, J.E. (2006). Liprin-alpha has LAR-independent functions in R7 photoreceptor axon targeting. Proc Natl Acad Sci USA, pp. 11595-11600.

Holmes, A.L., and Heilig, J.S. (1999). Fasciclin II and Beaten path modulate intercellular adhesion in Drosophila larval visual organ development. Development *126*, pp. 261-272.

Holt, C.E., and Harris, W.A. (1998). Target selection: invasion, mapping and cell choice. Current Opinion in Neurobiology, pp. 98-105.

Hong, K., Hinck, L., Nishiyama, M., Poo, M.M., Tessier-Lavigne, M., and Stein, E. (1999). A ligand-gated association between cytoplasmic domains of UNC5 and DCC family receptors converts netrin-induced growth cone attraction to repulsion. Cell, pp. 927-941.

Hornberger, M.R., Dutting, D., Ciossek, T., Yamada, T., Handwerker, C., Lang, S., Weth, F., Huf, J., Wessel, R., Logan, C., *et al*. (1999). Modulation of EphA receptor function by coexpressed ephrinA ligands on retinal ganglion cell axons. Neuron *22*, pp. 731-742.

Huang, Z., and Kunes, S. (1996). Hedgehog, transmitted along retinal axons, triggers neurogenesis in the developing visual centers of the Drosophila brain. Cell *86*, 411-422.

Huang, Z., Shilo, B.Z., and Kunes, S. (1998). A retinal axon fascicle uses spitz, an EGF receptor ligand, to construct a synaptic cartridge in the brain of Drosophila. Cell *95*, 693-703.

Huber, A.B., Kolodkin, A.L., Ginty, D.D., and Cloutier, J.-F. (2003). Signaling at the growth cone: ligand-receptor complexes and the control of axon growth and guidance. Annu Rev Neurosci, pp. 509-563.

Huberman, A.D., Clandinin, T.R., and Baier, H. (2010). Molecular and cellular mechanisms of lamina-specific axon targeting. Cold Spring Harbor Perspectives in Biology, pp. 1743.

Imai, T., Sakano, H., and Vosshall, L.B. (2010). Topographic mapping--the olfactory system. In Cold Spring Harbor Perspectives in Biology, pp. a001776.

Imai, T., Suzuki, M., and Sakano, H. (2006). Odorant receptor-derived cAMP signals direct axonal targeting. Science *314*, pp. 657-661.

Imai, T., Yamazaki, T., Kobayakawa, R., Kobayakawa, K., Abe, T., Suzuki, M., and Sakano, H. (2009). Pre-target axon sorting establishes the neural map topography. Science *325*, 585-590.

Imondi, R., Wideman, C., and Kaprielian, Z. (2000). Complementary expression of transmembrane ephrins and their receptors in the mouse spinal cord: a possible role in constraining the orientation of longitudinally projecting axons. Development, pp. 1397-1410.

Inan, M., and Crair, M.C. (2007). Development of cortical maps: perspectives from the barrel cortex. Neuroscientist *13*, 49-61.

Ishii, N., Wadsworth, W.G., Stern, B.D., Culotti, J.G., and Hedgecock, E.M. (1992). UNC-6, a laminin-related protein, guides cell and pioneer axon migrations in C. elegans. Neuron, pp. 873-881.

Jefferis, G.S.X.E., Vyas, R.M., Berdnik, D., Ramaekers, A., Stocker, R.F., Tanaka, N.K., Ito, K., and Luo, L. (2004). Developmental origin of wiring specificity in the olfactory system of Drosophila. Development, pp. 117-130.

Jiang, Y., Obama, H., Kuan, S.L., and Nakamoto, M. (2009). In vitro guidance of retinal axons by a tectal lamina-specific glycoprotein Nel. Mol Cell Neurosci.

Kalil, K., and Dent, E.W. (2005). Touch and go: guidance cues signal to the growth cone cytoskeleton. Current Opinion in Neurobiology, pp. 521-526.

Kamiguchi, H. (2007). The role of cell adhesion molecules in axon growth and guidance. Adv Exp Med Biol *621*, pp. 95-103.

Katz, L.C., and Shatz, C.J. (1996). Synaptic activity and the construction of cortical circuits. Science, pp. 1133-1138.

Keino-Masu, K., Masu, M., Hinck, L., Leonardo, E.D., Chan, S.S., Culotti, J.G., and Tessier-Lavigne, M. (1996). Deleted in Colorectal Cancer (DCC) encodes a netrin receptor. Cell *87*, pp. 175-185.

Keleman, K., and Dickson, B.J. (2001). Short- and long-range repulsion by the Drosophila Unc5 netrin receptor. Neuron *32*, pp. 605-617.

Keleman, K., Rajagopalan, S., Cleppien, D., Teis, D., Paiha, K., Huber, L.A., Technau, G.M., and Dickson, B.J. (2002a). Comm sorts robo to control axon guidance at the Drosophila midline. Cell *110*, 415-427.

Keleman, K., Rajagopalan, S., Cleppien, D., Teis, D., Paiha, K., Huber, L.A., Technau, G.M., and Dickson, B.J. (2002b). Comm sorts robo to control axon guidance at the Drosophila midline. In Cell, pp. 415-427.

Kelly, T.-A.N., Katagiri, Y., Vartanian, K.B., Kumar, P., Chen, I.-I., Rosoff, W.J., Urbach, J.S., and Geller, H.M. (2010). Localized alteration of microtubule polymerization in response to guidance cues. J Neurosci Res, pp. 3024-3033.

Kennedy, T.E., Serafini, T., de la Torre, J.R., and Tessier-Lavigne, M. (1994). Netrins are diffusible chemotropic factors for commissural axons in the embryonic spinal cord. Cell *78*, pp. 425-435.

Kennedy, T.E., Wang, H., Marshall, W., and Tessier-Lavigne, M. (2006). Axon guidance by diffusible chemoattractants: a gradient of netrin protein in the developing spinal cord. J Neurosci, pp. 8866-8874.

Kidd, T., Bland, K.S., and Goodman, C.S. (1999). Slit is the midline repellent for the robo receptor in Drosophila. Cell, pp. 785-794.

Kidd, T., Brose, K., Mitchell, K.J., Fetter, R.D., Tessier-Lavigne, M., Goodman, C.S., and Tear, G. (1998). Roundabout controls axon crossing of the CNS midline and defines a novel subfamily of evolutionarily conserved guidance receptors. Cell, pp. 205-215.

Kolodziej, P.A., Timpe, L.C., Mitchell, K.J., Fried, S.R., Goodman, C.S., Jan, L.Y., and Jan, Y.N. (1996). frazzled encodes a Drosophila member of the DCC immunoglobulin subfamily and is required for CNS and motor axon guidance. Cell *87*, pp. 197-204.

Komiyama, T., Sweeney, L.B., Schuldiner, O., Garcia, K.C., and Luo, L. (2007). Graded expression of semaphorin-1a cell-autonomously directs dendritic targeting of olfactory projection neurons. Cell *128*, pp. 399-410.

Krueger, N.X., Van Vactor, D., Wan, H.I., Gelbart, W.M., Goodman, C.S., and Saito, H. (1996). The transmembrane tyrosine phosphatase DLAR controls motor axon guidance in Drosophila. Cell, pp. 611-622.

Kruger, R.P., Lee, J., Li, W., and Guan, K.-L. (2004). Mapping netrin receptor binding reveals domains of Unc5 regulating its tyrosine phosphorylation. J Neurosci, pp. 10826-10834.

Labrador, J.P., O'Keefe, D., Yoshikawa, S., McKinnon, R.D., Thomas, J.B., and Bashaw, G.J. (2005). The homeobox transcription factor even-skipped regulates netrin-receptor expression to control dorsal motor-axon projections in Drosophila. Curr Biol *15*, pp. 1413-1419.

Lattemann, M., Zierau, A., Schulte, C., Seidl, S., Kuhlmann, B., and Hummel, T. (2007). Semaphorin-1a controls receptor neuron-specific axonal convergence in the primary olfactory center of Drosophila. Neuron *53*, 169-184.

Lee, C.H., Herman, T., Clandinin, T.R., Lee, R., and Zipursky, S.L. (2001). N-cadherin regulates target specificity in the Drosophila visual system. Neuron *30*, pp. 437-450.

Lee, R.C., Clandinin, T.R., Lee, C.-H., Chen, P.-L., Meinertzhagen, I.A., and Zipursky, S.L. (2003). The protocadherin Flamingo is required for axon target selection in the Drosophila visual system. Nat Neurosci, pp. 557-563.

Lee, T., and Luo, L. (2001). Mosaic analysis with a repressible cell marker (MARCM) for Drosophila neural development. Trends Neurosci *24*, 251-254.

Leonardo, E.D., Hinck, L., Masu, M., Keino-Masu, K., Ackerman, S.L., and Tessier-Lavigne, M. (1997). Vertebrate homologues of C. elegans UNC-5 are candidate netrin receptors. Nature *386*, pp. 833-838.

Leung-Hagesteijn, C., Spence, A.M., Stern, B.D., Zhou, Y., Su, M.W., Hedgecock, E.M., and Culotti, J.G. (1992). UNC-5, a transmembrane protein with immunoglobulin and thrombospondin type 1 domains, guides cell and pioneer axon migrations in C. elegans. Cell *71*, pp. 289-299.

Li, W., Aurandt, J., Jurgensen, C., Rao, Y., and Guan, K.L. (2006). FAK and Src kinases are required for netrin-induced tyrosine phosphorylation of UNC5. J Cell Sci *119*, pp. 47-55.

Li, X., Meriane, M., Triki, I., Shekarabi, M., Kennedy, T.E., Larose, L., and Lamarche-Vane, N. (2002). The adaptor protein Nck-1 couples the netrin-1 receptor DCC (deleted in colorectal cancer) to the activation of the small GTPase Rac1 through an atypical mechanism. J Biol Chem, pp. 37788-37797.

Lim, Y.-s., and Wadsworth, W.G. (2002). Identification of domains of netrin UNC-6 that mediate attractive and repulsive guidance and responses from cells and growth cones. J Neurosci, pp. 7080-7087.

Lin, D.M., Fetter, R.D., Kopczynski, C., Grenningloh, G., and Goodman, C.S. (1994). Genetic analysis of Fasciclin II in Drosophila: defasciculation, refasciculation, and altered fasciculation. Neuron, pp. 1055-1069.

Liu, G., Li, W., Wang, L., Kar, A., Guan, K.L., Rao, Y., and Wu, J.Y. (2009). DSCAM functions as a netrin receptor in commissural axon pathfinding. Proc Natl Acad Sci U S A *106*, pp. 2951-2956.

Lohmann, C., and Bonhoeffer, T. (2008). A role for local calcium signaling in rapid synaptic partner selection by dendritic filopodia. Neuron, pp. 253-260.

Long, H., Sabatier, C., Ma, L., Plump, A., Yuan, W., Ornitz, D.M., Tamada, A., Murakami, F., Goodman, C.S., and Tessier-Lavigne, M. (2004). Conserved roles for Slit and Robo proteins in midline commissural axon guidance. Neuron, pp. 213-223.

Lowery, L.A., and Van Vactor, D. (2009). The trip of the tip: understanding the growth cone machinery. Nat Rev Mol Cell Biol *10*, pp. 332-343.

Lu, B., Wang, K.H., and Nose, A. (2009). Molecular mechanisms underlying neural circuit formation. Curr Opin Neurobiol *19*, pp. 162-167.

Luo, L., and Flanagan, J.G. (2007). Development of continuous and discrete neural maps. Neuron *56*, pp. 284-300.

Ly, A., Nikolaev, A., Suresh, G., Zheng, Y., Tessier-Lavigne, M., and Stein, E. (2008). DSCAM is a netrin receptor that collaborates with DCC in mediating turning responses to netrin-1. Cell, pp. 1241-1254.

Ma, W., Shang, Y., Wei, Z., Wen, W., Wang, W., and Zhang, M. (2010). Phosphorylation of DCC by ERK2 Is Facilitated by Direct Docking of the Receptor P1 Domain to the Kinase. Structure, pp. 1502-1511.

Mambetisaeva, E.T., Andrews, W., Camurri, L., Annan, A., and Sundaresan, V. (2005). Robo family of proteins exhibit differential expression in mouse spinal cord and Robo-Slit interaction is required for midline crossing in vertebrate spinal cord. Dev Dyn, pp. 41-51.

Masland, R.H. (2001a). Neuronal diversity in the retina. Current Opinion in Neurobiology, pp. 431-436.

Masland, R.H. (2001b). The fundamental plan of the retina. Nat Neurosci *4*, pp. 877-886.

Mastick, G.S., Farmer, W.T., Altick, A.L., Nural, H.F., Dugan, J.P., Kidd, T., and Charron, F. (2010). Longitudinal axons are guided by Slit/Robo signals from the floor plate. Cell adhesion & migration, pp. 337-341.

Matsunaga, M., Hatta, K., Nagafuchi, A., and Takeichi, M. (1988). Guidance of optic nerve fibres by N-cadherin adhesion molecules. Nature *334*, pp. 62-64.

Matsumoto, H., and Nagashima, M. (2010). Netrin-1 elevates the level and induces cluster formation of its receptor DCC at the surface of cortical axon shafts in an exocytosis-dependent manner. Neurosci Res *67*, 99-107.

Matsuoka, R.L., Nguyen-Ba-Charvet, K.T., Parray, A., Badea, T.C., Chédotal, A., and Kolodkin, A.L. (2011). Transmembrane semaphorin signalling controls laminar stratification in the mammalian retina. Nature, pp. 259-263.

Maurel-Zaffran, C., Suzuki, T., Gahmon, G., Treisman, J.E., and Dickson, B.J. (2001). Cell-autonomous and -nonautonomous functions of LAR in R7 photoreceptor axon targeting. Neuron *32*, pp. 225-235.

Mauss, A., Tripodi, M., Evers, J.F., and Landgraf, M. (2009). Midline signalling systems direct the formation of a neural map by dendritic targeting in the Drosophila motor system. PLoS Biol *7*, e1000200.

Meinertzhagen IA, Hansen TE. 1993. The development of the optic lobe. In The Development of Drosophila melanogaster, Cold Spring Harbor Laboratory Press, pp. 1363–491.

Meinertzhagen, I.A., and Sorra, K.E. (2001). Synaptic organization in the fly's optic lamina: few cells, many synapses and divergent microcircuits. Prog Brain Res *131*, pp. 53-69.

Merz, D.C., and Culotti, J.G. (2000). Genetic analysis of growth cone migrations in Caenorhabditis elegans. J Neurobiol, pp. 281-288.

Merz, D.C., Zheng, H., Killeen, M.T., Krizus, A., and Culotti, J.G. (2001). Multiple signaling mechanisms of the UNC-6/netrin receptors UNC-5 and UNC-40/DCC in vivo. Genetics, pp. 1071-1080.

Millard, S.S., Flanagan, J.J., Pappu, K.S., Wu, W., and Zipursky, S.L. (2007). Dscam2 mediates axonal tiling in the Drosophila visual system. Nature, pp. 720-724.

Ming, G.-l., Wong, S.T., Henley, J., Yuan, X.-b., Song, H.-j., Spitzer, N.C., and Poo, M.-m. (2002). Adaptation in the chemotactic guidance of nerve growth cones. Nature, pp. 411-418.

Mitchell, K.J., Doyle, J.L., Serafini, T., Kennedy, T.E., Tessier-Lavigne, M., Goodman, C.S., and Dickson, B.J. (1996). Genetic analysis of Netrin genes in Drosophila: Netrins guide CNS commissural axons and peripheral motor axons. Neuron *17*, pp. 203-215.

Mombaerts, P. (1996). Targeting olfaction. Curr Opin Neurobiol *6*, pp. 481-486.

Mombaerts, P. (2006). Axonal wiring in the mouse olfactory system. Annu Rev Cell Dev Biol *22*, pp. 713-737.

Montell C, Jones K, Zuker C, Rubin G. 1987. A second opsin gene expressed in the ultraviolet-sensitive R7 photoreceptor cells of *Drosophila melanogaster*. J. Neurosci. 7, pp.1558–66.

Morante, J., and Desplan, C. (2004). Building a projection map for photoreceptor neurons in the Drosophila optic lobes. Semin Cell Dev Biol *15*, pp. 137-143.

Morante, J., and Desplan, C. (2008). The color-vision circuit in the medulla of Drosophila. Curr Biol *18*, pp. 553-565.

Morey, M., Yee, S.K., Herman, T., Nern, A., Blanco, E., and Zipursky, S.L. (2008). Coordinate control of synaptic-layer specificity and rhodopsins in photoreceptor neurons. Nature, pp. 795-799.

Mumm, J.S., Godinho, L., Morgan, J.L., Oakley, D.M., Schroeter, E.H., and Wong, R.O. (2005). Laminar circuit formation in the vertebrate retina. Prog Brain Res *147*, pp. 155-169.

Nawabi, H., Briançon-Marjollet, A., Clark, C., Sanyas, I., Takamatsu, H., Okuno, T., Kumanogoh, A., Bozon, M., Takeshima, K., Yoshida, Y., *et al.* (2010). A midline switch of receptor processing regulates commissural axon guidance in vertebrates. Genes Dev, pp. 396-410.

Nern, A., Nguyen, L.V., Herman, T., Prakash, S., Clandinin, T.R., and Zipursky, S.L. (2005). An isoform-specific allele of Drosophila N-cadherin disrupts a late step of R7 targeting. Proc Natl Acad Sci U S A *102*, pp. 12944-12949.

Nern, A., Zhu, Y., and Zipursky, S.L. (2008). Local N-cadherin interactions mediate distinct steps in the targeting of lamina neurons. Neuron, pp. 34-41.

Nishiyama, M., Hoshino, A., Tsai, L., Henley, J.R., Goshima, Y., Tessier-Lavigne, M., Poo, M.M., and Hong, K. (2003). Cyclic AMP/GMP-dependent modulation of Ca2+ channels sets the polarity of nerve growth-cone turning. Nature *423*, pp. 990-995.

Ostroy, S.E., Wilson, M., and Pak, W.L. (1974). Drosophila rhodopsin: photochemistry, extraction and differences in the norp AP12 phototransduction mutant. Biochem Biophys Res Commun *59*, pp. 960-966.

Palmer, A., and Klein, R. (2003). Multiple roles of ephrins in morphogenesis, neuronal networking, and brain function. Genes Dev, pp. 1429-1450.

Palmesino, E., Haddick, P.C.G., Tessier-Lavigne, M., and Kania, A. (2012). Genetic Analysis of DSCAM's Role as a Netrin-1 Receptor in Vertebrates. J Neurosci, pp. 411-416.

Papatsenko, D., Nazina, A., and Desplan, C. (2001). A conserved regulatory element present in all Drosophila rhodopsin genes mediates Pax6 functions and participates in the fine-tuning of cell-specific expression. Mech Dev *101*, pp. 143-153.

Papatsenko, D., Sheng, G., and Desplan, C. (1997). A new rhodopsin in R8 photoreceptors of Drosophila: evidence for coordinate expression with Rh3 in R7 cells. Development *124*, pp. 1665-1673.

Perrimon, N., and Mathey-Prevot, B. (2007). Applications of high-throughput RNA interference screens to problems in cell and developmental biology. Genetics *175*, 7-16.

Petrovic, M., and Hummel, T. (2008). Temporal identity in axonal target layer recognition. Nature.

Picard, M., Petrie, R.J., Antoine-Bertrand, J., Saint-Cyr-Proulx, E., Villemure, J.F., and Lamarche-Vane, N. (2009). Spatial and temporal activation of the small GTPases RhoA and Rac1 by the netrin-1 receptor UNC5a during neurite outgrowth. Cell Signal *21*, 1961-1973.

Pignoni, F., and Zipursky, S.L. (1997). Induction of Drosophila eye development by decapentaplegic. Development *124*, pp. 271-278.

Piper, M., Anderson, R., Dwivedy, A., Weinl, C., van Horck, F., Leung, K.M., Cogill, E., and Holt, C. (2006). Signaling mechanisms underlying Slit2-induced collapse of Xenopus retinal growth cones. Neuron, pp. 215-228.

Poeck, B., Fischer, S., Gunning, D., Zipursky, S.L., and Salecker, I. (2001). Glial cells mediate target layer selection of retinal axons in the developing visual system of Drosophila. Neuron, pp. 99-113.

Poskanzer, K., Needleman, L.A., Bozdagi, O., and Huntley, G.W. (2003). N-cadherin regulates ingrowth and laminar targeting of thalamocortical axons. J Neurosci *23*, pp. 2294-2305.

Prakash, S., Caldwell, J.C., Eberl, D.F., and Clandinin, T.R. (2005). Drosophila N-cadherin mediates an attractive interaction between photoreceptor axons and their targets. Nat Neurosci, pp. 443-450.

Rashid, T., Upton, A.L., Blentic, A., Ciossek, T., Knoll, B., Thompson, I.D., and Drescher, U. (2005). Opposing gradients of ephrin-As and EphA7 in the superior colliculus are essential for topographic mapping in the mammalian visual system. Neuron *47*, pp. 57-69.

Riehl, R., Johnson, K., Bradley, R., Grunwald, G.B., Cornel, E., Lilienbaum, A., and Holt, C.E. (1996). Cadherin function is required for axon outgrowth in retinal ganglion cells in vivo. Neuron *17*, pp. 837-848.

Rister, J., Pauls, D., Schnell, B., Ting, C.Y., Lee, C.H., Sinakevitch, I., Morante, J., Strausfeld, N.J., Ito, K., and Heisenberg, M. (2007). Dissection of the peripheral motion channel in the visual system of Drosophila melanogaster. Neuron *56*, pp. 155-170.

Rolls, M.M. (2011). Neuronal polarity in Drosophila: Sorting out axons and dendrites. Devel Neurobio, pp. 419-429.

Round, J., and Stein, E. (2007). Netrin signaling leading to directed growth cone steering. Curr Opin Neurobiol *17*, pp. 15-21.

Rutishauser, U., Acheson, A., Hall, A.K., Mann, D.M., and Sunshine, J. (1988). The neural cell adhesion molecule (NCAM) as a regulator of cell-cell interactions. Science *240*, pp. 53-57.

Sabatier, C., Plump, A.S., Le, M., Brose, K., Tamada, A., Murakami, F., Lee, E.Y., and Tessier-Lavigne, M. (2004). The divergent Robo family protein rig-1/Robo3 is a negative regulator of slit responsiveness required for midline crossing by commissural axons. Cell *117*, pp. 157-169.

Sakano, H. (2010). Neural map formation in the mouse olfactory system. Neuron *67*, pp. 530-542.

Salcedo, E., Huber, A., Henrich, S., Chadwell, L.V., Chou, W.H., Paulsen, R., and Britt, S.G. (1999). Blue- and green-absorbing visual pigments of Drosophila: ectopic expression and physiological characterization of the R8 photoreceptor cell-specific Rh5 and Rh6 rhodopsins. J Neurosci *19*, pp. 10716-10726.

Sanes, J.R., and Yamagata, M. (2009). Many paths to synaptic specificity. Annu Rev Cell Dev Biol, pp. 161-195.

Sanes, J.R., and Zipursky, S.L. (2010). Design principles of insect and vertebrate visual systems. Neuron, pp. 15-36.

Sato, M., Umetsu, D., Murakami, S., Yasugi, T., and Tabata, T. (2006). DWnt4 regulates the dorsoventral specificity of retinal projections in the Drosophila melanogaster visual system. Nat Neurosci *9*, pp. 67-75.

Schuster, C.M., Davis, G.W., Fetter, R.D., and Goodman, C.S. (1996a). Genetic dissection of structural and functional components of synaptic plasticity. I. Fasciclin II controls synaptic stabilization and growth. Neuron, pp. 641-654.

Schuster, C.M., Davis, G.W., Fetter, R.D., and Goodman, C.S. (1996b). Genetic dissection of structural and functional components of synaptic plasticity. II. Fasciclin II controls presynaptic structural plasticity. Neuron, pp. 655-667.

Schwarting, G.A., Raitcheva, D., Crandall, J.E., Burkhardt, C., and Puschel, A.W. (2004). Semaphorin 3A-mediated axon guidance regulates convergence and targeting of P2 odorant receptor axons. Eur J Neurosci *19*, pp. 1800-1810.

Seeger, M., Tear, G., Ferres-Marco, D., and Goodman, C.S. (1993). Mutations affecting growth cone guidance in Drosophila: genes necessary for guidance toward or away from the midline. Neuron, pp. 409-426.

Senti, K.-A., Usui, T., Boucke, K., Greber, U., Uemura, T., and Dickson, B.J. (2003). Flamingo regulates R8 axon-axon and axon-target interactions in the Drosophila visual system. Curr Biol, pp. 828-832.

Serafini, T., Colamarino, S.A., Leonardo, E.D., Wang, H., Beddington, R., Skarnes, W.C., and Tessier-Lavigne, M. (1996). Netrin-1 is required for commissural axon guidance in the developing vertebrate nervous system. Cell *87*, pp.1001-1014.

Serafini, T., Kennedy, T.E., Galko, M.J., Mirzayan, C., Jessell, T.M., and Tessier-Lavigne, M. (1994). The netrins define a family of axon outgrowth-promoting proteins homologous to C. elegans UNC-6. Cell *78*, 409-424.

Serizawa, S., Miyamichi, K., Takeuchi, H., Yamagishi, Y., Suzuki, M., and Sakano, H. (2006). A neuronal identity code for the odorant receptor-specific and activity-dependent axon sorting. Cell *127*, 1057-1069.

Shapiro, L., Fannon, A.M., Kwong, P.D., Thompson, A., Lehmann, M.S., Grubel, G., Legrand, J.F., Als-Nielsen, J., Colman, D.R., and Hendrickson, W.A. (1995). Structural basis of cell-cell adhesion by cadherins. Nature *374*, 327-337.

Shinza-Kameda, M., Takasu, E., Sakurai, K., Hayashi, S., and Nose, A. (2006). Regulation of layer-specific targeting by reciprocal expression of a cell adhesion molecule, capricious. Neuron *49*, pp. 205-213.

Shirasaki, R., Mirzayan, C., Tessier-Lavigne, M., and Murakami, F. (1996). Guidance of circumferentially growing axons by netrin-dependent and -independent floor plate chemotropism in the vertebrate brain. Neuron *17*, pp. 1079-1088.

Simpson, J.H., Bland, K.S., Fetter, R.D., and Goodman, C.S. (2000). Short-range and long-range guidance by Slit and its Robo receptors: a combinatorial code of Robo receptors controls lateral position. Cell, pp. 1019-1032.

Sperry, R.W. (1963). Chemoaffinity in the orderly growth of nerve fiber patterns and connections. Proc Natl Acad Sci U S A. 50(4): pp. 703–710.

Stein, E., and Tessier-Lavigne, M. (2001). Hierarchical organization of guidance receptors: silencing of netrin attraction by slit through a Robo/DCC receptor complex. Science, pp. 1928-1938.

Sun, Q., Bahri, S., Schmid, A., Chia, W., and Zinn, K. (2000). Receptor tyrosine phosphatases regulate axon guidance across the midline of the Drosophila embryo. Development, pp. 801-812.

Takemura, S.-Y., Lu, Z., and Meinertzhagen, I.A. (2008). Synaptic circuits of the Drosophila optic lobe: the input terminals to the medulla. J Comp Neurol, pp. 33.

Tayler, T.D., and Garrity, P.A. (2003). Axon targeting in the Drosophila visual system. In Current Opinion in Neurobiology, pp. 90-95.

Tcherkezian, J., Brittis, P.A., Thomas, F., Roux, P.P., and Flanagan, J.G. (2010). Transmembrane receptor DCC associates with protein synthesis machinery and regulates translation. Cell, pp. 632-644.

Tear, G., Harris, R., Sutaria, S., Kilomanski, K., Goodman, C.S., and Seeger, M.A. (1996). commissureless controls growth cone guidance across the CNS midline in Drosophila and encodes a novel membrane protein. Neuron, pp. 501-514.

Tessier-Lavigne, M., and Goodman, C.S. (1996). The molecular biology of axon guidance. Science *274*, pp. 1123-1133.

Ting, C.-Y., Herman, T., Yonekura, S., Gao, S., Wang, J., Serpe, M., O'Connor, M.B., Zipursky, S.L., and Lee, C.-H. (2007). Tiling of r7 axons in the Drosophila visual system is mediated both by transduction of an activin signal to the nucleus and by mutual repulsion. Neuron, pp. 793-806.

Ting, C.Y., Yonekura, S., Chung, P., Hsu, S.N., Robertson, H.M., Chiba, A., and Lee, C.H. (2005). Drosophila N-cadherin functions in the first stage of the two-stage layer-selection process of R7 photoreceptor afferents. Development *132*, pp. 953-963.

Tomasi, T., Hakeda-Suzuki, S., Ohler, S., Schleiffer, A., and Suzuki, T. (2008). The transmembrane protein Golden goal regulates R8 photoreceptor axon-axon and axon-target interactions. Neuron, pp. 691-704.

Umetsu, D., Murakami, S., Sato, M., and Tabata, T. (2006). The highly ordered assembly of retinal axons and their synaptic partners is regulated by Hedgehog/Single-minded in the Drosophila visual system. Development *133*, pp. 791-800.

Uryu, K., Butler, A.K., and Chesselet, M.F. (1999). Synaptogenesis and ultrastructural localization of the polysialylated neural cell adhesion molecule in the developing striatum. J Comp Neurol, pp. 216-232.

von Hilchen, C.M., Hein, I., Technau, G.M., and Altenhein, B. (2010). Netrins guide migration of distinct glial cells in the Drosophila embryo. Development, pp. 1251-1262.

Wadsworth, W.G., Bhatt, H., and Hedgecock, E.M. (1996). Neuroglia and pioneer neurons express UNC-6 to provide global and local netrin cues for guiding migrations in C. elegans. Neuron, pp. 35-46.

Wen, Z., and Zheng, J.Q. (2006). Directional guidance of nerve growth cones. Curr Opin Neurobiol *16*, pp. 52-58.

Xiao, T., Staub, W., Robles, E., Gosse, Nathan J., Cole, Gregory J., and Baier, H. (2011). Assembly of Lamina-Specific Neuronal Connections by Slit Bound to Type IV Collagen. Cell, pp. 164-176.

Yamagata, M., and Sanes, J.R. (2008). Dscam and Sidekick proteins direct lamina-specific synaptic connections in vertebrate retina. Nature *451*, pp. 465-469.

Yanagawa, S., Lee, J.S., and Ishimoto, A. (1998). Identification and characterization of a novel line of Drosophila Schneider S2 cells that respond to wingless signaling. J Biol Chem, pp. 32353-32359.

Yang, L., Garbe, D.S., and Bashaw, G.J. (2009). A frazzled/DCC-dependent transcriptional switch regulates midline axon guidance. Science, pp. 944-947.

Yonekura, S., Xu, L., Ting, C.-Y., and Lee, C.-H. (2007). Adhesive but not signaling activity of Drosophila N-cadherin is essential for target selection of photoreceptor afferents. Developmental Biology, pp. 759-770.

Yurchenco, P.D., and Wadsworth, W.G. (2004). Assembly and tissue functions of early embryonic laminins and netrins. Current Opinion in Cell Biology, pp. 572-579.

Zou, Y., Stoeckli, E., Chen, H., and Tessier-Lavigne, M. (2000). Squeezing axons out of the gray matter: a role for slit and semaphorin proteins from midline and ventral spinal cord. Cell, pp. 363-375.

Acknowledgements

I would like to express my special gratitude to Iris Salecker, who guided me during this PhD. Thank you for your support and for pushing me to be the best I could be.

I am immensely grateful to my friends in the lab – Holger Apitz, Dafni Hadjieconomou, Nana Shimosako, Willy Joly, Carole Chotard, Justine Oyallon, Emily Richardson, Benjamin Richier and Lauren Shaw. My special appreciation is for the support of Holger (whose modesty doesn't always allow for him to be so greatly appreciated, as he deserves! I am a lucky woman to have known you, Dr. A!) Dafni (my eternal comrade!) and Nana (the survivor!).

I am thankful to the fly community at the NIMR – the people in Alex Gould and JP Vincent labs for discussions and their expertise I have come to appreciate many times along the way. Especially here to Karen Beckett for helping me to learn about cell assays and Cyrille Alexandre for his advice in molecular cloning. Thank you as well to the Division of Molecular Neurobiology for a wonderful work atmosphere.

Many thanks also to my thesis committee, JP Vincent, Francois Guillemot and Vassilis Pachnis for their guidance during this PhD.
I greatly appreciate the support of my Viva committee, Lynda Erskine and Darren Williams.

Most importantly, I would like to thank my family, and especially Tobi, for believing in me and supporting me in pursuing this PhD, even though it meant to be away from home for a long time. This thesis is dedicated to you!